Tesis Doctoral

Silvia Mir Palomo

VNIVERSITAT DE VALÈNCIA

Facultat de Farmàcia

2020

VNIVERSITAT DE VALÈNCIA

Facultat de Farmàcia

Doctorado en Biomedicina y Farmacia

Nanoliposomas de baicalina y berberina en el tratamiento de afecciones cutáneas

TESIS DOCTORAL

Presentado por:
Silvia Mir Palomo

Directores:
Octavio Díez Sales
Amparo Nácher Alonso
Mª Amparo Ofelia Vila Busó

Valencia, 2020

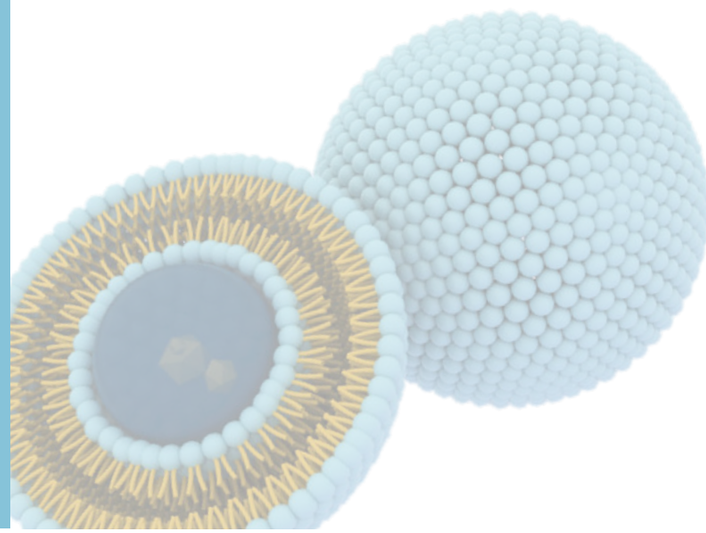

VNIVERSITAT DE VALÈNCIA

VNIVERSITAT DE VALÈNCIA Facultat de Farmàcia

Programa de Doctorado en Biomedicina y Farmacia

Nanoliposomas de baicalina y berberina en el tratamiento de afecciones cutáneas.

Tesis Doctoral presentada por:
Silvia Mir Palomo

Directores:
Octavio Díez Sales
Amparo Nácher Alonso
Mª Amparo Ofelia Vila Busó

Valencia, 2020

Facultat de Farmàcia

VNIVERSITAT DE VALÈNCIA

Doctorado en Biomedicina y Farmacia

D. Octavio Díez Sales, Dña. Amparo Nácher Alonso y Dña. María Amparo Ofelia Vila Busó, profesores Titulares, de la Universidad de València

CERTIFICAN:

Que la memoria de Tesis Doctoral realizada por Silvia Mir Palomo y que lleva por título "Nanoliposomas de baicalina y berberina en el tratamiento de afecciones cutáneas.", ha sido realizada bajo la dirección compartida de los mismos y reúne todos los requisitos necesarios para su presentación, juicio y calificación.

Valencia, a 25 de noviembre de 2020.

OCTAVIO|DIEZ|SALES Firmado digitalmente por OCTAVIO|DIEZ|SALES Fecha: 2020.11.18

MARIA AMPARO|NACHER|ALONSO Firmado digitalmente por MARIA AMPARO|NACHER|ALONSO Fecha: 2020.11.09 12:11:19 +01'00'

MARIA AMPARO OFELIA|VILA|BUSO 2020.11.18 20:31:21 +01'00'

Octavio Diez Sales Amparo Nácher Alonso Mª Amparo Ofelia Vila Busó

Departamento de Farmacia y Tecnología Farmacéutica y Parasitología.

Departamento de Quimica Física.

ÍNDICE

ABREVIATURAS

ATP	Adenosín trifosfato.
BA	Baicalina.
BE	Berberina.
BSC	Sistema de clasificación biofarmacéutica.
CLAE	Cromatografía líquida de alta eficacia.
Crio-TEM	Microscopía de transmisión criogénica.
DEX	Dexametasona.
DLS	“Dynamic Light Scattering”.
DMSO	Dimetilsulfóxido.
EE	Eficacia de encapsulación.
FDA	“Food and Drug Administration”.
FNS	Finasterida.
HaCat	Queratinocitos humanos inmortalizados.
HEMa	Melanocitos humanos hiperpigmentados.
HFDPC	Células de papila dérmica de folículo piloso humanas.
INF-γ	Interferon gamma.
IL-1	Interleuquina 1.
L-DOPA	Levodopa.
MPO	Mieloperoxidasa.
MTT	3-(4,5-dimethylthiazolyl-2)-2,5-diphenyltetrazolium bromide.
PBS	Tampón fosfato salino.
PI	Índice de polidispersión.
PRP	Plasma rico en plaquetas.

ROS	Especies reactivas del oxígeno.
TEM	Microscopía de transmisión electrónica.
TNF-α	Factor de necrosis tumoral.
TPA	13-acetato-12-O-tetradecanoilforbol.
UV	Ultravioleta.
3T3	Fibroblastos de ratón.

ÍNDICE DE FIGURAS

ÍNDICE DE TABLAS

PRÓLOGO

La presente Tesis Doctoral se estructura atendiendo a los requisitos establecidos por la Escuela de Doctorado de la Universidad de Valencia. Se presenta como compendio de artículos, publicados en revistas científicas indexadas en el "Journal Citation Reports (JCR)" y posicionados en el primer cuartil. Consta de una introducción, que trata los aspectos que actúan como vínculo de unión de los diferentes artículos publicados, seguida de una sección experimental, en la que se exponen, brevemente, los procedimientos realizados; a continuación se presentan los tres capítulos correspondientes al trabajo experimental desarrollado y, para finalizar, una discusión de los resultados y conclusiones globales.

El contenido de cada capítulo (artículo publicado en revista científica) refiere a la investigación que concierne al diseño y desarrollo de nanovesículas para el tratamiento de un tipo específico de alteración cutánea. Así, en el capítulo primero, se describe el estudio de la encapsulación de la baicalina, un flavonoide con diversas propiedades interesantes para el tratamiento psoriasis, en liposomas ultradeformables; se evalúa la liberación de la baicalina a partir de los liposomas, se analiza *in vitro* la biocompatibilidad de las formulaciones mediante el cultivo celular de fibroblastos; y finalmente se determina *in vivo*, el potencial antiinflamatorio de las formulaciones propuestas en un modelo animal de inflamación inducida por TPA en ratones CD-1.

El segundo capítulo se centra en la utilización de liposomas de baicalina y berberina, en combinación o de manera individualizada, para el tratamiento del vitíligo. Se analiza la permeabilidad cutánea de ambos productos naturales, encapsulados o no en liposomas ultradeformables, y se evalúa, mediante modelos *in vitro* de cultivos celulares de las principales células de la piel (queratinocitos, fibroblastos y melanocitos) la

biocompatibilidad de las formulaciones propuestas, el efecto protector que aportan frente a la radiación ultravioleta y frente al daño oxidativo y, para finalizar, el análisis de la capacidad hiperpigmentante, a través de la cuantificación de la melanina y la actividad tirosinasa.

El tercer capítulo evalúa el uso de vesículas innovadoras para mejorar la eficacia del tratamiento de la alopecia mediante la aplicación tópica local de finasterida, fármaco antiandrogénico derivado no hormonal de los esteroides, cargado individualmente o en combinación con baicalina, bioactivo antioxidante que actúa como coadyuvante. Se desarrollan liposomas convencionales, hialurosomas, glicerosomas y glicerohialurosomas. Los resultados *in vitro*, con cultivos de células de la papila dérmica del folículo piloso, e *in vivo*, con ratones C57BL/6, demuestran que los nanosistemas desarrollados son biocompatibles, capaces de estimular el crecimiento del cabello por la liberación folicular de la finasterida complementada con baicalina. En este trabajo, se pone de manifiesto la capacidad de estas nanovesículas de administrar la finasterida por vía transdérmica, como alternativa a la vía oral, que es la que se emplea habitualmente, consiguiendo un efecto local que minimice los efectos secundarios asociados a la administración de este fármaco por vía oral.

Por último, en el anexo se incluye una copia completa de los artículos publicados o aceptados para su publicación hasta la fecha.

RESUMEN

Las enfermedades cutáneas afectan a un gran número de personas y tienen un impacto negativo en la calidad de vida de los pacientes. Entre ellas destacan la psoriasis, una enfermedad crónica inflamatoria caracterizada por una excesiva proliferación de queratinocitos, y el vitíligo, caracterizada por la despigmentación gradual de la piel. Asimismo, la caída del cabello representa una de las patologías con mayor impacto sobre la calidad de vida de los pacientes, ya que suele afectar a su autoestima. Las tres patologías mencionadas tienen en común la ausencia, a día de hoy, de un tratamiento eficaz que no esté asociado a efectos adversos secundarios importantes. Una de las posibles estrategias terapéuticas que pueden contribuir a resolver este problema sería la administración por vía tópica de los fármacos propios del tratamiento, ya que presenta una serie de ventajas frente a otras vías, como son la facilidad de administración, lograr un efecto local y evitar las pérdidas presistémicas por el efecto de primer paso.

En la presente Tesis Doctoral se propone la administración por vía tópica de productos naturales como coadyuvantes en el tratamiento de las patologías descritas previamente.

La baicalina, un flavonoide natural aislado de la raíz de *Scutellaria baicalensis Georgi*, se propone como posible coadyuvante en el tratamiento de la psoriasis, el vitíligo y la caída capilar, ya que presenta diversas propiedades terapéuticas interesantes como antiinflamatorias, antioxidantes y estimulantes del crecimiento del cabello, entre otras. A su vez, la berberina es un alcaloide que presenta propiedades interesantes para el tratamiento del vitíligo, como la capacidad hiperpigmentante. Sin embargo, la aplicación por vía tópica de ambas se ve condicionada ya que presentan una hidrosolubilidad y permeabilidad cutánea baja. Se han

propuesto multitud de métodos para mejorar la aplicación de fármacos en la piel, ya que el estrato córneo forma una barrera muy efectiva que dificulta su paso a través; entre ellos, los liposomas son sistemas nanométricos y biocompatibles que tienen la capacidad de vehiculizar moléculas activas que presentan baja solubilidad en agua, mejorando la permeabilidad cutánea de las mismas.

Con el fin de desarrollar un tratamiento coadyuvante efectivo para la psoriasis, la baicalina se incorpora en liposomas ultradeformables a varias concentraciones, estos presentan un tamaño nanométrico, homogéneo y son biocompatibles, independientemente de la concentración de baicalina incorporada. Se ha podido observar que los liposomas ultradeformables de baicalina preparados mejoran la permeabilidad cutánea de la misma de manera concentración-dependiente y son capaces de reducir la inflamación inducida por TPA asociada a psoriasis en ratones CD-1, en proporción superior al tratamiento con dexametasona, un fármaco con propiedades antiinflamatorias. Los resultados obtenidos indican que los liposomas ultradeformables son nano-sistemas capaces de promover la permeabilidad cutánea de la baicalina, convirtiéndose así en una posible estrategia potencial para el tratamiento de la psoriasis al reducir la inflamación cutánea asociada a dicha enfermedad.

Para el estudio de un posible tratamiento coadyuvante del vitíligo se asocia baicalina y berberina, ambas encapsuladas, de manera individual o simultánea, en liposomas ultradeformables. Las vesículas, que presentan tamaños nanométricos con una distribución homogénea y carga negativa, son capaces de incorporar grandes cantidades de baicalina y berberina, así como de promover su permeabilidad cutánea. Los liposomas desarrollados muestran propiedades fotoprotectoras y antioxidantes

notables, así como una elevada capacidad de estimular la producción de melanina y la actividad de la tirosinasa. Los liposomas de baicalina o de berberina y particularmente, los liposomas que incluyen una combinación de ambos, representan una estrategia terapéutica prometedora para el tratamiento de los síntomas del vitíligo.

Por último, en la presente Tesis Doctoral se ha desarrollado un tratamiento innovador para la alopecia. La finasterida, un fármaco utilizado para el tratamiento de la caída del cabello, se incorpora en liposomas administrados por vía tópica, para evitar los efectos secundarios asociados a la administración oral, y se combina con baicalina como coadyuvante, para mejorar su eficacia, la cual es evaluada *in vitro* e *in vivo*. Se desarrollan liposomas, hialurosomas, glicerosomas y glicerohialurosomas que incorporan baicalina y finasterida; presentan un tamaño pequeño, con una distribución homogénea y carga negativa. Las formulaciones propuestas son capaces de estimular la proliferación de las células de la papila dérmica del folículo piloso y el estudio *in vivo* del crecimiento capilar y de los folículos pilosos en ratones C57BL/6 corrobora la capacidad de las vesículas de estimular el crecimiento del cabello. En consecuencia, los nano-sistemas que encapsulan baicalina y finasterida representan un tratamiento prometedor, seguro y eficaz para el tratamiento de la alopecia.

INTRODUCCIÓN

Piel y folículos pilosebáceos.

La piel es uno de los órganos más complejos y diversos del cuerpo humano. Presenta una superficie de aproximadamente 1,7 m^2 y se corresponde con el 10 % del peso total, siendo así el órgano más grande del cuerpo. La función principal de la piel es la de aportar una barrera robusta y flexible frente a agresiones externas. Esta barrera protege al ser humano frente a la radiación ultravioleta (UV), microorganismos patógenos, alérgenos, etc. Además, la piel tiene una función muy importante en homeostasis y en mantener los niveles de hidratación adecuados (1).

Estructura de la piel.

La piel está formada por varias capas, como se muestra en la figura 1. Estas se describen brevemente a continuación.

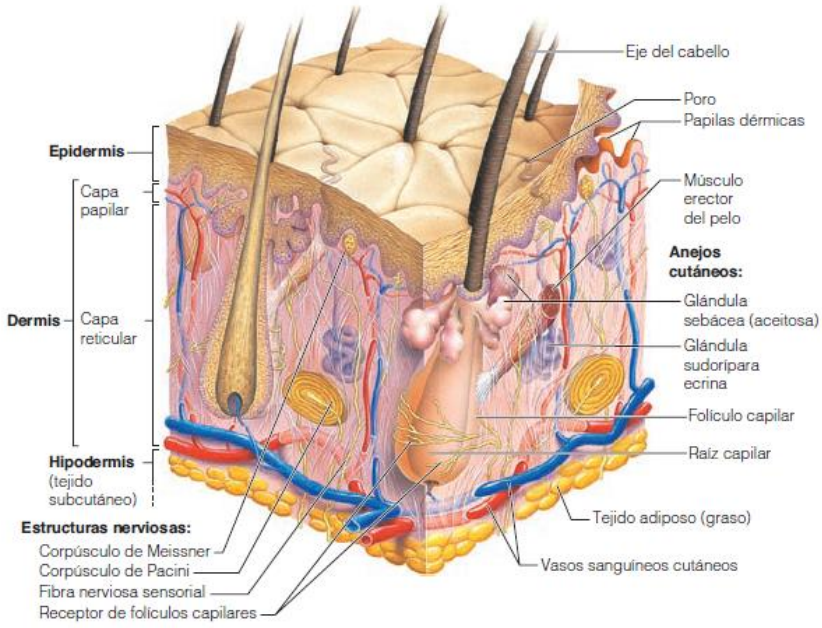

Figura 1. Estructura de la piel. Corte transversal (2).

Epidermis.

Es la epidermis, la capa más externa, la que evita y/o minimiza la entrada de microorganismos, toxinas, alérgenos o sustancias irritantes; absorbe radiación UV y reduce el daño producido por fuerzas mecánicas.

La epidermis está formada principalmente por queratinocitos; estos constituyen el 90% de las células, y están distribuidos, junto con melanocitos, células de Langerhans y células de Merkel, a lo largo de los estratos que la forman. El estrato basal, formado principalmente por queratinocitos que presentan una elevada actividad proliferativa, es la capa más interna. Los queratinocitos, a través del estrato espinoso y granuloso, se van diferenciando hasta formar finalmente corneocitos, células planas totalmente diferenciadas que constituyen principalmente el estrato córneo. En este estrato más externo se pueden encontrar, también, lípidos intercelulares, como ceramidas, fosfolípidos y colesterol, los cuales se organizan formando estructuras multilamelares similares a las de las membranas biológicas. Estas estructuras son las responsables de la permeabilidad selectiva de la piel (3).

La epidermis se encuentra sometida a un proceso de renovación celular continuo, ya que el estrato córneo se encuentra en un estado de formación constante (figura 2).

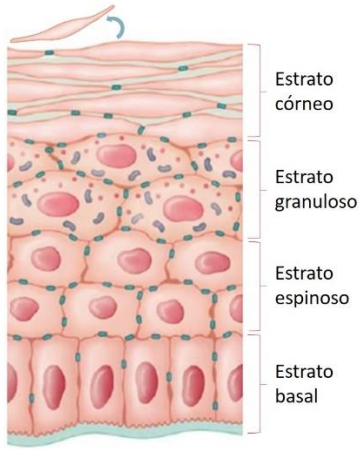

Figura 2. Esquema de las diferentes capas de la epidermis. Esquema de la diferenciación-renovación celular (4).

Los melanocitos son los responsables de la producción de melanina; sin embargo, suponen menos del 1% de las células presentes en la epidermis. Estos confieren protección frente a las radicaciones y permiten la pigmentación de la piel; producen un orgánulo llamado melanosoma, el cuál es transferido a los queratinocitos produciendo la deposición de melanina en la epidermis (5).

Las células de Langerhans son células dendríticas que tienen un papel crucial en aportar protección inmunológica a la piel, son las encargadas de fagocitar y eliminar cuerpos extraños, a través del complejo mayor de histocompatibilidad (6).

Las células menos numerosas de la epidermis son las células de Merkel, estas se encuentran en contacto con las células nerviosas y su función está relacionada con diferentes aspectos de las sensaciones táctiles (7).

Dermis.

La dermis es una capa formada por tejido conectivo que se localiza entre la epidermis y el tejido subcutáneo. Es una estructura fibrosa compuesta principalmente por colágeno y elastina, formados a partir de fibroblastos, el mayor tipo celular de esta capa. Es un tejido vascularizado que alberga nervios, terminaciones nerviosas, folículos pilosos y otras glándulas. La principal función de la dermis es la de servir como sostén y aportar protección a las capas más profundas; a su vez, juega un papel importante en la termorregulación y respuestas táctiles.

Como se observa en la figura 1, la dermis se divide en dos capas, un estrato de tejido conectivo laxo conocido como región papilar y la capa más profunda, que forma una capa gruesa de tejido conectivo denso que constituye la mayor parte de la dermis, denominada región reticular.

La región papilar de la dermis está conectada con el estrato basal de la epidermis formando la unión dermoepidermica. Esta zona de contacto actúa como barrera para el paso de algunas moléculas (8).

Hipodermis.

El tejido subcutáneo o hipodermis es, fundamentalmente, tejido adiposo y no se considera parte de la piel, sino que sirve de separación y anclaje de la piel a los diferentes tejidos.

Por otra parte, en la superficie de la piel se distinguen unas aberturas, a través de las cuales crece el pelo, denominadas **folículos pilosos**. Estos representan unas de las estructuras cutáneas más dinámicas y activas del organismo.

Anatomía del folículo piloso y del pelo.

El folículo piloso, junto al músculo piloerector y las glándulas sebáceas constituyen la unidad pilosebácea, una estructura compleja en la que coexisten diversos tipos celulares.

El folículo piloso se divide en dos zonas o segmentos delimitados por el musculo erector del pelo (figura 3).

- Segmento superior, compuesto del ostium (apertura del folículo en la piel), infundíbulo (desde ostium a la desembocadura de la glándula sebácea) y el istmo (de la glándula sebácea a la unión con el músculo erector del pelo). Este segmento no está influenciado por el ciclo de crecimiento del pelo.
- Segmento inferior, este segmento llega casi a desaparecer en fase telógena. Comprende desde el bulbo piloso a la unión con el músculo erector del pelo. Se compone del tallo y el bulbo, es en esta última zona donde se encuentran las células matriciales y los melanocitos, responsables de la pigmentación y formación del tallo piloso.

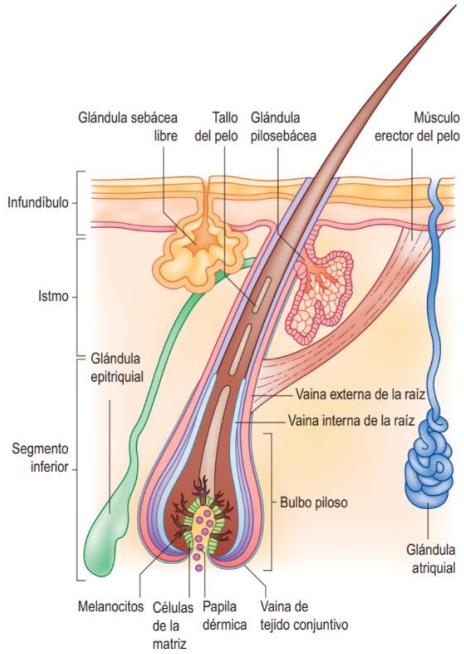

Figura 3. Diagrama del folículo piloso y anejos asociados (9).

El pelo está formado por queratina dura y se compone de tres regiones principales; la médula, la porción más interna responsable del aislamiento térmico; la corteza, la encargada de aportar resistencia al cabello; y la cutícula, la parte más externa que se encarga de conferir protección al cabello frente a agresiones externas. A su vez, los folículos pilosos están asociados a glándulas sebáceas, las cuales aportan lubricación al canal folicular y la superficie cutánea.

El folículo piloso está formado por componentes epiteliales y dérmicos, se distingue la papila dérmica en la base del folículo piloso. Las células de la papila dérmica son componentes mesenquimales especializados del cabello que juegan un papel importante en la morfogénesis y la regeneración del crecimiento capilar. Estas regulan el desarrollo y crecimiento del folículo piloso y actúan como un reservorio de células madre, nutrientes y factores de crecimiento. Estas células sirven como

modelo *in vitro* para evaluar la efectividad de terapias para el crecimiento del cabello, así como para definir el mecanismo de acción de fármacos o el funcionamiento de los folículos pilosos (10).

Ciclo de crecimiento capilar.

El folículo piloso sufre una regeneración continua en el ciclo de crecimiento del cabello. Durante este ciclo se producen cambios importantes en el segmento inferior del folículo piloso, así como en los vasos, nervios, tejido conjuntivo y células relacionadas con el folículo.
Este ciclo está formado por tres fases principalmente, tal como se muestra en la figura 4:

- la fase de crecimiento (anágena)
- la fase de transición (catágena) y
- la fase de reposo (telógena)

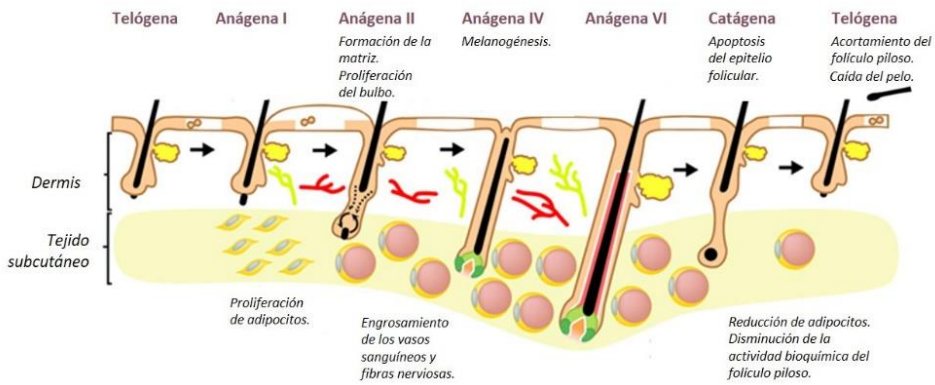

Figura 4. Descripción del ciclo de crecimiento capilar (11).

La fase anágena es la más duradera del ciclo, entre 2 y 7 años, por lo que más del 80% de los folículos pilosos se encuentran en esta fase. Durante esta fase la actividad mitótica del bulbo piloso se encuentra en pleno rendimiento, los folículos alcanzan su volumen y longitud máximos. Se

produce a su vez la pigmentación del pelo, debido a la interacción que se produce ente melanocitos, queratinocitos y fibroblastos de la papila dérmica.

La fase catágena o de transición es la más corta, con una duración de 2 a 4 semanas. Los folículos pilosos, durante este periodo, están en reposo; se produce la apoptosis del epitelio folicular y cesa la actividad mitótica y la pigmentación. El 1 -2 % de los folículos pilosos se encuentran en esta fase.

La fase telógena, en la que se encuentran el 10 – 15 % de los folículos, dura aproximadamente 3 meses. Durante esta fase, se produce el acortamiento del folículo piloso y se caracteriza por la disminución de la actividad bioquímica del mismo y la caída del cabello; a su vez, durante este periodo, los receptores de estrógenos se expresan al máximo.

Los cabellos se desprenden del tallo en la fase exógena. Tras esta fase y hasta que comienza de nuevo el ciclo, el folículo queda vacío, es lo que se conoce como fase kenógena (12).

Alteraciones de la piel.

Debido a que forma la barrera exterior del cuerpo, la piel se encuentra expuesta de manera permanente a patógenos y agentes externos nocivos. Es por ello que las alteraciones en la piel se dan con bastante frecuencia. En la mayoría de ellas, el sistema inmune juega un papel crucial. Esta Memoria se centra en tres de ellas, cuyas características se describen a continuación:

- Psoriasis
- Vitiligo
- Alopecia

Psoriasis.

Los procesos inflamatorios de la piel son muy heterogéneos e implican diversas vías de señalización complejas. La inflamación es un proceso que incluye la liberación de citoquinas proinflamatorias, entre las que el factor de necrosis tumoral (TNF-α) e interleuquinas juegan un papel muy importante (13).

Se considera un proceso de protección esencial para preservar la integridad del cuerpo contra los agentes físicos y químicos, así como las respuestas autoinmunes. La respuesta inflamatoria es considerada como un mecanismo de reparación; es útil para destruir al agente lesivo y simultáneamente iniciar una serie de acontecimientos que determinan la reconstrucción del tejido lesionado. Sin embargo, existen determinadas situaciones, como pueden ser las reacciones alérgicas, en las que la respuesta inflamatoria constituye un mecanismo patógeno y puede conllevar el daño de tejidos sanos, debido a una sobreproducción de especies reactivas de oxígeno (ROS), óxido nítrico y citoquinas (14).

De manera general, la inflamación se localiza en un órgano específico y normalmente es de corta duración, transcurre en unos minutos o pocos días y se caracteriza principalmente por la extravasación de líquidos plasmáticos, migración de proteínas y el movimiento de leucocitos hacia el área extravascular. Estas reacciones implicadas están mediadas por ciertos estímulos químicos producidos por las células y son los responsables de las manifestaciones de la inflamación, como hinchazón, rubor, dolor, etc. Principalmente se distinguen tres procesos, aumento del flujo sanguíneo al área inflamada, vasodilatación y aumento de la permeabilidad y migración de leucocitos fagocíticos al tejido circundante (15).

Aunque la inflamación es considerada como un mecanismo de protección, un exceso de respuesta inflamatoria puede causar un daño en tejidos sanos y causar una inflamación crónica, como ocurre en las enfermedades inflamatorias de la piel, muy comunes en dermatología. La psoriasis es una enfermedad inflamatoria cutánea crónicas de etiología desconocida; está causada por una interacción compleja de factores ambientales, genéticos e inmunológicos y tiene un impacto considerable en la calidad de vida de los pacientes (16).

El arsenal terapéutico actual para el abordaje de los procesos inflamatorios implica tratamientos sistémicos a largo plazo con fármacos antinflamatorios esteroideos y no esteroideos; sin embargo, su biodisponibilidad oral es baja y a menudo están asociados a la aparición de diversos efectos secundarios. Las terapias biológicas producen una supresión inespecífica de los procesos inflamatorios; sin embargo, son administradas por vía parenteral, presentan una eficacia limitada y no se encuentran exentos de efectos secundarios (17). La vía tópica puede ser una alternativa interesante ya que permite una acción localizada minimizando los efectos adversos del tratamiento (18). A su vez, ante las limitaciones y efectos secundarios que presentan las terapias antiinflamatorias actuales, los activos naturales se presentan como buenos candidatos coadyuvantes en el tratamiento de enfermedades inflamatorias cutáneas (15).

Vitíligo.

El vitíligo es una enfermedad cutánea caracterizada por una deficiente pigmentación de la piel; se manifiesta en forma de manchas o máculas bien definidas, que pueden ser acrómicas o hipocrómicas, en las que se ha observado el deterioro de la función del melanocito. La causa del vitíligo

es compleja y desconocida, implica una serie de factores genéticos, ambientales e inmunológicos. Afecta a un 0.5 – 1 % de la población a nivel mundial y puede desarrollarse a cualquier edad. No hay diferencias en la prevalencia en función del sexo, tipo de piel o raza (19).

La despigmentación de la piel es el signo clínico del vitíligo; se manifiesta con manchas blancas, a menudo simétricas, que generalmente aumentan en tamaño y número con el paso del tiempo. Existen varios tipos de vitíligo, descritos en la tabla 1, y es el patrón de las lesiones lo que predice la progresión de la enfermedad y las respuestas al tratamiento (20).

Tabla 1. Principales tipos de vitíligo (20).

No segmentado	**Generalizado**	Es la forma más común. Se caracteriza por la aparición, de manera asintomática, de manchas blancas más o menos simétricas. Puede empezar en cualquier parte del cuerpo, siendo los dedos, las manos y cara las regiones más frecuentes.
	Focal	Caracterizado por la aparición de una o varias manchas blancas localizadas, aisladas y pequeñas (10 – 15 cm^2), que no progresan durante al menos 2 años. Se distingue entre vitíligo acrofacial, que afecta a la cara, cabeza, manos y pies y vitíligo de mucosas, el cual afecta a zona genital o mucosas orales. Puede evolucionar a vitíligo generalizado.

No segmentado	**Universal**	Es una forma rara de la enfermedad, se caracteriza por la despigmentación completa o casi completa de la piel, puede incluir o no vello corporal (80 – 90 % de la superficie del cuerpo). Es la forma más extensa de la enfermedad y generalmente, tiene lugar en la edad adulta.
Segmentado		Es la forma menos común. La pérdida progresiva de melanocitos afecta solo a un segmento del cuerpo. Suele aparecer en la infancia. Se caracteriza por un inicio rápido de la enfermedad, frecuentemente en la cara; se estabiliza en 1 o 2 años y no afecta a otras áreas del cuerpo. Esta variante responde peor a tratamiento, probablemente debido a que se asocia con Leukotrichia y produce una pérdida de melanocitos necesaria para la repigmentación.

Existen diversas teorías sobre la causa del vitíligo. Se trata de una enfermedad multifactorial en cuyo inicio coexisten inflamación, defectos en los melanocitos y destrucción de los mismos (21).

La teoría autoinmune o autoinflamatoria se basa principalmente en la asociación clínica del vitíligo con trastornos autoinmunes, como tiroiditis, psoriasis, lupus eritematoso, etc. Hay un componente genético importante implicado en el desarrollo de la enfermedad, pues se ha observado una mayor incidencia de enfermedades autoinmunes en familiares de pacientes con vitíligo. A su vez, diversos estudios identificaron numerosas variantes genéticas comunes en pacientes con vitíligo (22).

Tal como se muestra en la figura 5, una gran cantidad de procesos en cadena están implicados en la destrucción de melanocitos y aparición de lesiones. Diversos estudios sugieren que el estrés oxidativo juega un importante papel en el inicio de esta enfermedad. Los melanocitos en las manchas de los pacientes de vitíligo muestran defectos intrínsecos que reducen su capacidad de contrarrestar el estrés oxidativo. Las células de la epidermis están constantemente expuestas a factores ambientales como la radiación ultravioleta, que puede aumentar la producción de ROS. Si bien los melanocitos sanos son capaces de mitigar estos daños, los melanocitos de las manchas de pacientes con vitíligo parecen ser más vulnerables, acumulando ROS y convirtiéndose en melanocitos estresados (23).

Finalmente, en el vitíligo se produce la destrucción de los melanocitos mediada por las células T $CD8^+$ citotóxicas. El número de estas células T se correlaciona con la intensidad de la gravedad. Varias citoquinas, como TNF-α e IFN-γ, están implicadas en la destrucción de los melanocitos. Estas se secretan como una señal para ayudar a las células T autorreactivas a localizar melanocitos estresados. TNF-α e IFN-γ inducen la liberación de varias quimiocinas (CXCL9 y CXCL10) que, en última instancia, producen la inhibición de la melanogénesis y la inducción de apoptosis de melanocitos (24).

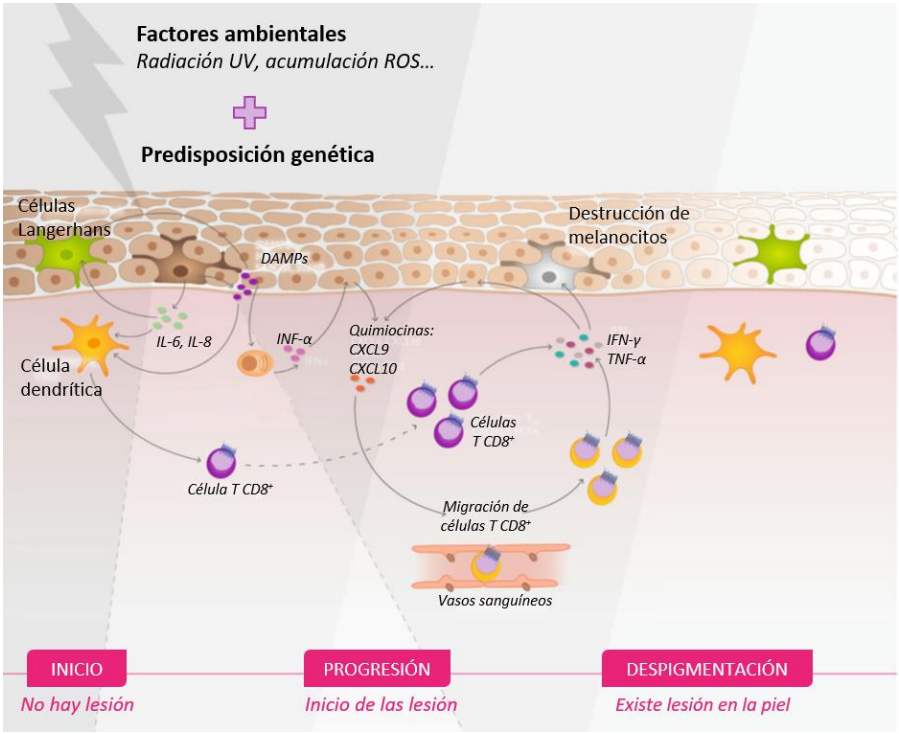

Figura 5. Esquema de la patología del vitíligo (25).

El tratamiento del vitíligo sigue siendo uno de los objetivos dermatológicos más difíciles. Los tratamientos actuales incluyen fototerapia, inmunosupresores y terapias quirúrgicas, que en conjunto pueden ayudar a frenar la enfermedad, estabilizar las lesiones despigmentadas y estimular la repigmentación. En la elección del tratamiento están implicados diversos factores como el tipo de vitíligo, la extensión y la distribución de la enfermedad, así como la edad del paciente y el fototipo. Existen diferencias en función del área a la que afecta la enfermedad, así pues la cara, el cuello, el tronco y las extremidades medias responden mejor al tratamiento, mientras que labios y extremidades distales son más resistentes. Sin embargo, se precisa un tratamiento de aproximadamente 3 meses para poder determinar la eficacia del mismo. La terapia con luz

UV es el tratamiento más común para el vitíligo y, asociado a una terapia adicional presenta mejores resultados (26).

Alopecias.

La caída de cabello, denominada alopecia, es un trastorno frecuente, en el que están involucrados gran cantidad de procesos genéticos, hormonales, traumáticos e iatrogénicos. Aunque se considera una patología benigna, la importancia de la alopecia estriba en la frecuencia, en el impacto psicológico que tiene o en la posibilidad de que se presente como un signo de enfermedades sistémicas o como consecuencia de efectos secundarios de fármacos (27).

Existen diversos tipos de alopecias que varían en extensión y gravedad, aunque el diagnóstico a menudo se atribuye a una pérdida de cabello provocada por andrógenos (28). Numerosos investigadores han propuesto diferentes sistemas de clasificación para la pérdida de cabello con patrones en función de la etapa evolutiva, estas van desde una simple clasificación de dos etapas propuesta por Beek en 1950 hasta una clasificación básica y específica avanzada reciente (Figura 6) (29).

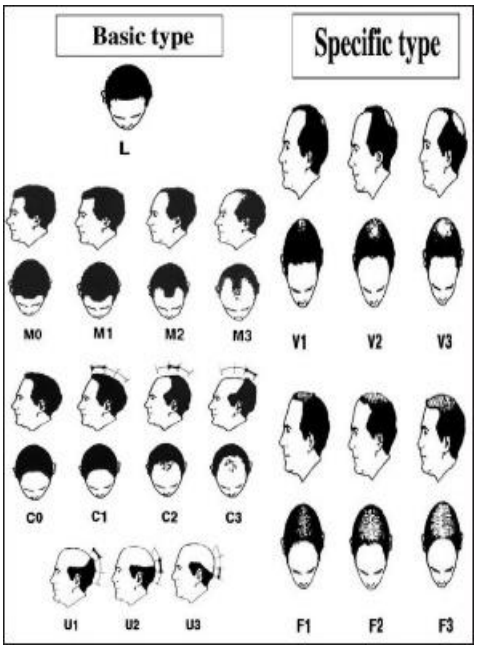

Figura 6. Clasificación básica de la pérdida de cabello (29).

Cada tipo de alopecia presenta un patrón definido. Siendo la alopecia androgénica, areata y cicatricial las más comunes.

Alopecia androgénica es un trastorno crónico y progresivo que afecta a un gran porcentaje de personas en el mundo. En la alopecia androgénica tiene lugar el acortamiento de la fase de crecimiento, la fase anágena; por lo que, como consecuencia, tiene lugar un aumento del porcentaje de pelos que se encuentran en fase telógena. Se caracteriza por una miniaturización del folículo piloso sensible a andrógenos, es causada por un aumento en los niveles de dihidrotestosterona, la alteración en la actividad de α-reductasa o la sobreexpresión de receptores de andrógenos. A menudo esta miniaturización está asociada a fibrosis y a inflamación del bulbo piloso (30).

Alopecia areata es una enfermedad autoinmune caracterizada por la pérdida de cabello sin cicatrices, se produce debido a una inflamación de los folículos pilosos (31). El inicio y progresión de la alopecia areata son impredecibles; se estima que aproximadamente un 80 % de los pacientes experimenta un crecimiento espontáneo del cabello tras un año de enfermedad, aunque la recaída o progresión a la alopecia total puede ocurrir en cualquier etapa. No existe tratamiento para este tipo de alopecia. La eficacia de las opciones terapéuticas disponibles es limitada y depende del paciente y de la etapa de la enfermedad en la que se encuentre (32).

El término **alopecia cicatricial** hace referencia a un grupo heterogéneo de trastornos capilares que conducen a la destrucción de los folículos pilosos y la consiguiente cicatrización. Esta forma de alopecia tiene lugar tras un daño físico, como quemadura, radiación, infecciones, tumores, etc. Se distinguen dos formas en función de los mecanismos de inflamación implicados; por un lado, la alopecia cicatricial primaria se produce como resultado de una destrucción inflamatoria directa del epitelio piloso, siendo el folículo piloso, el objetivo principal de la inflamación. Por otro lado, la alopecia cicatricial secundaria es causada por procesos inflamatorios o daños mecánicos en el tejido circundante del folículo piloso (33).

Una amplia variedad de terapias han sido descritas para el tratamiento de la caída del cabello o alopecia, tal como se describe en la tabla 2. Sin embargo, la FDA (“Food and Drug Administration”) solo ha aprobado dos fármacos, el minoxidilo, administrado por vía tópica, y la finasterida, administrada por vía oral (34).

Tabla 2. Tratamientos actuales para desordenes capilares (34).

Tratamiento de desórdenes capilares	
Minodixilo	La aplicación tópica de minoxidilo corresponde la primera línea de acción en el tratamiento de pérdida de cabello, independientemente del sexo. Está disponible como solución al 2 y 5 %. Aunque el minoxidilo ha demostrado ser efectivo por sí mismo, numerosos estudios señalan que su efectividad se ve incrementada cuando se usa en combinación con otros fármacos. El posible mecanismo de acción es debido a la vasodilatación que produce en el folículo. Estudios recientes apuntan a que puede tener un papel en la regulación de los niveles de potasio en los canales de ATP de las células dérmicas foliculares.
Finasterida	Es un inhibidor de la 5-α-reductasa tipo 2, impide la conversión de testosterona a dihidrotestosterona. Se administra por vía oral a dosis de 1 mg/día para el tratamiento de la alopecia androgénica. Sin embargo, presenta una amplia variedad de efectos adversos asociados, mayoritariamente de tipo sexuales y reproductivos. A su vez, se utiliza como tratamiento de la hiperplasia benigna de próstata, administrada a una dosis de 5 mg diarios.
Dutasterida	Es un inhibidor de la 5-α-reductasa tipo 1 y tipo 2. Diversos estudios demuestran que el tratamiento con dutasterida es más efectivo que con finasterida;

	sin embargo, presenta a su vez importantes efectos adversos asociados, como disminución de la libido, mareo, inflamación de los testículos, fallo cardíaco, etc.
Plasma rico en plaquetas (PRP)	Factores de crecimiento que pueden producir una reversión en el proceso de miniaturización del folículo y regula el ciclo de crecimiento de pelo.
Cimetidina	Es un bloqueante de histamina, produce a su vez, el bloqueo de la unión de dihidrotestosterona al receptor.
Anticonceptivos orales	Disminuyen la producción de andrógenos en mujeres. Se utiliza en el tratamiento de alopecia androgénica femenina.
Espironolactona	Bloquea la unión de dihidrotestosterona al receptor, a su vez, disminuye la producción de andrógenos.
Acetato de ciproterona	Bloquea la unión de dihidrotestosterona al receptor.

Tratamientos complementarios para las alteraciones cutáneas.

Tradicionalmente, los productos naturales han sido ampliamente utilizados para el cuidado de la piel y el tratamiento de enfermedades cutáneas. Hoy en día, cada vez son más frecuentes las formulaciones para el cuidado de la piel basadas en productos naturales. Se ha demostrado la eficacia de diferentes extractos de plantas como antioxidantes, antimicrobianas, despigmentantes, etc., que pueden resultar interesantes en la prevención y tratamiento de diversas afecciones cutáneas. Son varias

las ventajas que confieren este tipo de productos, además suelen ser una alternativa segura, en función de su dosis, a los productos de síntesis (35).

En la presente Tesis Doctoral se han seleccionado, para su formulación, los siguientes productos naturales, cuyas características se describen a continuación:

- Baicalina
- Berberina

Baicalina.

La medicina tradicional china está basada en más de 2000 años de conocimiento. Los aspectos principales de la práctica incluyen medicamentos a base de hierbas, acupuntura y otras terapias físicas como masajes. Esta práctica ha sido considerada fuera de China como una medicina alternativa; aunque su prevalencia internacional ha aumentado considerablemente, la aceptación de la medicina tradicional china por parte de la comunidad científica ha sido limitada. Sin embargo, hay ciertos aspectos de este tipo de medicina que son prometedores para la medicina moderna. El campo de los tratamientos basados en productos naturales de la medicina tradicional china ha ganado un gran interés como fuente de nuevos fármacos; un ejemplo claro de ello es el desarrollo de artemisina, un potente antipalúdico derivado de *Artemisia annua*, a base de hierbas, cuyo descubrimiento llevó a obtener el premio Nobel de medicina en 2015 (36).

Un producto natural utilizado ampliamente en la medicina tradicional china es la raíz de *Scutellaria Baicalensis Georgi.* Se utiliza de manera tradicional, tras su decocción, para el tratamiento de infecciones (37), hipertensión (38), diabetes, (39), hemorragia (40) e inflamación (41). Los

flavonoides se consideran los principales componentes de *Scutellaria Baicalensis Georgi*, entre los cuales la baicalina (BA), cuya estructura se muestra en la figura 7, ha sido considerada el componente activo esencial y uno de los flavonoides más abundantes (42).

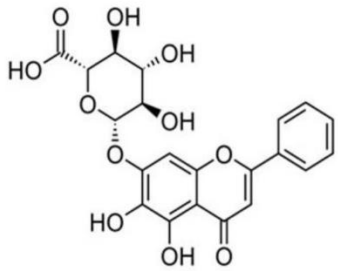

Figura 7. Estructura molecular de la baicalina (37).

Diversos estudios recientes han puesto de manifiesto numerosos efectos farmacológicos de la baicalina. Se ha demostrado, en un modelo animal, que podría utilizarse como un agente prebiótico para tratar la inflamación asociada a colitis ulcerosa (43). A su vez, ha demostrado un gran potencial en el tratamiento de la inflamación cutánea, inhibiendo la expresión y proliferación de citoquinas profinflamatorias en cultivos de queratinocitos estimulados por TNF-α (44). Por otro lado, la baicalina puede tener un papel importante en el tratamiento de enfermedades pulmonares, ya que, se demostró que ejerce un efecto supresor sobre la fibrosis pulmonar inducida por la proliferación de fibroblastos (45). Diversos estudios demuestran que la baicalina posee un potencial anticarcinogénico y, a su vez, se ha puesto de manifiesto una elevada capacidad de inhibir el crecimiento celular así como de inducir la apoptosis (46) (47) (48) (49).

Sin embargo, estudios farmacocinéticos han demostrado que su aplicación clínica es limitada debido a la escasa hidrosolubilidad (91 µg/mL) y baja biodisponibilidad (2.2 %), ya que, entre otros problemas, sufre pérdidas

presistémicas por hidrólisis en el tracto gastrointestinal (50) (51). La baicalina podría considerarse como un compuesto de clase IV de acuerdo con el Sistema de Clasificación Biofarmacéutica (BCS), a su vez, presenta un peso molecular (446.1 g/mol) y una lipofilia (log P octanol = 1.27) elevados (52) (53). Así pues, una posibilidad de soslayar parte de las limitaciones que sufre la baicalina sería su administración por vía tópica, mediante la encapsulación en sistemas de vehiculización que permitan obtener niveles de baicalina en piel adecuados.

Berberina.

La berberina (BE) es un alcaloide isoquinoleínico descubierto por primera vez en 1830. Su estructura se muestra en la figura 8. Este alcaloide puede encontrarse ampliamente en raíces, rizomas y tallos de diversas plantas como *Hydrastis canadensis, Berberis aristata, Coptis chinensis, Coptis rhizome, Coptis japonica, Phellondendron amurense, Phellondendron chinense schneid* (54), que han sido utilizadas en la medicina tradicional China, así como en India o Irán (55).

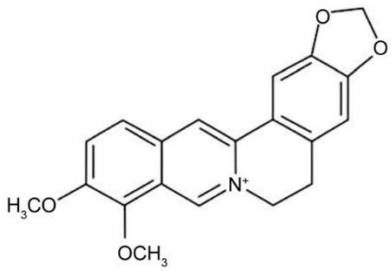

Figura 8. Estructura molecular de la berberina (56).

A principios de 1960, varios estudios demostraron que la berberina y sus sales, como el sulfato de berberina, eran efectivas para el tratamiento del cólera, la diarrea severa y la amebiasis (57) (58). A finales del siglo XX se realizaron estudios clínicos que demostraron que la berberina era eficaz

para el tratamiento de la diarrea asociada a infecciones con diversas bacterias (59) (60).

Actualmente, se ha demostrado que la berberina presenta múltiples beneficios terapéuticos como antiinflamatorio, antiinfeccioso, antiarritmico, hipolipemiante, hipoglicemiante, etc. Durante un proceso inflamatorio, la berberina demostró eficacia al inhibir la liberación de citoquinas proinflamatorias como IL-1, TNF-α e IFN-γ (61). Frente a infecciones, la berberina ha demostrado potencial frente a *Helicobacter pylori* (62) (63), así como en el tratamiento de cistitis (64). La berberina es también útil en la prevención de enfermedades cardiovasculares, ya que ha demostrado ser eficaz en la reducción de los niveles de colesterol (65). A su vez, en un ensayo clínico con pacientes prehipertensos, la berberina demostró ser segura, bien tolerada y efectiva para mejorar el patrón lipídico y los niveles de glucosa, previniendo así la progresión a hipertensión (66) (67). De la misma manera, debido a que es capaz de normalizar los niveles de glucosa, la berberina puede ser un coadyuvante potencial en el tratamiento de la diabetes (68).

Hoy en día, se utilizan las sales de berberina, como cloruro o sulfato de berberina con fines medicinales. Es un polvo amarillo intenso, inodoro con un sabor amargo alcaloide característico. Las limitaciones que presenta es su baja solubilidad en agua (69) y su baja biodisponibilidad (< 1%) (70). A su vez, el peso molecular la berberina es de 336.124 g/mol y el log P (octanol/agua) de 3.6. (71). El hecho de que sea una molécula de tamaño y lipofília elevados hace que su penetración por vía cutánea se vea comprometida, por lo que se hace necesario el planteamiento de diversas estrategias para mejorar su aplicación por vía cutánea.

Administración tópica de productos naturales.

La aplicación de principios activos por vía tópica puede ser una alternativa interesante frente a otras vías de administración, ya que ofrece una serie de ventajas. Es una opción prometedora al evitar las pérdidas presistémicas de activos que sufren un efecto de primer paso hepático, minimizar los efectos adversos y permitir la liberación controlada y sostenida en el tiempo.

Como se puede observar en la figura 9, existen varias vías para el paso de principios activos a través de la epidermis; la vía transapedicular, en la que los fármacos atraviesan la epidermis a través de los folículos pilosos, glándulas sebáceas asociadas y glándulas sudoríparas; y la vía transepidérmica, en la que hay descritas principalmente dos rutas, la ruta transcelular, en la que la sustancia activa atraviesa los corneocitos y la matriz lipídica; y la ruta paracelular, en la que el paso se produce mediante difusión pasiva, a través de los espacios libres de los corneocitos. La permeación de cada molécula a través de la piel no se realiza exclusivamente por una sola vía, si no que esta se realiza mediante una combinación de las mismas, en función de las características fisicoquímicas de cada sustancia, siendo la vía paracelular considerada como la vía principal de permeación para la mayoría de las moléculas (72).

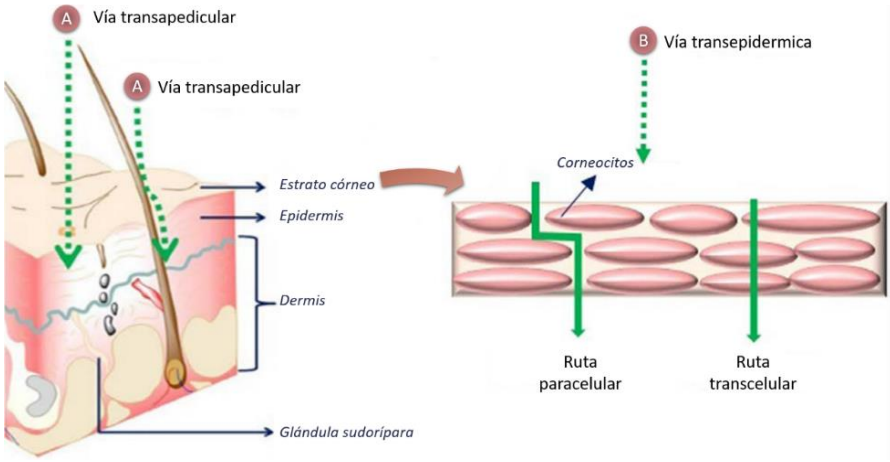

Figura 9. Esquema de las rutas descritas para el paso de sustancia a través de la piel (73).

A pesar de las numerosas ventajas que ofrece la vía tópica, el número de moléculas que pueden ser administradas por esta vía es limitado, ya que la piel forma una barrera muy efectiva, especialmente el estrato córneo, y la permeabilidad de la misma a compuestos muy hidrofílicos, hidrofóbicos o con un elevado peso molecular es muy baja.

Liposomas.

Con el fin de superar las limitaciones que presenta la vía tópica, en las últimas décadas, numerosos estudios se han centrado en el desarrollo de sistemas de transporte innovadores capaces de incorporar cantidades adecuadas de moléculas activas, tanto hidrófilas como lipófilas y promover la acumulación o el paso de las mismas a través de la piel para ejercer su acción farmacológica. Entre los vehículos propuestos, se ha centrado la atención en los de tamaño nanométrico; se han desarrollado numerosos nanotransportadores versátiles a base de lípidos con aplicación dermatológica, ya que, debido a su naturaleza lipídica poseen

la ventaja de que son capaces de facilitar la penetración de las moléculas a través del estrato córneo. Entre ellos, los liposomas son sistemas con gran potencial, ya que permiten la vehiculización de activos que por sí solos no son capaces de atravesar la epidermis y conducirlos al lugar de destino donde se liberan y ejercen su acción. Estas nanovesículas se preparan a base de fosfolípidos oleaginosos no tóxicos de origen natural que se organizan de forma similar a las membranas celulares (74).

Desde la primera observación de Alec Bangham, en la década de 1960, de que los fosfolípidos en medios acuosos pueden formar vesículas cerradas de bicapa lipídica, los liposomas se han convertido en una de las herramientas más prometedoras para la encapsulación de moléculas (75).

Composición de los liposomas.

Los liposomas, con una estructura similar a las bicapas de las membranas celulares y excelente biocompatibilidad, son cada vez más utilizados como sistemas de liberación de activos. Son sistemas vesiculares formados principalmente por fosfolípidos, los cuales se componen de cabezas hidrófilas y colas hidrófobas. Gracias a esta naturaleza anfifílica pueden formar bicapas en un medio acuoso, tal como se muestra en la figura 10 (76).

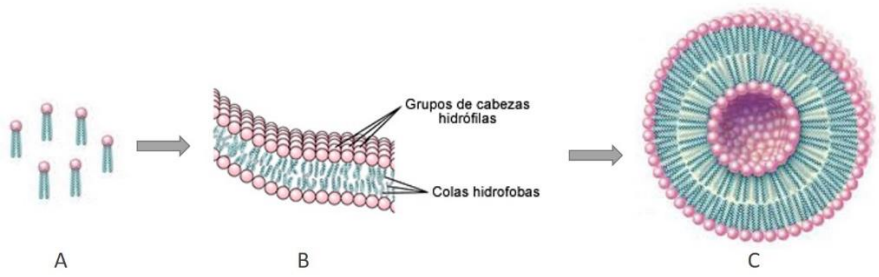

Figura 10. Esquema del fenómeno que sufren los fosfolípidos para conducir a la formación de liposomas: A) Moléculas de fosfolípido. B) Bicapa de fosfolípidos. C) Liposoma.

Los liposomas pueden estar formados por una o varias bicapas lipídicas que encierran un número igual de compartimentos acuosos. Son sistemas versátiles, ya que permiten la incorporación de moléculas lipófilas, localizadas en la bicapa lipídica, y moléculas hidrófilas, albergadas en el medio acuoso.

Los liposomas, como sistemas de transporte de activos, muestran una serie de ventajas ya que poseen una alta biocompatibilidad, confieren protección a los activos frente a su degradación, así como una prolongación de la vida media y tiempo de residencia de los mismos; todo esto se traduce en una reducción de la toxicidad y un aumento de la efectividad de los tratamientos.

Los fosfolípidos son el componente principal que les confiere las características fundamentales a los liposomas. Son moléculas en las que el grupo de la cabeza hidrófila y las cadenas de acilo hidrofóbicas están unidas al alcohol. La variación de los grupos de la cabeza, las cadenas hidrofóbicas y los alcoholes conduce a la existencia de una amplia variedad de fosfolípidos.

Existen dos tipos fundamentales de fosfolípidos en función de los alcoholes: glicerofosfolípidos y esfingolípidos. Como se muestra en la figura 11, los glicerofosfolípidos, que son los fosfolípidos principales en las células eucariotas, se refieren a los fosfolípidos en los que el glicerol actúa como nexo de unión. Existen diversos tipos de glicerofosfolípidos en función de modificaciones en el grupo hidrofílico de la cabeza, entre los que destacan fosfatidilcolina, fosfatidiletanolamina o fosfatidilserina, entre otros. Por otro lado, los esfingolípidos forman, también, parte de las membranas celulares, se diferencian de los glicerofosfolípidos en que la esfingosina ocupa el lugar del glicerol y las cadenas hidrófobas suelen ser más largas (77).

La fosfatidilcolina constituye el fosfolípido más ampliamente utilizado en la preparación de liposomas. Se trata de un glicerofosfolípido en el que una molécula de glicerol esterifica un par de cadenas hidrocarbonadas y una molécula de fosfocolina. Esta lecitina puede obtenerse a partir de fuentes naturales o por síntesis química. Es el más utilizado debido a su bajo coste de producción, carga neutra y comportamiento químicamente inerte (78).

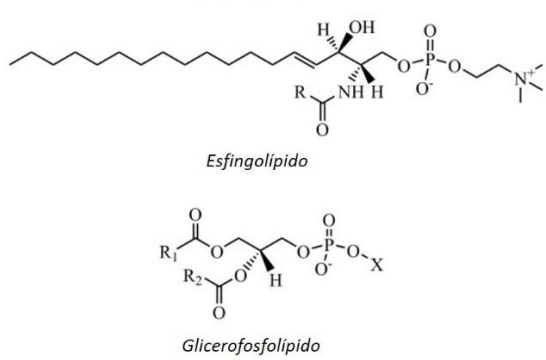

Figura 11. Estructura molecular de los principales tipos de fosfolípidos utilizados en la elaboración de liposomas (78).

Clasificación de los liposomas.

En función del tamaño, carga superficial, contenido en fosfolípidos y métodos de elaboración se pueden obtener diferentes tipos de liposomas. El tamaño de los mismos puede variar desde valores nanométricos a varios micrómetros. Además, pueden estar formados por una o varias bicapas concéntricas. Tanto el tamaño como el número de bicapas afectan a la eficacia de encapsulación de los liposomas. Atendiendo a estas variables, los liposomas se pueden clasificar en dos grandes categorías (figura 12) (79) (80):

- Vesículas multilamelares (MLV): se caracterizan por poseer varias bicapas lipídicas que encierran un número igual de compartimentos acuosos concéntricos. Presentan un tamaño comprendido entre valores nanométricos y 5 µm, así como una baja capacidad de encapsulación. Cuando poseen menos de cuatro capas se denominan oligolamelares y presentan una mejor capacidad de encapsulación.
- Vesículas unilamelares: formadas por una única bicapa fosfolipídica. En función del tamaño que presentan se distinguen dos tipos:
    - Vesículas unilamelares pequeñas (SUV): poseen un tamaño del orden de 25- 50 nm de diámetro y morfología principalmente esférica. Se caracterizan por presentar una distribución homogénea de tamaños; sin embargo, la capacidad de encapsulación de este tipo de vesículas es limitada.
    - Vesículas unilamelares grandes (LUV): de tamaño superior a 100 nm. Presentan ventajas, ya que se caracterizan por

poseer una buena capacidad de encapsulación, sobre todo si se trata de activos hidrosolubles, ya que posee un gran compartimento acuoso.

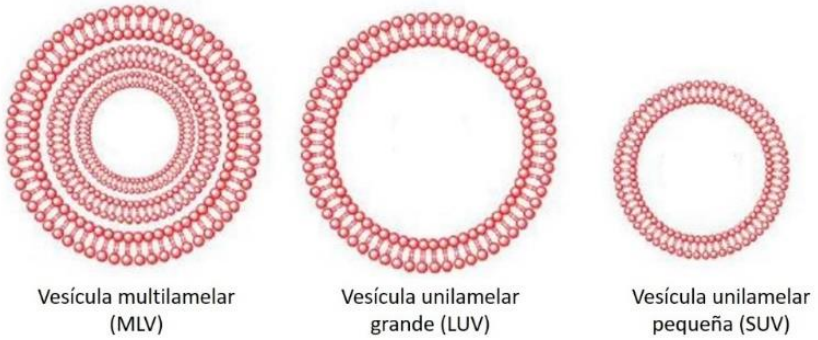

Figura 12. Tipos de liposomas (81)

Métodos de elaboración de los liposomas.

Existen una gran variedad de técnicas para la elaboración de estas vesículas, la elección de una u otra puede ser determinante para la formación de un tipo de vesícula concreto. El objetivo principal de un método de fabricación de liposomas es obtener partículas estables a largo plazo, con una buena distribución de tamaños y alta eficacia de encapsulación de la molécula activa (82).

Uno de los métodos más simples y utilizados es el método de Banghman, es el primer método que se desarrolló para la elaboración de liposomas. Implica la disolución de los fosfolípidos y componentes lipídicos en un solvente orgánico adecuado y la evaporación del mismo permitiendo la formación de una fina película lipídica en el fondo del matraz. A partir de la hidratación con un medio acuoso de la película lipídica se forman

vesículas liposomales. La molécula activa a encapsular se incluye, o bien en el medio acuoso de hidratación si es hidrófila, o bien en la fina película lipídica si es lipófila. Con este método se forman generalmente vesículas multilamelares muy heterogéneas en cuanto a tamaño y número de lamelas, es por ello que normalmente se requieren técnicas adicionales, como la sonicación o extrusión para la formación de vesículas unilamelares más pequeñas que presenten mejores características fisicoquímicas (83) (84).

La evaporación en fase reversa es un método alternativo que implica la hidratación de fosfolípidos (y principio activo si lo hubiere) disueltos en una fase orgánica mediante la adición de un medio acuoso (con el principio activo hidrosoluble). Se produce la formación de micelas invertidas, pequeñas gotas de agua estabilizadas por una monocapa de fosfolípidos dispersos en un exceso de solvente orgánico. Este método requiere una sonicación para la homogenización del sistema y la posterior eliminación del disolvente orgánico, generando la formación de un gel viscoso que da lugar a la formación de la suspensión liposomal. A partir de este método se generan normalmente vesículas multilamelares; sin embargo la utilización de concentraciones bajas de fosfolípidos puede conducir a la formación de vesículas unilamelares grandes (85) (79).

Con el fin de conseguir la formación de vesículas fisicoquímicamente homogéneas y de tamaño adecuado, normalmente es necesario llevar a cabo técnicas adicionales, entre las que destacan la sonicación y extrusión. Ambas llevan a la reducción de tamaño y del número de bicapas de las vesículas previamente formadas. La sonicación implica un gran aporte de energía que conduce a la formación de vesículas unilamelares pequeñas mientras que la extrusión reduce el tamaño de los liposomas y permite la

formación de sistemas homogéneos al forzarlos a pasar a través de un filtro con un tamaño de poro conocido. Para aumentar la capacidad de encapsulación de las vesículas previamente formadas se puede utilizar el método de congelación y calentamiento, basado en someter a las vesículas a ciclos de congelación y calentamiento por inmersión en nitrógeno líquido y posterior calentamiento en un baño termostatizado. Ambas fases deben tener una duración similar y el ciclo se repite un número determinado de veces. El activo a encapsular entra en contacto con la bicapa lipídica en la fase de congelación y al descongelar aumentan las probabilidades para atrapar a las moléculas activas (84).

La técnica de sonicación en sí misma se puede utilizar para la formación de liposomas que presentan un tamaño nanométrico, con una distribución homogénea y alta capacidad de encapsulación. Se puede considerar una técnica alternativa, de gran interés ecológico, ya que obvia el uso de disolventes orgánicos, con las ventajas que ello representa.

Nuevos avances en la formulación de liposomas.

Con el fin de optimizar el sistema de encapsulación y transporte, se han llevado a cabo ciertas modificaciones estructurales para generar nuevos liposomas con propiedades interesantes en el campo de la biomedicina (76). En muchos casos, los liposomas convencionales no tienen la capacidad de penetrar a través de la piel, sino que crean un remanente en las capas más superficiales. En las últimas décadas, se han desarrollado nuevos tipos de vesículas liposomales con el fin de modificar las características fisicoquímicas y funcionales de los liposomas, permitiendo así una liberación de la molécula activa más eficiente.

Se ha demostrado que la elasticidad de la bicapa lipídica de los liposomas es un factor clave para conseguir que el activo penetre a través de la piel en concentraciones suficientes. En este sentido, se han desarrollado unos nuevos sistemas de encapsulación liposomal llamados **transfersomas** o liposomas ultradeformables. Como se muestra en la figura 13, están compuestos por fosfolípidos y por un activador de borde de membrana, generalmente un tensioactivo, como polisorbato o colato, compuesto por moléculas anfifílicas y capaz de intercalarse entre la membrana liposomal. Estos tensioactivos, cuando se encuentran en una concentración superior a la concentración micelar crítica, se organizan en micelas. Cuando interactúan con la bicapa lipídica del liposoma, la estructura formada dependerá de la relación molar de tensioactivo:lípido, de esta manera, a bajas concentraciones de tensioactivo, la estructura liposomal se conserva. Al incluir ambos tipos de moléculas en una vesícula, esta es capaz de desestabilizar sus bicapas lipídicas y aumentar su deformación al disminuir la tensión interfacial sin modificar su estructura de bicapa lipídica (74) (86). Gracias a esta propiedad, los transfersomas son capaces de deformarse para pasar entre las células del estrato córneo y penetrar intactos a través de la piel, alcanzando así estratos más profundos.

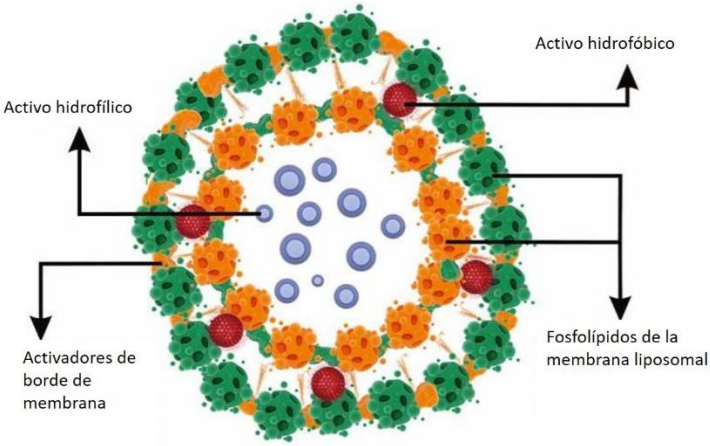

Figura 13. Estructura de un transfersoma o liposoma ultradeformable (86).

Un nuevo enfoque para aumentar la fluidez de la bicapa liposomal está representado por los **glicerosomas**. Son liposomas a los que se les ha incorporado un cierto porcentaje de glicerina (10 – 30 %), un humectante capaz de modificar la fluidez de la bicapa liposomal así como de hidratar la piel. Los glicerosomas son, por lo tanto, sistemas vesiculares flexibles capaces de transportar activos a capas más profundas de la piel (87). En este sentido, Manca et al. demostraron que los glicerosomas son un sistema de transporte interesante para la administración de diclofenaco. Son vesículas de elaboración sencilla que tienen la capacidad de promover la acumulación y permeación del fármaco a través de la piel (88). A su vez, la alta biocompatibilidad de estas nanovesículas las convierte en un sistema de administración tópica prometedor (89) (90).

La eficacia de estas formulaciones puede incrementarse también mediante el uso de material polimérico. En ocasiones, el uso tópico de las formulaciones vesiculares se ve obstaculizado por su estado líquido, que solo permite un breve tiempo de permanencia sobre la piel, debido a que

resbala y desaparece fácilmente del lugar de aplicación. La incorporación de las moléculas activas en un gel puede soslayar estos inconvenientes, sin embargo, este tipo de formulaciones puede reducir la liberación y acumulación del activo en los diferentes estratos de la piel. Como alternativa, se han propuesto vesículas de fosfolípidos o liposomas con un núcleo de gel como herramienta innovadora para la administración tópica de activos (91); en este sentido, el ácido hialurónico es un polímero idóneo para ello, ya que es soluble en agua y, a pH superior a 3, sus cadenas ácidas se ionizan formando fuertes interacciones intermoleculares, con el consiguiente desarrollo de una red estructurada de propiedades viscoelásticas interesantes, los **hialurosomas**. A su vez, el ácido hialurónico es un polímero altamente biocompatible y tiene un papel importante en la captación de agua y la cicatrización de las heridas de la piel. Es por ello que se convierte en un candidato muy atractivo para la formulación de sistemas de liberación de activos a través de la piel (92) (93) (94) (95).

OBJETIVOS

El objetivo principal es el diseño, elaboración y caracterización de diferentes tipos de liposomas, de tamaño nanométrico, que sirvan como vehículo de sustancias naturales destinadas al tratamiento coadyuvante de diversas patologías de la piel.

MATERIALES Y MÉTODOS

Elaboración de las vesículas.

La elaboración de los transfersomas, glicerosomas, hialurosomas o glicerohialurosomas se efectuó de manera similar; en primer lugar, fue necesario establecer la formulación que más se adecua al fin previsto, para ello se realizaron diversos estudios de preformulación. En cada caso, una solución acuosa adecuada se utilizó para hidratar la mezcla de fosfolípido y polisorbato; se agregaron diferentes concentraciones de baicalina, berberina o finasterida, según corresponda, y las dispersiones obtenidas se sometieron a un proceso de sonicación durante un periodo de tiempo estipulado. Finalmente, pasaron por un proceso de extrusión, en el que la suspensión es forzada a atravesar un filtro de policarbonato de 200 nm de tamaño de poro con el fin de mejorar la homogeneidad de tamaños de la preparación liposomal.

Caracterización de las vesículas.

Con el fin de confirmar la formación de liposomas y definir su morfología, las preparaciones se observaron mediante microscopía electrónica de transmisión (TEM) y microscopía electrónica de transmisión criogénica (Crio-TEM). Para el análisis de las vesículas mediante TEM, se utiliza un microscopio electrónico de transmisión (modelo JEOL 1010®, Francia); para ello las muestras se tiñen con ácido fosfotúngstico y la observación se lleva a cabo a un voltaje de aceleración de 60 kV mediante una cámara digital MegaView III. En el caso de crio-TEM, se forma una delgada película acuosa colocando una gota de muestra a analizar en una rejilla de carbón perforada con descarga luminosa. La película se vitrifica sumergiendo la rejilla en etano usando un Vitrobot. Las películas vítreas se transfirieren a un Tecnai F20 TEM y las muestras se observan en un modo de dosis baja a

200 kV y a una temperatura de ~ -173 °C. Los liposomas ultradeformables, o transfersomas, se observaron mediante TEM, mientras que los glicerosomas, hialurosomas y glicerohialurosomas se analizaron por crio-TEM.

A su vez, el diámetro medio, índice de polidispersidad y potencial Z que presentan las formulaciones elaboradas se midieron mediante una técnica por espectroscopía de difracción de luz láser conocida como "Dynamic Light Scattering" (DLS) utilizando un Zetasizer nano-S (Malvern Instruments, Worcestershire, Reino Unido).

La eficiencia de encapsulación (EE) de las nanovesículas se determinó mediante el método de diálisis; en este procedimiento se lleva a cabo una diálisis en medio acuoso, de manera que la proporción de principio activo que no se ha encapsulado atraviesa la membrana y difunde al medio de diálisis. La EE se expresa como el porcentaje de principio activo recuperado después de la diálisis frente a la cantidad utilizada inicialmente; para ello, tras el proceso de diálisis, se rompen las vesículas no dializadas, con Triton X-100 (10 %) o metanol (1:100), y se cuantifica el principio activo encapsulado mediante Cromatografía Liquida de Alta Eficacia (CLAE).

Método analítico.

La cuantificación de activos mediante Cromatografía Liquida de Alta Eficacia (CLAE) se llevó a cabo utilizando un Perkin Elmer® Series 200 equipado con un detector UV. La detección de baicalina tuvo lugar a 278 nm, utilizando como fase móvil una mezcla de agua y metanol (30:70) impulsada a 1 mL/min de manera isocrática. Para la detección de la berberina se utilizó una fase móvil compuesta de una mezcla de agua y

metanol (50:50) a un flujo de 1.2 mL/min y la detección se llevó a cabo a 346 nm.

Ensayos de permeabilidad cutánea.

El ensayo se realizó con células verticales de difusión "tipo Franz". Para ello, en el compartimento dador se añadió la formulación a ensayar y en el receptor una solución acuosa de polisorbato 80 (1%, p/V). Entre ambos compartimentos se interpuso la epidermis completa, obtenida mediante el método de separación por calor; para ello, la piel se sumergió en un baño de agua destilada a 60 °C y se mantuvo durante 90 segundos, la alta temperatura provoca un debilitamiento en las uniones existentes entre la dermis y la epidermis, favoreciendo así su separación. La célula completa se introdujo en un baño termostatado a 37 ° C y se mantuvo en constante agitación. Se tomaron muestras y se repuso el mismo volumen a distintos intervalos de tiempo. Finalmente se cuantificaron mediante CLAE. Para verificar la integridad de la epidermis, se aplicó 1 mL de solución de rojo fenol en la superficie de la piel.

Citotoxicidad de las formulaciones.

Con el fin de evaluar la viabilidad celular se utilizó el ensayo colorimétrico MTT (reducción metabólica del Bromuro de 3 (4,5-dimetiltiazolil-2) -2,5-difeniltetrazolio). En la presente Memoria se ensayó la citotoxicidad de las formulaciones propuestas en las siguientes líneas celulares, según corresponda:

- Fibroblastos de ratón – NIH-3T3
- Queratinocitos humanos inmortalizados - HaCaT
- Melanocitos humanos hiperpigmentados - HEMa

- Células de papila dérmica de folículo piloso humanas - HFDPC

Para llevar a cabo el análisis se sembraron las células correspondientes en placas de 96 pocillos y se cultivaron durante 24 h. Transcurrido ese tiempo se expusieron a las formulaciones, diluidas convenientemente con el medio de cultivo adecuado a cada tipo celular, con el fin de obtener una batería de concentraciones del producto natural a ensayar, durante 24 horas. Posteriormente se añadió una solución de MTT a cada pocillo y tras 3 horas de incubación, los cristales de formazán formados se disolvieron con dimetilsulfóxido (DMSO) con objeto de determinar el número de células vivas a través de la medición de la absorbancia a 570 nm. Los resultados se muestran como un porcentaje en comparación a las células control no tratadas (100 % de viabilidad).

Evaluación *in vivo* de la eficacia frente a la inflamación asociada a psoriasis.

La aplicación de TPA (12-O-Tetradecanoylphorbol 13-acetate) en ratones para inducir respuesta inflamatoria es uno de los modelos más comunes para la evaluación de la eficacia antiinflamatoria. El TPA induce una variedad de cambios histológicos y bioquímicos en la piel como infiltración de neutrófilos, hiperplasia epidérmica, aumento de los niveles de IL-1, etc. Para llevar a cabo este procedimiento (código del procedimiento: 2016/VSC/PEA/00112 tipo 2) es necesario inducir inflamación y ulceración tópica mediante la aplicación de TPA disuelto en acetona (243 µM) en la espalda de ratones CD-1 previamente afeitada. Tras 3 horas de la aplicación de TPA se aplicó en la misma zona las nanoformulaciones de baicalina a ensayar, dexametasona como control positivo o acetona como control negativo mediante condiciones no oclusivas. El protocolo se repitió durante 3 días. En el cuarto día los ratones se sacrificaron mediante

dislocación cervical y la piel tratada se extirpó con el fin de evaluar el edema y la inhibición de la actividad de la mieloperoxidasa, como un marcador del proceso inflamatorio; para ello, se homogenizaron las biopsias de la piel en tampón fosfato de sodio (pH 5.4) con bromuro de hexadeciltrimetilamonio al 0.5 % mediante un homogenizador Ultra-Turrax T25, la dispersión se centrifugó a 10.000 g durante 15 minutos a 1 °C y el sobrenadante obtenido se incubó durante 5 minutos a 37 °C con una mezcla de tampón fosfato de sodio (pH 5.4), tampón fosfato salino (pH 7.4) y peróxido de hidrógeno. Se añadió diclorhidrato de 3,30,5,50-tetrametilbencidina para inciar la reacción, la cual se detuvo a los 10 minutos usando acetato de sodio; la absorbancia de la solución final se midió a 620 nm. Para los ensayos histológicos, las muestras de piel se fijaron en formaldehído al 10 % y se analizaron con un microscopio óptico, después de haber teñido la piel con hematoxilina y eosina.

Evaluación *in vitro* de la eficacia frente al vitíligo.

Capacidad antioxidante *in vitro.*

Para evaluar la capacidad antioxidante de las nanoformulaciones de baicalina y/o berberina se utilizaron fibroblastos. Para ello, se indujo un daño oxidativo sometiendo a las células a peróxido de hidrógeno. Las células se sembraron en placas de 96 pocillos y tras 24 horas de incubación se expusieron simultáneamente a una dilución adecuada de peróxido de hidrógeno y concentraciones no citotóxicas de las formulaciones propuestas. Tras 4 horas, las células se lavaron con PBS y se determinó la viabilidad celular mediante el ensayo MTT, evaluando así el efecto protector de las formulaciones frente a la muerte celular causada por el estrés oxidativo. Las células expuestas al peróxido de hidrógeno que no fueron tratadas posteriormente con las formulaciones propuestas se

utilizaron como control positivo mientras que las células no tratadas ni sometidas a daño oxidativo se consideraron control negativo, con un 100 % de viabilidad.

Efecto fotoprotector *in vitro.*

El efecto fotoprotector de las diferentes formulaciones de baicalina y/o berberina se evaluó sometiendo a las células a una intensidad de radiación UV que produce un 50 % de la muerte celular. Para ello, inicialmente se determinó dicha intensidad en las diferentes líneas celulares, realizando un ensayo dosis – respuesta frente a varias intensidades de luz UV; se utilizaron queratinocitos y fibroblastos y se sembraron en placas de 96 pocillos, una vez alcanzaron la confluencia se irradiaron con luz UV (310 nm) a varias intensidades (100, 200, 400, 600, 800 y 1000 mJ / cm^2) usando una Cámara Crosslinker Bio-Link BLX 254 (5 × 8 W; Peqlab Biotechnologie GmbH, Erlangen, Alemania). Tras 24 horas, se realizó el ensayo de MTT para determinar el efecto de la irradiación con luz UV en comparación con células control no irradiadas (100 % de viabilidad). Una vez determinada la intensidad de radiación que causó el 50 % de muerte celular, los queratinocitos y fibroblastos se sembraron en placas de 96 pocillos y, tras 24 horas de incubación, se trataron con las diferentes formulaciones a ensayar a diferentes concentraciones no citotóxicas; una vez transcurrido el tratamiento, las células se irradiaron con la intensidad de luz UV adecuada, obtenida inicialmente. Tras 24 horas se determinó el efecto fotoprotector de las formulaciones, comparando la viabilidad de las células irradiadas con luz UV y tratadas con las diferentes formulaciones frente al control irradiado con luz UV y no tratado. Los resultados se muestran como porcentaje de fotoprotección en comparación con las células no tratadas (0 % de fotoprotección).

Análisis de la capacidad hiperpigmentante *in vitro.*

La capacidad de las formulaciones de baicalina y/o berberina de estimular la melanogénesis y la actividad de la tirosinasa se evaluó *in vitro* mediante cultivos de melanocitos.

Los melanocitos se sembraron en placas de 6 pocillos y se trataron, una vez alcanzada la confluencia, con concentraciones no citotóxicas de las diferentes formulaciones a ensayar. Una vez finalizado el tratamiento, transcurridas 48 horas, se lavaron las células con PBS y se despegaron de las placas con Tripsina/EDTA; tras un proceso de centrifugación, el sedimento celular se disolvió en hidróxido de sodio (NaOH) (1 N) y se incubó a 60 °C durante 1 hora. La cantidad de melanina se determinó mediante la medición de absorbancia a 470 nm usando un lector de microplacas (Multiskan EX, Thermo Fisher Scientific, Inc., Waltham, MA, EE. UU.). Los resultados se expresan como **porcentaje del contenido de melanina** respecto al que contienen las células no tratadas (100 % de melanina).

Para corroborar la vía implicada en la estimulación de la producción de melanina se determinó la actividad de la tirosinasa, ya que se considera la enzima clave en el proceso de síntesis de melanina.

La **actividad de tirosinasa** se estimó espectrofotométricamente utilizando L-DOPA como sustrato. Se sembraron los melanocitos en placas de 6 pocillos y se incubaron a 37 °C con 5 % de CO_2. Una vez se alcanzó la confluencia se trataron las células durante 48 horas con concentraciones no citotóxicas de las diferentes formulaciones propuestas. Al finalizar el tratamiento, las células se trataron con una solución tamponada de fosfato de sodio (0.1 M, pH 6.8) que contenía Triton X-100 al 1 % y se

sometieron a repetidos ciclos de congelación / descongelación a -20 °C durante 30 min. Los lisados se centrifugaron a 10.000 g durante 15 minutos y 90 µL de cada lisado se sembró en una placa de 96 pocillos y se añadió L-DOPA (10 µL, 10 mM). Después de la incubación a 37 °C en oscuridad durante 90 minutos, se midió la absorbancia por espectrofotometría a 475 nm utilizando un lector de microplacas (Multiskan EX, Thermo Fisher Scientific, Inc., Waltham, MA, EE. UU.). Los resultados se muestran como porcentaje de actividad de la enzima tirosinasa en comparación con el de las células no tratadas (100% de actividad).

Evaluación *in vitro* e *in vivo* de la eficacia frente a la alopecia androgénica.

Determinación del potencial estimulante del crecimiento del cabello *in vitro.*

Las células de la papila dérmica son las más utilizadas en modelos *in vitro* relacionados con el cabello, ya que se consideran células clave en la morfogénesis y la regeneración del crecimiento capilar, son las encargadas de regular el desarrollo y crecimiento de folículo piloso.

En la presente Memoria, las células de la papila dérmica se trataron con concentraciones no citotóxicas de diferentes formulaciones de finasterida y baicalina, con objeto de evaluar el efecto de las mismas sobre la proliferación de las células implicadas en el crecimiento capilar. Tras el tratamiento, la viabilidad celular se determinó mediante el ensayo colorimétrico de MTT. Transcurridas 3 horas, los cristales de formazán se disolvieron en DMSO y la reacción se midió espectroscópicamente a 570 nm con un lector de placas (Multiskan EX, Thermo Fisher Scientific, Inc.,

Waltham, MA, US). Los resultados se expresaron como porcentaje de proliferación celular en comparación con células control no tratadas (100 % de viabilidad).

Efecto promotor del crecimiento del cabello *in vivo.*

Para determinar la efectividad de las nanoformulaciones de baicalina y finasterida se realizaron estudios *in vivo* utilizando ratones C57BL / 6, ya que representan un modelo ideal que evita fluctuaciones en los resultados (código del procedimiento: 2019/VSC/PEA/0113 tipo 2). En estos animales, la morfogénesis del folículo piloso y el ciclo de crecimiento siguen un patrón establecido. Los experimentos *in vivo* se basaron en el modelo estandarizado del ciclo del folículo piloso inducido por depilación (96).

Se utilizaron ratones hembra sanos C57BL / 6 de seis semanas de edad (18-20 g). Los ratones se dividieron en 10 grupos (n = 5 por grupo) y los pelos, en fase telógena, del área dorsal se depilaron 24 h antes del tratamiento. El día 1, se aplicó tópicamente 100 µL de las formulaciones a ensayar en la zona dorsal depilada, en condiciones no oclusivas. El procedimiento se repitió una vez al día durante 21 días. El último día, los ratones fueron sacrificados por dislocación cervical. Durante el período de aplicación, se verificaron las diferencias entre los grupos tratados y no tratados en términos de peso corporal promedio o presencia de anomalías.

La pigmentación de la piel se considera como evidencia del crecimiento del cabello, ya que presenta color rosa brillante en la fase telógena (reposo) y se vuelve gris o negro en la fase anágena (crecimiento) (97). La longitud del cabello se midió los días 12, 16 y 21 a partir del promedio de la longitud de 10 pelos de la misma zona de los ratones de cada grupo; a

su vez, se determinó la fase de los folículos pilosos (anágena y telógena) utilizando un micrómetro ocular. El efecto promotor de los diferentes tratamientos se analizó como un indicador de la capacidad de las nanoformulaciones para mejorar el crecimiento del cabello en comparación con el grupo no tratado.

Al finalizar el experimento, las muestras de piel de los ratones de los diferentes grupos se incluyeron en parafina. Las secciones transversales (5 µm) se tiñeron con hematoxilina y eosina y se observaron con un microscopio óptico (Leica DM3000, Leica-Microsystems, Wetzlar, Alemania). El número y el diámetro de los folículos en los diferentes grupos también se midieron a través de Image Pro plus 7.0, Media Cybernetics.

CAPÍTULO 1

Inhibition of skin inflammation by baicalin ultradeformable vesicles.

Silvia Mir-Palomo[a,*], Amparo Nácher[a,b], Octavio Díez-Sales[a,b], M. A. Ofelia Vila Busó[c], Carla Caddeo[d], Maria Letizia Manca[d], Maria Manconi[d], Anna Maria Fadda[d], Amparo Ruiz Saurí[e].

[a] *Dept. Pharmacy and Pharmaceutical Technology, Faculty of Pharmacy, University of Valencia, Spain*

[b] *Institute of Molecular Recognition and Technological Development, Inter-Universitary Institute from Polytechnic University of Valencia and University of Valencia, Spain*

[c] *Dept. Physics and Chemistry, Faculty of Pharmacy, University of Valencia, Spain*

[d] *Dept. Farmaco Chimico Tecnologico, University of Cagliari, Cagliari 09124, Italy*

[e] *Dept. of Pathology, University of Valencia, Avda Blasco Ibañez 17, 46010 Valencia, Spain*

International Journal of Pharmaceutics 511 (2016) 23–29.

doi: 10.1016/j.ijpharm.2016.06.136

Abstract.

The topical efficacy of baicalin, a natural flavonoid isolated from *Scutellaria baicalensis Georgi*, which has several beneficial properties, such as antioxidative, antiviral, anti-inflammatory and antiproliferative, is hindered by its poor aqueous solubility and low skin permeability. Therefore, its incorporation into appropriate phospholipid vesicles could be a useful tool to improve its local activity. To this purpose, baicalin at increasing concentrations up to saturation, was incorporated in ultradeformable vesicles, which were small in size (~67 nm), monodispersed (PI<0.19) and biocompatible, regardless of the concentration of baicalin, as confirmed by *in vitro* studies using fibroblasts. On the other hand, transdermal flux through human epidermis was concentration dependent. The *in vivo* results showed the significant anti-inflammatory activity of baicalin loaded nanovesicles irrespective of the concentration used, as they were able to reduce the skin damage induced by the phorbol ester (TPA) application, even in comparison with dexamethasone, a synthetic drug with anti-inflammatory properties. Overall results indicate that ultradeformable vesicles are promising nanosystems for the improvement of cutaneous delivery of baicalin in the treatment of skin inflammation.

Keywords: baicalin, ultradeformable vesicles, skin, mice, topical delivery.

Introduction.

Baicalin (7-glucuronic acid 5, 6-dihydroxyflavone), is one of the most abundant flavonoid in the root of *Scutellaria baicalensis Georgi,* used as medical agent in traditional Chinese medicine thanks to its multiple therapeutic benefits. Indeed, it has shown strong anti-inflammatory (Chen et al., 2001) and anti-oxidant properties (Shi et al., 2015), as well as antimicrobial and antifungal activities (Shi et al., 2014) and a great potential to prevent and inhibit tumor (Chen et al., 2016). Further, baicalin is able to protect the skin from damages caused by exposure to solar ultraviolet (UV) radiations. Considering all the protective and beneficial effects and its low toxicity, baicalin can be considered a suitable molecule for eliminating causes and effects of skin aging and injuries, including UV radiation damages, wounds and burns (J. Zhang et al., 2014). Despite these promising properties, baicalin efficacy and actual use in topical formulations are hampered by its lipophilic nature and consequent low water solubility, which account for a poor bioavailability (Xing et al., 2005). To overcome this problem, baicalin has been loaded in different nanocarriers (Shi-Ying et al., 2014) (Zhang et al., 2014) for systemic, brain, corneal delivery and tumor targeting (Chen et al., 2016). In other studies, nanocarriers have been used to achieve effective transdermal delivery. Unfortunately, the barrier nature of the stratum corneum represents an important obstacle to drug accumulation into and passage through the skin, not only for conventional dosage forms, but also for some innovative dosage systems. To this purpose, several techniques or systems have been tested and the most widely studied approach in the last decades is the use of lipid nanocarriers, such as phospholipid vesicles and derived systems: ethosomes, glycerosomes and hyalurosomes (Manca et al., 2015) (Castangia et al., 2013). Their use for skin delivery can offer some

advantages over classical topical dosage forms, and some specially designed vesicular carriers can be able to efficiently increase drug penetration and permeation through the skin. Although there are several studies on the incorporation of baicalin in liposomes (Wei et al., 2014), only a few studies specifically addressed the enhancement of baicalin efficacy following application on the skin. Hence, alternative phospholipid vesicles can result in a greater improvement of its therapeutic index and effectiveness in skin protection.

In light of this, in the present study, baicalin was incorporated in ultradeformable liposomes made with a mixture of soy lecithin and polysorbate 80, used as edge activator to improve bilayer fluidity. Thanks to this property, vesicles can squeeze themselves between the cells in the stratum corneum driven by the hydration gradient and reaching deeper skin strata. In addition, considering that drug saturation may improve its thermodynamic activity, maximizing the flux through biological membranes, irrespective of the selected vehicle and the drug solubility, baicalin was incorporated into ultradeformable vesicles at increasing amounts up to the maximum possible concentration (2.5, 5 and 10 mg/mL) which is supposed to saturate the system. Vesicle morphology, size distribution, zeta potential, and entrapment efficiency were evaluated, as well as the ability of the vesicles to promote *in vitro* baicalin skin delivery. The cytotoxic effect of empty and baicalin loaded vesicles was evaluated in 3T3 mouse fibroblasts. The drug and carrier performances and their ability to reduce oxidative inflammation and neutrophil infiltration induced by TPA in mice were studied, as well. To detect the damages induced by TPA on the skin and the effect provided by the tested formulations, a histological evaluation was also carried out.

Materials and methods.

Materials.

Lipoid® S75, a mixture of soybean lecithin containing phosphatidylcholine (70%) and phosphatidylethanolamine (10%), lysophosphatidylcholine (3% maximum), triglycerides (3% maximum), fatty acids (0.5% maximum), tocopherol (0.1–0.2%) was a gift from Lipoid GmbH (Ludwigshafen, Germany). Polysorbate 80 and disodium phosphate were purchased from Scharlab S.L. (Barcelona, Spain). Monosodium phosphate was purchased from Panreac quimica S.A. (Barcelona, Spain). Dexamethasone 21-sodium phosphate (DEX) was from Acofarma S.A. (Madrid, Spain) and the DEX solution (2 µg/mL) was prepared in buffer solution (pH 7.4). Baicalin (BA) was purchased by Cymit química S.L. (Barcelona, Spain) and saturated solution was prepared.

Vesicle preparation.

Samples were prepared weighing Lipoid® S75 (180 mg/mL), polysorbate 80 (2.5 mg/mL) and BA (2.5, 5 and 10 mg/mL) in a glass vial and hydrating them overnight with a buffer solution (pH 7.4) composed by a mixture of monosodium phosphate (0.3 %) and disodium phosphate (2.9 %). Then, the dispersion was sonicated for 3 min with a CY-500 ultrasonic disintegrator (Optic Ivymen system, Barcelona, Spain) to obtain clear opalescent dispersions. To achieve a uniform particle size distribution, the liposomal suspension was extruded with an Avanti® Mini-Extruder (Avanti Polar Lipids, Alabaster, Alabama) through a 200 nm membrane (Whatman, GE Healthcare, Fairfield, Connecticut, US) (Manconi et al., 2003). Empty liposomes were prepared as reference.

Analytical method.

The BA content was quantified using a Perkin Elmer® Series 200 HPLC equipped with a UV detector and a column Teknokroma® Brisa "LC2" C18, 5.0 µm (150 cm × 4.6 mm). The mobile phase consisted of a mixture of water and methanol (30:70), delivered at a flow rate of 1 mL/min. BA content was measured at 278 nm. The limit of detection and quantification for the BA was 0.45 µg/mL and 1.36 µg/mL, respectively.

Vesicle characterization.

The formation and morphology of ultradeformable liposomes were checked by transmission electron microscopy (TEM) using a JEM-1010 microscope (Jeol Europe, Croissy-sur-Seine, France), equipped with a digital camera MegaView III at an accelerating voltage of 80 kV. Vesicles were examined using a negative staining technique: non-diluted dispersions were stained with 1% phosphotungstic acid on a carbon grid and examined/visualized.

The average diameter and polydispersity index (PI) of non-diluted samples were determined by Photon Correlation Spectroscopy using a Zetasizer nano-S (Malvern Instruments, Worcestershire, United Kingdom). Zeta potential was estimated using the Zetasizer nano-S by electrophoretic light scattering, which measures the particle electrophoretic mobility in a thermostated cell. Vesicles were purified from non-incorporated BA by dialysis. Each sample (1 mL) was loaded into Spectra/Por® tubing (12–14 kDa MW cut-off; Spectrum Laboratories Inc., DG Breda, The Netherlands) and dialyzed against buffer (1 L) for 2 h, at room temperature. Both non-dialyzed and dialyzed samples were disrupted with methanol (1:100) and assayed by HPLC to quantify the BA content in the vesicular systems. The

drug entrapment efficiency (EE %) of the three systems was calculated as follows (Eq. 1):

$$EE\ (\%) = \left(\frac{actual\ BA}{initial\ BA}\right) x100 \qquad \text{(Eq.1)}$$

where *actual BA* is the amount of BA in vesicles after dialysis, and *initial BA* is the amount of drug before dialysis, as calculated by HPLC.

Cell culture.

3T3 mouse fibroblasts (ATCC, Manassas, VA, USA) were cultured in Dulbecco's modified Eagle's medium (Sigma Aldrich, Spain), supplemented with 10% (v/v) foetal bovine serum, penicillin (100 U/mL), and streptomycin (100 µg/mL) (Sigma Aldrich, Spain) in 5% CO_2 incubator at 37°C to maintain exponential cell growth.

Cell viability studies.

3T3 cells were seeded in 96-well plates with cell density being approximately $5x10^5$ cells/well, at passages 11-12. After 24 h of incubation, 3T3 cells were treated for 2, 4, 8 and 24 h with ultradeformable vesicles, empty or loaded with BA at different concentrations: 2.5 BA (2.5 mg/mL), 5 BA (5 mg/mL) and 10 BA (10 mg/mL) or BA saturated solution (25µL of formulation in 250 µL of medium). Cell viability was determined by the MTT [3(4,5-dimethylthiazolyl-2)-2,5-diphenyltetrazolium bromide] colorimetric assay. Briefly, 200 µL of MTT reagent (0.5 mg/mL in PBS) was added to each well and after 2 h the formed formazan crystals were dissolved in DMSO. The reaction was spectrophotometrically measured at 570 nm with a microplate reader (Multiskan EX, Thermo Fisher Scientific, Inc., Waltham, Massachusetts, United States). All experiments were

repeated at least three times, each time in triplicate. Results are shown as percentage of cell viability in comparison with non-treated control cells (100% viability) (Eq. 2):

$$Cell\ Viability\ (\%) = \left(\frac{Absorbance_{sample}}{Absorbance_{control}}\right) x100 \text{ (Eq.2)}$$

where $Absorbance_{sample}$ is the absorbance of fibroblasts treated with the vesicular formulation and $Absorbance_{control}$ is the absorbance of non-treated cells, at 570 nm.

Skin permeation studies.

Permeation experiments were performed on Caucasian abdominal skin samples obtained from three randomly assigned female donors aged 38–48 years who had undergone cosmetic surgical procedures in the Hospital Clínico Universitario (Valencia, Spain). Informed consent was previously obtained from the patients, and their identity was masked to the researchers to guarantee their anonymity. Excess of fatty and connective tissues was removed, and the samples (full thickness skin) were stored at −40°C for no more than 1 month.

Experiments were performed non-occlusively by means of vertical Franz cells (effective diffusion area of 0.784 cm^2), using epidermis from human skin (Díez-Sales et al., 2005). Epidermis was sandwiched securely between donor and receptor compartments of the Franz cells, with the stratum corneum side facing the donor compartment (Manconi et al., 2012). The receptor compartment was filled with 6 mL of buffer solution (pH 7.4), which was continuously stirred with a small magnetic bar and thermostated (~37°C) throughout the experiments to reach the physiological skin temperature (~32°C). The different formulations (200

µL) were applied on the epidermis surface and at different time intervals, over 24 h, receptor solutions were withdrawn and analysed for BA content by HPLC (as described in Section 2.3). Finally, in order to check the integrity of the epidermis, 1 mL of phenol red solution (0.5 mg/mL) was applied in the donor compartment.

The cumulative amounts (Q) of drug permeated per cm^2 of skin were plotted against time, and the equation derived from the application of the Fick's Second Law to the diffusion process was fitted to the data (Eq. 4):

$$Q_{(t)} = A \cdot P \cdot L \cdot C \left[D \cdot \frac{t}{L^2} - \frac{1}{6} - \frac{2}{x^2} \cdot \sum_{n=1}^{\infty} \cdot Exp\left(\frac{-D \cdot n^2 \cdot x^2 \cdot t}{L^2} \right) \right] \qquad \text{(Eq. 4)}$$

where *Q (t)* is the quantity of BA passing across the skin and reaching the receptor solution at a given time, *t*; *A* is the actual diffusion surface area (0.784 cm^2); *P* is the partition coefficient of the permeant between the skin and the donor vehicle; *L* is the diffusion pathway; *D* is the diffusion coefficient of the permeant in the membrane; and *C* is the concentration of the permeant in the donor solution. The fitting procedures were carried out by means of nonlinear regression using Sigma Plot 10.0 (Pharsight corp, USA).

By fitting the equation 4, lag time (t_L, h) corresponding to $L^2/6D$ and the permeability coefficient ($Kp = P \cdot D/L$) were calculated. The flux values (*J*) were obtained by employing the expression: $J = Kp \cdot C$.

In vivo experimental design.

Female CD-1 mice (5-6 weeks old, 25-35 g) were bred in the animal facility of the Faculty of Pharmacy of the University of Valencia. All studies were performed in accordance with European Union regulations for the handling and use of laboratory animals and the protocols were approved

by the Institutional Animal Care and Use Committee of the University of Valencia (code A1456917886577). The back skin of mice was shaved one day before the experiment, and only animals showing no hair re-growth were selected for tests. On day 1, cutaneous inflammation was induced by applying on the shaved dorsal area (~2 cm^2) 20 µL of TPA dissolved in acetone (243 µM). After 3 h, empty or BA (2.5, 5 and 10 mg/mL) loaded liposomes, or BA saturated solution, or DEX solution (100 µL each) were topically smeared over the same dorsal site (non-occlusive conditions). The procedure was repeated on day 2 and 3. On day 4, mice were sacrificed by cervical dislocation. Each group comprised four mice.

In vivo inflammatory: myeloperoxidase determination.

After 72 h of treatment (on day 4), mice were sacrificed and the treated skin area was excised and immediately stored at −80°C (De Young et al., 1989) (Caddeo et al., 2013). The myeloperoxidase (MPO) activity was measured. The biopsies were dispersed in 750 µL of sodium phosphate buffer 80 mM (pH 5.4) containing 0.5% hexadecyltrimethylammonium bromide and homogenized in ice bath with an Ultra-Turrax® T25 homogenizer (IKA® Werke GmbH & Co. KG, Staufen, Germany). The dispersions were centrifuged at 10.000 rpm for 15 min at 1°C and the obtained supernatant (25 µL) was added to 75 µL saline phosphate buffer (pH 7.4), 10 µL sodium phosphate buffer (pH 5.4), 10 µL of 0.026% hydrogen peroxide and incubated at 37°C for 5 min. Then, 10 µL of 18 mM 3,3',5,5'-tetramethylbenzidine dihydrochloride hydrate in 8% aqueous N,N-dimethylformamide was added to start the reaction. After 10 min of incubation, the reaction was stopped with the addition of 15 µL of 1.5 M sodium acetate (pH 3.0), and the absorbance recorded at 620 nm using a microplate reader (Multiskan EX, Thermo Fisher Scientific, Inc., Waltham,

Massachusetts, United States). The MPO activity was calculated from the linear portion of a standard curve.

Histological examination.

Mice skin treated with the tested formulations was excised, fixed and stored in formaldehyde (10%). Tissue specimens were processed routinely and embedded in paraffin wax. Longitudinal sections (5 µm) were stained with haematoxylin and eosin (H&E) and observed by light microscope (DMD 108 DIGITAL Microimaging Device, Leica, Wetzlar, Germany).

Statistical analysis of data.

Data are shown as mean ± standard deviation. Statistical differences were determined by using one-way ANOVA test and Tukey´s test for multiple comparisons with a significance level of $P<0.05$. All statistical analyses were performed using IBM SPSS statistics 22 for Windows (Valencia, Spain).

Results and discussion.

BA is a flavonoid isolated from the dried roots of *Scutellaria baicalensis Georgi*. More precisely, it is a glycoside flavones formed by a benzene ring condensed with a six-member pyrone ring, which in the 2-position carries a phenyl benzene ring as a substituent (Figure 1). Taking into account its low skin bioavailability along with the beneficial effects on skin protection, and the lack of studies focusing on its topical delivery using innovative phospholipid vesicles, in the present work BA was incorporated in ultradeformable vesicles at increasing concentrations. Aiming at optimizing the formulation of ultradeformable vesicles, a preformulation study was carried out increasing the amount of BA loaded, so as to reach

the critical/maximum concentration (10 mg/mL) without affecting the main physico-chemical characteristics of the vesicles: small, homogenous size, and high stability. It was found that above such concentration, the vesicles were large and highly polydispersed, and aggregation and BA precipitation occurred in a short time. Hence, 2.5, 5 and 10 mg/mL were selected as the concentrations to be used for further studies.

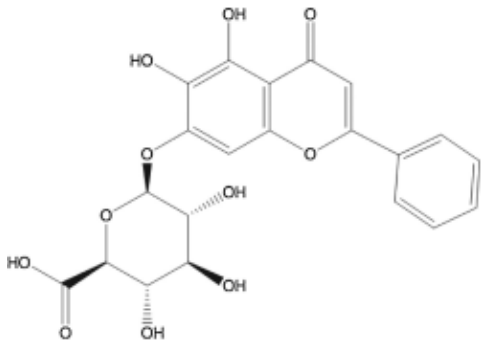

Figure 1. Chemical structure of Baicalin (BA).

Vesicle characterization.

TEM images provided evidence of vesicle formation, and showed that they were small, fairly spherical and multilamellar vesicles, regardless of the BA concentration (Figure 2).

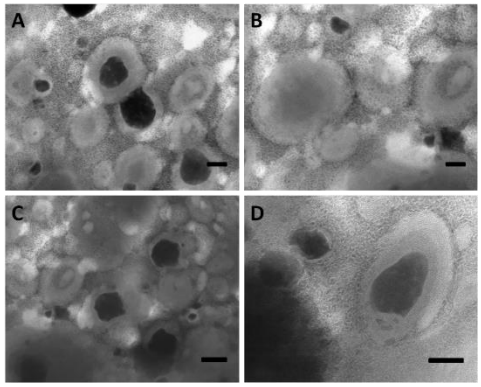

Figure 2. Representative TEM micrographs of ultradeformable vesicles loading BA: 2.5 BA (A and D), 5 BA (B) and 10 BA (C). Each bar corresponds to 100 nm.

Empty ultradeformable vesicles were small in size, around 82 nm (Table 1), and the incorporation of BA, whatever the concentration, led to a slight decrease of the mean diameter, from ~82 to ~67 nm, probably because the lipophilic BA interacts with the phospholipid chains, modifying their packing and permitting a reduction of the bilayer curvature. All the formulations were monodispersed (PI<0.19) and Photon Correlation Spectroscopy results were always repeatable, as indicated by the small standard deviations obtained from at least three repetitions (Table 1). The zeta potential was highly negative (≈−30 mV), irrespective of BA concentration. Ultradeformable vesicles were purified from the non-incorporated drug by dialysis for 2 h, which was long enough to eliminate the free drug. Ultradeformable vesicles were able to incorporate BA in good yields, as the entrapment efficiency value was ~80%, without differences among the groups (P>0.05). Physico-chemical properties of vesicles were very similar and were not affected by the different

concentrations of BA, confirming that even at the highest concentration (10 mg/mL), the flavonoid was optimally incorporated in vesicle structure ensuring the system saturation.

Table 1. Average size, polydispersity index (PI), zeta potential (ZP) and BA entrapment efficiency (EE, %) of empty ultradeformable vesicles and the same vesicles loading BA 2.5, 5 and 10 mg/ml (2.5 BA, 5 BA, 10 BA). Each value is the mean ± SD (n=4).

Sample	Sample size (nm)		PI		Z Potential (mV)		EE (%)
	Initial	30 days	Initial	30 days	Initial	30 days	
Empty vesicles	82.50 ±1.03	79.89 ±1.09	0.183	0.25	-31.1 ±0.5	-23.8 ±0.9	-
2.5BA vesicles	74.84 ±0.61	78.84 ±1.27	0.137	0.27	-27.0 ±1.1	-22.8 ±1.5	82.75 ±0.42
5BA vesicles	70.59 ±0.07	87.73 ±0.78	0.154	0.35	-30.4 ±1.3	-24.8 ±0.6	81.72 ±0.23
10BA vesicles	67.58 ±1.45	89.84 ±1.58	0.132	0.38	-30.8 ±1.9	-24.3 ±1.9	80.86 ±0.13

Toxicity studies on 3T3 cells.

When a new pharmaceutical formulation is designed, it is important to evaluate its safety, especially on the target tissue. *In vitro* toxicity study on cells represents a good and reliable method to select the formulations that will be used for further *in vivo* studies, so as to avoid the useless sacrifice of a high number of animals. 3T3 fibroblasts were used as a representative cell line of the dermis, and they were incubated with non-diluted formulations: empty or BA loaded vesicles and BA saturated solution.

The cytotoxicity was evaluated by the MTT assay. As shown in Figure 3, all the vesicular formulations did not show a significant cytotoxic effect in the first 8 h of incubation (80% viability), compared to untreated control cells (100% viability), while BA saturated solution exhibited greater cytotoxicity, as the viability was less than 70%. At longer incubation time (24 h), an increase in cell mortality was observed, especially for the fibroblasts treated with BA saturated solution (20% viability), while a ~50% viability was found when BA loaded ultradeformable vesicles were used, thus confirming the higher biocompatibility of the vesicles.

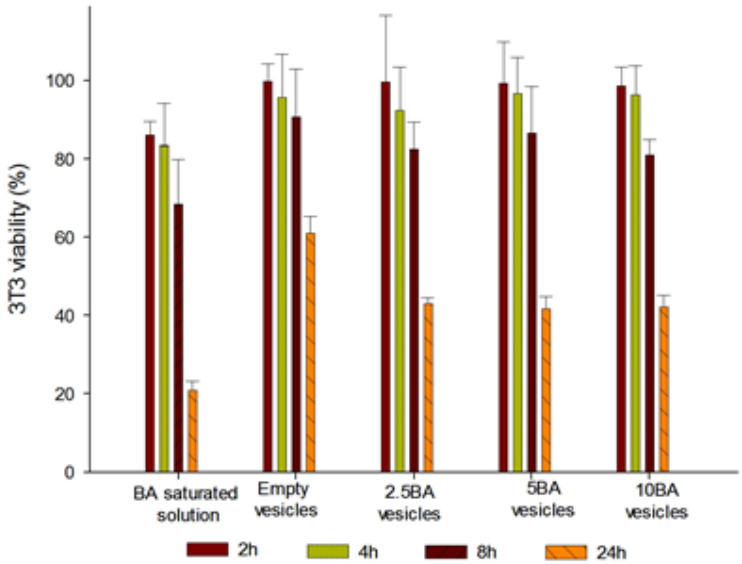

Figure 3. In vitro 3T3 fibroblast viability after incubation with BA saturated solution, empty ultradeformable vesicles and the same vesicles loading 2.5, 5 and 10 mg/mL (2.5 BA, 5 BA, 10 BA) at different incubation times (2, 4, 8 and 24 h). Mean values ± standard deviations (error bars) are reported.

Skin diffusion studies.

Ultradeformable vesicles contain an edge activator which is reported to make the bilayer flexible and the vesicles able to squeeze through the skin channels, improving the transdermal flux of the loaded molecules. To confirm this assumption, permeation study using human epidermis was carried out applying on the skin ultradeformable vesicles loaded with BA (2.5, 5 and 10 mg/mL) or BA saturated solution. The permeation profiles obtained from the different formulations are shown in Figure 4. The ultradeformable vesicles provided the greatest penetration rate of BA at 24 h, as compared to that obtained with the BA saturated solution. In particular, the vesicles loading the highest amount of BA (10 mg/mL) showed the best results in term of penetration (~5%) and flux (270.2±16.2 $\mu g/cm^2/h$). By decreasing the amount of BA, the amount permeated and the flux of the drug decreased as well, being 2.5% and 117.3±9.7 $\mu g/cm^2/h$ for the vesicles loading 5 mg/mL, and 1.5% and 190.11±16.63 $\mu g/cm^2/h$ for vesicles loading 2.5 mg/mL of BA. In all cases, the lag time (t_L) was around 9 h. Significant differences between the flux values and the amount of permeated BA provided by the three vesicles and saturated solution were detected ($P<0.05$), disclosing the concentration-dependent ability of the vesicles to deliver BA on the skin.

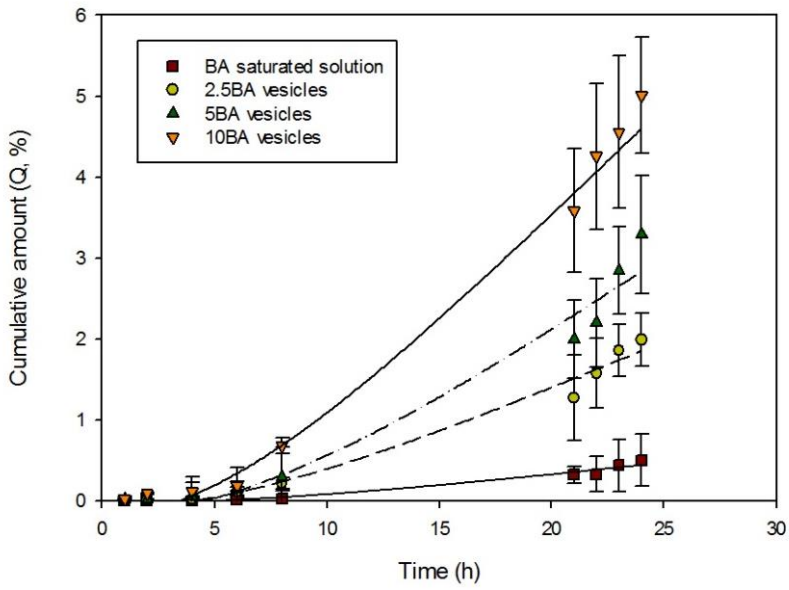

Figure 4. Amount of BA accumulated in receptor compartment after 24 h treatment with different formulations: BA saturated solution (- □ -) and ultradeformable vesicles loading different concentrations of BA: 2.5 BA (- o -), 5 BA (- Δ -) and 10 BA (- ∇ -) (n=4). Mean values ± standard deviations (error bars) are reported (n=4).

In vivo inflammatory response: myeloperoxidase assay.

The application of TPA in mice to induce inflammatory response is one of the most common model for the evaluation of the anti-inflammatory activity of drugs. TPA induces a variety of histological and biochemical changes in the skin, including neutrophil infiltration in epidermis and dermis, epidermal hyperplasia, activation of protein kinase C, induction of ornithine decarboxylase activity, and enhancement of IL-1 levels. In this work, TPA was daily applied on mouse dorsal skin for 3 days, inducing skin damages at the macroscopic level, such as skin ulceration, loss of epidermis integrity and crust formation, as well as biological alterations, such as neutrophil infiltration, as previously reported (Caddeo et al.,

2013). The MPO activity was quantified as a marker of the inflammatory process, since it is proportional to the neutrophil concentration in the inflamed tissue. The efficacy of BA loaded ultradeformable vesicles was tested and compared with that of DEX solution and BA saturated solution. The photographs of the treated mice clearly showed the therapeutic potential of BA loaded ultradeformable vesicles, as an amelioration of the TPA cutaneous damage was visible (Figure 5).

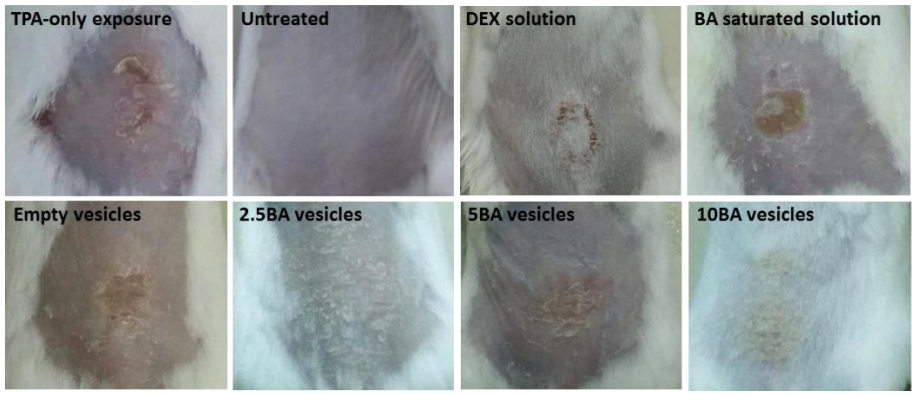

Figure 5. Macroscopic appearance of mice skin lesions inducted with TPA and treated with acetone (untreated skin), DEX solution, BA saturated solution, empty liposomes or the same vesicles loading BA 2.5, 5 and 10 mg/mL (2.5 BA, 5 BA, 10 BA).

The treatment with DEX solution reduced TPA skin lesion, but to a lesser extent: skin appeared diffusely dry, flaky, and crusted. These effects were much severe in mice treated with the BA saturated solution. The macroscopic observations are in agreement with the MPO values. The vesicles displayed a superior ability to reduce MPO activity in the injured tissue, and its inhibition was higher than that provided by both DEX

solution and BA saturated solution (Figure 6). No significant differences were observed (P>0.05) among the results provided by the three vesicular formulations containing different amounts of BA, which indicates that, in spite of the system saturation, ultradeformable vesicles can ensure a higher beneficial activity of BA than that obtained using the saturated solution. Differently to the *in vitro* transdermal delivery results, the *in vivo* treatment of damaged skin was not affected by the BA concentration in vesicles, probably because in this model the stratum corneum was thinner or disrupted, thus facilitating the vesicle passage and allowing a therapeutic effect even at the lower concentration. The importance of the vesicle saturation effect was underlined in transdermal studies, where the BA needs to overcome the intact skin barrier and transdermal flux was concentration-dependent.

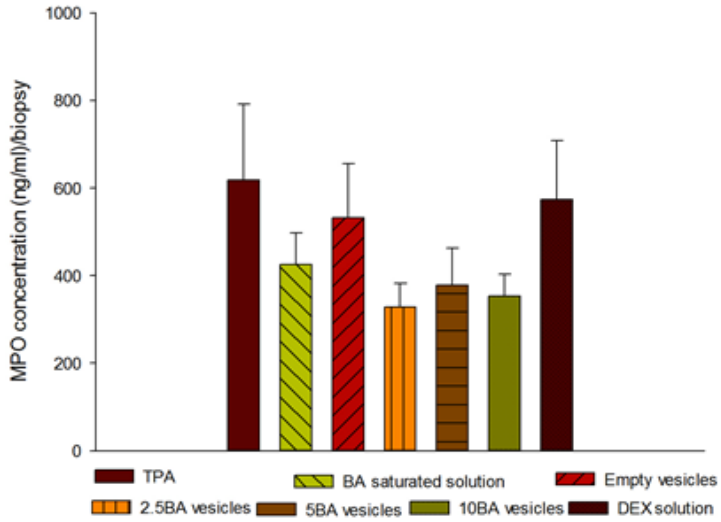

Figure 6. MPO activity in skin mice inflamed with TPA and treated with DEX solution, BA saturated solution, empty ultradeformable vesicles or the same vesicles loading BA 2.5, 5 and 10 mg/mL (2.5 BA, 5 BA, 10 BA). Mean values ± standard deviations (error bars) are reported (n=4).

Histological evaluation.

Morphological alterations of mouse skin exposed to TPA were assessed by H&E staining, in comparison with untreated skin (Figure 7B and A, respectively). As already demonstrated with the biomarker, the skin treated with acetone only showed a regular structure, epidermis and dermis had a normal appearance, as well as the tissues directly underneath (i.e., subcutaneous cellular tissue, skeletal muscle and adipose tissue), with only some mononuclear and polymorphonuclear cells in the muscular region (Figure 7A). Mouse skin treated with TPA displayed severe dermal and subcutaneous alteration, with a large number of leukocytes infiltrating these regions, as well as muscle and adipose tissues, also showing pathological features of inflammatory damage, such as vascular congestion (Figure 7B). Similar results of injured skin were obtained using the BA saturated solution and DEX solution (Figure 7C and F). On the other hand, the application of the BA loaded ultradeformable vesicles reduced TPA-induced lesions, along with mild to moderate inflammatory infiltrates of mononuclear cells, eosinophils and neutrophils (Figure 7E). The *in vivo* findings disclosed a great therapeutic efficacy of BA loaded ultradeformable vesicles, which unlike the transdermal flux, was not BA concentration/saturation dependent, probably because the transdermal flux depended on the passage of BA through the skin while, in the TPA model, the epidermis is disrupted, the skin's barrier function is impaired and BA can easily diffuse, whatever the concentration in the vesicles.

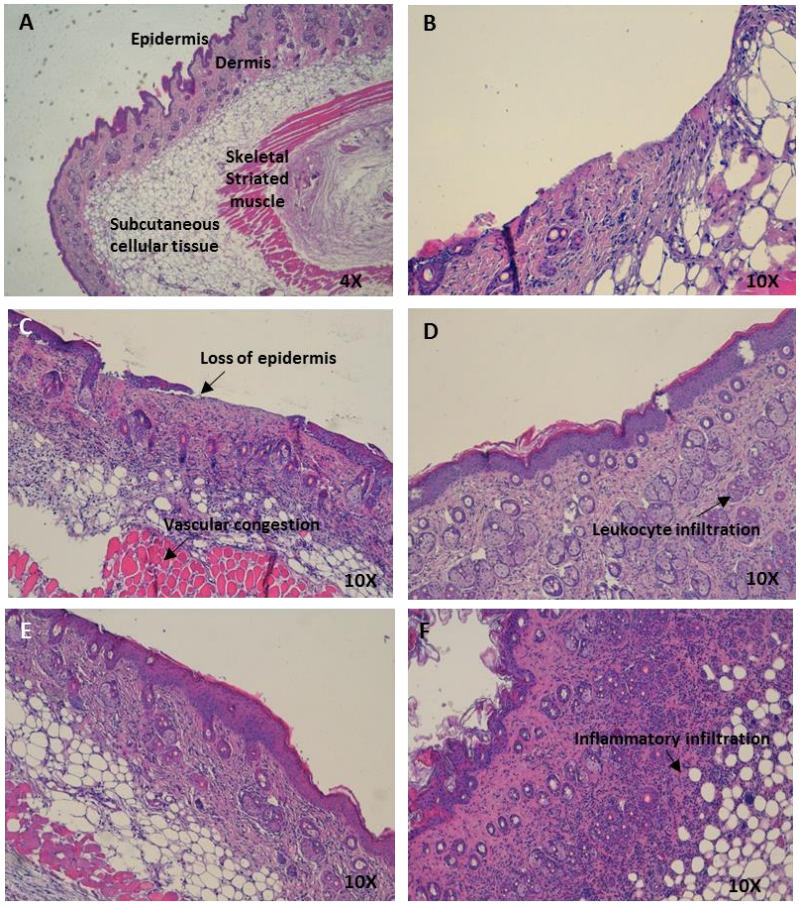

Figure 7. Representative histological sections of mouse skin: untreated skin (A); TPA-inflamed skin (B); TPA-inflamed and treated with BA saturated solution (C); inflamed and treated with empty ultradeformable vesicles (D); inflamed and treated with BA loaded ultradeformable vesicles (E) or inflamed and treated with DEX solution (F).

Conclusions.

Bearing in mind the few data reporting the design of baicalin loaded innovative phospholipid vesicles and their possible improvement of transdermal delivery, in the present work new, suitable and biocompatible ultradeformable vesicles loading baicalin were developed. We demonstrated that the ultradeformable vesicles play a key role in facilitating baicalin skin delivery and showed a great potential as anti-inflammatory systems and were more effective than dexamethasone in counteracting TPA inflammation and skin injury. Moreover, *in vivo* studies on damaged skin underlined that the efficacy of baicalin was not affected by the concentration, while *in vitro* studies performed using human intact skin, indicated that using BA vesicles (10 mg/mL) the highest penetration was obtained.

References.

Caddeo, C., Sales, O.D., Valenti, D., Saurí, A.R., Fadda, A.M., Manconi, M., 2013. Inhibition of skin inflammation in mice by diclofenac in vesicular carriers: Liposomes, ethosomes and PEVs. Int. J. Pharm. 443, 128–136. doi:10.1016/j.ijpharm.2012.12.041

Castangia, I., Manca, M.L., Matricardi, P., Sinico, C., Lampis, S., Fernàndez-Busquets, X., Fadda, A.M., Manconi, M., 2013. Effect of diclofenac and glycol intercalation on structural assembly of phospholipid lamellar vesicles. Int. J. Pharm. 456, 1–9. doi:10.1016/j.ijpharm.2013.08.034

Chen, Y.-C., Shen, S.-C., Chen, L.-G., Lee, T.J.-F., Yang, L.-L., 2001. Wogonin, baicalin, and baicalein inhibition of inducible nitric oxide synthase and cyclooxygenase-2 gene expressions induced by nitric oxide synthase inhibitors and lipopolysaccharide1. Biochem. Pharmacol. 61, 1417–1427. doi:10.1016/S0006-2952(01)00594-9

Chen, Y., Minh, L.V., Liu, J., Angelov, B., Drechsler, M., Garamus, V.M., Willumeit-Römer, R., Zou, A., 2016. Baicalin loaded in folate-PEG modified liposomes for enhanced stability and tumor targeting. Colloids Surf. B Biointerfaces 140, 74–82. doi:10.1016/j.colsurfb.2015.11.018

De Young, L.M., Kheifets, J.B., Ballaron, S.J., Young, J.M., 1989. Edema and cell infiltration in the phorbol ester-treated mouse ear are temporally separate and can be differentially modulated by pharmacologic agents. Agents Actions 26, 335–341.

Díez-Sales, O., Garrigues, T.M., Herráez, J.V., Belda, R., Martín-Villodre, A., Herráez, M., 2005. In Vitro Percutaneous Penetration of Acyclovir from Solvent Systems and Carbopol 971-P Hydrogels: Influence of Propylene Glycol. J. Pharm. Sci. 94, 1039–1047. doi:10.1002/jps.20317

Manca, M.L., Castangia, I., Zaru, M., Nácher, A., Valenti, D., Fernàndez-Busquets, X., Fadda, A.M., Manconi, M., 2015. Development of curcumin loaded sodium hyaluronate immobilized vesicles (hyalurosomes) and their potential on skin inflammation and wound restoring. Biomaterials 71, 100–109. doi:10.1016/j.biomaterials.2015.08.034

Manconi, M., Aparicio, J., Vila, A.O., Pendás, J., Figueruelo, J., Molina, F., 2003. Viscoelastic properties of concentrated dispersions in water of soy lecithin. Colloids Surf. Physicochem. Eng. Asp., A collection of papers presented at the International Symposium on Electrokinetic Phenomena, Cracow, Poland, August 18-22, 2003 222, 141–145. doi:10.1016/S0927-7757(03)00249-8

Manconi, M., Caddeo, C., Sinico, C., Valenti, D., Mostallino, M.C., Lampis, S., Monduzzi, M., Fadda, A.M., 2012. Penetration enhancer-containing vesicles: composition dependence of structural features and skin penetration ability. Eur. J. Pharm. Biopharm. Off. J. Arbeitsgemeinschaft Für Pharm. Verfahrenstechnik EV 82, 352–359. doi:10.1016/j.ejpb.2012.06.015

Shi, G.-F., Yao, R.-X., Wang, G.-Y., Wang, Z.-J., Chen, F.-W., 2015. Liquid Chromatography-Tandem Mass Spectrometry Screening Method for the Detection of Radical-Scavenging Natural Antioxidants from the

Whole Scutellariae (Radix, Stem and Leaf). J. Chromatogr. Sci. 53, 1140–1146. doi:10.1093/chromsci/bmu176

Shi, G.-X., Shao, J., Wang, T.-M., Wang, C.-Z., 2014. New advance in studies on antimicrobal activity of Scutellaria baicalensis and its effective ingredients. Zhongguo Zhong Yao Za Zhi Zhongguo Zhongyao Zazhi China J. Chin. Mater. Medica 39, 3713–3718.

Shi-Ying, J., Jin, H., Shi-Xiao, J., Qing-Yuan, L., Jin-Xia, B., CHEN, H.-G., Rui-Sheng, L., Wei, W., Hai-Long, Y., 2014. Characterization and evaluation in vivo of baicalin-nanocrystals prepared by an ultrasonic-homogenization-fluid bed drying method. Chin. J. Nat. Med. 12, 71–80. doi:10.1016/S1875-5364(14)60012-1

Wei, Y., Guo, J., Zheng, X., Wu, J., Zhou, Y., Yu, Y., Ye, Y., Zhang, L., Zhao, L., 2014. Preparation, pharmacokinetics and biodistribution of baicalin-loaded liposomes. Int. J. Nanomedicine 9, 3623–3630. doi:10.2147/IJN.S66312

Xing, J., Chen, X., Zhong, D., 2005. Absorption and enterohepatic circulation of baicalin in rats. Life Sci. 78, 140–146. doi:10.1016/j.lfs.2005.04.072

Zhang, H., Zhao, L., Chu, L., Han, X., Zhai, G., 2014. Preparation, optimization, characterization and cytotoxicity in vitro of Baicalin-loaded mixed micelles. J. Colloid Interface Sci. 434, 40–47. doi:10.1016/j.jcis.2014.07.045

Zhang, J., Yin, Z., Ma, L., Yin, Z., Hu, Y., Xu, Y., Wu, D., Permatasari, F., Luo, D., Zhou, B., 2014. The protective effect of baicalin against UVB

irradiation induced photoaging: an in vitro and in vivo study. PloS One 9, e99703. doi:10.1371/journal.pone.0099703.

CAPÍTULO 2

Baicalin and berberine ultradeformable vesicles as potential adjuvant in vitiligo therapy.

Silvia Mir-Palomo[a], Amparo Nácher[a,b,*], M. A. Ofelia Vila Busó[c], Carla Caddeo[d], Maria Letizia Manca[d], Maria Manconi[d] , Octavio Díez-Sales[a,b]

[a] *Dept. Pharmacy, Pharmaceutical Technology and Parasitology, Faculty of Pharmacy, University of Valencia, Spain*

[b] *Instituto Interuniversitario de Investigación de Reconocimiento Molecular y Desarrollo Tecnológico (IDM), Universitat Politècnica de València, Universitat de València, Av. Vicent Andrés Estellés s/n, 46100, Burjassot, Valencia, Spain*

[c] *Dept. Physics and Chemistry, Faculty of Pharmacy, University of Valencia, Spain*

[d] *Dept. of Scienze della Vita e dell'Ambiente, University of Cagliari, via Ospedale 72, 09124 Cagliari, Italy*

Colloids and Surfaces B: Biointerfaces 175 (2019) 654–662

doi: 10.1016/j.colsurfb.2018.12.055

Abstract.

0.5–1% of the world's population is affected by vitiligo, a disease characterized by a gradual depigmentation of the skin. Baicalin and berberine are natural compounds with beneficial activities, such as antioxidant, anti-inflammatory and proliferative effects. These polyphenols could be useful for the treatment of vitiligo symptoms, and their efficacy can be improved by loading in suitable carriers. The aim of this work was to formulate and characterize baicalin or berberine loaded ultradeformable vesicles, and demonstrate their potential as adjuvants in the treatment of vitiligo. The vesicles were produced using a previously reported simple, scalable method. Their morphology, size distribution, surface charge and entrapment efficiency were assessed. The ability of the vesicles to promote the permeation of the polyphenols was evaluated. The antioxidant and photoprotective effects were investigated *in vitro* using keratinocytes and fibroblasts. Further, the stimulation of melanin production and tyrosinase activity in melanocytes after treatment with the vesicles were assessed. Ultradeformable vesicles were small in size, homogeneously dispersed, and negatively charged. They were able to incorporate high amounts of baicalin and berberine, and promote their skin permeation. In fact, the polyphenols concentration in the epidermis was higher than 10%, which could be indicative of the formation of a depot in the epidermis. The vesicles showed remarkable antioxidant and photoprotective capabilities, presumably correlated with the stimulation of melanin production and tyrosinase activity. In conclusion, baicalin or berberine ultradeformable vesicles, and particularly their combination, may represent promising nanosystem-based adjuvants for the treatment of vitiligo symptoms.

Keywords: Ultradeformable vesicles; vitiligo; antioxidant; photoprotection; pigmentation.

Introduction.

Vitiligo is an autoimmune disease of the skin affecting 0.5–1% of the world's population [1]. It is clinically characterized by the appearance of disfiguring white patches caused by the loss of melanin pigment, which often negatively affects patients' self-esteem and quality of life [2]. Multiple mechanisms are involved in this disease: early factors include activation of innate immunity, inflammation, and oxidative stress [3]. Despite its occurrence, therapeutic options for patients are still limited. Current therapies exhibit considerable efficacy, but often the total repigmentation is not achieved [4]. One of the most common treatments involves the application of psoralens associated with ultraviolet (UV) light A exposure, topical corticosteroids, narrowband ultraviolet light B, which unfortunately cause important side effects [5].

In traditional Chinese medicine, different natural molecules and extracts have been successfully applied for the treatment of vitiligo [6]. The exact mechanism of action of these compounds is still unknown, but it seems to be related to their anti-inflammatory, immunomodulatory and antioxidant properties. Given that, antioxidant and anti-inflammatory natural molecules could be potential candidates for the vitiligo therapy, due to their efficacy and safety. Bearing in mind our previous results [7] [8] [9], baicalin and berberine were selected for this study. The former is a flavonoid with strong anti-inflammatory and antioxidant properties [10], antimicrobial and antifungal activities [11], a great potential in preventing and inhibiting tumours [12], and protecting the skin from the damages caused by intense exposure to solar UV radiations [13]; the latter is a quaternary isoquinoline alkaloid with several pharmacological effects, including anticarcinogenic [14], antioxidant, anti-inflammatory [15] and

pigmenting [16]. Both polyphenols have been used for the skin protection and the treatment of common dermatological disorders.

Despite the promising properties of baicalin and berberine, there are some limitations in their clinical applications, the most important being poor aqueous solubility and poor absorption after topical administration [17] [18]. To overcome these problems and taking into consideration previous results obtained for the skin delivery of baicalin, in the present work, baicalin and berberine were incorporated in ultradeformable vesicles. Elastic and flexible phospholipid vesicles have been developed by using different phospholipids and a surfactant that acts as edge activator, enhancing the fluidity and deformability of the vesicle bilayer [19]. In this work, ultradeformable vesicles were prepared with a mixture of phospholipids and polysorbate 80, and their ability to improve the vitiligo symptoms was evaluated. An extensive physico-chemical characterization of the vesicles was accomplished by investigating their ability to promote the passage of baicalin and berberine into/through the skin. The cytotoxicity of the formulations was evaluated *in vitro* using keratinocytes and fibroblasts, as well as their ability to promote the antioxidant and photoprotective activities of baicalin and berberine. Further, melanocytes were used to evaluate the ability of the formulations to promote melanogenesis and tyrosinase activity.

Material and methods.

Materials.

Lipoid S75, a mixture of soybean lecithin with phosphatidylcholine (~70%) and phosphatidylethanolamine (~10%), non-polar lipids and fatty acids (~20%), was a gift from Lipoid GmbH (Ludwigshafen, Germany). Disodium phosphate and polysorbate 80 were purchased from Scharlab S.L.

(Barcelona, Spain). Monosodium phosphate was purchased from Panreac quimica S.A. (Barcelona, Spain). Sorbitol was from Guinama SL (Valencia, Spain). Baicalin was purchased from Cymit quimica S.L. (Barcelona, Spain), and berberine from Sigma-Aldrich (Madrid, Spain).

Vesicle preparation.

Baicalin ultradeformable vesicles were prepared by dispersing baicalin (2.5 mg/mL), Lipoid S75 (60 mg/mL), and polysorbate 80 (2.5 mg/mL) in a buffered aqueous solution of monosodium phosphate and disodium phosphate (PBS, pH 7.4). Berberine ultradeformable vesicles were prepared by dispersing berberine (2.5 mg/mL), Lipoid S75 (120 mg/mL), and polysorbate 80 (2.5 mg/mL) with a solution of sorbitol (5 % v/v) in water. The phospholipid was left swelling overnight, and then the dispersions were sonicated for 3 min with a CY-500 ultrasonic disintegrator (Optic Ivymen system, Barcelona, Spain) to obtain transparent dispersions. Further, in order to achieve a homogeneous system, the dispersions were extruded with an Avanti® Mini-Extruder (Avanti Polar Lipids, Alabaster, Alabama) through a 200 nm membrane (Whatman, GE Healthcare, Fairfield, Connecticut, US). Empty vesicles were also prepared and compared with polyphenol loaded vesicles.

Analytical methods.

The baicalin and berberine content was quantified by using a Perkin Elmer® Series 200 HPLC equipped with a UV detector and a column Teknokroma® Brisa “LC2” C18, 5.0 µm (150 × 4.6 mm). Baicalin was detected at 278 nm by using a mixture of water and methanol (30:70) as mobile phase, delivered at a flow rate of 1 mL/min. Berberine

determination was carried out at 346 nm by using a mixture of water and methanol (50:50) as mobile phase, delivered at a flow rate of 1.2 mL/min.

Vesicle characterization.

Vesicle formation and morphology were evaluated by Transmission Electron Microscopy (TEM), by using a JEM-1010 microscope (Jeol Europe, Croissy-sur-Seine, France), equipped with a digital camera MegaView III, at an accelerating voltage of 100 kV. The vesicles were examined by using a negative staining technique: non-diluted samples were stained with 1% phosphotungstic acid on a carbon grid and visualized.

The mean diameter and the Polydispersity Index (PI, a dimensionless measure of the broadness of the size distribution) of empty, baicalin or berberine ultradeformable vesicles were measured by Photon Correlation Spectroscopy (PCS) using a Zetasizer nano-ZS® (Malvern Instruments, Worcestershire, UK). Zeta potential was measured by using the Zetasizer nano-ZS by means of the M3-PALS (Mixed Mode Measurement-Phase Analysis Light Scattering) technique, which measures the particle electrophoretic mobility.

The stability of the vesicles was evaluated for 30 days at 25 °C. During this period, size, size distribution and surface charge were measured.

The vesicles were purified from the non-incorporated berberine or baicalin by dialysis. Each sample (1 mL) was loaded into Spectra/Por® tubing (12–14 kDa MW cut-off; Spectrum Laboratories Inc., DG Breda, The Netherlands) and dialyzed against 1 L of buffered solution (pH 7.4) for 4 h, at room temperature. Both non-dialyzed and dialyzed samples were disrupted with Triton X-100 (10%) and assayed by HPLC to quantify the amount of baicalin and berberine (Section 2.3). The entrapment efficiency (EE %) was calculated as percentage as follows (Eq. 1):

$$EE\ (\%) = \left(\frac{\text{actual active agent}}{\text{initial active agent}}\right) \cdot 100 \qquad \text{(Eq. 1)}$$

where actual active agent is the amount of baicalin or berberine detected in the vesicles after dialysis, and initial active agent is the amount of baicalin or berberine detected before dialysis.

Skin permeation studies.

Permeation experiments were performed by using static vertical Franz diffusion cells and newborn pig skin provided by a local slaughterhouse. Excess of fatty and connective tissues were removed, and the specimens (full-thickness skin) were stored at −80 °C until use. For the experiments, only the epidermis (thickness ~200 μm) was used: it was securely clamped between the donor and receiver compartments of the Franz cells (effective diffusion area of 0.784 cm^2), with the stratum corneum side facing the donor compartment. The receptor compartment was filled with buffered solution (pH 7.4). The Franz cells were immersed in a bath system at 37±2°C and maintained under stirring in order to mimic physiological skin conditions. The different formulations (500 μL) were applied onto the epidermis surface, and at regular time intervals, up to 24 h, the receiving solution was withdrawn, replaced with pre-thermostated, fresh PBS, and analysed by HPLC for baicalin or berberine content (as described in Section 2.3). In addition, in order to verify the integrity of the epidermis, 1 mL of phenol red solution (0.5 mg/mL) was applied onto the skin surface in the donor compartment and quantified in the receptor compartment by spectrophotometry. When the values of phenol red were <1%, the epidermis was considered intact.

The cumulative amounts (Q, μg/cm^2) of baicalin or berberine permeated through the epidermis were plotted against time, and the equation derived from the application of the Fick's Second Law to the diffusion process was fitted to the data (Eq. 2):

$$Q_{(t)}=A\cdot P\cdot L\cdot C\left[D\cdot\frac{t}{L^2}-\frac{1}{6}-\frac{2}{x^2}\cdot\sum_{n=1}^{\infty}\cdot Exp\left(\frac{-D\cdot n^2\cdot x^2\cdot t}{L^2}\right)\right] \qquad \text{(Eq. 2)}$$

where *Q (t)* is the amount of active agent passing across the skin and reaching the receptor solution at a given time *t*; *A* is the actual diffusion surface area (0.784 cm^2); *P* is the partition coefficient of the permeant between the skin and the donor vehicle; *L* is the diffusion pathway; *D* is the diffusion coefficient of the permeant in the skin; and *C* is the concentration of the permeant in the donor vehicle. The fitting procedures were carried out by means of non-linear regression using Sigma Plot 10.0 (Pharsight corp, USA). By fitting the equation 2, lag time (t_L, h) corresponding to $L^2/6D$ and the permeability coefficient ($Kp = P\cdot D/L$) were calculated.

Cell culture.

Human immortalized keratinocytes (HaCaT) (Thermo Fisher Scientific Inc, Waltham, MA, USA) and 3T3 mouse fibroblasts (ATCC, Manassas, VA, USA) were cultured in Dulbecco's modified Eagle's medium (Sigma Aldrich, Spain), supplemented with 10% (v/v) foetal bovine serum, penicillin (100 U/mL), and streptomycin (100 μg/mL) (Sigma Aldrich, Spain) in 5% CO_2 incubator at 37 °C to allow exponential cell growth. Highly pigmented adult human epidermal melanocytes (HEMa) were purchased from Thermo Fisher Scientific Inc (Waltham, MA, USA). Cells were maintained in Medium 254 with the addition of Human Melanocyte Growth

Supplement-2, PMA-Free (HMGS-2) and 1% (V/V) gentamicin/amphothericin (Thermo Fisher Scientific Inc, Waltham, MA, USA) in a humidified incubator at 37 °C with 5% CO_2.

Cell viability studies.

Cytotoxicity studies were carried out using HaCaT keratinocytes at passages 31-32, 3T3 fibroblasts at passages 22-23 and HEMa melanocytes at passages 4-5. The cells were seeded into 96-well plates with a density of approximately 2.5, 2.9, and 1.4 ×·10^5 cells/well, for HaCaT, 3T3 and HEMa, respectively. After 24 h of incubation, when confluence was reached, the cells were exposed for 24 h to baicalin in PBS or berberine in 5%sorbitol water solution, or empty vesicles, or baicalin or berberine loaded vesicles, at different concentrations (200, 100, 50, 25, 12.5, 1.56 µg/mL) of baicalin or berberine. Cell viability was determined by the MTT [3(4,5-dimethylthiazolyl-2)-2,5-diphenyltetrazolium bromide] colorimetric assay. MTT reagent (100 µL, 0.5 mg/mL) was added to each well, and after 3 h the formed formazan crystals were dissolved in DMSO (100 µL). The reaction was spectrophotometrically measured at 570 nm with a microplate reader (Multiskan EX, Thermo Fisher Scientific, Inc., Waltham, MA, US). The experiments were performed in triplicate and repeated at least three times. Results are shown as percentage of cell viability in comparison with untreated control cells (100% viability) (Eq. 3):

$$\text{Cell Viability (\%)} = \left(\frac{\text{Absorbance}_{\text{sample}}}{\text{Absorbance}_{\text{control}}}\right) \text{x}100 \qquad \text{(Eq. 3)}$$

where $Absorbance_{sample}$ is the absorbance of cells treated with the formulations and $Absorbance_{control}$ is the absorbance of non-treated cells, at 570 nm.

Dose-response curves for different intensities of UV radiation.

In order to define the intensity of radiation that caused 50% cell death (LC_{50}), HaCaT and 3T3 were seeded into 96-well plates with a cell density of 1.7 and 2.0·× 10^6 cells/well, respectively. When confluence was reached, the cells were irradiated with different intensities of UVB rays (100, 200, 400, 600, 800 and 1000 mJ/cm^2) using a Crosslinker Bio-Link BLX 254 camera (5 x 8 W; Peqlab Biotechnologie GmbH, Erlangen, Germany) at a wavelength of 310 nm. After 24 h, the MTT assay was performed as described in Section 2.7. Results are shown as percentage of cell viability in comparison with untreated control cells (100% viability).

Photoprotective effect of formulations against UV radiation.

The photoprotective effect of the different formulations was assayed using the intensity of radiation that caused 50% cell death. HaCaT keratinocytes and 3T3 fibroblasts were seeded into 96-well plates, and after 24 h, were treated with baicalin in PBS or berberine in 5%sorbitol water solution, or empty vesicles, or baicalin or berberine loaded vesicles, at different concentrations of both polyphenols (12.5, 6.25, 3.12 and 1.56 μg/mL). In addition, the cells were treated simultaneously with both baicalin in PBS and berberine in 5%sorbitol water solution, or in the vesicles, at the above concentrations. 24 h after the treatment, the cells were irradiated with the appropriate intensity of UVB radiation, and incubated for 24 h at 37 °C with CO_2 (5%), then the cell viability was measured by MTT assay (as described in Section 2.7). Results are shown as percentage of photoprotection in comparison with untreated control cells (0% photoprotection): the percentage of photoprotection represents the percentage of live cells before and after treatment (Eq. 4).

$$\% \text{ Photoprotection} = \frac{\text{Absorbance of treated cells} - \text{Absorbance of non treated cells}}{\text{Absorbance of treated cells}} \cdot 100$$

(Eq. 4)

Efficacy of the formulations against oxidative stress in cells.

HaCaT cells were seeded into 96-well plates (3.1×10^5 cells/well) and incubated until confluence was reached. The cells were treated simultaneously with hydrogen peroxide and the formulations: baicalin in PBS or berberine in 5%sorbitol water solution, or empty vesicles, or baicalin or berberine loaded vesicles, at non-cytotoxic concentrations of the polyphenols of 12.5, 6.25, 3.12, and 1.56 µg/mL. In addition, the cells were treated simultaneously with both baicalin in PBS and berberine in 5%sorbitol water solution, or in vesicles, at the above concentrations. After 4 h of treatment, the cells were washed with PBS, and the MTT assay was performed to measure the cell viability (as decribed in Section 2.7). Untreated cells were used as a negative control, and cells treated with hydrogen peroxide without formulations were used as a positive control. Results are shown as percentage of antioxidant capability in comparison with untreated cells (0% antioxidant capability).

Melanin content determination.

HEMa cells at passages 5-6 were cultured on 6-well plates (2.2×10^5 cells/well) and incubated until confluence was reached. The cells were treated with baicalin in PBS or berberine in 5%sorbitol water solution, or empty vesicles, or baicalin or berberine loaded vesicles using non-cytotoxic concentrations (12.5, 6.25, 3.12 and 1.56 µg/mL) of baicalin or berberine. In addition, baicalin in PBS and berberine in 5%sorbitol water solution, or in vesicles were applied simultaneously, at the above concentrations. After 48 of incubation, the medium was removed, the cells

were washed twice with PBS and harvested using trypsin (0.05%) and EDTA (0.02%). The harvested cells were centrifuged, the pellet was dissolved in NaOH solution (1 N) and incubated at 60 °C for 1 h. The amount of melanin in solution was determined by measuring the absorbance at 470 nm using a microplate reader (Multiskan EX, Thermo Fisher Scientific, Inc., Waltham, MA, US). Results are shown as a percentage of melanin content in comparison with untreated cells (100% viability).

Tyrosinase activity assay.

Tyrosinase activity was estimated spectrophotometrically by using L-DOPA as substrate. HEMa cells at passages 5-6 were seeded into 6-well plates (approximately 2.0 ×·10^5 cells/well) and incubated until confluence was reached. The cells were treated for 48 h with baicalin in PBS or berberine in 5%sorbitol water solution, or empty vesicles, or baicalin or berberine vesicles at different concentrations of baicalin or berberine (12.5, 6.25, 3.125, and 1.56 µg/mL). A combined treatment of baicalin in PBS and berberine in 5%sorbitol water solution, or in vesicles at the above concentrations was also tested. At the end of each experiment, the cells were treated with sodium phosphate buffer (0.1 M, pH 6.8) containing 1% Triton X-100 and disrupted by repeated freeze/thaw cycles at −20 °C for 30 min. The lysates were clarified by centrifugation at 10,000 g for 15 min, then 90 µL of each lysate was seeded into a 96-well plate, and L-DOPA (10 µL, 10 mM) was added to each well. After incubation at 37 °C in the dark for 90 min, the end-point absorbance was measured spectrophotometrically at 475 nm using a microplate reader (Multiskan EX, Thermo Fisher Scientific, Inc., Waltham, MA, US). Results are shown as

a percentage of tyrosinase activity in comparison with untreated cells (100% viability).

Statistical analysis of data.

Data are shown as means ± standard deviation. Statistical differences were determined by using one-way ANOVA test and Tukey´s test for multiple comparisons with a significance level of $p<0.05$. All statistical analyses were performed using IBM SPSS statistics 22 for Windows (University of Valencia, Spain).

Results.

Vesicle characterization.

Based on our previous results [7], in the present study baicalin was incorporated in ultradeformable vesicles prepared with Lipoid S75 (60 mg/mL) and tween 80 (2.5 mg/mL) in PBS. To obtain berberine ultradeformable vesicles with size and polydispersity index comparable to those of baicalin vesicles, a higher amount of Lipoid S75 (120 mg/mL) was needed, as well as the addition of sorbitol (5% v/v in water). TEM images provided evidence of vesicle formation (Figure 1).

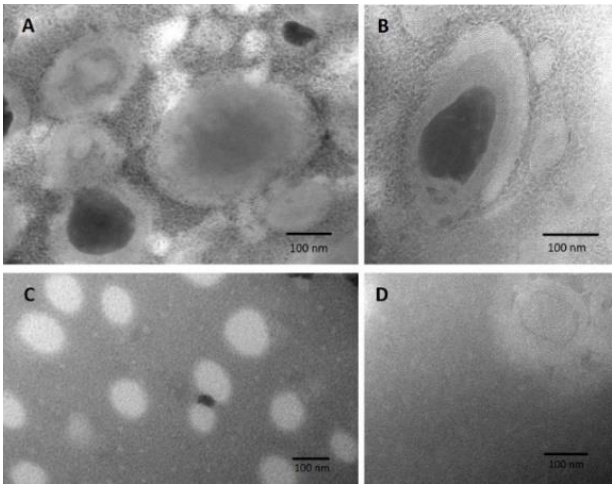

Figure 1. Representative TEM micrographs of ultradeformable vesicles loaded with baicalin (A and B) and berberine (C and D).

Baicalin ultradeformable vesicles were irregularly shaped and multilamellar, while berberine vesicles were mostly unilamellar, spherical in shape, and homogeneously dispersed. The size of the vesicles was measured by PCS, which provides a global value of mean size and size distribution as a function of the ability of the particles to scatter the incident light (Table 1). Empty formulations were also prepared and characterized to elucidate the effect of both active agents on bilayer-assembling features. Both baicalin and berberine vesicles were small in size, and the former were more monodispersed. All the vesicles were negatively charged, with berberine vesicles showing more negative values. The empty vesicles were larger than the corresponding baicalin or berberine loaded vesicles. This behaviour may be correlated with the intercalation of the polyphenols in the bilayer, which affected its assembly. Both baicalin and berberine were incorporated in high amounts in the vesicles. All the formulations were highly stable, since no significant

changes were detected after 30 days on storage at room temperature (25°C).

Table 1. Mean diameter (MD), polydispersity index (PI), zeta potential (ZP) and entrapment efficiency (EE) of baicalin or berberine loaded ultradeformable vesicles and the corresponding empty vesicles. Empty vesicles A and empty vesicles B were obtained by dispersing the phospholipid in PBS and 5%sorbitol water solution, respectively. Each value is the mean ± standard deviation (n = 3).

	Vesicle size (nm)		**PI**		**Z Potential (mV)**		**EE (%)**
	Day 0	Day 30	Day 0	Day 30	Day 0	Day 30	
Baicalin vesicles	64.8± 1.3	69.9± 1.6	0.14± 0.03	0.27± 0.03	-27.0± 1.1	-22.8± 1.5	82.7± 0.4
Empty vesicles A	80.4± 1.8	87.9± 1.1	0.18± 0.03	0.25± 0.03	-31.1± 1.6	-23.8± 2.8	-
Berberine vesicles	61.1± 1.4	69.7± 1.1	0.24± 0.01	0.34± 0.04	-38.1± 1.4	-20.7± 2.2	87.1± 1.2
Empty vesicles B	85.9± 0.8	90.7± 2.4	0.16± 0.02	0.32± 0.01	-33.3± 3.8	-13.7± 1.6	-

Skin permeation studies.

In order to evaluate the ability of ultradeformable vesicles to enhance the permeation of baicalin and berberine through the skin, *in vitro* studies were performed by applying the polyphenols in PBS or in 5%sorbitol water solution, or loaded in vesicles onto newborn pig skin. The permeation profiles are presented in Figure 2. The vesicles loaded with baicalin gave the best results in terms of penetration. The total amount of baicalin and

berberine penetrated was ~2% and 1%, respectively, which may be indicative of the formation of a depot in the epidermis. The permeability coefficients were 7.25 x 10^{-5} cm/s and 1.08 x 10^{-5} cm/s, respectively. Hence, the penetration of baicalin was 7-fold higher than berberine. These values are in accordance with the physico-chemical properties of the two polyphenols. The lag time (t_L) values for baicalin and berberine vesicles were around 6 and 4 h, respectively, which are favourable when a local effect is desired, decreasing the passage of the polyphenols into the bloodstream.

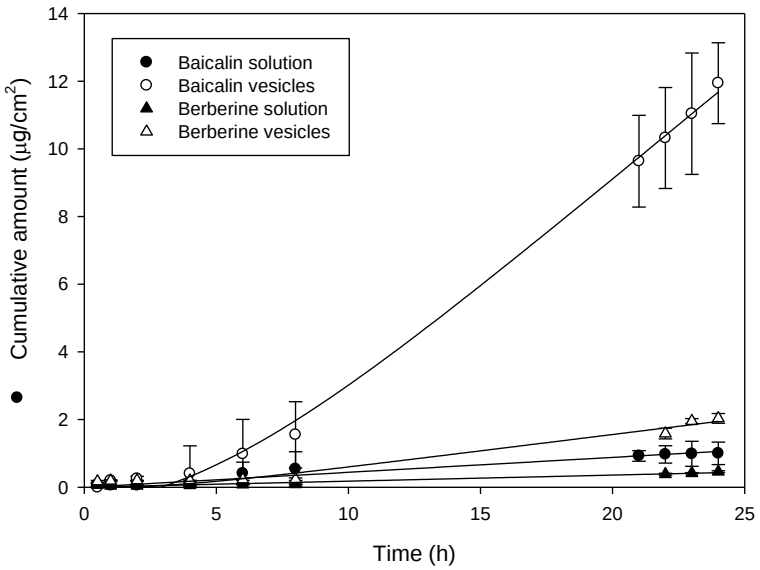

Figure 2. Amount of baicalin and berberine accumulated in the receptor compartment after a 24 h application of the polyphenols in PBS or in 5% sorbitol water solution, and vesicular formulations. Mean values and standard deviations (error bars) are reported (n=3).

Cell viability studies.

The cytotoxicity of baicalin and berberine formulations was evaluated using the main cells present in human skin: 3T3 fibroblasts, HaCaT keratinocytes and HEMa melanocytes (Figure 3). After incubation with empty vesicles, the viability of the three cell lines was always ~100%, regardless of the concentration tested. After incubation with baicalin in PBS or loaded vesicles, the viability values for HaCaT and HEMa were similar: ~100% using the lower concentrations (from 3.12 to 50 µg/mL), ~80% using 100 µg/mL of baicalin (regardless of the sample used) and ~70% ($p<0.05$) with 200 µg/mL of baicalin. The viability of 3T3 fibroblasts was always ≥100%, regardless of the tested sample or concentration.

A different behaviour was found incubating the cells with berberine in 5%sorbitol water solution or loaded in vesicles: the viability values were similar, irrespective of the cell type used. When the higher concentrations were used (from 200 to 25 µg/mL), the cell viability was between ~50 and ~75%, while at the lower concentrations (from 12.5 to 1.56 µg/mL) a 100% viability was reached. The non-cytotoxic concentrations were chosen to evaluate the efficacy of baicalin and berberine ultradeformable vesicles as antioxidants and photoprotectants of cells.

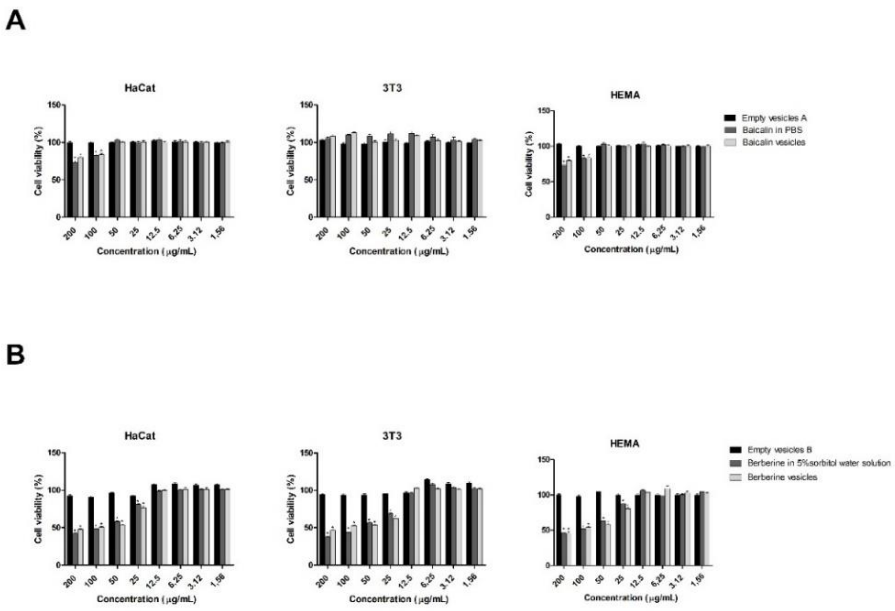

Figure 3. Viability of HaCaT, 3T3 and HEMa cells incubated with ultradeformable vesicles loaded with baicalin (1) or berberine (2). The viability of cells treated with the corresponding empty vesicles or the polyphenols in PBS or 5%sorbitol water solution was reported as a reference. Empty vesicles A and empty vesicles B were obtained by dispersing the phospholipid in PBS and 5%sorbitol water solution, respectively. Mean values ± standard deviations (error bars) are reported (n=16).

Dose-response curves for different intensities of UV radiation.

The effect of UV radiation at different intensities on cell viability was evaluated in HaCaT keratinocytes and 3T3 fibroblasts. In a preliminary study, the cell viability was measured as a function of the radiation intensity (Figure 4). Cell viability decreased as the radiation intensity increased, causing 50% cell death at 500 mJ/cm^2 for keratinocytes and at

400 mJ/cm^2 for fibroblasts. These UV intensities were chosen to evaluate the ability of baicalin and berberine vesicles to counteract the damaging effects of UV radiation.

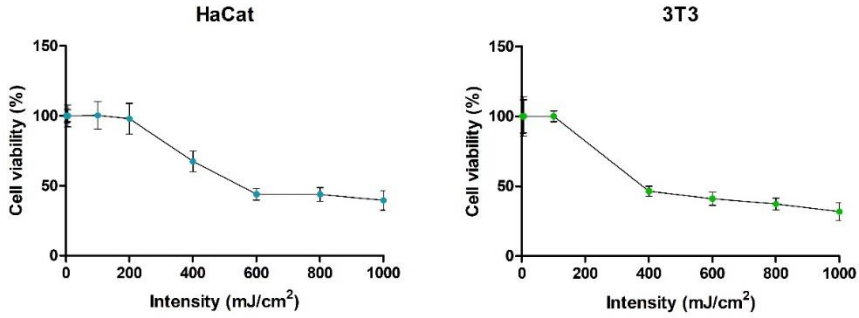

Figure 4. Effect of UVB (λ=310 nm) at different intensities on the viability of 3T3 fibroblasts and HaCaT keratinocytes. Values are given as means ± standard deviations (n=16).

Photoprotective effect of the formulations against UV radiation.

The ability of the formulations to counteract the deleterious effects of UV radiation was measured in keratinocytes and fibroblasts, because the UV radiation is able to penetrate the skin and reach the dermis (Figure 5). The photoprotective activity was calculated as a percentage of viability of treated versus untreated cells. Using the keratinocytes, the photoprotection provided by the baicalin in PBS or berberine in 5%sorbitol water solution at the different non-cytotoxic concentrations was very low (~7%). The efficacy increased up to ~34% thanks to the loading of baicalin in the ultradeformable vesicles, while the incorporation of berberine into the vesicles did not provide an important increase in the photoprotective activity (~13%). When the keratinocytes were treated simultaneously with baicalin vesicles and berberine vesicles, the photoprotective activity was similar to that provided by baicalin vesicles alone (~34%). In the

fibroblasts, the photoprotective activity was similar to that obtained in keratinocytes: ~13% with baicalin in PBS, ~27% with baicalin vesicles at the three higher non-cytotoxic concentrations (from 12.5 to 3.12 µg/mL), and ~14% at the lower non-cytotoxic concentration (1.56 µg/mL), ~8% with berberine in 5%sorbitol water solution, and ~18% with berberine vesicles. The association of baicalin vesicles and berberine vesicles provided values similar to those obtained with baicalin vesicles alone (~28% at the three higher concentrations, 12.5, 6.25 and 3.12 µg/mL, and ~16% at the lower concentration, 1.56 µg/mL). Overall results indicated that baicalin loaded vesicles showed a stronger photoprotective activity, which was not reinforced by the association with berberine.

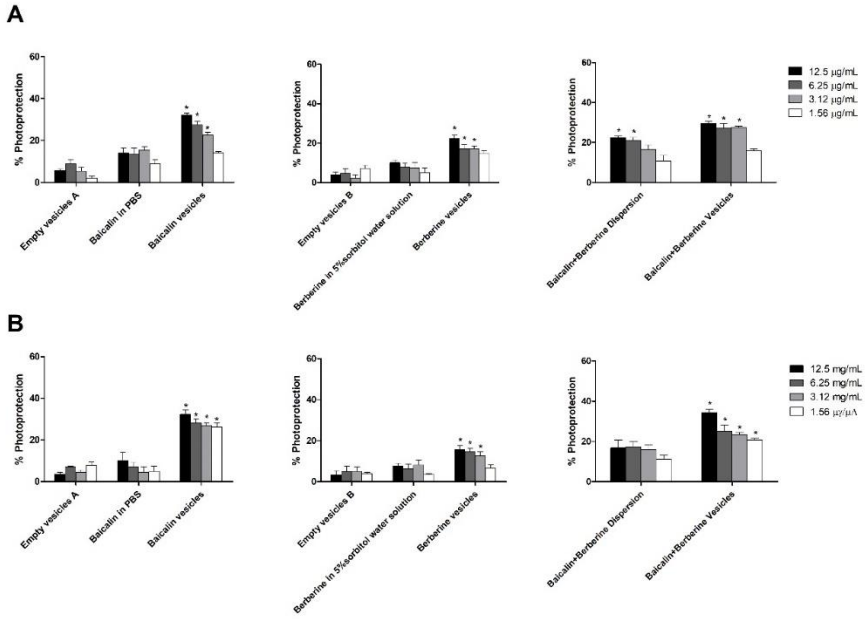

Figure 5. Effect of baicalin and berberine formulations against UVB-induced phototoxicity in 3T3 fibroblasts (A) and HaCaT keratinocytes (B). Empty vesicles and polyphenols in PBS or 5%sorbitol water solution were tested as controls. Empty vesicles A and empty vesicles B were obtained

by dispersing the phospholipid in PBS and 5%sorbitol water solution, respectively. Each bar represents the mean ± standard deviation (n=16). *p < 0.05 versus irradiated and untreated controls.

Efficacy of the formulations against oxidative stress damage in cells.

The ability of baicalin and berberine loaded vesicles to counteract the damages induced by oxidative stress was evaluated by using keratinocytes, which are the predominant cells in the outermost layer of the skin, thus more exposed to environmental contaminants and aggressors (Figure 6). The cells were stressed with hydrogen peroxide and treated with baicalin in PBS or berberine in 5%sorbitol water solution, or in vesicles at the different non-cytotoxic concentrations (12.5-1.56 µg/mL). Additionally, the cells were treated with empty vesicles or baicalin vesicles together with berberine vesicles. The exposure of the cells to hydrogen peroxide, which was indicated as 0% antioxidant capability, led to a significant reduction in cell viability (~65%). The antioxidant capability of the empty vesicles was around 30%, and increased using the polyphenols in PBS or in 5%sorbitol water solution, reaching ~38% at the lower concentration (1.56 µg/mL) and ~56% at the higher concentration (12.5 µg/mL) of baicalin in PBS, and ~42% at all the concentrations of berberine in 5%sorbitol water solution. The antioxidant capability of baicalin or berberine ultradeformable vesicles further increased to ~59% at the higher concentration (12.5 µg/mL), ~55% at 6.25 µg/mL, and ~47% at the other non-cytotoxic concentrations. Comparable results were obtained by treating the cells simultaneously with the baicalin vesicles and berberine vesicles, as the antioxidant activity reached ~55% at the higher concentration (12.5 µg/mL) and ~47% at the other non-cytotoxic

concentrations. The same values were obtained using baicalin in PBS together with berberine in 5%sorbitol water solution.

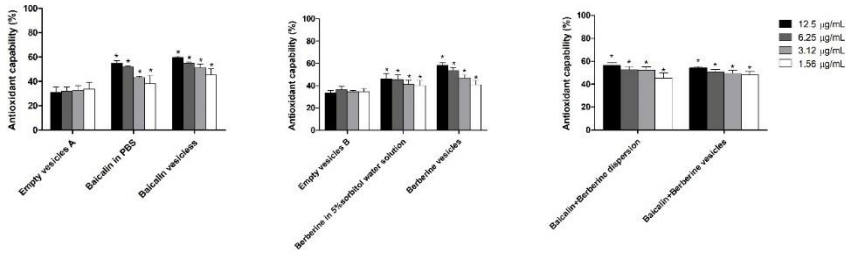

Figure 6. Protective effect of the different baicalin and berberine formulations against H_2O_2-induced oxidative stress in HaCaT keratinocytes. Empty vesicles A and empty vesicles B were obtained by dispersing the phospholipid in PBS or 5%sorbitol water solution, respectively. Each bar represents a mean ± standard deviation (n=16). *p < 0.05 versus untreated control.

Melanin content determination.

The ability of baicalin and berberine vesicles to facilitate melanogenesis and skin pigmentation was evaluated in melanocytes. The cells were treated for 48 h with the formulations, the amount of melanin was measured, and the melanogenetic activity was calculated as a percentage of untreated cells (Table 2). The melanogenetic activity was around 90% in cells treated with baicalin in PBS, and slightly increased to ~106% when the polyphenol was loaded in the vesicles. The melanogenetic activity increased especially using berberine vesicles at 12.5 and 6.25 µg/mL, reaching ~133%. The higher melanogenetic activity was achieved when the cells were treated with the combination of baicalin vesicles and berberine vesicles, reaching ~145% with the higher concentrations (12.5

and 6.25 µg/mL). The obtained data indicated that berberine vesicles stimulated the melanogenesis more than baicalin vesicles, and their combination further improved this activity, suggesting a possible use of these vesicles as adjuvants in repigmentation of skin affected by vitiligo.

Tyrosinase activity assay.

To corroborate the pathway involved in the stimulation of melanin production, the tyrosinase activity was measured, as it is the key enzyme involved in melanin synthesis. Results were expressed as a percentage of untreated cells (Table 2).

Similarly, to the melanogenetic activity, the tyrosinase activity was less stimulated by baicalin in PBS (~95%) or loaded in vesicles (~100%), and more by berberine in 5%sorbitol water solution (~110%) or loaded in vesicles (~130%). The tyrosinase activity was markedly stimulated by the combination of baicalin vesicles and berberine vesicles, especially at the lower concentrations (136%). This combination may represent a potential strategy to stimulate both tyrosinase enzyme activity and melanin production.

Table 2. Melanogenetic activity (%) and tyrosinase activity (%) of melanocytes after a 48 h treatment with baicalin or berberine in PBS or in 5%sorbitol water solution, or loaded in vesicles, at different concentrations (12.5, 6.25, 3.12 and 1.56 µg/mL). Baicalin and berberine were used alone or in association. Each value is the mean ± standard deviation (n = 16). *$p < 0.05$ versus untreated control cells (100%).

	Melanogenic activity (%)				Tyrosinase activity (%)			
µg/mL	**12.5**	**6.25**	**3.12**	**1.56**	**12.5**	**6.25**	**3.12**	**1.56**
Baicalin in PBS	91 ±3	94 ±2	93 ±3	93 ±6	95 ±2	97 ±4	98 ±3	96 ±5
Baicalin vesicles	106 ±1	109 ±6	105 ±5	105 ±6	101 ±4	101 ±3	100 ±5	99 ±5
Berberine in 5%sorbitol water solution	115 ±3	116 ±4	103 ±5	101 ±4	110 ±2	107 ±4	106 ±4	112 ±3
Berberine vesicles	135 ±3*	130 ±3*	110 ±6	113 ±5	129 ±3*	121 ±4*	119 ±3	116 ±4
Baicalin + Berberine dispersion	103 ±3	99 ±3	93 ±3	97 ±5	119 ±2	115 ±3	114 ±2	97 ±5
Baicalin + Berberine vesicles	153 ±4*	138 ±6*	110 ±5	115 ±5	136 ±4*	132 ±2*	125 ±4*	122 ±6

Discussion.

Vitiligo is a common skin disorder characterised by patchy areas of depigmentation due to the loss of melanin-forming cells, melanocytes, in the epidermis. Topical monotherapy is indicated for mild-to-moderate vitiligo [20]. Adequate modifications and innovations are still required to improve the local efficacy of active molecules, and phospholipid vesicles might represent the vehicle of choice for local treatments, as they can enhance the skin accumulation and efficacy of active molecules, such as baicalin and berberine. Taking into account previous results on the delivery of baicalin for the treatment of skin inflammation, elastic, ultradeformable vesicles, the so-called transfersomes, were chosen for this study [7] [19]. Baicalin was loaded in vesicles containing 60 mg/ml of Lipoid S75, and 2.5 mg/mL of tween 80. To load berberine into vesicles with characteristics comparable to those loading baicalin, 120 mg/mL of

the same phospholipid was needed, along with the addition of sorbitol (5%) in water as a stabilizer. The prepared ultradeformable vesicles were fairly spherical, small in size, homogeneously dispersed, negatively charged, capable of incorporating high amounts of baicalin or berberine. The incorporation of the polyphenols into the vesicles led to a reduction of the mean diameter, in comparison with that of empty vesicles ($p<0.05$), probably due to the intercalation of baicalin or berberine in the phospholipid bilayer, and the consequent modification of the vesicle assembly [7] [21] [22]. Size distribution and surface charge were monitored for 30 days at 25 °C: no significant variations were detected (Table 1), irrespective of the sample tested. Skin permeation of baicalin and berberine was improved by their incorporation in the ultradeformable vesicles. The concentration of the polyphenols in the receptor compartment was less than 2%, which can be indicative of the formation of a depot in the epidermis. No cytotoxic effects were detected upon treatment with empty vesicles (viability ≥100%), irrespective of the cells used. A high biocompatibility was also detected using baicalin in PBS or in vesicles, as the viability was always around 100% even using high concentrations (i.e., 100, 50 and 25 μg/mL). A different behaviour was observed for berberine in 5%sorbitol water solution or loaded in vesicles, as the viability was high (~100%) only using the lower concentrations (12.5-1.56 μg/mL). Taking into account these results, only the lower concentrations were chosen for further studies. Under these conditions, the polyphenols in PBS or in 5%sorbitol water solution were able to counteract the oxidative stress induced by H_2O_2, and this effect was slightly improved (~15%) using the vesicles. Baicalin vesicles provided the highest antioxidant activity, which was not significantly improved by the association with berberine vesicles. The antioxidant effect can be useful

against vitiligo symptoms, which are correlated with the accumulation of reactive oxygen species in the skin [23]. Additionally, the photoprotective effect of the formulations was evaluated. The highest photoprotective activity was achieved by using baicalin vesicles or when baicalin and berberine vesicles were used in combination. Vitiligo is phenotypically characterized by acquired depigmented spots in the skin. It is often necessary to use rotational therapy to decrease side effects and to achieve better repigmentation response [24]. Berberine vesicles, mostly when combined with baicalin vesicles, induced a significant increase in melanin production and tyrosinase activity. The latter is considered as the key determinant of pigmentation and the rate-limiting enzyme for melanin synthesis. The improved melanin production can ensure a suitable repigmentation of skin white spots. Currently, the main purpose of clinical treatment of vitiligo is to increase the melanogenesis and uniform skin colour. The findings of this study suggest that the association of baicalin vesicles with berberine vesicles may represent a promising strategy to counteract vitiligo progression, because the presence of baicalin vesicles ensures the antioxidant protection, and the presence of berberine vesicles ensures photoprotection and skin repigmentation. The delivery of bioactive molecules by ultradeformable vesicles capable of squeezing through the skin channels, facilitates the accumulation of the payload into the skin and the interaction with cells. Therefore, the association of these vesicles may represent a valid adjuvant to the generally used treatments of vitiligo.

Conclusion.

The association of baicalin and berberine ultradeformable vesicles showed a great potential as adjuvant therapy of vitiligo, because the baicalin vesicles exhibited good antioxidant and photoprotective abilities that were reinforced by repigmentation provided by the berberine vesicles.

References.

[1] O. Osinubi, M. j. Grainge, L. Hong, A. Ahmed, J. m. Batchelor, D. Grindlay, A. r. Thompson, S. Ratib, The prevalence of psychological comorbidity in people with vitiligo: a systematic review and meta-analysis, Br. J. Dermatol. (n.d.) n/a-n/a. doi:10.1111/bjd.16049.

[2] M.L. Frisoli, J.E. Harris, Vitiligo: Mechanistic insights lead to novel treatments, J. Allergy Clin. Immunol. 140 (2017) 654–662. doi:10.1016/j.jaci.2017.07.011.

[3] R. Speeckaert, N. van Geel, Vitiligo: An Update on Pathophysiology and Treatment Options, Am. J. Clin. Dermatol. 18 (2017) 733–744. doi:10.1007/s40257-017-0298-5.

[4] K. Boniface, J. Seneschal, M. Picardo, A. Taïeb, Vitiligo: Focus on Clinical Aspects, Immunopathogenesis, and Therapy, Clin. Rev. Allergy Immunol. 54 (2018) 52–67. doi:10.1007/s12016-017-8622-7.

[5] L. B Travis, N. Silverberg, Calcipotriene and Corticosteroid Combination Therapy for Vitiligo, Pediatr. Dermatol. 21 (2004) 495–8. doi:10.1111/j.0736-8046.2004.21418.x.

[6] S. Gianfaldoni, U. Wollina, M. Tirant, G. Tchernev, J. Lotti, F. Satolli, M. Rovesti, K. França, T. Lotti, Herbal Compounds for the Treatment of Vitiligo: A Review, Open Access Maced. J. Med. Sci. 6 (2018) 203–207. doi:10.3889/oamjms.2018.048.

[7] S. Mir-Palomo, A. Nácher, O. Díez-Sales, M.A. Ofelia Vila Busó, C. Caddeo, M.L. Manca, M. Manconi, A.M. Fadda, A.R. Saurí, Inhibition of skin inflammation by baicalin ultradeformable vesicles, Int. J. Pharm. 511 (2016) 23–29. doi:10.1016/j.ijpharm.2016.06.136.

[8] M. Manconi, M.L. Manca, C. Caddeo, D. Valenti, C. Cencetti, O. Diez-Sales, A. Nacher, S. Mir-Palomo, M.C. Terencio, D. Demurtas, J.C. Gomez-Fernandez, F.J. Aranda, A.M. Fadda, P. Matricardi, Nanodesign

of new self-assembling core-shell gellan-transfersomes loading baicalin and in vivo evaluation of repair response in skin, Nanomedicine Nanotechnol. Biol. Med. 14 (2018) 569–579. doi:10.1016/j.nano.2017.12.001.

[9] M. Manconi, M.L. Manca, C. Caddeo, C. Cencetti, C. di Meo, N. Zoratto, A. Nacher, A.M. Fadda, P. Matricardi, Preparation of gellan-cholesterol nanohydrogels embedding baicalin and evaluation of their wound healing activity, Eur. J. Pharm. Biopharm. 127 (2018) 244–249. doi:10.1016/j.ejpb.2018.02.015.

[10] B. Dinda, S. Dinda, S. DasSharma, R. Banik, A. Chakraborty, M. Dinda, Therapeutic potentials of baicalin and its aglycone, baicalein against inflammatory disorders, Eur. J. Med. Chem. 131 (2017) 68–80. doi:10.1016/j.ejmech.2017.03.004.

[11] G.-X. Shi, J. Shao, T.-M. Wang, C.-Z. Wang, [New advance in studies on antimicrobal activity of Scutellaria baicalensis and its effective ingredients], Zhongguo Zhong Yao Za Zhi Zhongguo Zhongyao Zazhi China J. Chin. Mater. Medica. 39 (2014) 3713–3718.

[12] Y. Chen, L.V. Minh, J. Liu, B. Angelov, M. Drechsler, V.M. Garamus, R. Willumeit-Römer, A. Zou, Baicalin loaded in folate-PEG modified liposomes for enhanced stability and tumor targeting, Colloids Surf. B Biointerfaces. 140 (2016) 74–82. doi:10.1016/j.colsurfb.2015.11.018.

[13] J. Zhang, Z. Yin, L. Ma, Z. Yin, Y. Hu, Y. Xu, D. Wu, F. Permatasari, D. Luo, B. Zhou, The Protective Effect of Baicalin against UVB Irradiation Induced Photoaging: An In Vitro and In Vivo Study, PLOS ONE. 9 (2014) e99703. doi:10.1371/journal.pone.0099703.

[14] Q. Liu, H. Jiang, Z. Liu, Y. Wang, M. Zhao, C. Hao, S. Feng, H. Guo, B. Xu, Q. Yang, Y. Gong, C. Shao, Berberine radiosensitizes human esophageal cancer cells by downregulating homologous

recombination repair protein RAD51, PloS One. 6 (2011) e23427. doi:10.1371/journal.pone.0023427.

[15] C.-L. Kuo, C.-W. Chi, T.-Y. Liu, The anti-inflammatory potential of berberine in vitro and in vivo, Cancer Lett. 203 (2004) 127–137.

[16] S.A. Ali, I. Naaz, R.K. Choudhary, Berberine-induced pigment dispersion in Bufo melanostictus melanophores by stimulation of beta-2 adrenergic receptors, J. Recept. Signal Transduct. 34 (2014) 15–20. doi:10.3109/10799893.2013.843193.

[17] E. Mirhadi, M. Rezaee, B. Malaekeh-Nikouei, Nano strategies for berberine delivery, a natural alkaloid of Berberis, Biomed. Pharmacother. Biomedecine Pharmacother. 104 (2018) 465–473. doi:10.1016/j.biopha.2018.05.067.

[18] N.R. Srinivas, Baicalin, an emerging multi-therapeutic agent: pharmacodynamics, pharmacokinetics, and considerations from drug development perspectives, Xenobiotica. 40 (2010) 357–367. doi:10.3109/00498251003663724.

[19] E. Romero, M. Jose Morilla, Ultradeformable phospholipid vesicles as a drug delivery system: a review, Res. Rep. Transdermal Drug Deliv. (2015) 55. doi:10.2147/RRTD.S50370.

[20] B.J. Garg, A. Saraswat, A. Bhatia, O.P. Katare, Topical treatment in vitiligo and the potential uses of new drug delivery systems, Indian J. Dermatol. Venereol. Leprol. 76 (2010) 231–238. doi:10.4103/0378-6323.62961.

[21] C. Caddeo, M. Manconi, M.C. Cardia, O. Díez-Sales, A.M. Fadda, C. Sinico, Investigating the interactions of resveratrol with phospholipid vesicle bilayer and the skin: NMR studies and confocal imaging, Int. J. Pharm. 484 (2015) 138–145. doi:10.1016/j.ijpharm.2015.02.049.

[22] C. Caddeo, M. Manconi, A.M. Fadda, F. Lai, S. Lampis, O. Diez-Sales, C. Sinico, Nanocarriers for antioxidant resveratrol: Formulation approach, vesicle self-assembly and stability evaluation, Colloids Surf. B Biointerfaces. 111 (2013) 327–332. doi:10.1016/j.colsurfb.2013.06.016.

[23] L. Qiu, Z. Song, V. Setaluri, Oxidative Stress and Vitiligo: The Nrf2–ARE Signaling Connection, J. Invest. Dermatol. 134 (2014) 2074–2076. doi:10.1038/jid.2014.241.

[24] C.G. Moreira, L.Z.B. Carrenho, P.L. Pawloski, B.S. Soley, D.A. Cabrini, M.F. Otuki, Pre-clinical evidences of Pyrostegia venusta in the treatment of vitiligo, J. Ethnopharmacol. 168 (2015) 315–325. doi:10.1016/j.jep.2015.03.080.

CAPÍTULO 3

Co-loading of finasteride and baicalin in phospholipid vesicles tailored for the treatment of hair disorders.

Silvia Mir-Palomo[a], Amparo Nácher[a,b], M.A. Ofelia Vila Busó[c], Carla Caddeo[d], Maria Letizia Manca[d], Amparo Ruiz Saurí[e], Elvira Escribano Ferrer[f], Maria Manconi[d] and Octavio Díez-Sales[a,b.]

[a] *Dept. Pharmacy, Pharmaceutical Technology and Parasitology, Faculty of Pharmacy, University of Valencia, Spain*

[b] *Instituto Interuniversitario de Investigación de Reconocimiento Molecular y Desarrollo Tecnológico (IDM), Universitat Politècnica de València, Universitat de València, Av. Vicent Andrés Estellés s/n, 46100, Burjassot, Valencia, Spain*

[c] *Dept. Physics and Chemistry, Faculty of Pharmacy, University of Valencia, Spain*

[d] *Dept. of Scienze della Vita e dell'Ambiente, University of Cagliari, via Ospedale 72, 09124 Cagliari, Italy*

[e] *Dept. of Pathology, University of Valencia, Avda Blasco Ibañez 17, 46010 Valencia, Spain*

[f] *Biopharmaceutics and Pharmacokinetics Unit, Institute for Nanoscience and Nanotechnology, University of Barcelona, Barcelona, Spain*

Nanoscale. 12(30) (2020) 16143:16152

doi: 10.1039/d0nr03357j.

Abstract.

Hair loss affects a large number of people worldwide and it has a negative impact on the quality of life. Despite the availability of different drugs for the treatment of hair disorders, therapeutic options are still limited and scarcely effective. An innovative strategy to improve the efficacy of alopecia treatment is pre-sented in this work. Finasteride, the only oral synthetic drug approved by Unites States Federal Drug Administration, was loaded in phospholipid vesicles. In addition, baicalin was co-loaded as an adjuvant. Their effect on hair growth was evaluated *in vitro* and *in vivo*. Liposomes, hyalurosomes, glycerosomes and glycerol-hyalurosomes were manufactured by using a simple method that avoids the use of organic solvents. All the vesicles were small in size (∼100 nm), homogeneously dispersed (polydispersity index ≤ 0.27) and negatively charged (−16 mV). The formulations were able to stimulate the proliferation of human dermal papilla cells, which are widely used in hair physiology studies. The analysis of hair growth and hair follicles of C57BL/6 mice, treated with the formulations for 21 days, underlined the ability of the vesicles to improve hair growth by the simultaneous follicular delivery of finasteride and baicalin. Therefore, the developed nanosystems can represent a promising tool to ensure the efficacy of the local treatment of hair loss.

Keywords: Finasteride; baicalin; phospholipid vesicles; hair disorders; hair follicle dermal papilla cells; *in vivo* hair growth.

Introduction.

Hair loss is a common dermatological disorder that can affect the quality of life of patients, as it has a relevant impact on their psychology.[1] The aetiology and subsequent development of hair loss or alopecia is not fully understood, but it is commonly accepted that it can be caused by a combination of genetic and environmental stimuli.[2]

Hair follicles control hair growth, which is a regenerating system that undergoes a cyclic process divided into different phases: hair generation and growth (anagen phase), regression (catagen phase) and rest (telogen phase). Moreover, hair follicles are supported by the dermal papilla cells, which play a crucial role in hair growth cycle and seem to be responsible for the key signals controlling hair follicle cycle during mammals life.[3,4]

The incorrect or slowed cyclic process of growth can cause hair loss, which is very common, especially in adults. Despite the high incidence of alopecia, the therapeutic treatments are still limited. Among those currently available, the majority of treatments exhibit low efficacy and important side effects.[5,6] Therefore, alternative treatment options, more effective and safer, are urgently needed. Among the different drugs available for the treatment of alopecia, finasteride is one of the most used. It is the only oral synthetic drug approved by Unites States Federal Drug Administration and is especially recommended for the treatment of hair loss connected to androgenic alopecia. Finasteride inhibits human 5α-reductase, which converts testosterone into the more potent 5α-dihydrotestosterone,[7] induces the passage of hair follicles from telogen to anagen phase, and inhibits miniaturization of hair follicles.[8]

In spite of its benefits, the chronic oral treatment with finasteride is associated with different side effects, such as gynecomastia, decreased libido, ejaculation disorder and others, which lead to a low treatment adherence. A significant reduction of the abovementioned side effects can be achieved by topical application, especially if the drug is locally delivered by ad hoc formulated nanocarriers.[9] The latter are nanoparticulate systems able to facilitate the passage of their cargo through the stratum corneum to the viable epidermis and dermis.

An additional strategy to improve the efficacy of topical finasteride could be its combination with natural active ingredients with complementary activity.[10] Among others, baicalin[11] has attracted the attention of the scientific community due to its potential ability to promote hair growth.[12–14] In addition, it possesses other beneficial properties, such as antioxidant,[15] antitumor,[3] anti-inflammatory,[17] and antibiofilm activity against *S. saprophyticus* infections.[18] Baicalin is extracted from the roots of Scutellaria baicalensis Georgi, which has been officially listed in the Chinese Pharmacopeia and was introduced in European Pharmacopoeia (9th Edition). Thanks to its high biocompatibility and promising activity on hair growth, baicalin can be considered a potential adjuvant to finasteride in the local treatment of hair loss and alopecia. Both finasteride and baicalin belong to Class II in the biopharmaceutical classification system,[19] as they show low aqueous solubility and permeability,20 which may limit their topical application. The loading of finasteride and baicalin in ad hoc formulated phospholipid vesicles can help to overcome these drawbacks by improving their local bioavailability.[21] Phospholipid vesicles are regarded as the most promising nanosystems for the delivery of a wide range of drugs. Thanks to their peculiar structure and versatility, they are able to incorporate both hydrophilic and lipophilic molecules, ensuring an

efficient co-delivery of different molecules. Moreover, phospholipid vesicles are highly biocompatible, safe, and capable of facilitating the passage of the payload through the stratum corneum, improving the accumulation in the deeper skin strata and the delivery at follicular level.[22] In addition, due to their composition similar to that of cellular membranes, the phospholipid vesi-cles are able to promote the interaction with cells and the release of the payload in the cytoplasm where the beneficial activity is exerted.

Recently, many authors have underlined the importance of the composition of phospholipid vesicles to their performance as topical delivery systems. New vesicles have been developed, such as transfersomes, also called ultradeformable liposomes, capable of squeezing through the intercellular spaces of the stratum corneum;[22,23] ethosomes, elastic vesicles containing high amounts of ethanol;[24,25] penetration enhancer-containing vesicles (PEVs);[26,27] glycerosomes, containing high amounts of glycerol,[28] capable, as well as PEVs, of enhancing the delivery of drugs to the skin;[29] and hyalurosomes, vesicles immobilized in a sodium hyaluronate network.[30,31]

In the present study, finasteride and baicalin were co-loaded in liposomes, hyalurosomes, glycerosomes and glycerol-hyalurosomes, while liposomes loaded with finasteride or baicalin individually were used as references. The vesicles were characterized and their ability to promote hair growth was evaluated both *in vitro*, by using human hair follicle dermal papilla cells, and *in vivo*, by applying the vesicle formulations on the shaved back skin of C57BL/6 mice.[32]

Material and methods.

Materials.

Lipoid® S75, a mixture of soybean lecithin, was a gift from Lipoid GmbH (Ludwigshafen, Germany). Disodium phosphate was purchased from Scharlab S.L. (Barcelona, Spain). Monosodium phosphate was obtained from Panreac quimica S.A. (Barcelona, Spain). Baicalin was purchased by Cymit química S.L. (Barcelona, Spain). Finasteride was purchased from Farmalabor Srl (Canosa di Puglia, Italy). Sodium Hyaluronate was purchased from DSM Nutritional Products AG Branch Pentapharm (Switzerland). Tetrazolium salt, 3-(4,5-dimethylthiazol-2-yl)-2,5-diphenyltetrazolium bromide (MTT), glycerol and all the other reagents of analytical grade were purchased from Sigma- Aldrich (Milan, Italy).

Vesicle preparation.

The phospholipid vesicles were prepared by hydration of lipid components, sonication and extrusion (when necessary), avoiding the use of organic solvents.[33] Briefly, Lipoid® S75 (210 mg mL^{-1}), baicalin (10 mg mL^{-1}) and finasteride (2.5 mg mL^{-1}) were weighed in a glass vial and hydrated overnight with PBS (pH 7.4) to obtain liposomes, with glycerol and PBS (1 : 1 v/v) to obtain glycerosomes, with an aqueous solution of sodium hyaluronate (0.1% w/v) to obtain hyalurosomes, or with a mixture of glycerol and 0.2% sodium hyaluronate solution (1 : 1 v/v) to obtain glycerol-hyalurosomes. Empty liposomes and liposomes loaded with finasteride or baicalin individually were prepared and used as references, to evaluate the effect of the payloads on vesicle assembly. All the dispersions were sonicated (25 cycles, 5 seconds on and 5 seconds off) with a Soniprep 150 ultrasonic disintegrator (MSE Crowley, London, UK) in

order to obtain small and homogeneous vesicles. Liposomes loaded with finasteride or baicalin individually were then extruded through a 200 nm membrane (Whatman, GE Healthcare, Fairfield, Connecticut, US) by using an Avanti® Mini-Extruder (Avanti Polar Lipids, Alabaster, AL, US) to improve the homogeneity of the dispersions.

Analytical methods.

Finasteride and baicalin were quantified by HPLC using a PerkinElmer® Series 200 equipped with a UV detector and a column Teknokroma® Brisa "LC2" C18, 5.0 µm (150 × 4.6 mm). Finasteride was quantified at 245 nm by using a mixture of water and methanol (75 : 25) as mobile phase, delivered at a flow rate of 1 mL min^{-1}. The limit of detection for finasteride was 5 µg and the limit of quantification was 15 µg mL^{-1}.

Baicalin content was measured at 278 nm by using a mixture of water and methanol (30 : 70) as mobile phase, delivered at a flow rate of 1 mL min^{-1}. The limit of detection for baicalin was 0.45 µg and the limit of quantification was 1.36 µg mL^{-1}.

Vesicle characterization

Vesicle formation and morphology were evaluated by cryo-TEM observation. A thin film of each sample was formed on a holey carbon grid and vitrified by plunging (kept at 100% humidity and room temperature) into ethane maintained at its melting point, using a Vitrobot (FEI Company, Eindhoven, Netherlands). The vitreous films were transferred to a Tecnai F20 TEM (FEI Company), and the samples were observed in a low-dose mode. Images were acquired at 200 kV at a temperature of −173 °C, using a CCD Eagle camera (FEI Company).

The average diameter and polydispersity index of the vesicle dispersions were determined by Photon Correlation Spectroscopy using a Zetasizer nano-ZS (Malvern Instruments, Worcestershire, UK). Zeta potential was estimated by using the Zetasizer nano-ZS by electrophoretic light scattering, which measures the particle electrophoretic mobility in a thermostated cell. All the measurements were performed after dilution (1 : 100) of the samples with PBS.[34]

The stability of vesicles was evaluated for 30 days at room temperature (25 °C). During this period, size, size distribution and surface charge were measured.

To evaluate the amount of finasteride and baicalin loaded into the vesicles, the samples (2 mL) were transferred into Spectra/Por® membranes (12–14 kDa MW cut-off; Spectrum Laboratories Inc., DG Breda, The Netherlands) and dialyzed against buffer (2 L) for 4 h, at room temperature (~25 °C) with water refreshed every hour to allow the complete removal of the non-entrapped molecules. Both non-dialyzed and dialyzed vesicles were disrupted with methanol (1 : 100) and analysed by HPLC (see analytical methods section) to quantify finasteride and baicalin contents. The entrapment efficiency (EE) was calculated as a percentage as follows (eqn (1)):

$$EE\ (\%) = [(\text{actual drug}) / (\text{initial drug})] \cdot 100 \qquad \text{(Eqn. 1)}$$

where actual drug is the amount of finasteride or baicalin detected in vesicles after dialysis, and initial drug is that before dialysis.

In vitro evaluation of cytotoxicity and cell proliferation.

Hair follicle dermal papilla cells (HFDPC, Cell Applications Inc., San Diego, CA, US) were grown as monolayers in 75 cm2 flasks and incubated at 37 °C in a controlled atmosphere containing 5% CO2 and 100% humidity. The growth medium (Cell Applications Inc., San Diego, CA, US) specific for hair follicle dermal papilla cells, supplemented with penicillin (100 U mL^{-1}) and streptomycin (100 mg mL^{-1}) (Sigma Aldrich, Spain), was used to culture them.

In order to evaluate the cytotoxicity of the formulations, the cells (5.5 × 10^4 cell per mL), at passage 2, were seeded in 96-well plates with 250 µL of culture medium. After 24 h, the cells were treated with the formulations at different dilutions (corresponding to concentrations of finasteride ranging from 800 to 0.390 µg mL^{-1} and baicalin ranging from 3200 to 1.56 µg mL^{-1}) for 48 h (n = 8). Untreated cells were used as a negative control. Non-cytotoxic concentrations (finasteride from 6.25 to 0.390 µg mL^{-1} and baicalin from 25 to 1.56 µg mL^{-1}) were then used to evaluate the effect of the formulations on the promotion of cell proliferation. The cells were treated with the formulations for 48 h (n = 8). Untreated cells were used as a negative control.

At the end of each experiment (cytotoxicity and proliferation), the cells were washed three times with PBS and their viability was determined by means of the MTT [3(4,5-dimethyl-thiazolyl-2)-2,5-diphenyltetrazolium bromide] colorimetric assay, adding 100 µL of MTT reagent (0.5 mg mL^{-1} in PBS, final concentration) to each well. After 3 h, the formed formazan crystals were dissolved in dimethyl sulfoxide. The reaction was spectrophotometrically measured at 570 nm with a microplate reader (Multiskan EX, Thermo Fisher Scientific, Inc., Waltham, MA, US).

Results were reported as a percentage of cell proliferation in comparison with untreated control cells (100% viability) according to eqn (2):

$$\text{Cell proliferation } (\%) = \left({}^{\text{Absorbance}_{\text{sample}}} \Big/ _{\text{Absorbance}_{\text{control}}} \right) \cdot 100$$

(Eqn. 2)

where $\text{Absorbance}_{\text{sample}}$ is the absorbance of treated cells and $\text{Absorbance}_{\text{control}}$ is the absorbance of untreated cells (100% viability), measured at 570 nm.

In vivo study design.

Healthy six-week-old C57BL/6 female mice (18–20 g) were used for the *in vivo* experiments. All studies were performed in accordance with European Union regulations for the handling and use of laboratory animals and the protocols were approved by the Institutional Animal Care and Use Committee of the University of Valencia (Code 2019/VSC/PA/0113 type 2). The number and suffering of the animals were kept to the minimum. In C57BL/6 mice, hair follicle morphogenesis and growth cycle follow a rather precise time-scale. However, the process is dependent on various factors, such as genetic background (mice strain) and sex (female mice show a prolonged telogen), among others. To avoid fluctuations in the results, *in vivo* experiments were based on the highly standardized C57BL/ 6 model of depilation-induced hair follicle cycling.[1]

Mice were divided into 10 groups (n = 5 per group) and the hairs, in telogen phase, on the dorsal area were gently shaved 24 h before treatment. On day 1, 100 µL of sample was topically smeared over the shaved dorsal site under non-occlusive conditions. The tested samples were finasteride and

baicalin co-loaded liposomes, glycerosomes, hyalurosomes and glycerol-hyalurosomes, along with finasteride dispersion, baicalin dispersion, finasteride loaded liposomes and baicalin loaded liposomes used as references. The procedure was repeated once per day during 21 days of experiment. On the final day, the mice were sacrificed by cervical dislocation. During the application period, differences between treated and non-treated groups in terms of average body weight or presence of abnormalities were checked.

Evaluation of *in vivo* hair growth. Skin pigmentation was taken as evidence of hair growth, as it is bright pink in the telogen phase and turns into grey or black in the anagen phase.[16] Hair length was determined on days 12, 16 and 21 from the same shaved area of all mice, by choosing 10 hairs to measure and calculate the mean length. The results were shown as average length ± standard deviation. The cyclic phase of hair follicles (anagen and telogen), along with the anagen percentage (eqn (3)) were determined by using an ocular micrometer:

$$\%\ \text{anagen} = \left(\text{number of hair in anagen phase} / \text{number total of hairs}\right) \cdot 100$$

(Eqn. 3)

The enhancing effect of the different treatments was also estimated (Eq. 4) as an indicator of the ability of the nanoformulations to improve hair growth in comparison with untreated group.

$$\text{Enhancing effect (EE)} = \text{treated mice hair lenght} / \text{control mice hair length}$$

(Eq. 4)

Histological observation of hair follicles. Mice skin treated with the tested formulations was excised, fixed and stored in 10% formaldehyde until use. Tissue specimens were processed routinely and embedded in paraffin. Transversal sections (5 µm) were stained with haematoxylin and eosin and observed under a light microscope (Leica DM3000, Leica-Microsystems, Wetzlar, Germany). Number and diameter of follicles in the different groups were also measured through Image Pro plus 7.0, Media Cybernetics.

Statistical analysis of data.

Data are shown as means ± standard deviations. Statistical differences were determined by using one-way ANOVA test and Tukey´s test for multiple comparisons with a significance level of $p < 0.05$. All statistical analyses were performed using IBM SPSS statistics 22 for Windows (Valencia, Spain).

Results.

Vesicle characterization.

Cryo-TEM images disclosed that liposomes, used as a reference, were spherical and unilamellar (Fig. 1A). The addition of glycerol and/or hyaluronan led to the formation of spherical, oligo-multilamellar vesicles (Fig. 1B–D). Multivesicular structures were detected in glycerosomes and glycerol-hyalurosomes (Fig. 1B and D).

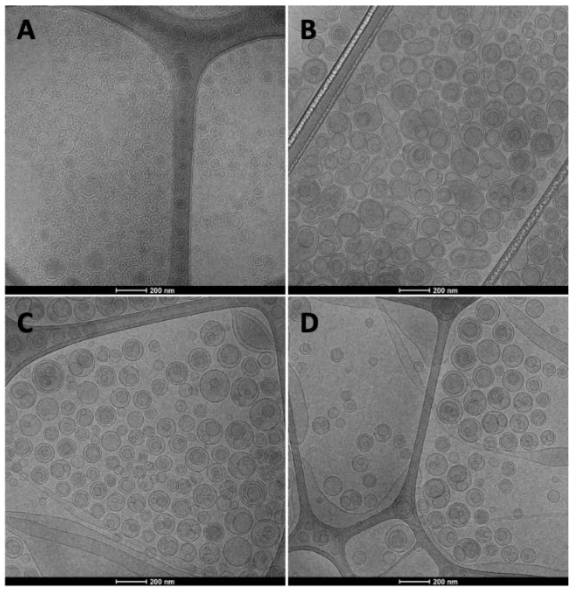

Figure 1. Representative cryo-TEM photographs of finasteride and baicalin co-loaded liposomes (A), glycerosomes (B), hyalurosomes (C) and glycerol-hyalurosomes (D). Bars correspond to 200 nm.

The size of the nanovesicles plays an important role, especially when they are specifically tailored for topical or follicular application. Indeed, it has been reported that follicular penetration of nanovesicles increases as their size decreases.[35]

Given that, and aiming at achieving a deep follicular pene-tration, small-sized vesicles, ranging from 65 to 110 nm, were prepared (Fig. 2). The mean diameter of empty liposomes (used as a reference) was ∼80 nm, with a low polydispersity index (0.18) and a negative zeta potential (−31 mV). The loading of finasteride did not affect the mean diameter of liposomes, but led to an increase in the polydispersity index. The loading of baicalin led to a decrease in the mean diameter and the polydispersity

index (Fig. 2). The simultaneous loading of finasteride and baicalin caused an increase in mean diameter and polydispersity index, and the zeta potential was much less negative (−13 mV), denoting an important impact of the co-loading, probably due to the distribution of both molecules in the vesicle bilayer and on the surface. The addition of glycerol and/or hyaluronan did not affect the physico-chemical features of the vesicles. Indeed, no significant differences were detected in comparison with co-loaded liposomes and between the samples ($p > 0.05$). Glycerosomes, hyalurosomes and glycerol-hyalurosomes were able to incorporate finasteride and baicalin in the same amounts, similarly to co-loaded liposomes (reference), as the entrapment efficiency was ∼80% for both molecules. The entrapment efficiency decreased when using finasteride alone or baicalin alone (∼65%). The nanovesicles showed a good stability at room temperature, as no significant changes were detected after 30 days on storage at room temperature (∼25 °C).

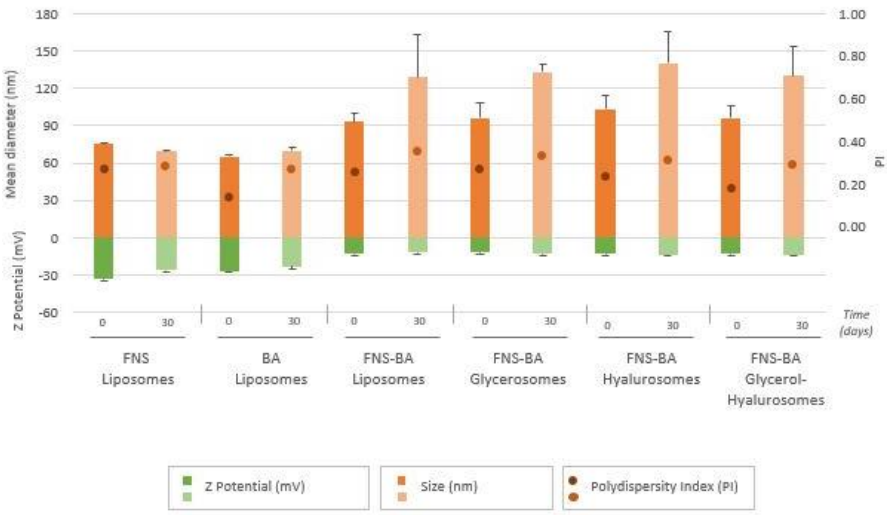

Figure 2. Mean diameter (MD), polydispersity index (PI) and zeta potential (ZP) values of finasteride (FNS) and baicalin (BA) loaded nanovesicles over 30 days of storage at room temperature (~25°C). Values correspond to means ± standard deviations (n=3).

In vitro cytotoxicity assay.

The biocompatibility of the formulations was evaluated by incubating hair follicle dermal papilla cells with samples at different dilutions (corresponding to concentrations of finasteride ranging from 800 to 0.390 μg mL^{-1} and baicalin ranging from 3200 to 1.56 μg mL^{-1}) for 48 h (Figure 3). The effect of finasteride or baicalin in dispersion or loaded individually in liposomes on the viability of papilla cells was concentration dependent: the viability was less than 50% when the lower dilutions (i.e., higher concentrations) were used, while the viability was always ≥100% when using higher dilutions (i.e., lower concentrations: ≤12.5 μg mL^{-1} of finasteride and ≤50 mg/mL of baicalin). The effect of finasteride and

baicalin co-loaded glycerosomes and hyalurosomes was very similar to that of liposomes, while it was found that glycerol-hyalurosomes, at dilutions corresponding to finasteride concentrations ≥6.3 μg mL^{-1} and baicalin ≥25 μg mL^{-1}, stimulated cell proliferation leading to ~179% viability.

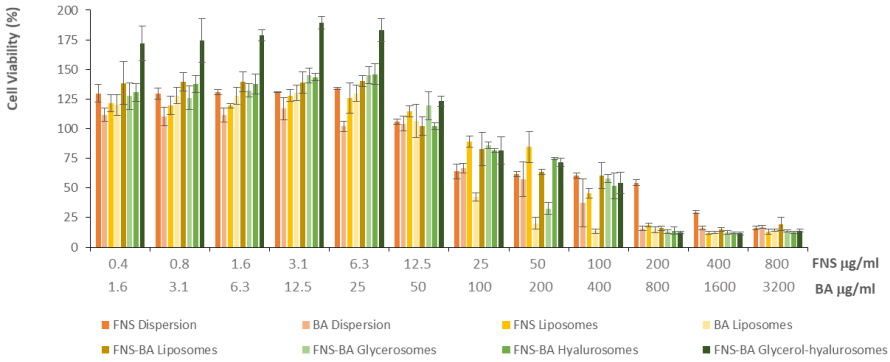

Figure 3. Viability of hair follicle dermal papilla cells after 48 h of incubation with formulations at different dilutions. Finasteride (FNS) dispersion and baicalin (BA) dispersion were used as references along with finasteride loaded liposomes and baicalin loaded liposomes. Bars represent mean values ± standard deviations (n=8)

In vitro cell proliferation assay.

Dermal papilla cells are considered the main responsible for controlling hair growth, and their proliferation can positively affect the process. Given that, the ability of the formulations to promote the proliferation of these cells, as a growth-related parameter, was investigated by using only non-cytotoxic dilutions (Figure 4). At these dilutions, finasteride and baicalin co-loaded into glycerol-hyalurosomes were able to stimulate cell growth to a greater extent (~179% viability) than the dispersions or the other vesicles, and irrespective of the concentration used ($p<0.05$ versus

untreated cells). The efficacy of both finasteride and baicalin co-loaded in phospholipid vesicles was compared with that of these molecules in dispersion or loaded individually in liposomes, in order to understand the positive contribution provided by both carrier and co-loading. The viability of the cells treated with the dispersions was ~122% using finasteride in dispersion or loaded in liposomes, and ~115% using baicalin in dispersion or loaded in liposomes. The co-loading in liposomes, glycerosomes and hyalurosomes led to a slight increase in cell proliferation (~132% viability without significant differences between these formulations), while the co-loading in glycerol-hyalurosomes significantly promoted the proliferation, as the cell viability reached ~179%. These results underline a synergistic effect of finasteride and baicalin on cell proliferation and an additional contribution of the glycerol-hyalurosomes on the achievement of the therapeutic efficacy. This can be mainly connected with their optimal carrier ability, which seems to be potentiated by the simultaneous presence of glycerol and sodium hyaluronate in phospholipid vesicles.

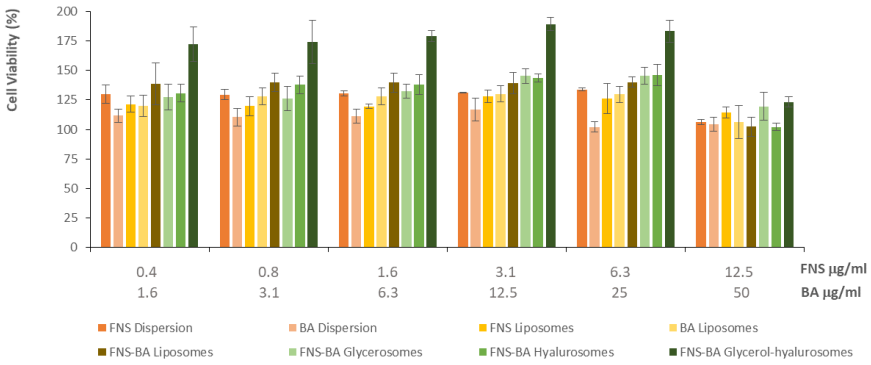

Figure 4. Effect of finasteride and baicalin co-loaded nanovesicles on proliferation of hair follicle dermal papilla cells after 48 h of treatment by using non-cytotoxic concentrations. Finasteride (FNS) dispersion and baicalin (BA) dispersion were used as references, along with finasteride

loaded liposomes and baicalin loaded liposomes. Bars represent the means ± standard deviations (n=8).

In vivo determination of hair length and anagen percentage.

In vivo studies were performed by using C57BL/6 mice, which represent an ideal model to avoid fluctuations of results. The differences in hair growth and colour for each treated group was evaluated by visual inspection on days 12, 16 and 21 of treatment. The shaved area of all mice appeared pink on day 0, and the re-growth of dark hair was clearly visible on day 21 (Figure 5). After 12 days, the finasteride or the baicalin in dispersion stimulated a moderate hair growth, which was more evident than that observed in untreated mice, but less than that provided by finasteride and baicalin loaded individually in liposomes. The co-loading of finasteride and baicalin in hyalurosomes and glycerol-hyalurosomes further improved the hair growth. On days 16 and 21, there were no significant differences between the treatments ($p > 0.05$), as the shaved area of all treated mice was completely covered by new hairs.

The length of the hair was also measured during the experiment to better evaluate the differences among the treatments (Table 1). On day 16, only finasteride and baicalin co-loaded glycerosomes, hyalurosomes and glycerol-hyalurosomes led to a significant improvement of the growth of hairs, with respect to untreated mice ($p < 0.01$). On day 21, all the treatments provided an increase in hair length (Enhancing effect, EE), especially using glycerol-hyalurosomes, which doubled the growth rate as compared to control untreated mice (EE= 2.1; Table 1). In addition, the anagen phase of hair follicles was immediately induced in the shaved area by using these formulations (Table 1) [36]. After the completion of the anagen phase, the other phases (catagen and telogen phases) started

spontaneously in a fairly homogeneous manner. The growth stages of hairs can be also detected by the colour of the skin, which became darker during the anagen phase because of the presence of melanocytes in hair follicles and the production of melanin, which in turn has an important role in controlling the cycle of hair growth. At the beginning of the experiment, immediately after the shaving procedure, the skin was pinkish, which is the characteristic colour of the telogen phase; during the treatment with the formulations, the colour of the skin surface turned to grey, which is the colour of the anagen phase [12]. The anagen phase started sooner when the mice were treated with the nanovesicles, as confirmed by visual inspection: the colour of the skin changed from pinkish to black due to an acceleration in hair growth rate.

Table 1. Hair length on days 12, 16 and 21, enhancing effect (EE) and hair anagen percentage (% anagen) on day 21 (n=10), recorded for each group of mice treated with finasteride (FNS) or baicalin (BA) co-loaded vesicles or finasteride dispersion and baicalin dispersion or finasteride loaded liposomes and baicalin loaded liposomes. The results are shown as means ± standard deviations (n=5).

Treatment	Hair Length (mm)			EE	% anagen
	Day 12	Day 16	Day 21	Day 21	Day 21
Control/ untreated	-	3.6±0.4	5.7±0.7	1	45
FNS Dispersion	-	5.1±0.4	6.5±0.9	1.1	55
BA Dispersion	-	4.2±0.5	7.2±1.1	1.3	70
FNS Liposomes	2.4±0.9	5.2±0.8	8.1±1.1	1.4	55
BA Liposomes	2.6±0.9	4.1±0.4	7.1±1.3	1.2	40
FNS-BA Liposomes	3.4±0.4	5.0±0.7	10.1±0.9	1.7	90
FNS-BA Glycerosomes	3.7±0.8	5.7±0.7	9.8±1.8	1.7	80
FNS-BA Hyalurosomes	4.3±0.4	8.6±0.7	9.9±1.4	1.7	75
FNS-BA Glycerol-hyalurosomes	3.6±0.5	7.4±1.1	12.1±1.6	2.1	80

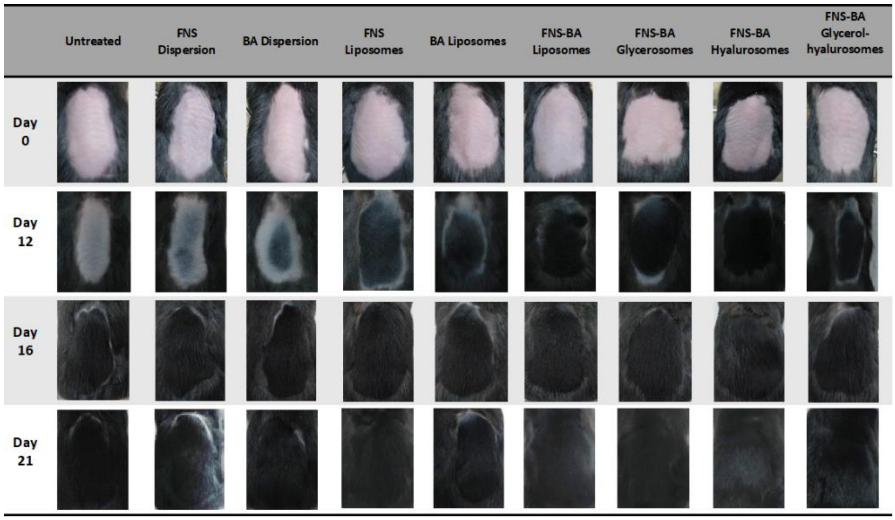

Figure 5. Representative images of dorsal skin of C57BL/6 shaved mice on day 0 and after 12, 16 and 21 days of topical treatment with finasteride (FNS) and baicalin (BA) co-loaded in phospholipid nanovesicles or finasteride dispersion and baicalin dispersion or finasteride loaded liposomes and baicalin loaded liposomes used as references

Measurement of the number and diameter of follicles.

Hair follicles are intimately connected with hair disorders: the higher the hair follicle number, the better the hair growth promotion. For this reason, the number and diameter of hair follicles were measured after 21 days of treatment. No significant differences were detected for the diameter of the follicles among the different groups versus control ($p > 0.05$). This parameter was not affected by the treatments with the formulations (data not shown). On the contrary, the number of follicles was significantly increased when the mice were treated with finasteride and baicalin co-loaded in the nanovesicles (Figure 6). The treatment with finasteride or baicalin loaded individually in liposomes led to a slight increase in the

number of follicles, which points to a crucial contribution provided by the co-loading.

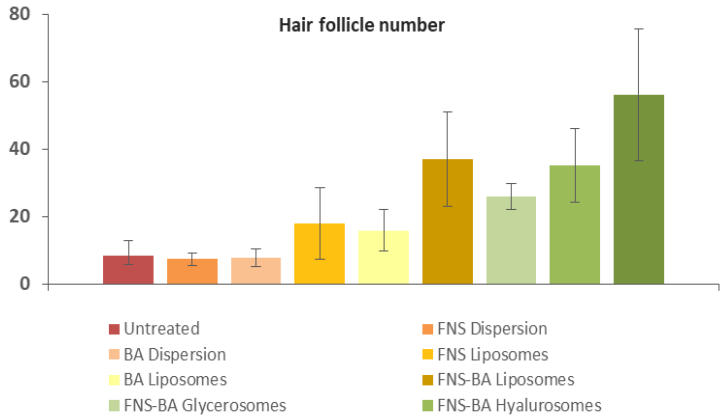

Figure 6. Number of hair follicles in C57BL/6 mice after 21 days of treatment with finasteride (FNS) or baicalin (BA) co-loaded vesicles or finasteride dispersion and baicalin dispersion or finasteride loaded liposomes and baicalin loaded liposomes. Values are presented as means ± standard deviations (n=5).

Histological observation of hair follicles.

In order to confirm the efficacy of the phospholipid vesicles in promoting hair growth, the dorsal skin of mice treated with the different formulations was excised, stained with haematoxylin and eosin, and observed under a light microscope. The morphological differences of the skin treated with finasteride and baicalin co-loaded vesicles were evaluated and compared with untreated skin and skin treated with finasteride in dispersion or loaded in liposomes and baicalin in dispersion or loaded in liposomes (Figure 7). Histological results confirmed the promoting effect of the co-

loading of finasteride and baicalin in all the vesicles in increasing the number of follicles in C57BL/6 mice.

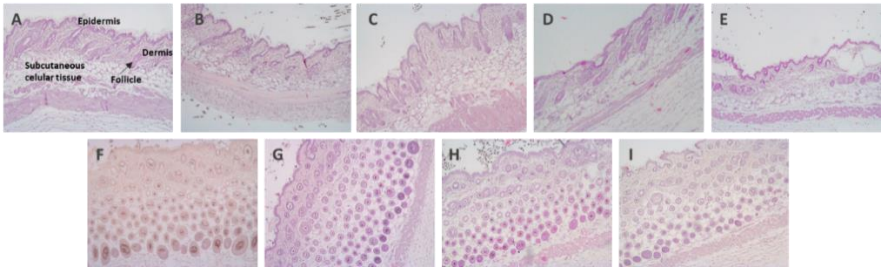

Figure 7. Representative images of histological sections of mouse skin: untreated skin (A); skin treated with finasteride dispersion (B), baicalin dispersion (C), baicalin loaded liposomes (D), finasteride loaded liposomes (E), finasteride and baicalin co-loaded liposomes (F), glycerosomes (G), hyalurosomes (H) and glycerol-hyalurosomes (I). All images were taken at 10x magnification.

Discussion.

Considering the great number of patients affected by hair loss and alopecia and the lack of effective therapies, often associated with undesired side effects, in this work, glycerosomes, hyalurosomes and glycerol-hyalurosomes specifically tailored for the simultaneous delivery of finasteride and baicalin were developed and tested [37,38]. The use of phospholipid vesicles for the treatment of skin disorders seems to be a good strategy, as these nanocarriers can enhance skin bioavailability, penetration depth, and prolong the residence time of the payload [21]. Nanocarriers are also considered good candidates for the treatment of follicle diseases, such as hair loss or alopecia, as they may deliver the therapeutic agents specifically to the follicular area, improving their efficacy [22]. Finasteride and baicalin co-loaded liposomes, finasteride

loaded liposomes and baicalin loaded liposomes were used as references to better evaluate the effect of additives (i.e., glycerol and/or sodium hyaluronate) in phospholipid vesicles and the efficacy of the single therapeutic agents (i.e., finasteride and baicalin).

Among the newest phospholipid vesicles developed in the last years, glycerosomes and hyalurosomes seemed to be the most appropriate for skin delivery [30,39]. Moreover, in this work, for the first time, sodium hyaluronate and glycerol were combined to obtain the so-called glycerol-hyalurosomes. The combination of the co-solvent and the polymer strengthened the effectiveness of the single components, presumably because glycerol-hyalurosomes, by being highly viscous, were capable of staying in the application site for a prolonged time during which glycerol can modify the ordered structure of the stratum corneum allowing the diffusion of the vesicles, while sodium hyaluronate, by interacting with dermal papilla cells, can stimulate their proliferation and the hair growth cycle. Further, the ability of these vesicles to interact with cells ensures the entry of the payloads in the cytoplasm, where the therapeutic activity is exerted.

Finasteride is a drug widely used for the treatment of androgenetic alopecia but, because of the numerous side effects associated with the oral use, the long-term treatment is generally avoided, thus resulting in an ineffective therapeutic response [40]. In particular, the oral administration of finasteride (1 mg/day) resulted to be effective in men [41] and less in women [42]. The use of higher doses in women represents a possible alternative, which still is controversial and deserves further investigation [43]. The delivery of finasteride by phospholipid vesicles can represent a valuable alternative to ensure topical efficacy and avoid the side effects

associated with oral administration [44]. In addition, the therapeutic efficacy of drugs can be potentiated by their association with natural adjuvants with complementary properties. Baicalin is a natural and safe active molecule capable of controlling and promoting hair growth [12], thus it can be used to improve the local efficacy of finasteride. Our results confirmed that the co-loading of finasteride and baicalin accelerated the anagen phase and hair growth rate, as well as the number of follicles in treated mice, as compared to finasteride or baicalin loaded individually in liposomes. On the other hand, the co-loading was not as relevant to stimulating the proliferation of papilla cells *in vitro.*

The use of modified phospholipid vesicles (glycerosomes, hyalurosomes and glycerol-hyalurosomes) was expected to improve the skin and follicular delivery of the payloads [44]. Previous works reported the importance of the lamellarity and size of vesicles as key factors for the improvement of both bioavailability at skin and follicular levels and therapeutic efficacy of loaded drugs [45]. According to this, the mean diameter of the prepared vesicles was around 100 nm. Liposomes and hyalurosomes were mainly unilamellar and oligomellar and the number of lamellae increased in glycerosomes and glycerol-hyalurosomes, probably due to the presence of glycerol [46]. Previous studies disclosed optimal performances of ethosomes in favouring percutaneous absorption of finasteride, especially into the dermis layer [47,48], thanks to the moisturizing properties of ethanol. In the present study, the phospholipid vesicles were modified with glycerol and/or sodium hyaluronate. The former is a trihydroxy alcohol widely used in dermatological preparations for its hydrating and moisturizing properties [49], which can induce significant changes in the mechanical properties of human skin *in vivo,* even after a 10-min application [50]. Sodium hyaluronate is a naturally-occurring

polyanionic polysaccharide present in the intercellular matrix of vertebrate connective tissues. It is present in the skin where it plays protective, stabilizing and shock-absorbing functions [51]. The combination of these components in phospholipid vesicles can improve skin hydration, facilitating the passage of intact vesicles to the dermis and follicles. In addition, they made the dispersions more viscous, facilitating the topical application, avoiding the loss of material and prolonging its residence time on the application site. Our results demonstrate that glycerol-hyalurosomes were able to promote the complete growth of hair in the shaved area of C57BL/6 mice at a faster rate than the other vesicles, besides providing a significant increase in hair length (12.1±1.6 mm on day 21) and number of follicles. Therefore, the association of phospholipid, glycerol and sodium hyaluronate maximized the performances of the nanovesicles in the *in vivo* co-delivery of finasteride and baicalin. Moreover, glycerol-hyalurosomes were also the most effective formulation in promoting the growth of dermal papilla cells *in vitro*, which can positively affect hair growth process.

Conclusions.

The results suggest that the co-loading of finasteride and baicalin in phospholipid vesicles can improve their efficacy against hair loss, but only if the vesicles are properly formulated. Indeed, when finasteride and baicalin were co-loaded in glycerol-hyalurosomes, hair follicle dermal papilla cells were stimulated to proliferate, hair growth was accelerated, and the number of follicles was increased in treated mice. These effects seem to be adequate to ensure the efficacy of the local treatment of hair loss and androgenetic alopecia.

References.

1. Y. Zhang, L. Han, S. S. Chen, J. Guan, F. Z. Qu and Y. Q. Zhao, Biomed. Pharmacother., 2016, 83, 641–647.

2. Z. Santos, P. Avci and M. R. Hamblin, Expert Opin. Drug Discovery, 2015, 10, 269–292.

3. L. Dong, H. Hao, L. Xia, J. Liu, D. Ti, C. Tong, Q. Hou, Q. Han, Y. Zhao, H. Liu, X. Fu and W. Han, Sci. Rep., 2014, 4, 5432.

4. S. Müller-Röver, K. Foitzik and R. Paus, B. H.-J. of I. and undefined, Elsevier, 2001.

5. J. Ocampo-Garza, J. Griggs and A. Tosti, Expert Opin. Invest. Drugs, 2019, 28, 275–284.

6. Y. Feng, L. Ma, X. Li and W. Ding, X. C.-B. & Pharmacotherapy and undefined, Elsevier, 2017.

7. M. Górecki, A. Dziedzic and R. Luboradzki, A. O.-Steroids and undefined, Elsevier, 2017.

8. N. Rattanachitthawat, T. Pinkhien, P. Opanasopit, T. Ngawhirunpat and P. Chanvorachote, In Vivo, 2019, 33, 1209–1220.

9. M. Z. U. Khan, S. A. Khan, M. Ubaid, A. Shah, R. Kousar and G. Murtaza, Curr. Drug Delivery, 2018, 15, 1100–1111.

10. A.-M. Hosking, M. Juhasz and N. A. Mesinkovska, Skin Appendage Disord., 2018, 5, 72–89.

11. G. Jakab, D. Bogdán, K. Mazák, R. Deme, Z. Mucsi, I. M. Mándity, B. Noszál, N. Kállai-Szabó and I. Antal, AAPS PharmSciTech, 2019, 20, 314.

12. S. H. Shin, S. S. Bak, M. K. Kim, Y. K. Sung and J. C. Kim, Naunyn-Schmiedeberg's Arch. Pharmacol., 2015, 388, 583– 586.

13. F. Xing, W. J. Yi, F. Miao, M. Y. Su and T. C. Lei, Int. J. Mol. Med., 2018, 41, 2079–2085.

14. A. R. Kim, S. N. Kim, I. K. Jung, H. H. Kim, Y. H. Park and W. S. Park, Planta Med., 2014, 80, 153–158.

15. Y. Qian, Y. Chen and L. Wang, J. T.-A. cirurgica brasileira and undefined, SciELO Bras, 2018.

16. C. Gao, Y. Zhou, H. Li, X. Cong, Z. Jiang, X. Wang, R. Cao and W. Tian, Mol. Med. Rep., 2017, 16, 8729–8734.

17. S. Mir-Palomo, A. Nácher, O. Díez-Sales, O. M. A. Vila Busó, C. Caddeo, M. L. Manca, M. Manconi, A. M. Fadda and A. R. Saurí, Int. J. Pharm., 2016, 511, 23–29.

18. J. Wang, H. Jiao, J. Meng, M. Qiao, H. Du, M. He, K. Ming, J. Liu, D. Wang and Y. Wu, Front. Microbiol., 2019, 10, 2800.

19. T. Ahmed, M. K.-E. J. of P. Sciences and undefined, Elsevier, 2016.

20. R. El-Gogary and S. Gaber, M. N.-S. reports and undefined, nature.com, 2019.

21. H. A. E. Benson, J. E. Grice, Y. Mohammed, S. Namjoshi and M. S. Roberts, Curr. Drug Delivery, 2019, 16, 444–460.

22. C. L. Fang, I. A. Aljuffali, Y. C. Li and J. Y. Fang, Ther. Delivery, 2014, 5, 991–1006.

23. A. Zeb, O. Qureshi and H. Kim, J. C.-I. journal of and undefined, ncbi.nlm.nih.gov, 2016.

24. M. L. Manca, I. Usach, J. E. Peris, A. Ibba, G. Orrù, D. Valenti, E. Escribano-Ferrer, J. C. Gomez-Fernandez, F. J. Aranda, A. M. Fadda and M. Manconi, Pharmaceutics, 2019, 11, 263.

25. A. Ascenso, S. Raposo, C. Batista, P. Cardoso, T. Mendes, F. G. Praça, M. V. Bentley and S. Simões, Int. J. Nanomed., 2015, 10, 5837–5851.

26. I. Castangia, M. L. Manca, C. Caddeo, A. Maxia, S. Murgia, R. Pons, D. Demurtas, D. Pando, D. Falconieri, J. E. Peris, A. M. Fadda and M. Manconi, Colloids Surf., B, 2015, 132, 185–193.

27. M. Manconi, F. Marongiu, M. L. Manca, C. Caddeo, G. Sarais, C. Cencetti, L. Pucci, V. Longo, G. Bacchetta and A. M. Fadda, Int. J. Pharm., 2017, 523, 159–166.

28. M. L. Manca, C. Cencetti, P. Matricardi, I. Castangia, M. Zaru, O. D. Sales, A. Nacher, D. Valenti, A. M. Maccioni, A. M. Fadda and M. Manconi, Int. J. Pharm., 2016, 511, 198–204.

29. N. Bavarsad, A. Akhgari, S. Seifmanesh, A. Salimi and A. Rezaie, Daru, J. Pharm. Sci., 2016, 24, 7.

30. M. L. Manca, I. Castangia, M. Zaru, A. Nácher, D. Valenti, X. Fernàndez-Busquets, A. M. Fadda and M. Manconi, Biomaterials, 2015, 71, 100–109.

31. I. Castangia, C. Caddeo, M. L. Manca, L. Casu, A. C. Latorre, O. Díez-Sales, A. Ruiz-Saurí, G. Bacchetta, A. M. Fadda and M. Manconi, Carbohydr. Polym., 2015, 134, 657–663.

32. V. Truong, M. Bak, C. Lee and M. Jun, W. J.- Molecules and undefined, mdpi.com, 2017.

33. M. Manconi, J. Aparicio, A. O. Vila, J. Pendás, J. Figueruelo and F. Molina, Colloids Surf., A, 2003, 222, 141–145.

34. A. Catalan-Latorre, M. Ravaghi, M. L. Manca, C. Caddeo, F. Marongiu, G. Ennas, E. Escribano-Ferrer, J. E. Peris, O. Diez-Sales, A. M. Fadda and M. Manconi, Eur. J. Pharm. Biopharm., 2016, 107, 49–55.

35. E. Abd, M. S. Roberts and J. E. Grice, Skin Pharmacol. Physiol., 2016, 29, 24–30.

36. R. Sennett and M. Rendl, Semin. Cell Dev. Biol., 2012, 23, 917–927.

37. L. L. Levy and J. J. Emer, Int. J. Women's Health, 2013, 5, 541–556.

38. S. Arias-Santiago, A. Buendía-Eisman, M. T. Gutiérrez- Salmerón and S. Serrano-Ortega, in Handbook of Hair in Health and Disease, MDText.com, Inc., 2012, pp. 99–116.

39. M. L. Manca, M. Manconi, M. Zaru, D. Valenti, J. E. Peris, P. Matricardi, A. M. Maccioni and A. M. Fadda, Int. J. Pharm., 2017, 532, 401–407.

40. S. W. Lee, M. Juhasz, P. Mobasher, C. Ekelem and N. A. Mesinkovska, J. Drugs Dermatol., 2018, 17, 457–463.

41. J. Shapiro and K. D. Kaufman, J. Invest. Dermatol. Symp. Proc., 2003, 8, 20–23.

42. V. H. Price, J. L. Roberts, M. Hordinsky, E. A. Olsen, R. Savin, W. Bergfeld, V. Fiedler, A. Lucky, D. A. Whiting, F. Pappas, J. Culbertson, P. Kotey, A. Meehan and J. Waldstreicher, J. Am. Acad. Dermatol., 2000, 43, 768–776.

43. R. Oliveira-Soares, J. E. Silva, M. Correia and M. André, Int. J. Trichol., 2013, 5, 22–25.

44. M. Tabbakhian, N. Tavakoli, M. R. Jaafari and S. Daneshamouz, Int. J. Pharm., 2006, 323, 1–10.

45. D. D. Verma, S. Verma, G. Blume and A. Fahr, Int. J. Pharm., 2003, 258, 141–151.

46. M. Manconi, S. Mura, C. Sinico, A. M. Fadda, A. O. Vila and F. Molina, Colloids Surf., A, 2009, 342, 53–58.

47. Y. Rao, F. Zheng, X. Zhang, J. Gao and W. Liang, AAPS PharmSciTech, 2008, 9, 860–865.

48. Y. Rao, F. Zheng, X. Liang, H. Wang, J. Zhang and X. Lu, Drug Delivery, 2015, 22, 1003–1009.

49. J. W. Fluhr, R. Darlenski and C. Surber, Br. J. Dermatol., 2008, 159, 23–34.

50. L. Overgaard Olsen and G. B. E. Jemec, Acta Derm.- Venereol., 1993, 73, 404–406.

51. M. B. Brown and S. A. Jones, J. Eur. Acad. Dermatol. Venereol., 2005, 19, 308–318.

DISCUSIÓN

Capítulo 1. Evaluación de la eficacia de liposomas ultradeformables de baicalina frente a la inflamación asociada a psoriasis.

Caracterización fisicoquímica de las vesículas.

Tamaño, índice de polidispersión, potencial Z, eficacia de encapsulación y microscopía.

Se utilizan liposomas ultradeformables de baicalina a diferentes concentraciones (2.5, 5 y 10 mg/mL) como coadyuvantes en el tratamiento de la inflamación cutánea ligada a psoriasis. Tal como se observa en las imágenes obtenidas por microscopía electrónica de transmisión (Figura 2 del Capítulo 1), los liposomas formados presentaron una forma irregular y fueron multilamelares, independientemente de la concentración de baicalina incorporada. Como se muestra en la Tabla 1 del Capítulo 1 todos los liposomas elaborados presentaron un tamaño de partícula inferior a 100 nm; asimismo, se puede observar que la incorporación de baicalina se acompaña de una ligera disminución del diámetro, independientemente de la concentración, si se compara con los liposomas vacíos control; probablemente, debido a que la baicalina, de naturaleza lipofílica, interacciona con las cadenas de fosfolípidos modificando su ensamblaje produciendo así, una reducción en la curvatura de la bicapa. Por otro lado, todas las formulaciones fueron monodispersas, con un índice de polidispersión inferior a 0.2 y presentaron un potencial Z negativo y elevado (~-30 mV), independientemente de la concentración de baicalina incorporada. Las vesículas elaboradas fueron capaces de incorporar baicalina en un alto porcentaje; con una eficacia de encapsulación próxima al 80 % en todos los casos ($p < 0.05$). Las características fisicoquímicas de las vesículas son muy similares entre sí; no afecta la cantidad de baicalina

incorporada, confirmando que los liposomas diseñados son capaces de incorporar con éxito incluso la cantidad más elevada de flavonoide propuesta (10 mg/mL). Además, los liposomas mostraron una buena estabilidad en el tiempo.

Ensayos de permeabilidad cutánea in vitro.

Los liposomas ultradeformables contienen un activador de membrana capaz de flexibilizar la bicapa del liposoma, facilitando su paso a través de la piel. Con objeto de poner de manifiesto esta capacidad en los liposomas de baicalina, se realizaron estudios *in vitro* de permeabilidad cutánea con células de difusión "tipo Franz". Los perfiles de permeabilidad obtenidos se muestran en la Figura 4 del Capítulo 1; se observa la capacidad de los liposomas ultradeformables para promover el paso de baicalina a través de la piel, en comparación con la solución de baicalina (control). A su vez, los valores de flujo y cantidad de baicalina permeada a partir de los liposomas ultradeformables (2.5, 5 y 10 mg/mL) y de la solución presentaron diferencias estadísticamente significativas ($p < 0.05$), demostrando que la capacidad de las vesículas para liberar baicalina en la piel es concentración-dependiente. En concreto, los liposomas ultradeformables con mayor carga de baicalina (10 mg/mL) fueron capaces de promover el paso de la misma a través de la epidermis en mayor porcentaje, consiguiendo un 5 % de baicalina permeada aproximadamente; por el contrario, una reducción en la carga de baicalina en los liposomas supuso una disminución en la cantidad permeada, siendo la más baja la obtenida a partir de los liposomas ultradeformables que contienen 2.5 mg/mL de baicalina (~2%).

Análisis de la citotoxicidad de las formulaciones de baicalina *in vitro* en cultivos de fibroblastos.

Cuando se diseña una nueva formulación es necesario evaluar su seguridad, especialmente en el tejido diana. El estudio de citotoxicidad *in vitro* en cultivos celulares representa un método de screening adecuado y fiable para seleccionar las formulaciones que se probarán más adelante en los estudios *in vivo*, con el fin de reducir el uso innecesario de animales. Se utilizaron fibroblastos (NIH-3T3) para evaluar la citotoxicidad de las formulaciones de baicalina propuestas, debido a que es la línea celular más representativa de la dermis. Como se muestra en la Figura 3 del Capítulo 1, los liposomas ultradeformables que incorporan baicalina (2.5, 5 y 10 mg/mL) no mostraron un efecto citotóxico importante tras 8 horas de incubación con los fibroblastos (~80 % de viabilidad celular); mientras que la incubación de las células con baicalina en solución supuso una reducción de la viabilidad celular al 70 %. La biocompatibilidad de los liposomas ultradeformables de baicalina se confirmó al aumentar el tiempo de incubación con las células a 24 horas, la viabilidad celular obtenida en todos los casos fue del 50 % aproximadamente, independientemente de la concentración utilizada; mientras que, al incorporar la baicalina en solución, la viabilidad celular se redujo al 20 %.

Estudio *in vivo* de la eficacia de la baicalina frente a la inflamación ligada a psoriasis.

La psoriasis es una enfermedad inflamatoria crónica de la piel muy común, con una patogénesis muy compleja, ya que es el resultado de la combinación de factores genéticos y ambientales. La psoriasis se caracteriza por una excesiva proliferación de queratinocitos, dilatación de vasos sanguíneos e infiltración inflamatoria de leucocitos, principalmente

en la dermis. Los procesos inflamatorios de la piel implicados en la psoriasis son muy complejos y resultan de la participación de varias vías de señalización. Hasta la actualidad no existe un tratamiento efectivo sin efectos secundarios, por ello se ha seleccionado la baicalina, un flavonoide con propiedades antiinflamatorias, para su encapsulación en liposomas ultradeformables, como un posible coadyuvante al tratamiento actual de esta enfermedad, que contribuya a reducir los posibles efectos adversos asociados.

Se aplicó TPA (12-O-tetradecanoilforbol-13-acetato) en ratones con el fin de inducir una respuesta inflamatoria, ya que es el modelo más común en el estudio de la actividad antiinflamatoria de moléculas asociada a psoriasis.

Análisis macroscópico y de la actividad de la mieloperoxidasa.

Tras la aplicación diaria de una solución de TPA durante 3 días en la piel de los ratones se indujo una lesión cutánea. Se apreció ulceración, pérdida de la integridad de la epidermis y formación de costra. La actividad de la enzima mieloperoxidasa (MPO) se cuantificó como un marcador del proceso inflamatorio, ya que es indicativo de la concentración de neutrófilos en el tejido inflamado.

Se comparó la eficacia de los liposomas ultradeformables de baicalina con una solución de la misma, una solución de dexametasona, como control positivo, y un control negativo no tratado.

Las fotografías de los ratones tratados (Figura 5 del Capítulo 1) ponen de manifiesto el potencial terapéutico de los liposomas ultradeformables de baicalina, ya que tras el tratamiento con los mismos se observa una reducción del daño cutáneo, respecto al control negativo no tratado. A su

vez, la aplicación de baicalina en solución mostró una capacidad antiinflamatoria menor, ya que las lesiones en los ratones fueron mucho más severas que en el caso del tratamiento con baicalina en liposomas. Por otro lado, el tratamiento con dexametasona (control positivo) condujo a una reducción de las lesiones cutáneas en menor medida que el tratamiento con liposomas ultradeformables de baicalina, ya que la piel aparecía escamosa, seca y con costra.

El potencial de los liposomas ultradeformables de baicalina en el tratamiento de la inflamación asociada a psoriasis se confirmó con el análisis de la actividad MPO. Como se observa en la Figura 6 del Capítulo 1, la capacidad de las vesículas de baicalina para reducir la actividad de MPO fue superior a la de baicalina en solución y dexametasona. A su vez, el potencial de los liposomas de baicalina de inhibir la MPO no es concentración-dependiente, ya que no se encontraron diferencias estadísticamente significativas entre el tratamiento con los liposomas cargados con las diferentes concentraciones de baicalina (2.5, 5 y 10 mg/mL) ($p > 0.05$).

A diferencia de los resultados de permeabilidad cutánea *in vitro,* la reducción de la lesión cutánea *in vivo* de los ratones no dependió de la concentración de baicalina utilizada, cuando se incorpora en liposomas ultradeformables, probablemente debido a que en el modelo *in vitro* el estrato córneo es más fino o está dañado, lo cual facilita el paso de las vesículas a través del mismo y permite un efecto terapéutico incluso a concentraciones más bajas.

Análisis histológico.

Las alteraciones morfológicas de la piel de los ratones expuestos a TPA se analizaron mediante tinciones Hematoxilina/Eosina. Como se observa en la Figura 7 del Capítulo 1, la epidermis y dermis de los ratones no tratados presentaron una apariencia normal; sin embargo, la piel de los ratones tratados con TPA mostraron alteraciones severas en la dermis y tejido subcutáneo, presentando una gran cantidad de infiltraciones de leucocitos, así como diferentes características patológicas como congestión vascular. Si bien la piel de los ratones tratados con dexametasona o baicalina en solución presentaba una apariencia similar, la aplicación de baicalina encapsulada en liposomas ultradeformables redujo las lesiones inducidas por el TPA, así como los infiltrados inflamatorios de células mononucleares, eosinófilos y neutrófilos.

Los resultados *in vivo* obtenidos confirmaron el potencial de los liposomas de baicalina como coadyuvantes en el tratamiento de la psoriasis independientemente de la concentración utilizada.

Capítulo 2. Evaluación de la eficacia de liposomas ultradeformables de baicalina y berberina frente al vitíligo.

Caracterización fisicoquímica de las vesículas.

Tamaño, índice de polidispersión, potencial Z, eficacia de encapsulación y microscopía.

A la vista de los resultados del estudio anterior, se propuso utilizar los liposomas ultradeformables de baicalina de más baja concentración (2.5 mg/mL) junto con liposomas de berberina como posibles coadyuvantes en el tratamiento del vitíligo. Para obtener unas vesículas de berberina que presentaran un tamaño e índice de polidispersión comparables a los obtenidos para los liposomas de baicalina se requirió incrementar la cantidad de fosfolípido, así como la adición de sorbitol (5 % v/V en agua). Los liposomas vacíos en base a la cantidad superior de fosfolípido y sorbitol se prepararon como control. Las imágenes obtenidas por microscopía electrónica de transmisión proporcionaron evidencia de la formación de las vesículas (Figura 1 del Capítulo 2). Los liposomas de baicalina fueron multilamelares y presentaron una forma irregular, mientras que los liposomas de berberina fueron mayoritariamente unilamelares y de forma esférica.

Como se puede observar en la Tabla 1 del Capítulo 2, los liposomas de berberina presentaron un tamaño de partícula inferior a 100 nm. De manera similar a la baicalina, la incorporación de berberina en los liposomas produjo una reducción del tamaño de los mismos; este comportamiento puede relacionarse con la intercalación de baicalina y berberina que tiene lugar en la bicapa lipídica, afectando a su ensamblaje. Tanto baicalina como berberina se incorporaron en los liposomas en un

porcentaje elevado. Las formulaciones fueron monodispersas y presentaron carga negativa, más elevada en el caso de liposomas de berberina. Tanto las vesículas de baicalina como de berberina fueron estables en el tiempo, ya que no se observaron cambios significativos en los parámetros fisicoquímicos tras 30 días de almacenamiento a temperatura ambiente (25 °C).

Ensayos de permeabilidad cutánea in vitro.

Con el fin de evaluar la capacidad de los liposomas ultradeformables de promover el paso de baicalina y berberina a través de la piel, se realizaron estudios *in vitro* de permeabilidad cutánea con células de difusión "tipo Franz". Los perfiles obtenidos se muestran en la Figura 2 del Capítulo 2. Se observa como los liposomas ultradeformables son capaces de estimular el paso, tanto de baicalina como de berberina, a través de la piel, en mayor magnitud que cuando se encuentran en solución (control); sin embargo, una concentración similar de baicalina incorporada en liposomas es capaz de penetrar en un porcentaje superior a la berberina, el porcentaje de baicalina permeado fue del 2 %, mientras que la berberina alcanzó el 1 %. Asimismo, la baicalina experimentó un periodo de latencia de 6 horas, mientras que en la berberina de 4 horas y la concentración de ambas moléculas en el compartimento receptor fue inferior al 2 %, lo que puede ser un indicio de la formación de un reservorio en la epidermis. Este comportamiento resulta deseable cuando se persigue un efecto local.

Análisis de la citotoxicidad de las formulaciones de baicalina y berberina *in vitro* en cultivos de fibroblastos, queratinocitos y melanocitos.

La citotoxicidad de las formulaciones de baicalina y berberina se evaluó en cultivos de las principales células presentes en la piel humana: fibroblastos (NIH-3T3), queratinocitos (HaCat) y melanocitos (HEMa).

Los liposomas ultradeformables propuestos demostraron ser biocompatibles, ya que, como se observa en la Figura 3 del Capítulo 2, la viabilidad de las tres líneas celulares fue del 100 % tras la incubación con los liposomas vacíos. Sin embargo, cuando se incuban las células con baicalina en solución o incorporada en los liposomas, la viabilidad de queratinocitos y melanocitos fue del 100 % cuando se utilizan las concentraciones más bajas (de 3.12 a 50 µg/mL), 80 % con 100 µg/mL de baicalina y 70 % con 200 µg/mL de baicalina, independientemente de la formulación utilizada. En el caso de fibroblastos, la viabilidad celular obtenida fue siempre del 100 %, independientemente de la concentración o formulación utilizada.

La berberina se comportó de manera similar independientemente de la línea celular utilizada: fibroblastos, queratinocitos o melanocitos. Cuando se incuban las células con berberina a concentraciones más elevadas (de 200 a 25 µg/mL), la viabilidad obtenida estuvo comprendida entre el 50 y el 75 %, mientras que a concentraciones más bajas (de 12.5 a 1.56 µg/mL) la viabilidad de todos los tipos celulares fue del 100 %, independientemente de si la berberina se encuentra libre en solución o incorporada en liposomas

Estudio *in vitro* de la eficacia de las formulaciones de baicalina y berberina frente al vitíligo.

El vitíligo se caracteriza fenotípicamente por manchas despigmentadas en la piel debidas a la pérdida de melanocitos. El tratamiento eficaz del vitíligo sigue siendo uno de los objetivos dermatológicos más complicados. El arsenal terapéutico disponible incluye fototerapia, inmunosupresores y terapias quirúrgicas. Sin embargo, se necesitan modificaciones e innovación para mejorar la eficacia del tratamiento actual. Los liposomas pueden representar un vehículo adecuado para tratamientos locales por vía tópica, ya que son capaces de aumentar la eficacia de los activos, como baicalina y berberina, dos productos naturales con propiedades interesantes para el tratamiento de esta enfermedad.

Protección frente a la radiación ultravioleta (UV).

La radiación UV es capaz de penetrar la epidermis y alcanzar la dermis, es por ello que se utilizan cultivos de queratinocitos y fibroblastos para determinar la capacidad de las formulaciones de baicalina y berberina para proteger a la piel frente a la radiación UV.

El efecto fotoprotector de las formulaciones de baicalina y berberina se expresa como el porcentaje de viabilidad de las células tratadas con las formulaciones a ensayar en comparación a células control no tratadas (0 % de fotoprotección), ambas expuestas a una dosis de radiación UV que produjo el 50 % de muerte celular previamente determinada (500 mJ/cm^2 para el caso de queratinocitos y 400 mJ/cm^2 para fibroblastos) (Figura 4 del Capítulo 2).

Los resultados obtenidos se muestran en la Figura 5 del Capítulo 2; se observa como la encapsulación en liposomas es una estrategia

prometedora para aumentar el potencial fotoprotector de la baicalina y la berberina; los liposomas de baicalina a dosis no citotóxicas (12.5 – 1.56 µg/mL) fueron capaces de ofrecer una potente protección frente a la radiación UV (~ 35%); sin embargo, cuando la baicalina se administra en forma de solución, la fotoprotección que ofrece es menor. Asimismo, un fenómeno similar se observa en el caso de la berberina, administrada en solución libre ofrece una fotoprotección del 7 % aproximadamente, y, por el contrario, cuando se incorpora en liposomas, la capacidad de protección frente a la radiación UV aumenta hasta un 15 % aproximadamente. Sin embargo, la berberina confiere una fotoprotección más limitada que la baicalina; el tratamiento simultáneo con liposomas de baicalina y liposomas de berberina confirió a los queratinocitos una fotoprotección similar a la proporcionada con el tratamiento con liposomas de baicalina individual.

El tratamiento con liposomas de baicalina es una estrategia prometedora para ofrecer una fotoprotección adecuada; esta afirmación se confirmó a la vista de los resultados obtenidos en cultivos de fibroblastos, ya que, a su vez, fue el tratamiento con liposomas de baicalina el que mayor efecto fotoprotector confirió a las células, ya sea de manera individual o reforzada con la asociación de berberina

Capacidad antioxidante.

La acumulación de especies reactivas del oxígeno está implicada en la patología del vitíligo, los melanocitos afectados por esta enfermedad presentan defectos que limitan su capacidad de contrarrestar el estrés oxidativo, es por ello que el tratamiento antioxidante puede resultar de utilizad frente a los síntomas del vitíligo. Los queratinocitos son las células predominantes en la epidermis que, al ser la capa más externa de la piel,

se encuentra más expuesta a agresiones y agentes patógenos. Por esta razón, los queratinocitos fueron seleccionados para evaluar la capacidad de las formulaciones de baicalina y berberina de contrarrestar el daño inducido por estrés oxidativo.

Los queratinocitos fueron expuestos a peróxido de hidrógeno, capaz de inducir un daño oxidativo (redujo la viabilidad celular a un 65 %), y, posteriormente fueron tratados con concentraciones no citotóxicas de las diferentes formulaciones a ensayar (12.5 – 1.56 µg/mL).

En la Figura 6 del Capítulo 2 se representa el porcentaje de capacidad antioxidante que confiere el tratamiento de las células con las diferentes formulaciones; expresado como porcentaje de capacidad antioxidante en comparación con las células control dañadas con peróxido de hidrógeno (0 % de capacidad antioxidante). Se ha demostrado que, tanto la baicalina como la berberina, son dos productos naturales con una potente capacidad antioxidante. Ambos, administrados en solución son capaces de contrarrestar el daño oxidativo inducido por peróxido de hidrógeno; asimismo, su efectividad se ve reforzada mediante su incorporación en liposomas, confiere a los queratinocitos una protección frente al daño oxidativo del 60 % aproximadamente. El tratamiento combinado de liposomas de baicalina y berberina no aportó ninguna mejoría respecto al tratamiento con liposomas de baicalina o liposomas de berberina individualmente.

Contenido de melanina.

El vitíligo se caracteriza por la aparición de manchas sin pigmentación en la piel, es por ello que se evalúo la capacidad de los liposomas de baicalina y berberina para estimular la melanogénesis y la pigmentación cutánea,

mediante cultivos de melanocitos. Se determinó la actividad melanogénica tras el tratamiento de las células con las diferentes formulaciones, como porcentaje de melanina en comparación a las células no tratadas (0 % de actividad melanogénica).

Como se muestra en la tabla 2 del Capítulo 2, el tratamiento con baicalina en solución produjo un aumento del contenido de melanina de las células (~ 90 % de actividad melanogénica) y su incorporación en liposomas conllevó un ligero aumento de la misma (~100 %). Por otro lado, la berberina encapsulada en liposomas demostró ser un tratamiento muy efectivo capaz de aumentar el contenido de melanina de las células en mayor medida que la baicalina, logrando un 130 % de actividad melanogénica aproximadamente. Un efecto sinérgico se observó entre ambos tratamientos, pues la actividad melanogénica más elevada se observó con el tratamiento simultáneo de las células con liposomas de baicalina y liposomas de berberina (~150 %). Los resultados obtenidos sugieren un posible uso de estas vesículas como coadyuvantes en la repigmentación de la piel afectada por vitíligo.

Evaluación de la actividad tirosinasa.

Para corroborar la vía involucrada en la estimulación de la producción de melanina, se determinó la actividad de la tirosinasa, una enzima clave en la síntesis de melanina. Los resultados se expresan como porcentaje de actividad tirosinasa, frente a las células control no tratadas (0 % de actividad tirosinasa).

Los resultados obtenidos (tabla 2 del Capítulo 2) sugieren que el tratamiento propuesto con liposomas ultradeformables que incorporan baicalina y berberina es capaz de aumentar la actividad de la enzima

tirosinasa, de manera similar a como sucede con la estimulación de la actividad melanogénica, demostrando así que es la tirosinasa la enzima implicada en la repigmentación.

Los liposomas ultradeformables de berberina mostraron mayor capacidad de aumentar la actividad de la enzima, se logra un 130 % de actividad tirosinasa tras el tratamiento con liposomas de berberina, frente a un 100 % obtenido con liposomas de baicalina. A su vez, el tratamiento combinado con liposomas de baicalina y berberina consiguió estimular de forma considerable la actividad de la tirosinasa y producción de melanina en cultivos celulares. Esta combinación representa una estrategia potencial para el tratamiento del vitíligo, ya que es capaz de producir la repigmentación adecuada de las manchas, logrando un tono de piel uniforme.

Los resultados obtenidos en el presente capítulo sugieren que la asociación de liposomas de berberina y de baicalina puede representar una estrategia prometedora para frenar la progresión del vitíligo, ya que las vesículas de baicalina aportan una protección frente a la radiación UV y al estrés oxidativo importante y su asociación con las vesículas de berberina garantizan la repigmentación de la piel.

Capítulo 3. Evaluación de la eficacia de liposomas ultradeformables, glicerosomas, hialurosomas y glicerohialurosomas de baicalina y finasterida frente a la alopecia androgénica.

Caracterización fisicoquímica de las vesículas.

Tamaño, índice de polidispersión, potencial Z, eficacia de encapsulación y microscopía.

Por último, se evalúo el potencial de la baicalina como coadyuvante en el tratamiento de la alopecia androgénica, para ello se combinó con finasterida. En este caso, el tamaño de las nanovesículas desempeña un papel muy importante, ya que la penetración folicular aumenta a medida que disminuye el tamaño de los liposomas. En estudios previos se ha puesto de manifiesto la capacidad de los liposomas formulados con etanol para favorecer la absorción percutánea de finasterida. En la presente Tesis Doctoral, las vesículas fosfolipídicas se modifican con glicerol y/o hialuronato de sodio. El glicerol es un poliol ampliamente utilizado por sus propiedades hidratantes y el hialuronato de sodio es un polisacárido presente de manera natural en la piel. La combinación de ambos componentes en los liposomas podría mejorar la hidratación de la piel, facilitando el paso de las vesículas intactas a la dermis y a los folículos. A su vez, incrementa la viscosidad de las formulaciones liposomales, facilitando su aplicación y prolongando el periodo de residencia de la formulación en el lugar de acción. Así pues, la finasterida y la baicalina se incorporaron de manera simultánea en liposomas ultradeformables, hialurosomas, glicerosomas y glicerohialurosomas, mientras que los liposomas vacíos o cargados solo con finasterida o baicalina se utilizaron como controles.

Como se puede observar en la Figura 1 del Capítulo 3, las imágenes obtenidas por Crio-TEM revelaron que los liposomas, utilizados como referencia, eran esféricos y unilamelares, mientras que la presencia de glicerol y/o hialuronato de sodio conduce a la formación de vesículas multiamelares. El diámetro medio de los liposomas vacíos, utilizados como referencia, fue de 80 nm aproximadamente, con un índice de polidispersidad bajo (0.18) y un potencial Z negativo (-30 mV). La incorporación de baicalina, como se puede comprobar en la Figura 2 del Capítulo 3, se acompañó de una reducción del tamaño de las vesículas, y del índice de polidispersidad; sin embargo, la incorporación de finasterida no afectó al tamaño de los liposomas, pero condujo a un aumento en el índice de polidispersidad. La incorporación simultánea de baicalina y finasterida produjo un aumento del diámetro medio de las nanovesículas (~100 nm) y del índice de polidispersidad (~ 0.25); a su vez, el potencial Z fue mucho menos negativo (~ -13 mV), lo que denota que la incorporación simultánea tiene un impacto importante, probablemente debido a la intercalación simultánea de ambas moléculas en la bicapa lipídica de la vesícula. La adición de glicerol y/o hialuronato de sodio no modificó las propiedades fisicoquímicas de las vesículas. Por otra parte, las nanovesículas incorporaron la finasterida y baicalina en un porcentaje adecuado (~ 80 %) y presentaron buena estabilidad a lo largo del tiempo, ya que no se detectaron cambios significativos después de 30 días de almacenamiento a temperatura ambiente (25 °C).

Análisis de la citotoxicidad de las formulaciones de baicalina *in vitro* en cultivos de células de papila dérmica del folículo piloso.

La biocompatibilidad de las formulaciones propuestas se corroboró mediante la incubación *in vitro* de células de la papila dérmica del folículo

piloso con diferentes concentraciones de las formulaciones seleccionadas, de 800 a 0.39 µg/mL en el caso de finasterida y de 3200 a 1.56 µg/mL en el caso de baicalina.

Los resultados (Figura 3 del Capítulo 3) muestran como el tratamiento con finasterida o con baicalina, de manera individual o combinada, produjo un efecto dependiente de la concentración utilizada, ya sean administradas en solución o incorporadas en los sistemas nanovesiculares propuestos; pues en todos los casos, la viabilidad celular obtenida tras la incubación con las formulaciones a concentraciones elevadas fue inferior al 50 %, mientras que las concentraciones más bajas (inferior a 12.5 µg/mL de finasterida y a 50 µg/mL de baicalina) no produjeron muerte celular, la viabilidad obtenida fue del 100 %. Las concentraciones no citotóxicas se utilizaron para ensayos de efectividad *in vitro* posteriores.

Estudio de la eficacia de las formulaciones de baicalina frente a la alopecia androgénica.

Un gran número de pacientes están afectados por la caída del cabello, sin embargo, se observa una baja adherencia terapéutica a los fármacos utilizados para la alopecia, como la finasterida oral, debido a los efectos secundarios asociados al tratamiento. La administración de finasterida por vía tópica, mediante su incorporación en vesículas fosfolipídicas, se plantea como una alternativa prometedora capaz de asegurar su eficacia y evitar los efectos secundarios asociados a su administración por vía oral, ya que los liposomas son capaces de dirigir las moléculas activas al área folicular. Por otro lado, la eficacia terapéutica de la finasterida puede verse potenciada por su asociación con productos naturales que ejerzan acciones complementarias, como por ejemplo la baicalina, un flavonoide capaz de estimular el crecimiento capilar. Por ello, se ha analizado el

efecto de glicerosomas, hialurosomas y glicerohialurosomas diseñados específicamente para la encapsulación de finasterida y baicalina, en la estimulación del crecimiento del cabello. Asimismo, la finasterida y la baicalina incorporadas de manera individual o simultánea en liposomas y en suspensión, se utilizaron como control para evaluar los efectos de la incorporación del glicerol y del hialuronato de sodio en las vesículas fosfolipídicas.

Estudio in vitro del potencial estimulante del crecimiento del cabello.

La capacidad de las formulaciones nanovesiculares de baicalina y finasterida de estimular el crecimiento del cabello se determinó mediante el análisis de la proliferación *in vitro* de las células de la papila dérmica del folículo piloso, consideradas como las principales responsables del control del crecimiento del cabello, tras su incubación con concentraciones no citotóxicas de las formulaciones propuestas. Como se muestra en la Figura 4 del Capítulo 3, se comparó la capacidad de estimular la proliferación celular de las nanovesículas que incorporan baicalina y finasterida de manera simultánea con los liposomas que las encapsulan de manera individual y con las dispersiones control, con el objetivo de evaluar la posible influencia del tipo de vehículo utilizado y de la cantidad encapsulada de cada sustancia, sola o conjuntamente.

Los resultados muestran como el tratamiento con baicalina y finasterida produce un aumento en la proliferación de las células del folículo piloso, pues la viabilidad celular obtenida tras el tratamiento de las células con finasterida, incorporada en liposomas o en suspensión de manera individual, fue del 120 % aproximadamente y mediante el tratamiento con baicalina, libre en solución o en liposomas, se logró un 115 % de viabilidad celular. Sin embargo, la incorporación simultánea de baicalina y finasterida

en las vesículas produjo un aumento mayor de la proliferación celular, en comparación tanto con las vesículas que contenían estos productos de forma individual, como con las suspensiones de las mismos; en concreto, los glicerohialurosomas que incorporan baicalina y finasterida de manera combinada fueron los sistemas que estimularon en mayor medida la proliferación de las células, logrando un 180 % de viabilidad celular. Estos resultados ponen de manifiesto el sinergismo de la finasterida con la baicalina sobre la proliferación celular, así como la influencia del vehículo utilizado, pues la presencia de glicerol y hialuronato de sodio en los sistemas vesiculares parece potenciar la capacidad de la finasterida y baicalina de estimular el crecimiento del cabello.

Estudio in vivo del efecto estimulante del crecimiento del cabello.

Los estudios *in vivo* se llevaron a cabo utilizando ratones C57BL/6, ya que representan un modelo estandarizado para evitar alteraciones en los resultados.

Se realizó una **inspección visual** del crecimiento del pelo y el color de la piel de los ratones en los días 12, 16 y 21 post-tratamiento, ya que la pigmentación de la piel se considera un factor clave que determina el crecimiento del cabello, pues presenta color rosa en la fase telógena (reposo) y se vuelve gris o negro en la fase anágena (crecimiento); así pues, como se muestra en la Figura 5 del Capítulo 3, en el día 0 de tratamiento la piel depilada de cada ratón presentaba color rosa y en el día 21 se observó de manera clara como la piel presentaba color negro y se hizo evidente el crecimiento de pelo.

Tras 12 días de tratamiento, se corroboró la capacidad de la baicalina y la finasterida de estimular el crecimiento del pelo, pues los ratones a los que

se les administró tanto baicalina como finasterida en suspensión presentaron la piel con pigmentación gris-negra, significativo de que se indujo la fase anágena más rápidamente que en el caso de los ratones no tratados, que presentaron pigmentación rosácea; sin embargo, se demostró como la incorporación de dichas moléculas activas en sistemas nanovesiculares adecuados aumenta su efectividad, ya que el crecimiento de pelo resultó notable en los ratones a los que se les administró baicalina o finasterida incorporadas en liposomas; a su vez, el tratamiento con las vesículas cargadas simultáneamente con finasterida y baicalina resultó ser el tratamiento más eficaz, pues mejoró de manera aún más significativa el crecimiento capilar, mostrándose más visible cuando se emplearon hialurosomas y glicerohialurosomas. En los días 16 y 21 de tratamiento, no pudieron observarse diferencias a nivel visual entre los ratones tratados con las diferentes formulaciones, ya que la zona de tratamiento se encontró cubierta de pelo en todos los casos.

Asimismo, se determinó la **longitud** alcanzada por los pelos de los ratones de cada grupo con el fin de evaluar las diferencias entre los tratamientos con las diferentes formulaciones (Tabla 1 del Capítulo 3). En el día 16 post-tratamiento, solo los ratones tratados con glicerosomas, hialurosomas y glicerohialurosomas cargados con baicalina y finasterida simultáneamente mostraron una longitud de pelo significativamente superior a los ratones no tratados ($p < 0.01$).

En el día 21 se observó como todos los tratamientos propuestos lograron provocar un aumento en la longitud del pelo, determinado mediante el parámetro EE (efecto estimulante), un indicador de la capacidad de las formulaciones de estimular el crecimiento del pelo, en comparación con el grupo de ratones no tratados. Los resultados obtenidos revelan como el

tratamiento combinado de finasterida y baicalina incorporadas en nanovesículas es una estrategia prometedora para estimular el crecimiento del pelo, pues en todos los casos se logró un ratio de efecto estimulante superior al 1.5 respecto al grupo de ratones no tratados, más evidente en el caso del tratamiento con glicerohialurosomas de baicalina y finasterida, ya que el ratio de efecto estimulante fue el doble al de los ratones no tratados.

Los folículos pilosos están íntimamente relacionados con los desórdenes capilares, un mayor **número de folículos pilosos** suponen una mejor estimulación del crecimiento del cabello. Es por ello que se determinó el número y diámetro de los folículos pilosos tras 21 días de tratamiento. El diámetro de los folículos de los ratones de los diferentes grupos de tratamiento no presentaron diferencias estadísticamente significativas respecto al grupo control de ratones no tratados ($p > 0.05$). Sin embargo, se observó un aumento significativo en el número de folículos en los ratones que fueron tratados con las nanovesículas que incorporan baicalina y finasterida simultáneamente, tanto liposomas, como glicerosomas, hialurosomas y glicerohialurosomas, tal como se muestra en la Figura 6 del capítulo 3. El tratamiento con finasterida o baicalina incorporadas de manera individual en liposomas produjo un incremento menos notable en el número de folículos, lo que apunta a que la incorporación simultánea de baicalina y finasterida refuerza la acción estimulante de la génesis de folículos pilosos.

Para confirmar la eficacia estimulante del crecimiento capilar de las diferentes nanovesículas de baicalina y finasterida propuestas, se procedió al **análisis histológico** de la piel de los ratones tratados con las diferentes formulaciones a ensayar, tras su aislamiento y tinción con

Hematoxilina/Eosina (Figura 7 del Capítulo 3). Los resultados histológicos confirman la capacidad las nanovesículas que incorporan baicalina y finasterida de estimular el crecimiento del cabello, ya que el tratamiento con las mismas supone un incremento en el número de folículos pilosos en ratones C57BL/6.

En consecuencia, los resultados *in vitro* demuestran que la encapsulación combinada de finasterida y baicalina en sistemas nanovesiculares adecuados (liposomas, glicerosomas, hialurosomas y glicerohialurosomas) supone el desarrollo de un nuevo tratamiento capaz de estimular la proliferación de las células de la papila dérmica y del folículo piloso, y los resultados *in vivo* confirman su capacidad de acelerar la fase anágena y la tasa de crecimiento del cabello, así como de aumentar la cantidad de folículos pilosos. Por ello, se puede afirmar que las formulaciones de finasterida suplementadas con baicalina en liposomas, glicerosomas, hialurosomas o glicerohialurosomas supone un tratamiento eficaz y alternativo a los existentes en la actualidad frente a la caída del cabello.

CONCLUSIONES

Las principales conclusiones obtenidas del trabajo desarrollado se exponen a continuación:

1. Todos los sistemas liposomales desarrollados presentaron un tamaño nanométrico (inferior a 150 nm), con una distribución de tamaños homogénea (inferior a 0.3) y un potencial Z negativo (superior a - 10 mV); así como una elevada capacidad de encapsulación de las moléculas activas propuestas (superior al 80 %). Además mostraron una elevada estabilidad a lo largo del tiempo.
2. Los liposomas ultradeformables son capaces de promover la permeación de baicalina y berberina a través de la piel.
3. Las formulaciones propuestas son biocompatibles en los diferentes modelos celulares utilizados: fibroblastos, queratinocitos, melanocitos y células de la papila dérmica del folículo piloso.
4. Los liposomas de baicalina suponen una buena estrategia terapéutica como coadyuvantes en el tratamiento de la psoriasis independientemente de la concentración utilizada, ya que reducen la inflamación inducida por TPA asociada a psoriasis.
5. La asociación de liposomas de baicalina y de berberina puede representar una estrategia prometedora para frenar la progresión del vitíligo, ya que las vesículas de baicalina aportan una protección frente a la radiación UV y al estrés oxidativo importante y su asociación con las vesículas de berberina garantizan la repigmentación de la piel.
6. La combinación de finasterida y baicalina encapsuladas en los liposomas propuestos puede considerarse un tratamiento eficaz

frente a la caída del cabello, pues los resultados *in vitro* demuestran que son capaces de estimular la proliferación de las células de la papila dérmica y del folículo y los resultados *in vivo* confirman que son capaces de acelerar la fase anágena y la tasa de crecimiento del cabello, así como de aumentar la cantidad de folículos pilosos.

BIBLIOGRAFÍA

1. Thakur Raghu Raj Singh RFD. Novel Delivery Systems for Transdermal and Intradermal Drug Delivery. 1st ed. School of Pharmacy, Queen's University Belfast, UK: Wiley; 2015.

2. Elaine N. Marieb. Anatomía y fisiología humana. 9th ed. Madrid: Pearson Educacion; 2008.

3. Eckhart L, Zeeuwen PLJM. The skin barrier: Epidermis vs environment. Exp Dermatol. 2018 Aug 1;27(8):805–6.

4. Haftek M. Queratinización epidérmica. EMC - Dermatol. 2011 Jan 1;45(1):1–13.

5. Lambert MW, Maddukuri S, Karanfilian KM, Elias ML, Lambert WC. The physiology of melanin deposition in health and disease. Clin Dermatol. 2019 Sep 1;37(5):402–17.

6. Deckers J, Hammad H, Hoste E. Langerhans Cells: Sensing the Environment in Health and Disease. Front Immunol. 2018 Feb 1;9:93.

7. Abraham J, Mathew S. Merkel Cells: A Collective Review of Current Concepts. Int J Appl Basic Med Res. 2019;9(1):9–13.

8. Brown TM, Krishnamurthy K. Histology, Dermis. StatPearls Publishing; 2020.

9. Patel A, Forsythe P, Smith S. Dermatología de pequeños animales. 1st ed. Barcelona, España: Elsevier Saunders; 2010.

10. Madaan A, Verma R, Singh AT, Jaggi M. Review of Hair Follicle Dermal Papilla cells as in vitro screening model for hair growth. Int J Cosmet Sci. 2018 Oct 1;40(5):429–50.

11. Geyfman M, Plikus MV, Treffeisen E, Andersen B, Paus R. Resting no more: re-defining telogen, the maintenance stage of the hair growth cycle. Biol Rev Camb Philos Soc. 2015 Nov;90(4):1179–96.

12. Houschyar KS, Borrelli MR, Tapking C, Popp D, Puladi B, Ooms M, et al. Molecular Mechanisms of Hair Growth and Regeneration: Current Understanding and Novel Paradigms. Dermatol Basel Switz. 2020 Mar 12;1–10.

13. Dinarello CA. Anti-inflammatory Agents: Present and Future. Cell. 2010 Mar 19;140(6):935–50.

14. León Regal M, Alvarado Borges A, de Armas García J, Miranda Alvarado L, Varens Cedeño J, Cuesta del Sol J. Respuesta inflamatoria aguda. Consideraciones bioquímicas y celulares: cifras alarmantes. Rev Finlay. 2015 Mar;5(1):47–62.

15. Arulselvan P, Fard MT, Tan WS, Gothai S, Fakurazi S, Norhaizan ME, et al. Role of Antioxidants and Natural Products in Inflammation. Oxid Med Cell Longev. 2016;2016: 5276130.

16. Maniadakis N, Toth E, Schiff M, Wang X, Nassim M, Szegvari B, et al. A Targeted Literature Review Examining Biologic Therapy Compliance and Persistence in Chronic Inflammatory Diseases to Identify the Associated Unmet Needs, Driving Factors, and Consequences. Adv Ther. 2018;35(9):1333–55.

17. Martínez-Montiel MP, Muñoz-Yagüe MT. Tratamientos biológicos en la enfermedad inflamatoria crónica intestinal. Rev Esp Enfermedades Dig. 2006 Apr;98(4):265–91.

18. Pireddu R, Caddeo C, Valenti D, Marongiu F, Scano A, Ennas G, et al. Diclofenac acid nanocrystals as an effective strategy to reduce in vivo skin inflammation by improving dermal drug bioavailability. Colloids Surf B Biointerfaces. 2016 Jul 1;143:64–70.

19. Speeckaert R, Geel N van. Vitiligo: An Update on Pathophysiology and Treatment Options. Am J Clin Dermatol. 2017 Dec 1;18(6):733–44.

20. Rodrigues M, Ezzedine K, Hamzavi I, Pandya AG, Harris JE. New discoveries in the pathogenesis and classification of vitiligo. J Am Acad Dermatol. 2017 Jul 1;77(1):1–13.

21. Rashighi M, Harris JE. Vitiligo pathogenesis and emerging treatments. Dermatol Clin. 2017 Apr;35(2):257–65.

22. Ezzedine K, Eleftheriadou V, Whitton M, van Geel N. Vitiligo. The Lancet. 2015 Jul 4;386(9988):74–84.

23. Wang Y, Li S, Li C. Perspectives of New Advances in the Pathogenesis of Vitiligo: From Oxidative Stress to Autoimmunity. Med Sci Monit Int Med J Exp Clin Res. 2019 Feb 6;25:1017–23.

24. Benzekri L, Gauthier Y. Clinical markers of vitiligo activity. J Am Acad Dermatol. 2017 May;76(5):856–62.

25. Boniface K, Seneschal J, Picardo M, Taïeb A. Vitiligo: Focus on Clinical Aspects, Immunopathogenesis, and Therapy. Clin Rev Allergy Immunol. 2018 Feb 1;54(1):52–67.

26. Bergqvist C, Ezzedine K. Vitiligo: A Review. Dermatology. 2020 Mar 10;1–22.

27. Lacueva Modrego L, Ferrando Barberá J. Alopecias: orientación diagnóstica, clínica y terapéutica. Med Integral. 2000 Feb 15;35(2):54–71.

28. Lin RL, Garibyan L, Kimball AB, Drake LA. Systemic causes of hair loss. Ann Med. 2016;48(6):393–402.

29. Gupta M, Mysore V. Classifications of Patterned Hair Loss: A Review. J Cutan Aesthetic Surg. 2016 Mar;9(1):3–12.

30. Girijala RL, Riahi RR, Cohen PR. Platelet-rich plasma for androgenic alopecia treatment: A comprehensive review. Dermatol Online J. 2018 Jul 15;24(7).

31. Juárez-Rendón KJ, Rivera Sánchez G, Reyes-López MÁ, García-Ortiz JE, Bocanegra-García V, Guardiola-Avila I, et al. Alopecia Areata. Current situation and perspectives. Arch Argent Pediatr. 2017 Dec 1;115(6):404–11.

32. Simakou T, Butcher JP, Reid S, Henriquez FL. Alopecia areata: A multifactorial autoimmune condition. J Autoimmun. 2019;98:74–85.

33. Kanti V, Röwert-Huber J, Vogt A, Blume-Peytavi U. Cicatricial alopecia. JDDG J Dtsch Dermatol Ges. 2018;16(4):435–61.

34. Park AM, Khan S, Rawnsley J. Hair Biology: Growth and Pigmentation. Facial Plast Surg Clin N Am. 2018 Nov;26(4):415–24.

35. Ribeiro AS, Estanqueiro M, Oliveira MB, Sousa Lobo JM. Main Benefits and Applicability of Plant Extracts in Skin Care Products. Cosmetics. 2015 Jun;2(2):48–65.

36. Wang J, Wong Y-K, Liao F. What has traditional Chinese medicine delivered for modern medicine? Expert Rev Mol Med. 2018;20:4.

37. Shi H, Ren K, Lv B, Zhang W, Zhao Y, Tan RX, et al. Baicalin from Scutellaria baicalensis blocks respiratory syncytial virus (RSV) infection and reduces inflammatory cell infiltration and lung injury in mice. Sci Rep. 2016 Oct 21;6(1):1–12.

38. Ding L, Jia C, Zhang Y, Wang W, Zhu W, Chen Y, et al. Baicalin relaxes vascular smooth muscle and lowers blood pressure in spontaneously hypertensive rats. Biomed Pharmacother Biomedecine Pharmacother. 2019 Mar;111:325–30.

39. Fang P, Yu M, Shi M, Bo P, Gu X, Zhang Z. Baicalin and its aglycone: a novel approach for treatment of metabolic disorders. Pharmacol Rep PR. 2020 Feb;72(1):13–23.

40. Zhou Q-B, Jin Y-L, Jia Q, Zhang Y, Li L-Y, Liu P, et al. Baicalin attenuates brain edema in a rat model of intracerebral hemorrhage. Inflammation. 2014 Feb;37(1):107–15.

41. Dinda B, Dinda S, DasSharma S, Banik R, Chakraborty A, Dinda M. Therapeutic potentials of baicalin and its aglycone, baicalein against inflammatory disorders. Eur J Med Chem. 2017 May 5;131:68–80.

42. Zhao Q, Chen X-Y, Martin C. Scutellaria baicalensis, the golden herb from the garden of Chinese medicinal plants. Sci Bull. 2016;61(18):1391–8.

43. Zhu L, Xu L-Z, Zhao S, Shen Z-F, Shen H, Zhan L-B. Protective effect of baicalin on the regulation of Treg/Th17 balance, gut microbiota and short-chain fatty acids in rats with ulcerative colitis. Appl Microbiol Biotechnol. 2020 Apr 22; 104(12):5449-5460.

44. Wu X, Deng X, Wang J, Li Q. Baicalin Inhibits Cell Proliferation and Inflammatory Cytokines Induced by Tumor Necrosis Factor α (TNF-α) in Human Immortalized Keratinocytes (HaCaT) Human Keratinocytes by Inhibiting the STAT3/Nuclear Factor kappa B (NF-κB) Signaling Pathway. Med Sci Monit Int Med J Exp Clin Res. 2020 Apr 23;26:919392.

45. Zhao H, Li C, Li L, Liu J, Gao Y, Mu K, et al. Baicalin alleviates bleomycin-induced pulmonary fibrosis and fibroblast proliferation in

rats via the PI3K/AKT signaling pathway. Mol Med Rep. 2020 Jun;21(6):2321–34.

46. Yu Z, Zhan C, Du H, Zhang L, Liang C, Zhang L. Baicalin suppresses the cell cycle progression and proliferation of prostate cancer cells through the CDK6/FOXM1 axis. Mol Cell Biochem. 2020 May 8; 469:169–178

47. Yang B, Bai H, Sa Y, Zhu P, Liu P. Inhibiting EMT, stemness and cell cycle involved in baicalin-induced growth inhibition and apoptosis in colorectal cancer cells. J Cancer. 2020;11(8):2303–17.

48. Jin B-R, An H-J. Baicalin alleviates benign prostate hyperplasia through androgen-dependent apoptosis. Aging. 2020 04;12(3):2142–55.

49. Duan X, Guo G, Pei X, Wang X, Li L, Xiong Y, et al. Baicalin Inhibits Cell Viability, Migration and Invasion in Breast Cancer by Regulating miR-338-3p and MORC4. OncoTargets Ther. 2019;12:11183–93.

50. Huang T, Liu Y, Zhang C. Pharmacokinetics and Bioavailability Enhancement of Baicalin: A Review. Eur J Drug Metab Pharmacokinet. 2019 Apr;44(2):159–68.

51. Luan J, Zheng F, Yang X, Yu A, Zhai G. Nanostructured lipid carriers for oral delivery of baicalin: In vitro and in vivo evaluation. Colloids Surf Physicochem Eng Asp. 2015 Feb 5;466:154–9.

52. Wu H, Long X, Yuan F, Chen L, Pan S, Liu Y, et al. Combined use of phospholipid complexes and self-emulsifying microemulsions for improving the oral absorption of a BCS class IV compound, baicalin. Acta Pharm Sin B. 2014 Jun 1;4(3):217–26.

53. Jakab G, Bogdán D, Mazák K, Deme R, Mucsi Z, Mándity IM, et al. Physicochemical Profiling of Baicalin Along with the Development and Characterization of Cyclodextrin Inclusion Complexes. AAPS PharmSciTech. 2019 Sep 16;20(8):314.

54. Tillhon M, Guamán Ortiz LM, Lombardi P, Scovassi AI. Berberine: New perspectives for old remedies. Biochem Pharmacol. 2012 Nov 15;84(10):1260–7.

55. Gao Y, Wang F, Song Y, Liu H. The status of and trends in the pharmacology of berberine: a bibliometric review [1985–2018]. Chin Med. 2020;15:7.

56. JIANG W, LI S, LI X. Therapeutic potential of berberine against neurodegenerative diseases. Sci China Life Sci. 2015 Jun;58(6):564–9.

57. Dutta NK, Panse MV. Usefulness of Berberine (an Alkaloid from Berberis aristata) in the Treatment of Cholera (Experimental). Indian J Med Res. 1962;50(5):732–6.

58. Subbaiah TV, Amin AH. Effect of berberine sulphate on Entamoeba histolytica. Nature. 1967 Jul 29;215(5100):527–8.

59. Rabbani GH, Butler T, Knight J, Sanyal SC, Alam K. Randomized controlled trial of berberine sulfate therapy for diarrhea due to enterotoxigenic Escherichia coli and Vibrio cholerae. J Infect Dis. 1987 May;155(5):979–84.

60. Khin-Maung-U, Myo-Khin, Nyunt-Nyunt-Wai, Aye-Kyaw, Tin-U. Clinical trial of berberine in acute watery diarrhoea. Br Med J Clin Res Ed. 1985 Dec 7;291(6509):1601–5.

61. Kalmarzi RN, Naleini SN, Ashtary-Larky D, Peluso I, Jouybari L, Rafi A, et al. Anti-Inflammatory and Immunomodulatory Effects of Barberry (Berberis vulgaris) and Its Main Compounds. Oxid Med Cell Longev. 2019;2019:6183965.

62. Zhang D, Ke L, Ni Z, Chen Y, Zhang L-H, Zhu S-H, et al. Berberine containing quadruple therapy for initial Helicobacter pylori eradication. Medicine (Baltimore). 2017 Aug 11;96(32):7697.

63. Peng C, Hu Y, Ge Z-M, Zou Q-M, Lyu N-H. Diagnosis and treatment of Helicobacter pylori infections in children and elderly populations. Chronic Dis Transl Med. 2020 Jan 8;5(4):243–51.

64. Genovese C, Davinelli S, Mangano K, Tempera G, Nicolosi D, Corsello S, et al. Effects of a new combination of plant extracts plus d-mannose for the management of uncomplicated recurrent urinary tract infections. J Chemother Florence Italy. 2018 Apr;30(2):107–14.

65. Cicero AFG, Fogacci F, Bove M, Giovannini M, Veronesi M, Borghi C. Short-Term Effects of Dry Extracts of Artichokeand Berberis in

Hypercholesterolemic Patients Without Cardiovascular Disease. Am J Cardiol. 2019 15;123(4):588–91.

66. Mazza A, Schiavon L, Rigatelli G, Torin G, Lenti S. The Effects of a New Generation of Nutraceutical Compounds on Lipid Profile and Glycaemia in Subjects with Pre-hypertension. High Blood Press Cardiovasc Prev Off J Ital Soc Hypertens. 2019 Aug;26(4):345–50.

67. Cicero AFG, Baggioni A. Berberine and Its Role in Chronic Disease. Adv Exp Med Biol. 2016;928:27–45.

68. Wang L, Kong H, Jin M, Li X, Stoika R, Lin H, et al. Synthesis of disaccharide modified berberine derivatives and their anti-diabetic investigation in zebrafish using a fluorescence-based technology. Org Biomol Chem. 2020 May 13;18(18):3563–74.

69. Kumar A, Ekavali, Chopra K, Mukherjee M, Pottabathini R, Dhull DK. Current knowledge and pharmacological profile of berberine: An update. Eur J Pharmacol. 2015 Aug 15;761:288–97.

70. Imenshahidi M, Hosseinzadeh H. Berberis Vulgaris and Berberine: An Update Review. Phytother Res PTR. 2016 Nov;30(11):1745–64.

71. National Center for Biotechnology Information. PubChem Database. Berberine, CID=2353, [Internet]. Available from: https://pubchem.ncbi.nlm.nih.gov/compound/Berberine

72. Keng Wooi N, Wing Man L. Skin Deep: The Basics of Human Skin Structure and Drug Penetration. In: Percutaneous Penetration Enhancers: Chemical Methods in Penetration Enhancement. 1st ed. Springer Berlin Heidelberg; 2015. 3-11.

73. Razavi H, Darvishi MH, Janfaza S. Silver Sulfadiazine Encapsulated in Lipid-Based Nanocarriers for Burn Treatment. J Burn Care Res Off Publ Am Burn Assoc. 2018 20;39(3):319–25.

74. Carita AC, Eloy JO, Chorilli M, Lee RJ, Leonardi GR. Recent Advances and Perspectives in Liposomes for Cutaneous Drug Delivery. Curr Med Chem. 2018 Feb 13;25(5):606–35.

75. Weissig V. Liposomes Came First: The Early History of Liposomology. In: Liposomes: Methods and Protocols. New York: Springer; 2017. 1–15.

76. Li M, Du C, Guo N, Teng Y, Meng X, Sun H, et al. Composition design and medical application of liposomes. Eur J Med Chem. 2019 Feb 15;164:640–53.

77. Ahmed KS, Hussein SA, Ali AH, Korma SA, Lipeng Q, Jinghua C. Liposome: composition, characterisation, preparation, and recent innovation in clinical applications. J Drug Target. 2019 Aug 9;27(7):742–61.

78. Li J, Wang X, Zhang T, Wang C, Huang Z, Luo X, et al. A review on phospholipids and their main applications in drug delivery systems. Asian J Pharm Sci. 2015 Apr 1;10(2):81–98.

79. Akbarzadeh A, Rezaei-Sadabady R, Davaran S, Joo SW, Zarghami N, Hanifehpour Y, et al. Liposome: classification, preparation, and applications. Nanoscale Res Lett. 2013 Feb 22;8(1):102.

80. Torchilin V.P, Weissig V. Liposomes - A Practical Approach. 2nd Edition. Oxford: Oxford University Press; 2003.

81. Pandey H, Rani R, Agarwal V, Pandey H, Rani R, Agarwal V. Liposome and Their Applications in Cancer Therapy. Braz Arch Biol Technol. 2016;20:59.

82. Popovska O, Simonovska J, Kavrakovski Z, Rafajlovska V. An Overview: Methods for Preparation and Characterization of Liposomes as Drug Delivery Systems. Int J Pharm Phytopharmacol Res. 2013;3(3):182–9.

83. Zhang H. Thin-Film Hydration Followed by Extrusion Method for Liposome Preparation. Methods Mol Biol Clifton NJ. 2017;1522:17–22.

84. Nkanga CI, Bapolisi AM, Okafor NI, Krause RWM. Liposomes: Advances and Perspectives. IntechOpen;2019.

85. Patil YP, Jadhav S. Novel methods for liposome preparation. Chem Phys Lipids. 2014 Jan 1;177:8–18.

86. Rai S, Pandey V, Rai G. Transfersomes as versatile and flexible nano-vesicular carriers in skin cancer therapy: the state of the art. Nano Rev Exp. 2017 Jun 7;8(1): 1325708.

87. Manca ML, Zaru M, Manconi M, Lai F, Valenti D, Sinico C, et al. Glycerosomes: a new tool for effective dermal and transdermal drug delivery. Int J Pharm. 2013 Oct 15;455(1–2):66–74.

88. Manca ML, Cencetti C, Matricardi P, Castangia I, Zaru M, Sales OD, et al. Glycerosomes: Use of hydrogenated soy phosphatidylcholine mixture and its effect on vesicle features and diclofenac skin penetration. Int J Pharm. 2016 Sep 10;511(1):198–204.

89. Manca ML, Manconi M, Zaru M, Valenti D, Peris JE, Matricardi P, et al. Glycerosomes: Investigation of role of 1,2-dimyristoyl-sn-glycero-3-phosphatidycholine (DMPC) on the assembling and skin delivery performances. Int J Pharm. 2017 Oct 30;532(1):401–7.

90. Salem HF, Kharshoum RM, Sayed OM, Abdel Hakim LF. Formulation design and optimization of novel soft glycerosomes for enhanced topical delivery of celecoxib and cupferron by Box-Behnken statistical design. Drug Dev Ind Pharm. 2018 Nov;44(11):1871–84.

91. Manca ML, Castangia I, Zaru M, Nácher A, Valenti D, Fernàndez-Busquets X, et al. Development of curcumin loaded sodium hyaluronate immobilized vesicles (hyalurosomes) and their potential on skin inflammation and wound restoring. Biomaterials. 2015 Dec;71:100–9.

92. Salwowska NM, Bebenek KA, Żądło DA, Wcisło-Dziadecka DL. Physiochemical properties and application of hyaluronic acid: a systematic review. J Cosmet Dermatol. 2016;15(4):520–6.

93. Manca ML, Lattuada D, Valenti D, Marelli O, Corradini C, Fernàndez-Busquets X, et al. Potential therapeutic effect of curcumin loaded hyalurosomes against inflammatory and oxidative processes involved in the pathogenesis of rheumatoid arthritis: The use of fibroblast-like synovial cells cultured in synovial fluid. Eur J Pharm Biopharm. 2019 Mar 1;136:84–92.

94. Castangia I, Caddeo C, Manca ML, Casu L, Latorre AC, Díez-Sales O, et al. Delivery of liquorice extract by liposomes and hyalurosomes to protect the skin against oxidative stress injuries. Carbohydr Polym. 2015 Dec 10;134:657–63.

95. Castangia I, Manca ML, Catalán-Latorre A, Maccioni AM, Fadda AM, Manconi M. Phycocyanin-encapsulating hyalurosomes as carrier for

skin delivery and protection from oxidative stress damage. J Mater Sci Mater Med. 2016 Feb 17;27(4):75.

96. Müller-Röver S, Handjiski B, van der Veen C, Eichmüller S, Foitzik K, McKay IA, et al. A comprehensive guide for the accurate classification of murine hair follicles in distinct hair cycle stages. J Invest Dermatol. 2001 Jul;117(1):3–15.

97. Zhang Y, Han L, Chen S-S, Guan J, Qu F-Z, Zhao Y-Q. Hair growth promoting activity of cedrol isolated from the leaves of Platycladus orientalis. Biomed Pharmacother. 2016 Oct 1;83:641–7.

ANEXOS

International Journal of Pharmaceutics 511 (2016) 23–29

Contents lists available at ScienceDirect

International Journal of Pharmaceutics

journal homepage: www.elsevier.com/locate/ijpharm

Inhibition of skin inflammation by baicalin ultradeformable vesicles

Silvia Mir-Palomo[a,*], Amparo Nácher[a,b], Octavio Díez-Sales[a,b], M.A. Ofelia Vila Busó[c], Carla Caddeo[d], Maria Letizia Manca[d], Maria Manconi[d], Anna Maria Fadda[d], Amparo Ruiz Saurí[e]

[a] Dept. Pharmacy and Pharmaceutical Technology, Faculty of Pharmacy, University of Valencia, Spain
[b] Institute of Molecular Recognition and Technological Development, Inter-Universitary Institute from Polytechnic University of Valencia and University of Valencia, Spain
[c] Dept. Physics and Chemistry, Faculty of Pharmacy, University of Valencia, Spain
[d] Dept. Farmaco Chimico Tecnologico, University of Cagliari, Cagliari 09124, Italy
[e] Dept. of Pathology, University of Valencia, Avda Blasco Ibañez 17, 46010 Valencia, Spain

ARTICLE INFO

Article history:
Received 26 May 2016
Received in revised form 27 June 2016
Accepted 29 June 2016
Available online 30 June 2016

Keywords:
Baicalin
Ultradeformable vesicles
Skin
Mice
Topical delivery

ABSTRACT

The topical efficacy of baicalin, a natural flavonoid isolated from *Scutellaria baicalensis Georgi*, which has several beneficial properties, such as antioxidative, antiviral, anti-inflammatory and antiproliferative, is hindered by its poor aqueous solubility and low skin permeability. Therefore, its incorporation into appropriate phospholipid vesicles could be a useful tool to improve its local activity. To this purpose, baicalin at increasing concentrations up to saturation, was incorporated in ultradeformable vesicles, which were small in size (~67 nm), monodispersed (PI < 0.19) and biocompatible, regardless of the concentration of baicalin, as confirmed by *in vitro* studies using fibroblasts. On the other hand, transdermal flux through human epidermis was concentration dependent. The *in vivo* results showed the significant anti-inflammatory activity of baicalin loaded nanovesicles irrespective of the concentration used, as they were able to reduce the skin damage induced by the phorbol ester (TPA) application, even in comparison with dexamethasone, a synthetic drug with anti-inflammatory properties. Overall results indicate that ultradeformable vesicles are promising nanosystems for the improvement of cutaneous delivery of baicalin in the treatment of skin inflammation.

1. Introduction

Baicalin (7-glucuronic acid 5, 6-dihydroxyflavone), is one of the most abundant flavonoid in the root of *Scutellaria baicalensis Georgi*, used as medical agent in traditional Chinese medicine thanks to its multiple therapeutic benefits. Indeed, it has shown strong anti-inflammatory (Chen et al., 2001) and anti-oxidant properties (Shi et al., 2015), as well as antimicrobial and antifungal activities (Shi et al., 2014) and a great potential to prevent and inhibit tumor (Chen et al., 2016). Further, baicalin is able to protect the skin from damages caused by exposure to solar ultraviolet (UV) radiations. Considering all the protective and beneficial effects and its low toxicity, baicalin can be considered a suitable molecule for eliminating causes and effects of skin aging and injuries, including UV radiation damages, wounds and burns (Zhang et al., 2014a,b). Despite these promising properties, baicalin efficacy and actual use in topical formulations are hampered by its lipophilic nature and consequent low water solubility, which account for a poor bioavailability (Xing et al., 2005). To overcome this problem, baicalin has been loaded in different nanocarriers (Shi-Ying et al., 2014; Zhang et al., 2014a,b) for systemic, brain, corneal delivery and tumor targeting (Chen et al., 2016). In other studies, nanocarriers have been used to achieve effective transdermal delivery. Unfortunately, the barrier nature of the stratum corneum represents an important obstacle to drug accumulation into and passage through the skin, not only for conventional dosage forms, but also for some innovative dosage systems. To this purpose, several techniques or systems have been tested and the most widely studied approach in the last decades is the use of lipid nanocarriers, such as phospholipid vesicles and derived systems: ethosomes, glycerosomes and hyalurosomes (Manca et al., 2015; Castangia et al., 2013). Their use for skin delivery can offer some advantages over classical topical dosage forms, and some specially designed vesicular carriers can be able to efficiently increase drug penetration and permeation through the skin. Although there are

* Corresponding author.
E-mail address: silmirpa@gmail.com (S. Mir-Palomo).

http://dx.doi.org/10.1016/j.ijpharm.2016.06.136
0378-5173/

several studies on the incorporation of baicalin in liposomes (Wei et al., 2014), only a few studies specifically addressed the enhancement of baicalin efficacy following application on the skin. Hence, alternative phospholipid vesicles can result in a greater improvement of its therapeutic index and effectiveness in skin protection.

In light of this, in the present study, baicalin was incorporated in ultradeformable liposomes made with a mixture of soy lecithin and polysorbate 80, used as edge activator to improve bilayer fluidity. Thanks to this property, vesicles can squeeze themselves between the cells in the stratum corneum driven by the hydration gradient and reaching deeper skin strata. In addition, considering that drug saturation may improve its thermodynamic activity, maximizing the flux through biological membranes, irrespective of the selected vehicle and the drug solubility, baicalin was incorporated into ultradeformable vesicles at increasing amounts up to the maximum possible concentration (2.5, 5 and 10 mg/mL) which is supposed to saturate the system. Vesicle morphology, size distribution, zeta potential, and entrapment efficiency were evaluated, as well as the ability of the vesicles to promote *in vitro* baicalin skin delivery. The cytotoxic effect of empty and baicalin loaded vesicles was evaluated in 3T3 mouse fibroblasts. The drug and carrier performances and their ability to reduce oxidative inflammation and neutrophil infiltration induced by TPA in mice were studied, as well. To detect the damages induced by TPA on the skin and the effect provided by the tested formulations, a histological evaluation was also carried out.

2. Materials and methods

2.1. Materials

Lipoid® S75, a mixture of soybean lecithin containing phosphatidylcholine (70%) and phosphatidylethanolamine (10%), lysophosphatidylcholine (3% maximum), triglycerides (3% maximum), fatty acids (0.5% maximum), tocopherol (0.1–0.2%) was a gift from Lipoid GmbH (Ludwigshafen, Germany). Polysorbate 80 and disodium phosphate were purchased from Scharlab S.L. (Barcelona, Spain). Monosodium phosphate was purchased from Panreac quimica S.A. (Barcelona, Spain). Dexamethasone 21-sodium phosphate (DEX) was from Acofarma S.A. (Madrid, Spain) and the DEX solution (2 μg/mL) was prepared in buffer solution (pH 7.4). Baicalin (BA) was purchased by Cymit química S.L. (Barcelona, Spain) and saturated solution was prepared.

2.2. Vesicle preparation

Samples were prepared weighing Lipoid® S75 (180 mg/mL), polysorbate 80 (2.5 mg/mL) and BA (2.5, 5 and 10 mg/mL) in a glass vial and hydrating them overnight with a buffer solution (pH 7.4) composed by a mixture of monosodium phosphate (0.3%) and disodium phosphate (2.9%). Then, the dispersion was sonicated for 3 min with a CY-500 ultrasonic disintegrator (Optic Ivymen system, Barcelona, Spain) to obtain clear opalescent dispersions. To achieve a uniform particle size distribution, the liposomal suspension was extruded with an Avanti® Mini-Extruder (Avanti Polar Lipids, Alabaster, Alabama) through a 200 nm membrane (Whatman, GE Healthcare, Fairfield, Connecticut, US) (Manconi et al., 2003). Empty liposomes were prepared as reference.

2.3. Analytical method

The BA content was quantified using a PerkinElmer® Series 200 HPLC equipped with a UV detector and a column Teknokroma® Brisa "LC2" C18, 5.0 μm (150 cm × 4.6 mm). The mobile phase consisted of a mixture of water and methanol (30:70), delivered at a flow rate of 1 mL/min. BA content was measured at 278 nm. The limit of detection and quantification for the BA was 0.45 μg/mL and 1.36 μg/mL, respectively.

2.4. Vesicle characterization

The formation and morphology of ultradeformable liposomes were checked by transmission electron microscopy (TEM) using a JEM-1010 microscope (Jeol Europe, Croissy-sur-Seine, France), equipped with a digital camera MegaView III at an accelerating voltage of 80 kV. Vesicles were examined using a negative staining technique: non-diluted dispersions were stained with 1% phosphotungstic acid on a carbon grid and examined/visualized.

The average diameter and polydispersity index (PI) of non-diluted samples were determined by Photon Correlation Spectroscopy using a Zetasizer nano-S (Malvern Instruments, Worcestershire, United Kingdom). Zeta potential was estimated using the Zetasizer nano-S by electrophoretic light scattering, which measures the particle electrophoretic mobility in a thermostated cell. Vesicles were purified from non-incorporated BA by dialysis. Each sample (1 mL) was loaded into Spectra/Por® tubing (12–14 kDa MW cut-off; Spectrum Laboratories Inc., DG Breda, The Netherlands) and dialyzed against buffer (1 L) for 2 h, at room temperature. Both non-dialyzed and dialyzed samples were disrupted with methanol (1:100) and assayed by HPLC to quantify the BA content in the vesicular systems. The drug entrapment efficiency (EE%) of the three systems was calculated as follows (Eq. (1)):

$$EE(\%) = \left(\frac{actualBA}{initialBA}\right) \times 100 \quad (1)$$

where *actual BA* is the amount of BA in vesicles after dialysis, and *initial BA* is the amount of drug before dialysis, as calculated by HPLC.

2.5. Cell culture

3T3 mouse fibroblasts (ATCC, Manassas, VA, USA) were cultured in Dulbecco's modified Eagle's medium (Sigma Aldrich, Spain), supplemented with 10% (v/v) foetal bovine serum, penicillin (100 U/mL), and streptomycin (100 μg/mL) (Sigma Aldrich, Spain) in 5% CO_2 incubator at 37 °C to maintain exponential cell growth.

2.6. Cell viability studies

3T3 cells were seeded in 96-well plates with cell density being approximately 5×10^5 cells/well, at passages 11–12. After 24 h of incubation, 3T3 cells were treated for 2, 4, 8 and 24 h with ultradeformable vesicles, empty or loaded with BA at different concentrations: 2.5 BA (2.5 mg/mL), 5 BA (5 mg/mL) and 10 BA (10 mg/mL) or BA saturated solution (25 μL of formulation in 250 μL of medium). Cell viability was determined by the MTT [3 (4,5-dimethylthiazolyl-2)-2,5-diphenyltetrazolium bromide] colorimetric assay. Briefly, 200 μL of MTT reagent (0.5 mg/mL in PBS) was added to each well and after 2 h the formed formazan crystals were dissolved in DMSO. The reaction was spectrophotometrically measured at 570 nm with a microplate reader (Multiskan EX, Thermo Fisher Scientific, Inc., Waltham, Massachusetts, United States). All experiments were repeated at least three times, each time in triplicate. Results are shown as percentage of cell viability in comparison with non-treated control cells (100% viability) (Eq. (2)):

$$CellViability(\%) = \left(\frac{Absorbance_{sample}}{Absorbance_{control}}\right) \times 100 \quad (2)$$

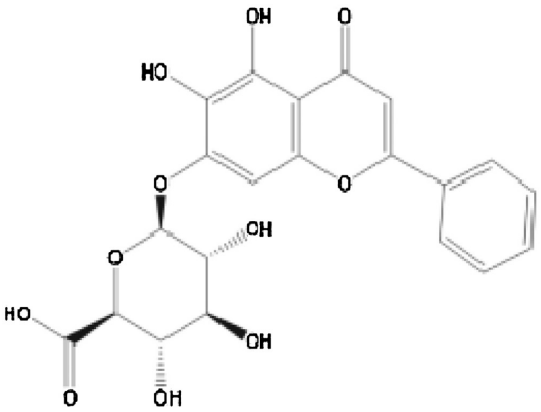

Fig. 1. Chemical structure of Baicalin (BA).

where $Absorbance_{sample}$ is the absorbance of fibroblasts treated with the vesicular formulation and $Absorbance_{control}$ is the absorbance of non-treated cells, at 570 nm.

2.7. Skin permeation studies

Permeation experiments were performed on Caucasian abdominal skin samples obtained from three randomly assigned female donors aged 38–48 years who had undergone cosmetic surgical procedures in the Hospital Clínico Universitario (Valencia, Spain). Informed consent was previously obtained from the patients, and their identity was masked to the researchers to guarantee their anonymity. Excess of fatty and connective tissues was removed, and the samples (full thickness skin) were stored at −40 °C for no more than 1 month.

Experiments were performed non-occlusively by means of vertical Franz cells (effective diffusion area of 0.784 cm^2), using epidermis from human skin (Díez-Sales et al., 2005). Epidermis was sandwiched securely between donor and receptor compartments of the Franz cells, with the stratum corneum side facing the donor compartment (Manconi et al., 2012). The receptor compartment was filled with 6 mL of buffer solution (pH 7.4), which was continuously stirred with a small magnetic bar and thermostated (~37 °C) throughout the experiments to reach the physiological skin temperature (~32 °C). The different formulations (200 μL) were applied on the epidermis surface and at different time intervals, over 24 h, receptor solutions were withdrawn and analysed for BA content by HPLC (as described in Section 2.3). Finally, in order to check the integrity of the epidermis, 1 mL of phenol red solution (0.5 mg/mL) was applied in the donor compartment.

The cumulative amounts (Q) of drug permeated per cm^2 of skin were plotted against time, and the equation derived from the application of the Fick's Second Law to the diffusion process was fitted to the data (Eq. (4)):

$$Q_{(t)} = A \cdot P \cdot L \cdot C\left[D \cdot \frac{t}{L^2} - \frac{1}{6} - \frac{2}{x^2} \cdot \sum_{n=1}^{\infty} \cdot Exp\left(\frac{-D \cdot n^2 \cdot x^2 \cdot t}{L^2}\right)\right] \quad (4)$$

where $Q\ (t)$ is the quantity of BA passing across the skin and reaching the receptor solution at a given time, t; A is the actual diffusion surface area (0.784 cm^2); P is the partition coefficient of the permeant between the skin and the donor vehicle; L is the diffusion pathway; D is the diffusion coefficient of the permeant in the membrane; and C is the concentration of the permeant in the donor solution. The fitting procedures were carried out by means of nonlinear regression using Sigma Plot 10.0 (Pharsight corp, USA).

By fitting the Eq. (4), lag time (t_L, h) corresponding to $L^2/6D$ and the permeability coefficient ($Kp = P{\cdot}D/L$) were calculated. The flux values (J) were obtained by employing the expression: $J = Kp{\cdot}C$.

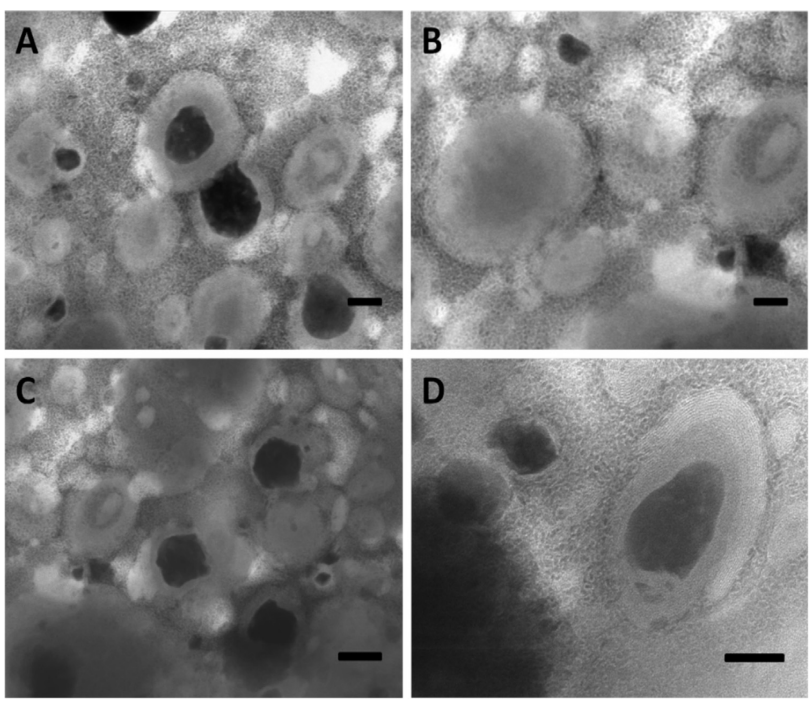

Fig. 2. Representative TEM micrographs of ultradeformable vesicles loading BA: 2.5 BA (A and D), 5 BA (B) and 10 BA (C). Each bar corresponds to 100 nm.

Table 1
Average size, polydispersity index (PI), zeta potential (ZP) and BA entrapment efficiency (EE, %) of empty ultradeformable vesicles and the same vesicles loading BA 2.5, 5 and 10 mg/ml (2.5 BA, 5 BA, 10 BA). Each value is the mean ± SD (n = 4).

Sample	Sample size (nm)		PI		Z Potential (mV)		EE (%)
	Initial	30 days	Initial	30 days	Initial	30 days	
Empty vesicles	82.50 ± 1.03	79.89 ± 1.09	0.183	0.25	−31.1 ± 0.5	−23.8 ± 0.9	–
2.5BA vesicles	74.84 ± 0.61	78.84 ± 1.27	0.137	0.27	−27.0 ± 1.1	−22.8 ± 1.5	82.75 ± 0.42
5BA vesicles	70.59 ± 0.07	87.73 ± 0.78	0.154	0.35	−30.4 ± 1.3	−24.8 ± 0.6	81.72 ± 0.23
10BA vesicles	67.58 ± 1.45	89.84 ± 1.58	0.132	0.38	−30.8 ± 1.9	−24.3 ± 1.99	80.86 ± 0.13

2.8. In vivo *experimental design*

Female CD-1 mice (5–6 weeks old, 25–35 g) were bred in the animal facility of the Faculty of Pharmacy of the University of Valencia. All studies were performed in accordance with European Union regulations for the handling and use of laboratory animals and the protocols were approved by the Institutional Animal Care and Use Committee of the University of Valencia (code A1456917886577). The back skin of mice was shaved one day before the experiment, and only animals showing no hair re-growth were selected for tests. On day 1, cutaneous inflammation was induced by applying on the shaved dorsal area (~2 cm^2) 20 μL of TPA dissolved in acetone (243 μM). After 3 h, empty or BA (2.5, 5 and 10 mg/mL) loaded liposomes, or BA saturated solution, or DEX solution (100 μL each) were topically smeared over the same dorsal site (non-occlusive conditions). The procedure was repeated on day 2 and 3. On day 4, mice were sacrificed by cervical dislocation. Each group comprised four mice.

2.9. In vivo *inflammatory: myeloperoxidase determination*

After 72 h of treatment (on day 4), mice were sacrificed and the treated skin area was excised and immediately stored at −80 °C (De Young et al., 1989; Caddeo et al., 2013). The myeloperoxidase (MPO) activity was measured. The biopsies were dispersed in 750 μL of sodium phosphate buffer 80 mM (pH 5.4) containing 0.5% hexadecyltrimethylammonium bromide and homogenized in ice bath with an Ultra-Turrax® T25 homogenizer (IKA® Werke GmbH & Co. KG, Staufen, Germany). The dispersions were centrifuged at 10.000 rpm for 15 min at 1 °C and the obtained supernatant (25 μL) was added to 75 μL saline phosphate buffer (pH 7.4), 10 μL sodium phosphate buffer (pH 5.4), 10 μL of 0.026% hydrogen peroxide and incubated at 37 °C for 5 min. Then, 10 μL of 18 mM 3,3′,5,5′-tetramethylbenzidine dihydrochloride hydrate in 8% aqueous *N*,*N*-dimethylformamide was added to start the reaction. After 10 min of incubation, the reaction was stopped with the addition of 15 μL of 1.5 M sodium acetate (pH 3.0), and the absorbance recorded at 620 nm using a microplate reader (Multiskan EX, Thermo Fisher Scientific, Inc., Waltham, Massachusetts, United States). The MPO activity was calculated from the linear portion of a standard curve.

2.10. *Histological examination*

Mice skin treated with the tested formulations was excised, fixed and stored in formaldehyde (10%). Tissue specimens were processed routinely and embedded in paraffin wax. Longitudinal sections (5 μm) were stained with haematoxylin and eosin (H&E) and observed by light microscope (DMD 108 DIGITAL Micro-imaging Device, Leica, Wetzlar, Germany).

2.11. *Statistical analysis of data*

Data are shown as mean ± standard deviation. Statistical differences were determined by using one-way ANOVA test and Tukey's test for multiple comparisons with a significance level of $P < 0.05$. All statistical analyses were performed using IBM SPSS statistics 22 for Windows (Valencia, Spain).

3. Results and discussion

BA is a flavonoid isolated from the dried roots of *Scutellaria baicalensis Georgi*. More precisely, it is a glycoside flavones formed by a benzene ring condensed with a six-member pyrone ring,

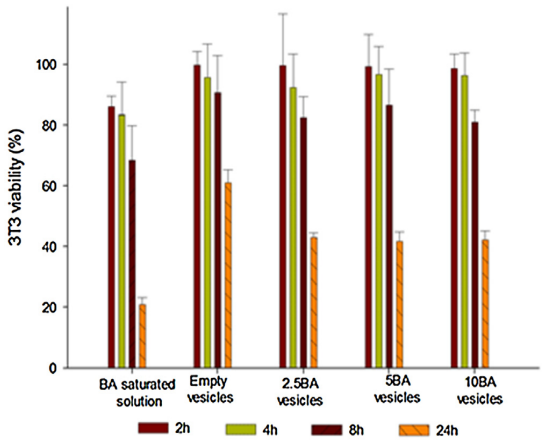

Fig. 3. In vitro 3T3 fibroblast viability after incubation with BA saturated solution, empty ultradeformable vesicles and the same vesicles loading 2.5, 5 and 10 mg/ml (2.5 BA, 5 BA, 10 BA) at different incubation times (2, 4, 8 and 24 h). Mean values ± standard deviations (error bars) are reported.

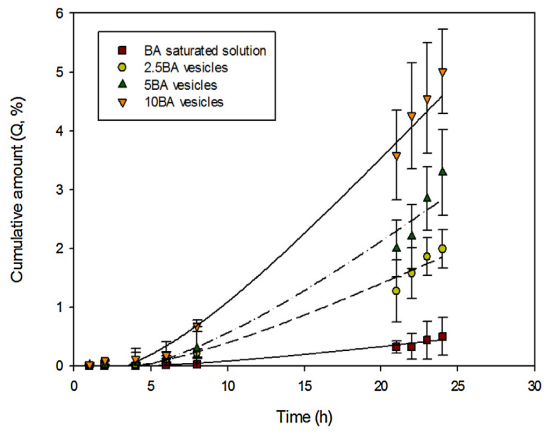

Fig. 4. Amount of BA accumulated in receptor compartment after 24 h treatment with different formulations: BA saturated solution (- □ -) and ultradeformable vesicles loading different concentrations of BA: 2.5 BA (- ○ -), 5 BA (- △ -) and 10 BA (- ▽ -) (n = 4). Mean values ± standard deviations (error bars) are reported (n = 4).

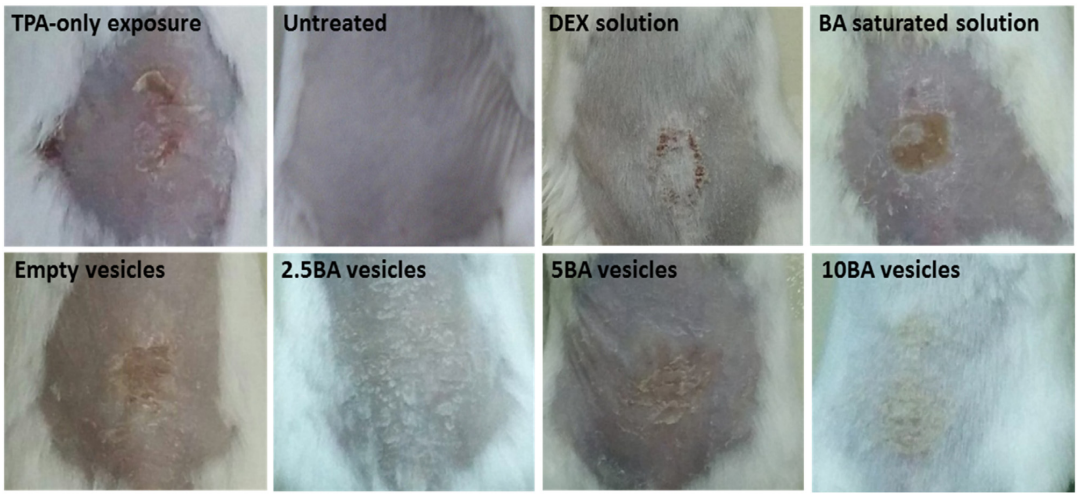

Fig. 5. Macroscopic appearance of mice skin lesions inducted with TPA and treated with acetone (untreated skin), DEX solution, BA saturated solution, empty liposomes or the same vesicles loading BA 2.5, 5 and 10 mg/ml (2.5 BA, 5 BA, 10 BA).

which in the 2-position carries a phenyl benzene ring as a substituent (Fig. 1). Taking into account its low skin bioavailability along with the beneficial effects on skin protection, and the lack of studies focusing on its topical delivery using innovative phospholipid vesicles, in the present work BA was incorporated in ultradeformable vesicles at increasing concentrations. Aiming at optimizing the formulation of ultradeformable vesicles, a preformulation study was carried out increasing the amount of BA loaded, so as to reach the critical/maximum concentration (10 mg/mL) without affecting the main physico-chemical characteristics of the vesicles: small, homogenous size, and high stability. It was found that above such concentration, the vesicles were large and highly polydispersed, and aggregation and BA precipitation occurred in a short time. Hence, 2.5, 5 and 10 mg/mL were selected as the concentrations to be used for further studies.

3.1. Vesicle characterization

TEM images provided evidence of vesicle formation, and showed that they were small, fairly spherical and multilamellar vesicles, regardless of the BA concentration (Fig. 2). Empty ultradeformable vesicles were small in size, around 82 nm (Table 1), and the incorporation of BA, whatever the concentration, led to a slight decrease of the mean diameter, from ~82 to ~67 nm, probably because the lipophilic BA interacts with the phospholipid chains, modifying their packing and permitting a reduction of the bilayer curvature. All the formulations were monodispersed (PI < 0.19) and Photon Correlation Spectroscopy results were always repeatable, as indicated by the small standard deviations obtained from at least three repetitions (Table 1). The zeta potential was highly negative (≈−30 mV), irrespective of BA concentration. Ultradeformable vesicles were purified from the non-incorporated drug by dialysis for 2 h, which was long enough to eliminate the free drug. Ultradeformable vesicles were able to incorporate BA in good yields, as the entrapment efficiency value was ~80%, without differences among the groups ($P > 0.05$). Physico-chemical properties of vesicles were very similar and were not affected by the different concentrations of BA, confirming that even at the highest concentration (10 mg/mL), the flavonoid was optimally incorporated in vesicle structure ensuring the system saturation.

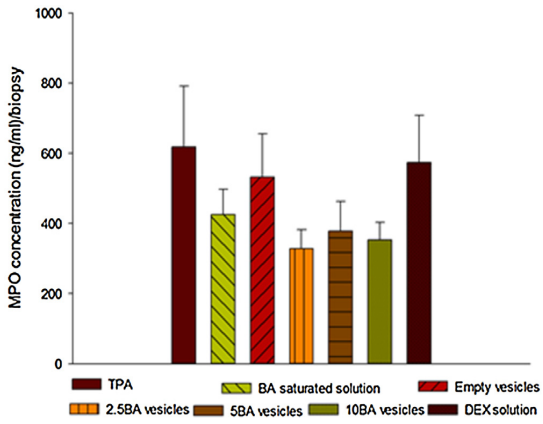

Fig. 6. MPO activity in skin mice inflamed with TPA and treated with DEX solution, BA saturated solution, empty ultradeformable vesicles or the same vesicles loading BA 2.5, 5 and 10 mg/ml (2.5 BA, 5 BA, 10 BA). Mean values ± standard deviations (error bars) are reported (n = 4).

3.2. Toxicity studies on 3T3 cells

When a new pharmaceutical formulation is designed, it is important to evaluate its safety, especially on the target tissue. *In vitro* toxicity study on cells represents a good and reliable method to select the formulations that will be used for further *in vivo* studies, so as to avoid the useless sacrifice of a high number of animals. 3T3 fibroblasts were used as a representative cell line of the dermis, and they were incubated with non-diluted formulations: empty or BA loaded vesicles and BA saturated solution.

The cytotoxicity was evaluated by the MTT assay. As shown in Fig. 3, all the vesicular formulations did not show a significant cytotoxic effect in the first 8 h of incubation (80% viability), compared to untreated control cells (100% viability), while BA saturated solution exhibited greater cytotoxicity, as the viability was less than 70%. At longer incubation time (24 h), an increase in cell mortality was observed, especially for the fibroblasts treated with BA saturated solution (20% viability), while a ~50% viability was found when BA loaded ultradeformable vesicles were used, thus confirming the higher biocompatibility of the vesicles.

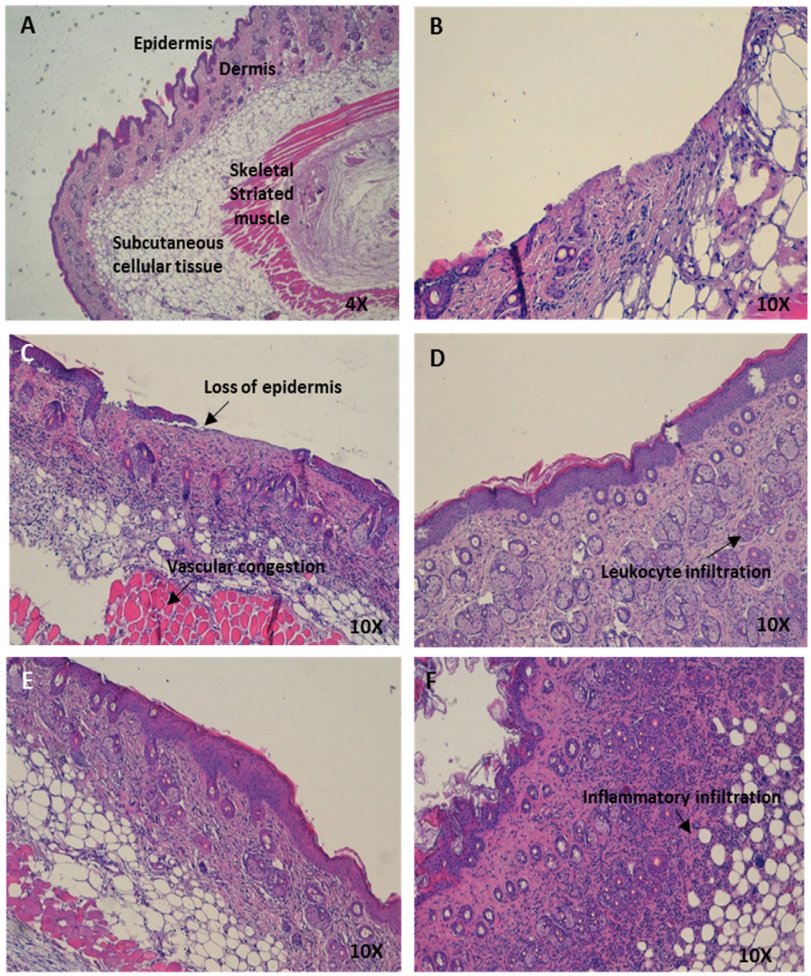

Fig. 7. Representative histological sections of mouse skin: untreated skin (A); TPA-inflamed skin (B); TPA-inflamed and treated with BA saturated solution (C); inflamed and treated with empty ultradeformable vesicles (D); inflamed and treated with BA loaded ultradeformable vesicles (E) or inflamed and treated with DEX solution (F).

3.3. Skin diffusion studies

Ultradeformable vesicles contain an edge activator which is reported to make the bilayer flexible and the vesicles able to squeeze through the skin channels, improving the transdermal flux of the loaded molecules. To confirm this assumption, permeation study using human epidermis was carried out applying on the skin ultradeformable vesicles loaded with BA (2.5, 5 and 10 mg/mL) or BA saturated solution. The permeation profiles obtained from the different formulations are shown in Fig. 4. The ultradeformable vesicles provided the greatest penetration rate of BA at 24 h, as compared to that obtained with the BA saturated solution. In particular, the vesicles loading the highest amount of BA (10 mg/mL) showed the best results in term of penetration (~5%) and flux (270.2 ± 16.2 μg/cm^2/h). By decreasing the amount of BA, the amount permeated and the flux of the drug decreased as well, being 2.5% and 117.3 ± 9.7 μg/cm^2/h for the vesicles loading 5 mg/mL, and 1.5% and 190.11 ± 16.63 μg/cm^2/h for vesicles loading 2.5 mg/mL of BA. In all cases, the lag time (t_L) was around 9 h. Significant differences between the flux values and the amount of permeated BA provided by the three vesicles and saturated solution were detected ($P < 0.05$), disclosing the concentration-dependent ability of the vesicles to deliver BA on the skin.

3.4. In vivo *inflammatory response: myeloperoxidase assay*

The application of TPA in mice to induce inflammatory response is one of the most common model for the evaluation of the anti-inflammatory activity of drugs. TPA induces a variety of histological and biochemical changes in the skin, including neutrophil infiltration in epidermis and dermis, epidermal hyperplasia, activation of protein kinase C, induction of ornithine decarboxylase activity, and enhancement of IL-1 levels. In this work, TPA was daily applied on mouse dorsal skin for 3 days, inducing skin damages at the macroscopic level, such as skin ulceration, loss of epidermis integrity and crust formation, as well as biological alterations, such as neutrophil infiltration, as previously reported (Caddeo et al., 2013). The MPO activity was quantified as a marker of the inflammatory process, since it is proportional to the neutrophil concentration in the inflamed tissue. The efficacy of BA loaded ultradeformable vesicles was tested and compared with that of DEX solution and BA saturated solution. The photographs of the treated mice clearly showed the therapeutic potential of BA loaded ultradeformable vesicles, as an amelioration of the TPA cutaneous damage was visible (Fig. 5). The treatment with DEX solution reduced TPA skin lesion, but to a lesser extent: skin appeared diffusely dry, flaky, and crusted. These effects were much severe in

mice treated with the BA saturated solution. The macroscopic observations are in agreement with the MPO values. The vesicles displayed a superior ability to reduce MPO activity in the injured tissue, and its inhibition was higher than that provided by both DEX solution and BA saturated solution (Fig. 6). No significant differences were observed ($P > 0.05$) among the results provided by the three vesicular formulations containing different amounts of BA, which indicates that, in spite of the system saturation, ultradeformable vesicles can ensure a higher beneficial activity of BA than that obtained using the saturated solution. Differently to the *in vitro* transdermal delivery results, the *in vivo* treatment of damaged skin was not affected by the BA concentration in vesicles, probably because in this model the stratum corneum was thinner or disrupted, thus facilitating the vesicle passage and allowing a therapeutic effect even at the lower concentration. The importance of the vesicle saturation effect was underlined in transdermal studies, where the BA needs to overcome the intact skin barrier and transdermal flux was concentration-dependent.

3.5. Histological evaluation

Morphological alterations of mouse skin exposed to TPA were assessed by H&E staining, in comparison with untreated skin (Fig. 7B and A, respectively). As already demonstrated with the biomarker, the skin treated with acetone only showed a regular structure, epidermis and dermis had a normal appearance, as well as the tissues directly underneath (*i.e.*, subcutaneous cellular tissue, skeletal muscle and adipose tissue), with only some mononuclear and polymorphonuclear cells in the muscular region (Fig. 7A). Mouse skin treated with TPA displayed severe dermal and subcutaneous alteration, with a large number of leukocytes infiltrating these regions, as well as muscle and adipose tissues, also showing pathological features of inflammatory damage, such as vascular congestion (Fig. 7B). Similar results of injured skin were obtained using the BA saturated solution and DEX solution (Fig. 7C and F). On the other hand, the application of the BA loaded ultradeformable vesicles reduced TPA-induced lesions, along with mild to moderate inflammatory infiltrates of mononuclear cells, eosinophils and neutrophils (Fig. 7E). The *in vivo* findings disclosed a great therapeutic efficacy of BA loaded ultradeformable vesicles, which unlike the transdermal flux, was not BA concentration/saturation dependent, probably because the transdermal flux depended on the passage of BA through the skin while, in the TPA model, the epidermis is disrupted, the skin's barrier function is impaired and BA can easily diffuse, whatever the concentration in the vesicles.

4. Conclusions

Bearing in mind the few data reporting the design of baicalin loaded innovative phospholipid vesicles and their possible improvement of transdermal delivery, in the present work new, suitable and biocompatible ultradeformable vesicles loading baicalin were developed. We demonstrated that the ultradeformable vesicles play a key role in facilitating baicalin skin delivery and showed a great potential as anti-inflammatory systems and were more effective than dexamethasone in counteracting TPA inflammation and skin injury. Moreover, *in vivo* studies on damaged skin underlined that the efficacy of baicalin was not affected by the concentration, while *in vitro* studies performed using human intact skin, indicated that using BA vesicles (10 mg/mL) the highest penetration was obtained.

References

Caddeo, C., Sales, O.D., Valenti, D., Saurí, A.R., Fadda, A.M., Manconi, M., 2013. Inhibition of skin inflammation in mice by diclofenac in vesicular carriers: liposomes, ethosomes and PEVs. Int. J. Pharm. 443, 128–136. doi:http://dx.doi.org/10.1016/j.ijpharm.2012.12.041.

Castangia, I., Manca, M.L., Matricardi, P., Sinico, C., Lampis, S., Fernàndez-Busquets, X., Fadda, A.M., Manconi, M., 2013. Effect of diclofenac and glycol intercalation on structural assembly of phospholipid lamellar vesicles. Int. J. Pharm. 456, 1–9. doi:http://dx.doi.org/10.1016/j.ijpharm.2013.08.034.

Chen, Y.-C., Shen, S.-C., Chen, L.-G., Lee, T.J.-F., Yang, L.-L., 2001. Wogonin, baicalin, and baicalein inhibition of inducible nitric oxide synthase and cyclooxygenase-2 gene expressions induced by nitric oxide synthase inhibitors and lipopolysaccharide1. Biochem. Pharmacol. 61, 1417–1427. doi:http://dx.doi.org/10.1016/S0006-2952(01)00594-9.

Chen, Y., Minh, L.V., Liu, J., Angelov, B., Drechsler, M., Garamus, V.M., Willumeit-Römer, R., Zou, A., 2016. Baicalin loaded in folate-PEG modified liposomes for enhanced stability and tumor targeting. Colloids Surf. B Biointerfaces 140, 74–82. doi:http://dx.doi.org/10.1016/j.colsurfb.2015.11.018.

Díez-Sales, O., Garrigues, T.M., Herráez, J.V., Belda, R., Martín-Villodre, A., Herráez, M., 2005. In vitro percutaneous penetration of acyclovir from solvent systems and carbopol 971-P hydrogels: influence of propylene glycol. J. Pharm. Sci. 94, 1039–1047. doi:http://dx.doi.org/10.1002/jps.20317.

De Young, L.M., Kheifets, J.B., Ballaron, S.J., Young, J.M., 1989. Edema and cell infiltration in the phorbol ester-treated mouse ear are temporally separate and can be differentially modulated by pharmacologic agents. Agents Actions 26, 335–341.

Manca, M.L., Castangia, I., Zaru, M., Nácher, A., Valenti, D., Fernàndez-Busquets, X., Fadda, A.M., Manconi, M., 2015. Development of curcumin loaded sodium hyaluronate immobilized vesicles (hyalurosomes) and their potential on skin inflammation and wound restoring. Biomaterials 71, 100–109. doi:http://dx.doi.org/10.1016/j.biomaterials.2015.08.034.

Manconi, M., Aparicio, J., Vila, A.O., Pendás, J., Figueruelo, J., Molina, F., 2003. Viscoelastic properties of concentrated dispersions in water of soy lecithin. Colloids Surf. Physicochem. Eng. Asp., A collection of papers presented at the International Symposium on Electrokinetic Phenomena, Cracow, Poland, August 18–22, 2003 222, 141–145. 10.1016/S0927-7757(03)00249-8.

Manconi, M., Caddeo, C., Sinico, C., Valenti, D., Mostallino, M.C., Lampis, S., Monduzzi, M., Fadda, A.M., 2012. Penetration enhancer-containing vesicles: composition dependence of structural features and skin penetration ability. Eur. J. Pharm. Biopharm. 82, 352–359. doi:http://dx.doi.org/10.1016/j.ejpb.2012.06.015.

Shi, G.-X., Shao, J., Wang, T.-M., Wang, C.-Z., 2014. New advance in studies on antimicrobal activity of Scutellaria baicalensis and its effective ingredients. J. Chin. Mater. Medica 39, 3713–3718.

Shi, G.-F., Yao, R.-X., Wang, G.-Y., Wang, Z.-J., Chen, F.-W., 2015. Liquid Chromatography-tandem mass spectrometry screening method for the detection of radical-scavenging natural antioxidants from the whole scutellariae (radix stem and leaf). J. Chromatogr. Sci. 53, 1140–1146. doi:http://dx.doi.org/10.1093/chromsci/bmu176.

Shi-Ying, J., Jin, H., Shi-Xiao, J., Qing-Yuan, L., Jin-Xia, B., CHEN, H.-G., Rui-Sheng, L., Wei, W., Hai-Long, Y., 2014. Characterization and evaluation in vivo of baicalin-nanocrystals prepared by an ultrasonic-homogenization-fluid bed drying method. Chin. J. Nat. Med. 12, 71–80. doi:http://dx.doi.org/10.1016/S1875-5364(14)60012-1.

Wei, Y., Guo, J., Zheng, X., Wu, J., Zhou, Y., Yu, Y., Ye, Y., Zhang, L., Zhao, L., 2014. Preparation, pharmacokinetics and biodistribution of baicalin-loaded liposomes. Int. J. Nanomed. 9, 3623–3630. doi:http://dx.doi.org/10.2147/IJN.S66312.

Xing, J., Chen, X., Zhong, D., 2005. Absorption and enterohepatic circulation of baicalin in rats. Life Sci. 78, 140–146. doi:http://dx.doi.org/10.1016/j.lfs.2005.04.072.

Zhang, H., Zhao, L., Chu, L., Han, X., Zhai, G., 2014a. Preparation, optimization, characterization and cytotoxicity in vitro of Baicalin-loaded mixed micelles. J. Colloid Interface Sci. 434, 40–47. doi:http://dx.doi.org/10.1016/j.jcis.2014.07.045.

Zhang, J., Yin, Z., Ma, L., Yin, Z., Hu, Y., Xu, Y., Wu, D., Permatasari, F., Luo, D., Zhou, B., 2014b. The protective effect of baicalin against UVB irradiation induced photoaging: an in vitro and in vivo study. PLoS One 9, e99703. doi:http://dx.doi.org/10.1371/journal.pone.0099703.

Colloids and Surfaces B: Biointerfaces 175 (2019) 654–662

Contents lists available at ScienceDirect

Colloids and Surfaces B: Biointerfaces

journal homepage: www.elsevier.com/locate/colsurfb

Baicalin and berberine ultradeformable vesicles as potential adjuvant in vitiligo therapy

Silvia Mir-Palomo[a], Amparo Nácher[a,b,*], M.A. Ofelia Vila Busó[c], Carla Caddeo[d], Maria Letizia Manca[d], Maria Manconi[d], Octavio Díez-Sales[a,b]

[a] Dept. Pharmacy, Pharmaceutical Technology and Parasitology, Faculty of Pharmacy, University of Valencia, Spain
[b] Instituto Interuniversitario de Investigación de Reconocimiento Molecular y Desarrollo Tecnológico (IDM), Universitat Politècnica de València, Universitat de València, Av. Vicent Andrés Estellés s/n, 46100, Burjassot, Valencia, Spain
[c] Dept. Physics and Chemistry, Faculty of Pharmacy, University of Valencia, Spain
[d] Dept. of Scienze della Vita e dell'Ambiente, University of Cagliari, via Ospedale 72, 09124, Cagliari, Italy

ARTICLE INFO

Keywords:
Ultradeformable vesicles
Vitiligo
Antioxidant
Photoprotection
Pigmentation

ABSTRACT

0.5–1% of the world's population is affected by vitiligo, a disease characterized by a gradual depigmentation of the skin. Baicalin and berberine are natural compounds with beneficial activities, such as antioxidant, anti-inflammatory and proliferative effects. These polyphenols could be useful for the treatment of vitiligo symptoms, and their efficacy can be improved by loading in suitable carriers. The aim of this work was to formulate and characterize baicalin or berberine loaded ultradeformable vesicles, and demonstrate their potential as adjuvants in the treatment of vitiligo. The vesicles were produced using a previously reported simple, scalable method. Their morphology, size distribution, surface charge and entrapment efficiency were assessed. The ability of the vesicles to promote the permeation of the polyphenols was evaluated. The antioxidant and photoprotective effects were investigated *in vitro* using keratinocytes and fibroblasts. Further, the stimulation of melanin production and tyrosinase activity in melanocytes after treatment with the vesicles were assessed. Ultradeformable vesicles were small in size, homogeneously dispersed, and negatively charged. They were able to incorporate high amounts of baicalin and berberine, and promote their skin permeation. In fact, the polyphenols concentration in the epidermis was higher than 10%, which could be indicative of the formation of a depot in the epidermis. The vesicles showed remarkable antioxidant and photoprotective capabilities, presumably correlated with the stimulation of melanin production and tyrosinase activity. In conclusion, baicalin or berberine ultradeformable vesicles, and particularly their combination, may represent promising nanosystem-based adjuvants for the treatment of vitiligo symptoms.

1. Introduction

Vitiligo is an autoimmune disease of the skin affecting 0.5–1% of the world's population [1]. It is clinically characterized by the appearance of disfiguring white patches caused by the loss of melanin pigment, which often negatively affects patients' self-esteem and quality of life [2]. Multiple mechanisms are involved in this disease: early factors include activation of innate immunity, inflammation, and oxidative stress [3]. Despite its occurrence, therapeutic options for patients are still limited. Current therapies exhibit considerable efficacy, but often the total repigmentation is not achieved [4]. One of the most common treatments involves the application of psoralens associated with ultraviolet (UV) light A exposure, topical corticosteroids, narrowband ultraviolet light B, which unfortunately cause important side effects [5].

In traditional Chinese medicine, different natural molecules and extracts have been successfully applied for the treatment of vitiligo [6]. The exact mechanism of action of these compounds is still unknown, but it seems to be related to their anti-inflammatory, immunomodulatory and antioxidant properties. Given that, antioxidant and anti-inflammatory natural molecules could be potential candidates for the vitiligo therapy, due to their efficacy and safety. Bearing in mind our previous results [7–9], baicalin and berberine were selected for this study. The former is a flavonoid with strong anti-inflammatory and antioxidant properties [10], antimicrobial and antifungal activities [11], a great potential in preventing and inhibiting tumours [12], and protecting the skin from the damages caused by intense exposure to

* Corresponding author at: Dept. Pharmacy, Pharmaceutical Technology and Parasitology, Faculty of Pharmacy, University of Valencia, Spain.
E-mail address: amparo.nacher@uv.es (A. Nácher).

https://doi.org/10.1016/j.colsurfb.2018.12.055
Received 11 September 2018; Received in revised form 29 November 2018; Accepted 19 December 2018
Available online 20 December 2018
0927-7765/

solar UV radiations [13]; the latter is a quaternary isoquinoline alkaloid with several pharmacological effects, including anticarcinogenic [14], antioxidant, anti-inflammatory [15] and pigmenting [16]. Both polyphenols have been used for the skin protection and the treatment of common dermatological disorders.

Despite the promising properties of baicalin and berberine, there are some limitations in their clinical applications, the most important being poor aqueous solubility and poor absorption after topical administration [17,18]. To overcome these problems and taking into consideration previous results obtained for the skin delivery of baicalin, in the present work, baicalin and berberine were incorporated in ultradeformable vesicles. Elastic and flexible phospholipid vesicles have been developed by using different phospholipids and a surfactant that acts as edge activator, enhancing the fluidity and deformability of the vesicle bilayer [19]. In this work, ultradeformable vesicles were prepared with a mixture of phospholipids and polysorbate 80, and their ability to improve the vitiligo symptoms was evaluated. An extensive physico-chemical characterization of the vesicles was accomplished by investigating their ability to promote the passage of baicalin and berberine into/through the skin. The cytotoxicity of the formulations was evaluated *in vitro* using keratinocytes and fibroblasts, as well as their ability to promote the antioxidant and photoprotective activities of baicalin and berberine. Further, melanocytes were used to evaluate the ability of the formulations to promote melanogenesis and tyrosinase activity.

2. Material and methods

2.1. Materials

Lipoid S75, a mixture of soybean lecithin with phosphatidylcholine (˜70%) and phosphatidylethanolamine (˜10%), non-polar lipids and fatty acids (˜20%), was a gift from Lipoid GmbH (Ludwigshafen, Germany). Disodium phosphate and polysorbate 80 were purchased from Scharlab S.L. (Barcelona, Spain). Monosodium phosphate was purchased from Panreac quimica S.A. (Barcelona, Spain). Sorbitol was from Guinama SL (Valencia, Spain). Baicalin was purchased from Cymit quimica S.L. (Barcelona, Spain), and berberine from Sigma-Aldrich (Madrid, Spain).

2.2. Vesicle preparation

Baicalin ultradeformable vesicles were prepared by dispersing baicalin (2.5 mg/mL), Lipoid S75 (60 mg/mL), and polysorbate 80 (2.5 mg/mL) in a buffered aqueous solution of monosodium phosphate and disodium phosphate (PBS, pH 7.4). Berberine ultradeformable vesicles were prepared by dispersing berberine (2.5 mg/mL), Lipoid S75 (120 mg/mL), and polysorbate 80 (2.5 mg/mL) with a solution of sorbitol (5% v/v) in water. The phospholipid was left swelling overnight, and then the dispersions were sonicated for 3 min with a CY-500 ultrasonic disintegrator (Optic Ivymen system, Barcelona, Spain) to obtain transparent dispersions. Further, in order to achieve a homogeneous system, the dispersions were extruded with an Avanti® Mini-Extruder (Avanti Polar Lipids, Alabaster, Alabama) through a 200 nm membrane (Whatman, GE Healthcare, Fairfield, Connecticut, US). Empty vesicles were also prepared and compared with polyphenol loaded vesicles.

2.3. Analytical methods

The baicalin and berberine content was quantified by using a Perkin Elmer® Series 200 HPLC equipped with a UV detector and a column Teknokroma® Brisa "LC2" C18, 5.0 µm (150 × 4.6 mm). Baicalin was detected at 278 nm by using a mixture of water and methanol (30:70) as mobile phase, delivered at a flow rate of 1 mL/min. Berberine determination was carried out at 346 nm by using a mixture of water and methanol (50:50) as mobile phase, delivered at a flow rate of 1.2 mL/min.

2.4. Vesicle characterization

Vesicle formation and morphology were evaluated by Transmission Electron Microscopy (TEM), by using a JEM-1010 microscope (Jeol Europe, Croissy-sur-Seine, France), equipped with a digital camera MegaView III, at an accelerating voltage of 100 kV. The vesicles were examined by using a negative staining technique: non-diluted samples were stained with 1% phosphotungstic acid on a carbon grid and visualized.

The mean diameter and the Polydispersity Index (PI, a dimensionless measure of the broadness of the size distribution) of empty, baicalin or berberine ultradeformable vesicles were measured by Photon Correlation Spectroscopy (PCS) using a Zetasizer nano-ZS® (Malvern Instruments, Worcestershire, UK). Zeta potential was measured by using the Zetasizer nano-ZS by means of the M3-PALS (Mixed Mode Measurement-Phase Analysis Light Scattering) technique, which measures the particle electrophoretic mobility.

The stability of the vesicles was evaluated for 30 days at 25 °C. During this period, size, size distribution and surface charge were measured.

The vesicles were purified from the non-incorporated berberine or baicalin by dialysis. Each sample (1 mL) was loaded into Spectra/Por® tubing (12–14 kDa MW cut-off; Spectrum Laboratories Inc., DG Breda, The Netherlands) and dialyzed against 1 L of buffered solution (pH 7.4) for 4 h, at room temperature. Both non-dialyzed and dialyzed samples were disrupted with Triton X-100 (10%) and assayed by HPLC to quantify the amount of baicalin and berberine (Section 2.3). The entrapment efficiency (EE%) was calculated as percentage as follows (Eq. (1)):

$$EE(\%) = \left(\frac{actualactiveagent}{initialactiveagent}\right) \cdot 100 \quad (1)$$

where actual active agent is the amount of baicalin or berberine detected in the vesicles after dialysis, and initial active agent is the amount of baicalin or berberine detected before dialysis.

2.5. Skin permeation studies

Permeation experiments were performed by using static vertical Franz diffusion cells and newborn pig skin provided by a local slaughterhouse. Excess of fatty and connective tissues were removed, and the specimens (full-thickness skin) were stored at −80 °C until use. For the experiments, only the epidermis (thickness ˜200 µm) was used: it was securely clamped between the donor and receiver compartments of the Franz cells (effective diffusion area of 0.784 cm^2), with the stratum corneum side facing the donor compartment. The receptor compartment was filled with buffered solution (pH 7.4). The Franz cells were immersed in a bath system at 37 ± 2 °C and maintained under stirring in order to mimic physiological skin conditions. The different formulations (500 µL) were applied onto the epidermis surface, and at regular time intervals, up to 24 h, the receiving solution was withdrawn, replaced with pre-thermostated, fresh PBS, and analysed by HPLC for baicalin or berberine content (as described in Section 2.3). In addition, in order to verify the integrity of the epidermis, 1 mL of phenol red solution (0.5 mg/mL) was applied onto the skin surface in the donor compartment and quantified in the receptor compartment by spectrophotometry. When the values of phenol red were < 1%, the epidermis was considered intact.

The cumulative amounts (Q, µg/cm^2) of baicalin or berberine permeated through the epidermis were plotted against time, and the equation derived from the application of the Fick's Second Law to the diffusion process was fitted to the data (Eq. (2)):

$$Q_{(t)} = A \bullet P \bullet L \bullet C \left[D \bullet \frac{t}{L^2} - \frac{1}{6} - \frac{2}{x^2} \bullet \sum_{n=1}^{\infty} \bullet Exp\left(\frac{-D \bullet n^2 \bullet x^2 \bullet t}{L^2} \right) \right] \quad (2)$$

where $Q\ (t)$ is the amount of active agent passing across the skin and reaching the receptor solution at a given time t; A is the actual diffusion surface area (0.784 cm^2); P is the partition coefficient of the permeant between the skin and the donor vehicle; L is the diffusion pathway; D is the diffusion coefficient of the permeant in the skin; and C is the concentration of the permeant in the donor vehicle. The fitting procedures were carried out by means of non-linear regression using Sigma Plot 10.0 (Pharsight corp, USA). By fitting the equation 2, lag time (t_L, h) corresponding to $L^2/6D$ and the permeability coefficient ($Kp = P{\cdot}D/L$) were calculated.

2.6. Cell culture

Human immortalized keratinocytes (HaCaT) (Thermo Fisher Scientific Inc, Waltham, MA, USA) and 3T3 mouse fibroblasts (ATCC, Manassas, VA, USA) were cultured in Dulbecco's modified Eagle's medium (Sigma Aldrich, Spain), supplemented with 10% (v/v) foetal bovine serum, penicillin (100 U/mL), and streptomycin (100 µg/mL) (Sigma Aldrich, Spain) in 5% CO_2 incubator at 37 °C to allow exponential cell growth. Highly pigmented adult human epidermal melanocytes (HEMa) were purchased from Thermo Fisher Scientific Inc (Waltham, MA, USA). Cells were maintained in Medium 254 with the addition of Human Melanocyte Growth Supplement-2, PMA-Free ($HMGS^{-2}$) and 1% (V/V) gentamicin/amphothericin (Thermo Fisher Scientific Inc, Waltham, MA, USA) in a humidified incubator at 37 °C with 5% CO_2.

2.7. Cell viability studies

Cytotoxicity studies were carried out using HaCaT keratinocytes at passages 31–32, 3T3 fibroblasts at passages 22–23 and HEMa melanocytes at passages 4-5. The cells were seeded into 96-well plates with a density of approximately 2.5, 2.9, and 1.4 $\times \cdot 10^5$ cells/well, for HaCaT, 3T3 and HEMa, respectively. After 24 h of incubation, when confluence was reached, the cells were exposed for 24 h to baicalin in PBS or berberine in 5%sorbitol water solution, or empty vesicles, or baicalin or berberine loaded vesicles, at different concentrations (200, 100, 50, 25, 12.5, 1.56 µg/mL) of baicalin or berberine. Cell viability was determined by the MTT [3(4,5-dimethylthiazolyl-2)-2,5-diphenyltetrazolium bromide] colorimetric assay. MTT reagent (100 µL, 0.5 mg/mL) was added to each well, and after 3 h the formed formazan crystals were dissolved in DMSO (100 µL). The reaction was spectrophotometrically measured at 570 nm with a microplate reader (Multiskan EX, Thermo Fisher Scientific, Inc., Waltham, MA, US). The experiments were performed in triplicate and repeated at least three times. Results are shown as percentage of cell viability in comparison with untreated control cells (100% viability) (Eq. 3):

$$Cell\ Viability\ (\%) = \left(\frac{Absorbance_{sample}}{Absorbance_{control}} \right) x100 \quad (3)$$

where $Absorbance_{sample}$ is the absorbance of cells treated with the formulations and $Absorbance_{control}$ is the absorbance of non-treated cells, at 570 nm.

2.8. Dose-response curves for different intensities of UV radiation

In order to define the intensity of radiation that caused 50% cell death (LC_{50}), HaCaT and 3T3 were seeded into 96-well plates with a cell density of 1.7 and 2.0$\cdot \times$ 10^6 cells/well, respectively. When confluence was reached, the cells were irradiated with different intensities of UVB rays (100, 200, 400, 600, 800 and 1000 mJ/cm^2) using a Crosslinker Bio-Link BLX 254 camera (5 × 8 W; Peqlab Biotechnologie GmbH, Erlangen, Germany) at a wavelength of 310 nm. After 24 h, the MTT assay was performed as described in Section 2.7. Results are shown as percentage of cell viability in comparison with untreated control cells (100% viability).

2.9. Photoprotective effect of formulations against UV radiation

The photoprotective effect of the different formulations was assayed using the intensity of radiation that caused 50% cell death. HaCaT keratinocytes and 3T3 fibroblasts were seeded into 96-well plates, and after 24 h, were treated with baicalin in PBS or berberine in 5%sorbitol water solution, or empty vesicles, or baicalin or berberine loaded vesicles, at different concentrations of both polyphenols (12.5, 6.25, 3.12 and 1.56 µg/mL). In addition, the cells were treated simultaneously with both baicalin in PBS and berberine in 5%sorbitol water solution, or in the vesicles, at the above concentrations. 24 h after the treatment, the cells were irradiated with the appropriate intensity of UVB radiation, and incubated for 24 h at 37 °C with CO_2 (5%), then the cell viability was measured by MTT assay (as described in Section 2.7). Results are shown as percentage of photoprotection in comparison with untreated control cells (0% photoprotection): the percentage of photoprotection represents the percentage of live cells before and after treatment (Eq. (4)).

$$\%\ Photoprotection = \frac{Absorbance\ of\ treated\ cells - Absorbance\ of\ non\ treated\ cells}{Absorbance\ of\ treated\ cells} \bullet 100 \quad (4)$$

2.10. Efficacy of the formulations against oxidative stress in cells

HaCaT cells were seeded into 96-well plates (3.1 × 10^5 cells/well) and incubated until confluence was reached. The cells were treated simultaneously with hydrogen peroxide and the formulations: baicalin in PBS or berberine in 5%sorbitol water solution, or empty vesicles, or baicalin or berberine loaded vesicles, at non-cytotoxic concentrations of the polyphenols of 12.5, 6.25, 3.12, and 1.56 µg/mL. In addition, the cells were treated simultaneously with both baicalin in PBS and berberine in 5%sorbitol water solution, or in vesicles, at the above concentrations. After 4 h of treatment, the cells were washed with PBS, and the MTT assay was performed to measure the cell viability (as decribed in Section 2.7). Untreated cells were used as a negative control, and cells treated with hydrogen peroxide without formulations were used as a positive control. Results are shown as percentage of antioxidant capability in comparison with untreated cells (0% antioxidant capability).

2.11. Melanin content determination

HEMa cells at passages 5–6 were cultured on 6-well plates (2.2 × 10^5 cells/well) and incubated until confluence was reached. The cells were treated with baicalin in PBS or berberine in 5%sorbitol water solution, or empty vesicles, or baicalin or berberine loaded vesicles using non-cytotoxic concentrations (12.5, 6.25, 3.12 and 1.56 µg/mL) of baicalin or berberine. In addition, baicalin in PBS and berberine in 5%sorbitol water solution, or in vesicles were applied simultaneously, at the above concentrations. After 48 of incubation, the medium was removed, the cells were washed twice with PBS and harvested using trypsin (0.05%) and EDTA (0.02%). The harvested cells were centrifuged, the pellet was dissolved in NaOH solution (1 N) and incubated at 60 °C for 1 h. The amount of melanin in solution was determined by measuring the absorbance at 470 nm using a microplate reader (Multiskan EX, Thermo Fisher Scientific, Inc., Waltham, MA, US). Results are shown as a percentage of melanin content in comparison with untreated cells (100% viability).

2.12. Tyrosinase activity assay

Tyrosinase activity was estimated spectrophotometrically by using L-DOPA as substrate. HEMa cells at passages 5–6 were seeded into 6-well plates (approximately 2.0×10^5 cells/well) and incubated until confluence was reached. The cells were treated for 48 h with baicalin in PBS or berberine in 5%sorbitol water solution, or empty vesicles, or baicalin or berberine vesicles at different concentrations of baicalin or berberine (12.5, 6.25, 3.125, and 1.56 μg/mL). A combined treatment of baicalin in PBS and berberine in 5%sorbitol water solution, or in vesicles at the above concentrations was also tested. At the end of each experiment, the cells were treated with sodium phosphate buffer (0.1 M, pH 6.8) containing 1% Triton X-100 and disrupted by repeated freeze/thaw cycles at −20 °C for 30 min. The lysates were clarified by centrifugation at 10,000 *g* for 15 min, then 90 μL of each lysate was seeded into a 96-well plate, and L-DOPA (10 μL, 10 mM) was added to each well. After incubation at 37 °C in the dark for 90 min, the end-point absorbance was measured spectrophotometrically at 475 nm using a microplate reader (Multiskan EX, Thermo Fisher Scientific, Inc., Waltham, MA, US). Results are shown as a percentage of tyrosinase activity in comparison with untreated cells (100% viability).

2.13. Statistical analysis of data

Data are shown as means ± standard deviation. Statistical differences were determined by using one-way ANOVA test and Tukey´s test for multiple comparisons with a significance level of $p < 0.05$. All statistical analyses were performed using IBM SPSS statistics 22 for Windows (University of Valencia, Spain).

3. Results

3.1. Vesicle characterization

Based on our previous results [7], in the present study baicalin was incorporated in ultradeformable vesicles prepared with Lipoid S75 (60 mg/mL) and tween 80 (2.5 mg/mL) in PBS. To obtain berberine ultradeformable vesicles with size and polydispersity index comparable to those of baicalin vesicles, a higher amount of Lipoid S75 (120 mg/mL) was needed, as well as the addition of sorbitol (5% v/v in water). TEM images provided evidence of vesicle formation (Fig. 1). Baicalin ultradeformable vesicles were irregularly shaped and multilamellar, while berberine vesicles were mostly unilamellar, spherical in shape, and homogeneously dispersed. The size of the vesicles was measured by PCS, which provides a global value of mean size and size distribution as a function of the ability of the particles to scatter the incident light (Table 1). Empty formulations were also prepared and characterized to elucidate the effect of both active agents on bilayer-assembling features. Both baicalin and berberine vesicles were small in size, and the former were more monodispersed. All the vesicles were negatively charged, with berberine vesicles showing more negative values. The empty vesicles were larger than the corresponding baicalin or berberine loaded vesicles. This behaviour may be correlated with the intercalation of the polyphenols in the bilayer, which affected its assembly. Both baicalin and berberine were incorporated in high amounts in the vesicles. All the formulations were highly stable, since no significant changes were detected after 30 days on storage at room temperature (25 °C).

3.2. Skin permeation studies

In order to evaluate the ability of ultradeformable vesicles to enhance the permeation of baicalin and berberine through the skin, in vitro studies were performed by applying the polyphenols in PBS or in 5%sorbitol water solution, or loaded in vesicles onto newborn pig skin. The permeation profiles are presented in Fig. 2. The vesicles loaded with baicalin gave the best results in terms of penetration. The total amount of baicalin and berberine penetrated was ˜2% and 1%, respectively, which may be indicative of the formation of a depot in the epidermis. The permeability coefficients were 7.25×10^{-5} cm/s and 1.08×10^{-5} cm/s, respectively. Hence, the penetration of baicalin was 7-fold higher than berberine. These values are in accordance with the physico-chemical properties of the two polyphenols. The lag time (t_L) values for baicalin and berberine vesicles were around 6 and 4 h, respectively, which are favourable when a local effect is desired, decreasing the passage of the polyphenols into the bloodstream.

3.3. Cell viability studies

The cytotoxicity of baicalin and berberine formulations was evaluated using the main cells present in human skin: 3T3 fibroblasts, HaCaT keratinocytes and HEMa melanocytes (Fig. 3). After incubation with empty vesicles, the viability of the three cell lines was always ˜100%, regardless of the concentration tested. After incubation with baicalin in PBS or loaded vesicles, the viability values for HaCaT and HEMa were similar: ˜100% using the lower concentrations (from 3.12–50 μg/mL), ˜80% using 100 μg/mL of baicalin (regardless of the sample used) and ˜70% ($p < 0.05$) with 200 μg/mL of baicalin. The viability of 3T3 fibroblasts was always ≥100%, regardless of the tested sample or concentration.

A different behaviour was found incubating the cells with berberine in 5%sorbitol water solution or loaded in vesicles: the viability values were similar, irrespective of the cell type used. When the higher concentrations were used (from 200 to 25 μg/mL), the cell viability was between ˜50 and ˜75%, while at the lower concentrations (from 12.5 to 1.56 μg/mL) a 100% viability was reached. The non-cytotoxic concentrations were chosen to evaluate the efficacy of baicalin and berberine ultradeformable vesicles as antioxidants and photoprotectants of cells.

3.4. Dose-response curves for different intensities of UV radiation

The effect of UV radiation at different intensities on cell viability was evaluated in HaCaT keratinocytes and 3T3 fibroblasts. In a preliminary study, the cell viability was measured as a function of the radiation intensity (Fig. 4). Cell viability decreased as the radiation intensity increased, causing 50% cell death at 500 mJ/cm^2 for keratinocytes and at 400 mJ/cm^2 for fibroblasts. These UV intensities were chosen to evaluate the ability of baicalin and berberine vesicles to counteract the damaging effects of UV radiation.

3.5. Photoprotective effect of the formulations against UV radiation

The ability of the formulations to counteract the deleterious effects of UV radiation was measured in keratinocytes and fibroblasts, because the UV radiation is able to penetrate the skin and reach the dermis (Fig. 5). The photoprotective activity was calculated as a percentage of viability of treated versus untreated cells. Using the keratinocytes, the photoprotection provided by the baicalin in PBS or berberine in 5% sorbitol water solution at the different non-cytotoxic concentrations was very low (˜7%). The efficacy increased up to ˜34% thanks to the loading of baicalin in the ultradeformable vesicles, while the incorporation of berberine into the vesicles did not provide an important increase in the photoprotective activity (˜13%). When the keratinocytes were treated simultaneously with baicalin vesicles and berberine vesicles, the photoprotective activity was similar to that provided by baicalin vesicles alone (˜34%). In the fibroblasts, the photoprotective activity was similar to that obtained in keratinocytes: ˜13% with baicalin in PBS, ˜27% with baicalin vesicles at the three higher non-cytotoxic concentrations (from 12.5 to 3.12 μg/mL), and ˜14% at the lower non-cytotoxic concentration (1.56 μg/mL), ˜8% with berberine in 5% sorbitol water solution, and ˜18% with berberine vesicles. The

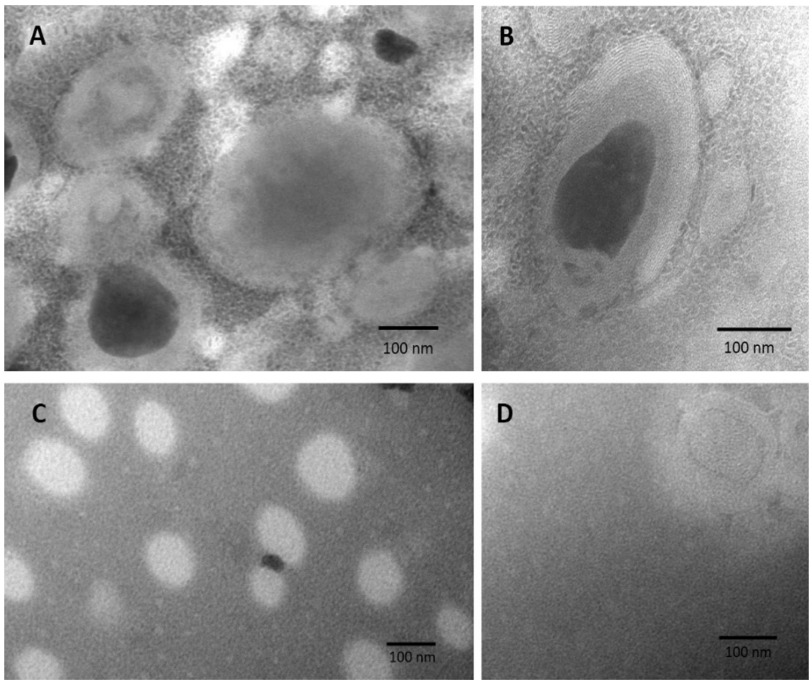

Fig. 1. Representative TEM micrographs of ultradeformable vesicles loaded with baicalin (A and B) and berberine (C and D).

association of baicalin vesicles and berberine vesicles provided values similar to those obtained with baicalin vesicles alone (˜28% at the three higher concentrations, 12.5, 6.25 and 3.12 μg/mL, and ˜16% at the lower concentration, 1.56 μg/mL). Overall results indicated that baicalin loaded vesicles showed a stronger photoprotective activity, which was not reinforced by the association with berberine.

3.6. Efficacy of the formulations against oxidative stress damage in cells

The ability of baicalin and berberine loaded vesicles to counteract the damages induced by oxidative stress was evaluated by using keratinocytes, which are the predominant cells in the outermost layer of the skin, thus more exposed to environmental contaminants and aggressors (Fig. 6). The cells were stressed with hydrogen peroxide and treated with baicalin in PBS or berberine in 5%sorbitol water solution, or in vesicles at the different non-cytotoxic concentrations (12.5-1.56 μg/mL). Additionally, the cells were treated with empty vesicles or baicalin vesicles together with berberine vesicles. The exposure of the cells to hydrogen peroxide, which was indicated as 0% antioxidant capability, led to a significant reduction in cell viability (˜65%). The antioxidant capability of the empty vesicles was around 30%, and increased using the polyphenols in PBS or in 5%sorbitol water solution, reaching ˜38% at the lower concentration (1.56 μg/mL) and ˜56% at the higher

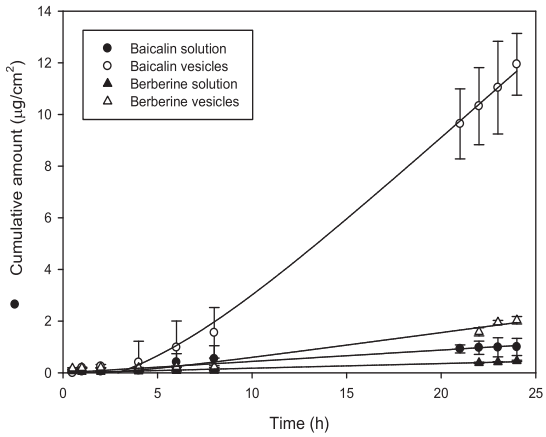

Fig. 2. Amount of baicalin and berberine accumulated in the receptor compartment after a 24 h application of the polyphenols in PBS or in 5%sorbitol water solution, and vesicular formulations. Mean values and standard deviations (error bars) are reported (n = 3).

Table 1
Mean diameter (MD), polydispersity index (PI), zeta potential (ZP) and entrapment efficiency (EE) of baicalin or berberine loaded ultradeformable vesicles and the corresponding empty vesicles. Empty vesicles A and empty vesicles B were obtained by dispersing the phospholipid in PBS and 5%sorbitol water solution, respectively. Each value is the mean ± standard deviation (n = 3).

	Vesicle size (nm)		PI		Z Potential (mV)		EE (%)
	Day 0	Day 30	Day 0	Day 30	Day 0	Day 30	
Baicalin vesicles	64.8 ± 1.3	69.9 ± 1.6	0.14 ± 0.03	0.27 ± 0.03	−27.0 ± 1.1	−22.8 ± 1.5	82.7 ± 0.4
Empty vesicles A	80.4 ± 1.8	87.9 ± 1.1	0.18 ± 0.03	0.25 ± 0.03	−31.1 ± 1.6	−23.8 ± 2.8	–
Berberine vesicles	61.1 ± 1.4	69.7 ± 1.1	0.24 ± 0.01	0.34 ± 0.04	−38.1 ± 1.4	−20.7 ± 2.2	87.1 ± 1.2
Empty vesicles B	85.9 ± 0.8	90.7 ± 2.4	0.16 ± 0.02	0.32 ± 0.01	−33.3 ± 3.8	−13.7 ± 1.6	–

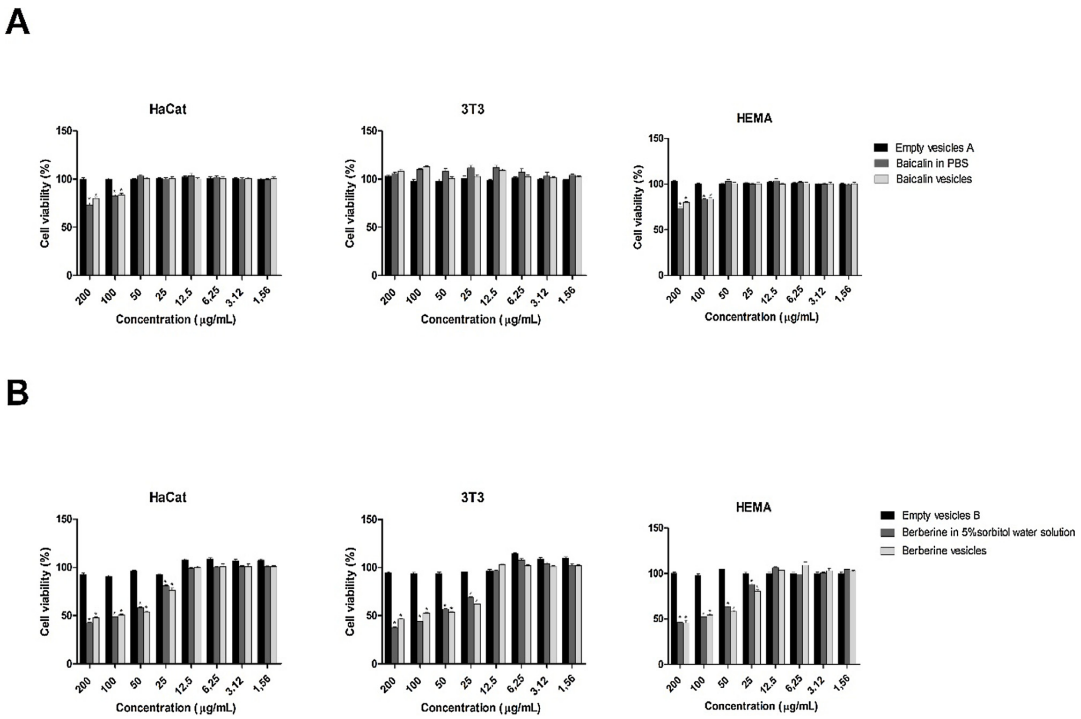

Fig. 3. Viability of HaCaT, 3T3 and HEMa cells incubated with ultradeformable vesicles loaded with baicalin (1) or berberine (2). The viability of cells treated with the corresponding empty vesicles or the polyphenols in PBS or 5%sorbitol water solution was reported as a reference. Empty vesicles A and empty vesicles B were obtained by dispersing the phospholipid in PBS and 5%sorbitol water solution, respectively. Mean values ± standard deviations (error bars) are reported (n = 16).

concentration (12.5 μg/mL) of baicalin in PBS, and ˜42% at all the concentrations of berberine in 5%sorbitol water solution. The antioxidant capability of baicalin or berberine ultradeformable vesicles further increased to ˜59% at the higher concentration (12.5 μg/mL), ˜55% at 6.25 μg/mL, and ˜47% at the other non-cytotoxic concentrations. Comparable results were obtained by treating the cells simultaneously with the baicalin vesicles and berberine vesicles, as the antioxidant activity reached ˜55% at the higher concentration (12.5 μg/mL) and ˜47% at the other non-cytotoxic concentrations. The same values were obtained using baicalin in PBS together with berberine in 5% sorbitol water solution.

3.7. Melanin content determination

The ability of baicalin and berberine vesicles to facilitate melanogenesis and skin pigmentation was evaluated in melanocytes. The cells were treated for 48 h with the formulations, the amount of melanin was measured, and the melanogenetic activity was calculated as a percentage of untreated cells (Table 2). The melanogenetic activity was around 90% in cells treated with baicalin in PBS, and slightly increased to ˜106% when the polyphenol was loaded in the vesicles. The melanogenetic activity increased especially using berberine vesicles at 12.5 and 6.25 μg/mL, reaching ˜133%. The higher melanogenetic activity was achieved when the cells were treated with the combination of baicalin vesicles and berberine vesicles, reaching ˜145% with the higher concentrations (12.5 and 6.25 μg/mL). The obtained data indicated that berberine vesicles stimulated the melanogenesis more than baicalin vesicles, and their combination further improved this activity, suggesting a possible use of these vesicles as adjuvants in repigmentation of skin affected by vitiligo.

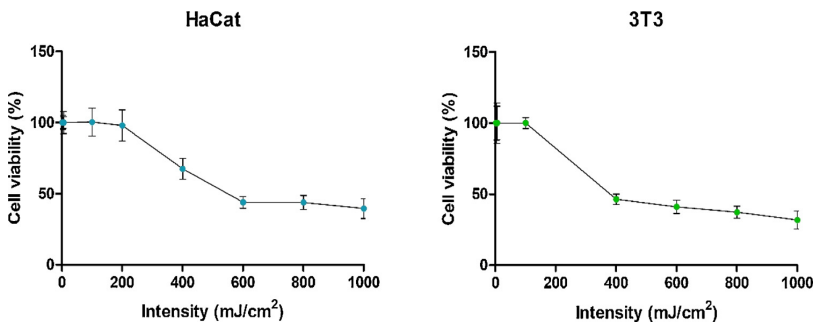

Fig. 4. Effect of UVB (λ = 310 nm) at different intensities on the viability of 3T3 fibroblasts and HaCaT keratinocytes. Values are given as means ± standard deviations (n = 16).

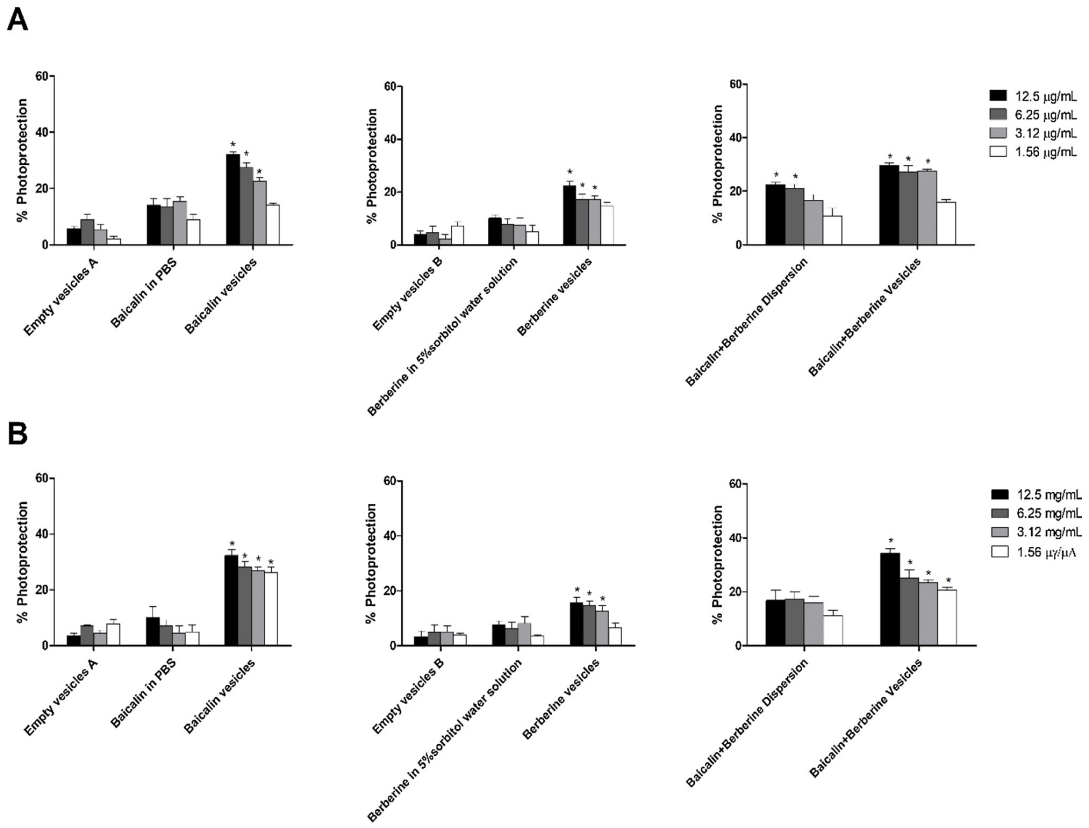

Fig. 5. Effect of baicalin and berberine formulations against UVB-induced phototoxicity in 3T3 fibroblasts (A) and HaCaT keratinocytes (B). Empty vesicles and polyphenols in PBS or 5%sorbitol water solution were tested as controls. Empty vesicles A and empty vesicles B were obtained by dispersing the phospholipid in PBS and 5%sorbitol water solution, respectively. Each bar represents the mean ± standard deviation (n = 16). *$p < 0.05$ versus irradiated and untreated controls.

3.8. Tyrosinase activity assay

To corroborate the pathway involved in the stimulation of melanin production, the tyrosinase activity was measured, as it is the key enzyme involved in melanin synthesis. Results were expressed as a percentage of untreated cells (Table 2).

Similarly, to the melanogenetic activity, the tyrosinase activity was less stimulated by baicalin in PBS (˜95%) or loaded in vesicles (˜100%), and more by berberine in 5%sorbitol water solution (˜110%) or loaded in vesicles (˜130%). The tyrosinase activity was markedly stimulated by the combination of baicalin vesicles and berberine vesicles, especially at the lower concentrations (136%). This combination may represent a potential strategy to stimulate both tyrosinase enzyme activity and melanin production.

4. Discussion

Vitiligo is a common skin disorder characterised by patchy areas of depigmentation due to the loss of melanin-forming cells, melanocytes, in the epidermis. Topical monotherapy is indicated for mild-to-

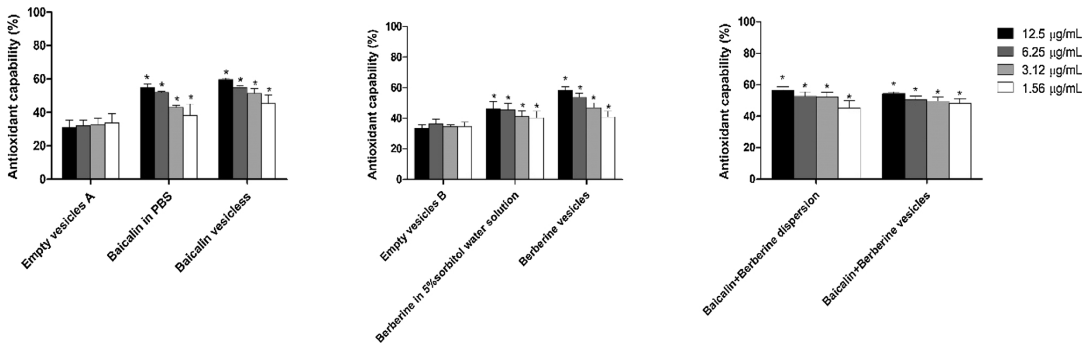

Fig. 6. Protective effect of the different baicalin and berberine formulations against H_2O_2-induced oxidative stress in HaCaT keratinocytes. Empty vesicles A and empty vesicles B were obtained by dispersing the phospholipid in PBS or 5%sorbitol water solution, respectively. Each bar represents a mean ± standard deviation (n = 16). *$p < 0.05$ versus untreated control.

Table 2
Melanogenetic activity (%) and tyrosinase activity (%) of melanocytes after a 48 h treatment with baicalin or berberine in PBS or in 5%sorbitol water solution, or loaded in vesicles, at different concentrations (12.5, 6.25, 3.12 and 1.56 μg/mL). Baicalin and berberine were used alone or in association. Each value is the mean ± standard deviation (n = 16).

	Melanogenic activity (%)				Tyrosinase activity (%)			
	12.5 μg/mL	6.25 μg/mL	3.12 μg/mL	1.56 μg/mL	12.5 μg/mL	6.25 μg/mL	3.12 μg/mL	1.56 μg/mL
Baicalin in PBS	91 ± 3	94 ± 2	93 ± 3	93 ± 6	95 ± 2	97 ± 4	98 ± 3	96 ± 5
Baicalin vesicles	106 ± 1	109 ± 6	105 ± 5	105 ± 6	101 ± 4	101 ± 3	100 ± 5	99 ± 5
Berberine in 5%sorbitol water solution	115 ± 3	116 ± 4	103 ± 5	101 ± 4	110 ± 2	107 ± 4	106 ± 4	112 ± 3
Berberine vesicles	135 ± 3*	130 ± 3*	110 ± 6	113 ± 5	129 ± 3*	121 ± 4*	119 ± 3	116 ± 4
Baicalin + Berberine dispersion	103 ± 3	99 ± 3	93 ± 3	97 ± 5	119 ± 2	115 ± 3	114 ± 2	97 ± 5
Baicalin + Berberine vesicles	153 ± 4*	138 ± 6*	110 ± 5	115 ± 5	136 ± 4*	132 ± 2*	125 ± 4*	122 ± 6

* $p < 0.05$ versus untreated control cells (100%).

moderate vitiligo [20]. Adequate modifications and innovations are still required to improve the local efficacy of active molecules, and phospholipid vesicles might represent the vehicle of choice for local treatments, as they can enhance the skin accumulation and efficacy of active molecules, such as baicalin and berberine. Taking into account previous results on the delivery of baicalin for the treatment of skin inflammation, elastic, ultradeformable vesicles, the so-called transfersomes, were chosen for this study [7,19]. Baicalin was loaded in vesicles containing 60 mg/ml of Lipoid S75, and 2.5 mg/mL of tween 80. To load berberine into vesicles with characteristics comparable to those loading baicalin, 120 mg/mL of the same phospholipid was needed, along with the addition of sorbitol (5%) in water as a stabilizer. The prepared ultradeformable vesicles were fairly spherical, small in size, homogeneously dispersed, negatively charged, capable of incorporating high amounts of baicalin or berberine. The incorporation of the polyphenols into the vesicles led to a reduction of the mean diameter, in comparison with that of empty vesicles ($p < 0.05$), probably due to the intercalation of baicalin or berberine in the phospholipid bilayer, and the consequent modification of the vesicle assembly [7,21,22]. Size distribution and surface charge were monitored for 30 days at 25 °C: no significant variations were detected (Table 1), irrespective of the sample tested. Skin permeation of baicalin and berberine was improved by their incorporation in the ultradeformable vesicles. The concentration of the polyphenols in the receptor compartment was less than 2%, which can be indicative of the formation of a depot in the epidermis. No cytotoxic effects were detected upon treatment with empty vesicles (viability ≥100%), irrespective of the cells used. A high biocompatibility was also detected using baicalin in PBS or in vesicles, as the viability was always around 100% even using high concentrations (i.e., 100, 50 and 25 μg/mL). A different behaviour was observed for berberine in 5% sorbitol water solution or loaded in vesicles, as the viability was high (˜100%) only using the lower concentrations (12.5-1.56 μg/mL). Taking into account these results, only the lower concentrations were chosen for further studies. Under these conditions, the polyphenols in PBS or in 5%sorbitol water solution were able to counteract the oxidative stress induced by H_2O_2, and this effect was slightly improved (˜15%) using the vesicles. Baicalin vesicles provided the highest antioxidant activity, which was not significantly improved by the association with berberine vesicles. The antioxidant effect can be useful against vitiligo symptoms, which are correlated with the accumulation of reactive oxygen species in the skin [23]. Additionally, the photoprotective effect of the formulations was evaluated. The highest photoprotective activity was achieved by using baicalin vesicles or when baicalin and berberine vesicles were used in combination. Vitiligo is phenotypically characterized by acquired depigmented spots in the skin. It is often necessary to use rotational therapy to decrease side effects and to achieve better repigmentation response [24]. Berberine vesicles, mostly when combined with baicalin vesicles, induced a significant increase in melanin production and tyrosinase activity. The latter is considered as the key determinant of pigmentation and the rate-limiting enzyme for melanin synthesis. The improved melanin production can ensure a suitable repigmentation of skin white spots. Currently, the main purpose of clinical treatment of vitiligo is to increase the melanogenesis and uniform skin colour. The findings of this study suggest that the association of baicalin vesicles with berberine vesicles may represent a promising strategy to counteract vitiligo progression, because the presence of baicalin vesicles ensures the antioxidant protection, and the presence of berberine vesicles ensures photoprotection and skin repigmentation. The delivery of bioactive molecules by ultradeformable vesicles capable of squeezing through the skin channels, facilitates the accumulation of the payload into the skin and the interaction with cells. Therefore, the association of these vesicles may represent a valid adjuvant to the generally used treatments of vitiligo.

5. Conclusion

The association of baicalin and berberine ultradeformable vesicles showed a great potential as adjuvant therapy of vitiligo, because the baicalin vesicles exhibited good antioxidant and photoprotective abilities that were reinforced by repigmentation provided by the berberine vesicles.

References

[1] O. Osinubi, M. j. Grainge, L. Hong, A. Ahmed, J. m. Batchelor, D. Grindlay, A. r. Thompson, S. Ratib, The prevalence of psychological comorbidity in people with vitiligo: a systematic review and meta-analysis, Br. J. Dermatol. (n.d.) n/a-n/a. doi:10.1111/bjd.16049.
[2] M.L. Frisoli, J.E. Harris, Vitiligo: mechanistic insights lead to novel treatments, J. Allergy Clin. Immunol. 140 (2017) 654–662, https://doi.org/10.1016/j.jaci.2017.07.011.
[3] R. Speeckaert, N. van Geel, Vitiligo: an update on pathophysiology and treatment options, Am. J. Clin. Dermatol. 18 (2017) 733–744, https://doi.org/10.1007/s40257-017-0298-5.
[4] K. Boniface, J. Seneschal, M. Picardo, A. Taïeb, Vitiligo: focus on clinical aspects, immunopathogenesis, and therapy, Clin. Rev. Allergy Immunol. 54 (2018) 52–67, https://doi.org/10.1007/s12016-017-8622-7.
[5] L.B. Travis, N. Silverberg, Calcipotriene and corticosteroid combination therapy for vitiligo, Pediatr. Dermatol. 21 (2004) 495–498, https://doi.org/10.1111/j.0736-8046.2004.21418.x.
[6] S. Gianfaldoni, U. Wollina, M. Tirant, G. Tchernev, J. Lotti, F. Satolli, M. Rovesti, K. França, T. Lotti, Herbal compounds for the treatment of vitiligo: a review, open access maced, J. Med. Sci. 6 (2018) 203–207, https://doi.org/10.3889/oamjms.2018.048.
[7] S. Mir-Palomo, A. Nácher, O. Díez-Sales, M.A. Ofelia Vila Busó, C. Caddeo, M.L. Manca, M. Manconi, A.M. Fadda, A.R. Saurí, Inhibition of skin inflammation by baicalin ultradeformable vesicles, Int. J. Pharm. 511 (2016) 23–29, https://doi.org/10.1016/j.ijpharm.2016.06.136.
[8] M. Manconi, M.L. Manca, C. Caddeo, D. Valenti, C. Cencetti, O. Diez-Sales, A. Nacher, S. Mir-Palomo, M.C. Terencio, D. Demurtas, J.C. Gomez-Fernandez, F.J. Aranda, A.M. Fadda, P. Matricardi, Nanodesign of new self-assembling core-shell gellan-transfersomes loading baicalin and in vivo evaluation of repair response in skin, Nanomed. Nanotechnol. Biol. Med. 14 (2018) 569–579, https://doi.org/10.1016/j.nano.2017.12.001.
[9] M. Manconi, M.L. Manca, C. Caddeo, C. Cencetti, C. di Meo, N. Zoratto, A. Nacher, A.M. Fadda, P. Matricardi, Preparation of gellan-cholesterol nanohydrogels embedding baicalin and evaluation of their wound healing activity, Eur. J. Pharm. Biopharm. 127 (2018) 244–249, https://doi.org/10.1016/j.ejpb.2018.02.015.

[10] B. Dinda, S. Dinda, S. DasSharma, R. Banik, A. Chakraborty, M. Dinda, Therapeutic potentials of baicalin and its aglycone, baicalein against inflammatory disorders, Eur. J. Med. Chem. 131 (2017) 68–80, https://doi.org/10.1016/j.ejmech.2017.03.004.

[11] G.-X. Shi, J. Shao, T.-M. Wang, C.-Z. Wang, [New advance in studies on antimicrobal activity of Scutellaria baicalensis and its effective ingredients], Zhongguo Zhong Yao Za Zhi Zhongguo Zhongyao Zazhi China, J. Chin. Mater. Medica. 39 (2014) 3713–3718.

[12] Y. Chen, L.V. Minh, J. Liu, B. Angelov, M. Drechsler, V.M. Garamus, R. Willumeit-Römer, A. Zou, Baicalin loaded in folate-PEG modified liposomes for enhanced stability and tumor targeting, Colloids Surf. B Biointerfaces 140 (2016) 74–82, https://doi.org/10.1016/j.colsurfb.2015.11.018.

[13] J. Zhang, Z. Yin, L. Ma, Z. Yin, Y. Hu, Y. Xu, D. Wu, F. Permatasari, D. Luo, B. Zhou, The protective effect of Baicalin against UVB irradiation induced photoaging: an in vitro and in vivo study, PLoS One 9 (2014) e99703, , https://doi.org/10.1371/journal.pone.0099703.

[14] Q. Liu, H. Jiang, Z. Liu, Y. Wang, M. Zhao, C. Hao, S. Feng, H. Guo, B. Xu, Q. Yang, Y. Gong, C. Shao, Berberine radiosensitizes human esophageal cancer cells by downregulating homologous recombination repair protein RAD51, PLoS One 6 (2011) e23427, , https://doi.org/10.1371/journal.pone.0023427.

[15] C.-L. Kuo, C.-W. Chi, T.-Y. Liu, The anti-inflammatory potential of berberine in vitro and in vivo, Cancer Lett. 203 (2004) 127–137.

[16] S.A. Ali, I. Naaz, R.K. Choudhary, Berberine-induced pigment dispersion in Bufo melanostictus melanophores by stimulation of beta-2 adrenergic receptors, J. Recept. Signal Transduct. Res. 34 (2014) 15–20, https://doi.org/10.3109/10799893.2013.843193.

[17] E. Mirhadi, M. Rezaee, B. Malaekeh-Nikouei, Nano strategies for berberine delivery, a natural alkaloid of Berberis, Biomed. Pharmacother. Biomedecine Pharmacother. 104 (2018) 465–473, https://doi.org/10.1016/j.biopha.2018.05.067.

[18] N.R. Srinivas, Baicalin, an emerging multi-therapeutic agent: pharmacodynamics, pharmacokinetics, and considerations from drug development perspectives, Xenobiotica. 40 (2010) 357–367, https://doi.org/10.3109/00498251003663724.

[19] E. Romero, M. Jose Morilla, Ultradeformable phospholipid vesicles as a drug delivery system: a review, Res. Rep. Transdermal Drug Deliv. (2015) 55, https://doi.org/10.2147/RRTD.S50370.

[20] B.J. Garg, A. Saraswat, A. Bhatia, O.P. Katare, Topical treatment in vitiligo and the potential uses of new drug delivery systems, Indian J. Dermatol. Venereol. Leprol. 76 (2010) 231–238, https://doi.org/10.4103/0378-6323.62961.

[21] C. Caddeo, M. Manconi, M.C. Cardia, O. Díez-Sales, A.M. Fadda, C. Sinico, Investigating the interactions of resveratrol with phospholipid vesicle bilayer and the skin: NMR studies and confocal imaging, Int. J. Pharm. 484 (2015) 138–145, https://doi.org/10.1016/j.ijpharm.2015.02.049.

[22] C. Caddeo, M. Manconi, A.M. Fadda, F. Lai, S. Lampis, O. Diez-Sales, C. Sinico, Nanocarriers for antioxidant resveratrol: formulation approach, vesicle self-assembly and stability evaluation, Colloids Surf, B Biointerfaces 111 (2013) 327–332, https://doi.org/10.1016/j.colsurfb.2013.06.016.

[23] L. Qiu, Z. Song, V. Setaluri, Oxidative stress and vitiligo: the Nrf2–ARE signaling connection, J. Invest. Dermatol. 134 (2014) 2074–2076, https://doi.org/10.1038/jid.2014.241.

[24] C.G. Moreira, L.Z.B. Carrenho, P.L. Pawloski, B.S. Soley, D.A. Cabrini, M.F. Otuki, Pre-clinical evidences of Pyrostegia venusta in the treatment of vitiligo, J. Ethnopharmacol. 168 (2015) 315–325, https://doi.org/10.1016/j.jep.2015.03.080.

Nanoscale

ROYAL SOCIETY OF CHEMISTRY

PAPER

View Article Online
View Journal | View Issue

Cite this: *Nanoscale*, 2020, **12**, 16143

Co-loading of finasteride and baicalin in phospholipid vesicles tailored for the treatment of hair disorders

Silvia Mir-Palomo, [a] Amparo Nácher, *[a,b] M. A. Ofelia Vila-Busó,[c] Carla Caddeo,[d] Maria Letizia Manca, [d] Amparo Ruiz Saurí,[e] Elvira Escribano-Ferrer,[f] Maria Manconi[d] and Octavio Díez-Sales[a,b]

Hair loss affects a large number of people worldwide and it has a negative impact on the quality of life. Despite the availability of different drugs for the treatment of hair disorders, therapeutic options are still limited and scarcely effective. An innovative strategy to improve the efficacy of alopecia treatment is presented in this work. Finasteride, the only oral synthetic drug approved by Unites States Federal Drug Administration, was loaded in phospholipid vesicles. In addition, baicalin was co-loaded as an adjuvant. Their effect on hair growth was evaluated *in vitro* and *in vivo*. Liposomes, hyalurosomes, glycerosomes and glycerol-hyalurosomes were manufactured by using a simple method that avoids the use of organic solvents. All the vesicles were small in size (~100 nm), homogeneously dispersed (polydispersity index ≤0.27) and negatively charged (~−16 mV). The formulations were able to stimulate the proliferation of human dermal papilla cells, which are widely used in hair physiology studies. The analysis of hair growth and hair follicles of C57BL/6 mice, treated with the formulations for 21 days, underlined the ability of the vesicles to improve hair growth by the simultaneous follicular delivery of finasteride and baicalin. Therefore, the developed nanosystems can represent a promising tool to ensure the efficacy of the local treatment of hair loss.

Received 29th April 2020,
Accepted 15th July 2020

DOI: 10.1039/d0nr03357j

rsc.li/nanoscale

Introduction

Hair loss is a common dermatological disorder that can affect the quality of life of patients, as it has a relevant impact on their psychology.[1] The aetiology and subsequent development of hair loss or alopecia is not fully understood, but it is commonly accepted that it can be caused by a combination of genetic and environmental stimuli.[2]

Hair follicles control hair growth, which is a regenerating system that undergoes a cyclic process divided into different phases: hair generation and growth (anagen phase), regression (catagen phase) and rest (telogen phase). Moreover, hair follicles are supported by the dermal papilla cells, which play a crucial role in hair growth cycle and seem to be responsible for the key signals controlling hair follicle cycle during mammals life.[3,4]

The incorrect or slowed cyclic process of growth can cause hair loss, which is very common, especially in adults. Despite the high incidence of alopecia, the therapeutic treatments are still limited. Among those currently available, the majority of treatments exhibit low efficacy and important side effects.[5,6] Therefore, alternative treatment options, more effective and safer, are urgently needed.

Among the different drugs available for the treatment of alopecia, finasteride is one of the most used. It is the only oral synthetic drug approved by Unites States Federal Drug Administration and is especially recommended for the treatment of hair loss connected to androgenic alopecia. Finasteride inhibits human 5α-reductase, which converts testosterone into the more potent 5α-dihydrotestosterone,[7] induces the passage of hair follicles from telogen to anagen phase, and inhibits miniaturization of hair follicles.[8]

In spite of its benefits, the chronic oral treatment with finasteride is associated with different side effects, such as

[a]*Department of Pharmacy and Pharmaceutical Technology, Faculty of Pharmacy, University of Valencia, Spain. E-mail: Amparo.Nacher@uv.es*
[b]*Instituto Interuniversitario de Investigación de Reconocimiento Molecular y Desarrollo Tecnológico (IDM), Universitat Politècnica de València, Universitat de València, Valencia, Spain*
[c]*Department of Physics and Chemistry, Faculty of Pharmacy, University of Valencia, Spain*
[d]*Department of Life and Environmental Sciences, Drug Sciences Division, University of Cagliari, via Ospedale 72, 09124 Cagliari, Italy*
[e]*Department of Pathology, University of Valencia, Avda Blasco Ibañez 17, 46010 Valencia, Spain*
[f]*Biopharmaceutics and Pharmacokinetics Unit, Institute for Nanoscience and Nanotechnology, University of Barcelona, Barcelona, Spain*

gynecomastia, decreased libido, ejaculation disorder and others, which lead to a low treatment adherence. A significant reduction of the abovementioned side effects can be achieved by topical application, especially if the drug is locally delivered by *ad hoc* formulated nanocarriers.[9] The latter are nanoparticulate systems able to facilitate the passage of their cargo through the stratum corneum to the viable epidermis and dermis.

An additional strategy to improve the efficacy of topical finasteride could be its combination with natural active ingredients with complementary activity.[10] Among others, baicalin[11] has attracted the attention of the scientific community due to its potential ability to promote hair growth.[12–14] In addition, it possesses other beneficial properties, such as antioxidant,[15] antitumor,[3] anti-inflammatory,[17] and antibiofilm activity against *S. saprophyticus* infections.[18] Baicalin is extracted from the roots of *Scutellaria baicalensis Georgi*, which has been officially listed in the Chinese Pharmacopeia and was introduced in European Pharmacopoeia (9th Edition). Thanks to its high biocompatibility and promising activity on hair growth, baicalin can be considered a potential adjuvant to finasteride in the local treatment of hair loss and alopecia. Both finasteride and baicalin belong to Class II in the biopharmaceutical classification system,[19] as they show low aqueous solubility and permeability,[20] which may limit their topical application. The loading of finasteride and baicalin in *ad hoc* formulated phospholipid vesicles can help to overcome these drawbacks by improving their local bioavailability.[21] Phospholipid vesicles are regarded as the most promising nanosystems for the delivery of a wide range of drugs. Thanks to their peculiar structure and versatility, they are able to incorporate both hydrophilic and lipophilic molecules, ensuring an efficient co-delivery of different molecules. Moreover, phospholipid vesicles are highly biocompatible, safe, and capable of facilitating the passage of the payload through the stratum corneum, improving the accumulation in the deeper skin strata and the delivery at follicular level.[22] In addition, due to their composition similar to that of cellular membranes, the phospholipid vesicles are able to promote the interaction with cells and the release of the payload in the cytoplasm where the beneficial activity is exerted.

Recently, many authors have underlined the importance of the composition of phospholipid vesicles to their performance as topical delivery systems. New vesicles have been developed, such as transfersomes, also called ultradeformable liposomes, capable of squeezing through the intercellular spaces of the stratum corneum;[22,23] ethosomes, elastic vesicles containing high amounts of ethanol;[24,25] penetration enhancer-containing vesicles (PEVs);[26,27] glycerosomes, containing high amounts of glycerol,[28] capable, as well as PEVs, of enhancing the delivery of drugs to the skin;[29] and hyalurosomes, vesicles immobilized in a sodium hyaluronate network.[30,31]

In the present study, finasteride and baicalin were co-loaded in liposomes, hyalurosomes, glycerosomes and glycerol-hyalurosomes, while liposomes loaded with finasteride or baicalin individually were used as references. The vesicles were characterized and their ability to promote hair growth was evaluated both *in vitro*, by using human hair follicle dermal papilla cells, and *in vivo*, by applying the vesicle formulations on the shaved back skin of C57BL/6 mice.[32]

Experimental

Materials

Lipoid® S75, a mixture of soybean lecithin, was a gift from Lipoid GmbH (Ludwigshafen, Germany). Disodium phosphate was purchased from Scharlab S.L. (Barcelona, Spain). Monosodium phosphate was obtained from Panreac quimica S.A. (Barcelona, Spain). Baicalin was purchased from Cymit química S.L. (Barcelona, Spain). Finasteride was purchased from Farmalabor Srl (Canosa di Puglia, Italy). Sodium hyaluronate was purchased from DSM Nutritional Products AG Branch Pentapharm (Switzerland). Tetrazolium salt, 3-(4,5-dimethylthiazol-2-yl)-2,5-diphenyltetrazolium bromide (MTT), glycerol and all the other reagents of analytical grade were purchased from Sigma-Aldrich (Milan, Italy).

Vesicle preparation

The phospholipid vesicles were prepared by hydration of lipid components, sonication and extrusion (when necessary), avoiding the use of organic solvents.[33] Briefly, Lipoid® S75 (210 mg mL^{-1}), baicalin (10 mg mL^{-1}) and finasteride (2.5 mg mL^{-1}) were weighed in a glass vial and hydrated overnight with PBS (pH 7.4) to obtain liposomes, with glycerol and PBS (1 : 1 v/v) to obtain glycerosomes, with an aqueous solution of sodium hyaluronate (0.1% w/v) to obtain hyalurosomes, or with a mixture of glycerol and 0.2% sodium hyaluronate solution (1 : 1 v/v) to obtain glycerol-hyalurosomes. Empty liposomes and liposomes loaded with finasteride or baicalin individually were prepared and used as references, to evaluate the effect of the payloads on vesicle assembly. All the dispersions were sonicated (25 cycles, 5 seconds on and 5 seconds off) with a Soniprep 150 ultrasonic disintegrator (MSE Crowley, London, UK) in order to obtain small and homogeneous vesicles. Liposomes loaded with finasteride or baicalin individually were then extruded through a 200 nm membrane (Whatman, GE Healthcare, Fairfield, Connecticut, US) by using an Avanti® Mini-Extruder (Avanti Polar Lipids, Alabaster, AL, US) to improve the homogeneity of the dispersions.

Analytical methods

Finasteride and baicalin were quantified by HPLC using a PerkinElmer® Series 200 equipped with a UV detector and a column Teknokroma® Brisa "LC2" C18, 5.0 μm (150 × 4.6 mm). Finasteride was quantified at 245 nm by using a mixture of water and methanol (75 : 25) as mobile phase, delivered at a flow rate of 1 mL min^{-1}. The limit of detection for finasteride was 5 μg and the limit of quantification was 15 μg mL^{-1}.

Baicalin content was measured at 278 nm by using a mixture of water and methanol (30 : 70) as mobile phase, deli-

vered at a flow rate of 1 mL min^{-1}. The limit of detection for baicalin was 0.45 μg and the limit of quantification was 1.36 μg mL^{-1}.

Vesicle characterization

Vesicle formation and morphology were evaluated by cryo-TEM observation. A thin film of each sample was formed on a holey carbon grid and vitrified by plunging (kept at 100% humidity and room temperature) into ethane maintained at its melting point, using a Vitrobot (FEI Company, Eindhoven, Netherlands). The vitreous films were transferred to a Tecnai F20 TEM (FEI Company), and the samples were observed in a low-dose mode. Images were acquired at 200 kV at a temperature of ~−173 °C, using a CCD Eagle camera (FEI Company).

The average diameter and polydispersity index of the vesicle dispersions were determined by Photon Correlation Spectroscopy using a Zetasizer nano-ZS (Malvern Instruments, Worcestershire, UK). Zeta potential was estimated by using the Zetasizer nano-ZS by electrophoretic light scattering, which measures the particle electrophoretic mobility in a thermostated cell. All the measurements were performed after dilution (1 : 100) of the samples with PBS.[34]

The stability of vesicles was evaluated for 30 days at room temperature (25 °C). During this period, size, size distribution and surface charge were measured.

To evaluate the amount of finasteride and baicalin loaded into the vesicles, the samples (2 mL) were transferred into Spectra/Por® membranes (12–14 kDa MW cut-off; Spectrum Laboratories Inc., DG Breda, The Netherlands) and dialyzed against buffer (2 L) for 4 h, at room temperature (~25 °C) with water refreshed every hour to allow the complete removal of the non-entrapped molecules. Both non-dialyzed and dialyzed vesicles were disrupted with methanol (1 : 100) and analysed by HPLC (see analytical methods section) to quantify finasteride and baicalin contents. The entrapment efficiency (EE) was calculated as a percentage as follows (eqn (1)):

$$\text{EE}\ (\%) = [(\text{actual drug})/(\text{initial drug})] \times 100 \qquad (1)$$

where actual drug is the amount of finasteride or baicalin detected in vesicles after dialysis, and initial drug is the amount detected before dialysis.

In vitro evaluation of cytotoxicity and cell proliferation

Hair follicle dermal papilla cells (HFDPC, Cell Applications Inc., San Diego, CA, US) were grown as monolayers in 75 cm^2 flasks and incubated at 37 °C in a controlled atmosphere containing 5% CO_2 and 100% humidity. The growth medium (Cell Applications Inc., San Diego, CA, US) specific for hair follicle dermal papilla cells, supplemented with penicillin (100 U mL^{-1}) and streptomycin (100 mg mL^{-1}) (Sigma Aldrich, Spain), was used to culture them.

In order to evaluate the cytotoxicity of the formulations, the cells (5.5×10^4 cell per mL), at passage 2, were seeded in 96-well plates with 250 μL of culture medium. After 24 h, the cells were treated with the formulations at different dilutions (corresponding to concentrations of finasteride ranging from 800 to 0.390 μg mL^{-1} and baicalin ranging from 3200 to 1.56 μg mL^{-1}) for 48 h (n = 8). Untreated cells were used as a negative control.

Non-cytotoxic concentrations (finasteride from 6.25 to 0.390 μg mL^{-1} and baicalin from 25 to 1.56 μg mL^{-1}) were then used to evaluate the effect of the formulations on the promotion of cell proliferation. The cells were treated with the formulations for 48 h (n = 8). Untreated cells were used as a negative control.

At the end of each experiment (cytotoxicity and proliferation), the cells were washed three times with PBS and their viability was determined by means of the MTT [3(4,5-dimethylthiazolyl-2)-2,5-diphenyltetrazolium bromide] colorimetric assay, adding 100 μL of MTT reagent (0.5 mg mL^{-1} in PBS, final concentration) to each well. After 3 h, the formed formazan crystals were dissolved in dimethyl sulfoxide. The reaction was spectrophotometrically measured at 570 nm with a microplate reader (Multiskan EX, Thermo Fisher Scientific, Inc., Waltham, MA, US).

Results were reported as a percentage of cell proliferation in comparison with untreated control cells (100% viability) according to eqn (2):

$$\text{Cell proliferation}(\%) = \left(\frac{\text{Absorbance}_{\text{sample}}}{\text{Absorbance}_{\text{control}}}\right) \times 100 \qquad (2)$$

where $\text{Absorbance}_{\text{sample}}$ is the absorbance of treated cells and $\text{Absorbance}_{\text{control}}$ is the absorbance of untreated cells (100% viability), measured at 570 nm.

In vivo study design

Healthy six-week-old C57BL/6 female mice (18–20 g) were used for the *in vivo* experiments. All studies were performed in accordance with European Union regulations for the handling and use of laboratory animals and the protocols were approved by the Institutional Animal Care and Use Committee of the University of Valencia (Code 2019/VSC/PA/0113 type 2). The number and suffering of the animals were kept to the minimum.

In C57BL/6 mice, hair follicle morphogenesis and growth cycle follow a rather precise time-scale. However, the process is dependent on various factors, such as genetic background (mice strain) and sex (female mice show a prolonged telogen), among others. To avoid fluctuations in the results, *in vivo* experiments were based on the highly standardized C57BL/6 model of depilation-induced hair follicle cycling.[1]

Mice were divided into 10 groups (n = 5 per group) and the hairs, in telogen phase, on the dorsal area were gently shaved 24 h before treatment. On day 1, 100 μL of sample was topically smeared over the shaved dorsal site under non-occlusive conditions. The tested samples were finasteride and baicalin co-loaded liposomes, glycerosomes, hyalurosomes and glycerol-hyalurosomes, along with finasteride dispersion, baicalin dispersion, finasteride loaded liposomes and baicalin loaded liposomes used as references. The procedure was repeated once per day during 21 days of experiment. On the final day,

the mice were sacrificed by cervical dislocation. During the application period, differences between treated and non-treated groups in terms of average body weight or presence of abnormalities were checked.

Evaluation of *in vivo* hair growth. Skin pigmentation was taken as evidence of hair growth, as it is bright pink in the telogen phase and turns into grey or black in the anagen phase.[16] Hair length was determined on days 12, 16 and 21 from the same shaved area of all mice, by choosing 10 hairs to measure and calculate the mean length. The results were shown as average length ± standard deviation. The cyclic phase of hair follicles (anagen and telogen), along with the anagen percentage (eqn (3)) were determined by using an ocular micrometer:

$$\%\ \text{anagen} = (\text{Hair}_{\text{anagen}}/\text{Hair}_{\text{total}}) \times 100 \quad (3)$$

where $\text{Hair}_{\text{anagen}}$ is the number of hairs in anagen phase and $\text{Hair}_{\text{total}}$ is the total number of hairs.

The enhancing effect of the different treatments was also estimated (eqn (4)) as an indicator of the ability of the nanoformulations to improve hair growth in comparison with untreated group.

$$\text{Enhancing effect} = \text{Hair length}_{\text{treated}}/\text{Hair lenght}_{\text{control}} \quad (4)$$

where $\text{Hair lenght}_{\text{treated}}$ is the hair length of treated mice and $\text{hair length}_{\text{control}}$ is the hair length of non-treated mice.

Histological observation of hair follicles. Mice skin treated with the tested formulations was excised, fixed and stored in 10% formaldehyde until use. Tissue specimens were processed routinely and embedded in paraffin. Transversal sections (5 μm) were stained with haematoxylin and eosin and observed under a light microscope (Leica DM3000, Leica-Microsystems, Wetzlar, Germany). Number and diameter of follicles in the different groups were also measured through Image Pro plus 7.0, Media Cybernetics.

Statistical analysis of data

Data are shown as means ± standard deviations. Statistical differences were determined by using one-way ANOVA test and Tukey's test for multiple comparisons with a significance level of $p < 0.05$. All statistical analyses were performed using IBM SPSS statistics 22 for Windows (Valencia, Spain).

Results

Vesicle characterization

Cryo-TEM images disclosed that liposomes, used as a reference, were spherical and unilamellar (Fig. 1A). The addition of glycerol and/or hyaluronan led to the formation of spherical, oligo-multilamellar vesicles (Fig. 1B–D). Multivesicular structures were detected in glycerosomes and glycerol-hyalurosomes (Fig. 1B and D).

The size of the nanovesicles plays an important role, especially when they are specifically tailored for topical or follicular application. Indeed, it has been reported that follicular penetration of nanovesicles increases as their size decreases.[35]

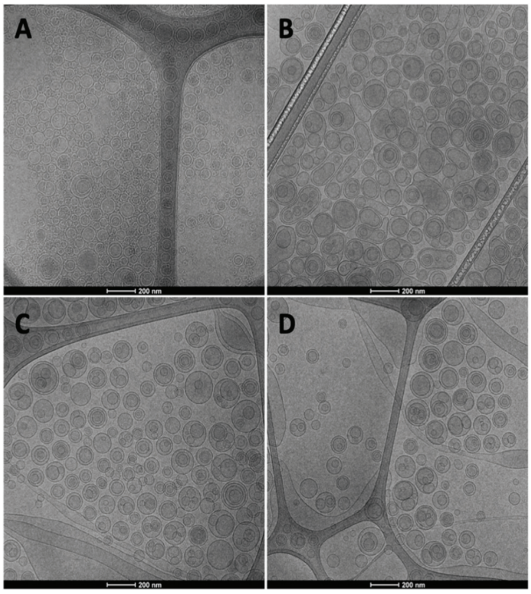

Fig. 1 Representative cryo-TEM photographs of finasteride and baicalin co-loaded liposomes (A), glycerosomes (B), hyalurosomes (C) and glycerol-hyalurosomes (D). Bars correspond to 200 nm.

Given that, and aiming at achieving a deep follicular penetration, small-sized vesicles, ranging from 65 to 110 nm, were prepared (Fig. 2). The mean diameter of empty liposomes (used as a reference) was ~80 nm, with a low polydispersity index (0.18) and a negative zeta potential (~−31 mV). The loading of finasteride did not affect the mean diameter of liposomes, but led to an increase in the polydispersity index. The loading of baicalin led to a decrease in the mean diameter and the polydispersity index (Fig. 2). The simultaneous loading of finasteride and baicalin caused an increase in mean diameter and polydispersity index, and the zeta potential was much less negative (−13 mV), denoting an important impact of the co-loading, probably due to the distribution of both molecules in the vesicle bilayer and on the surface. The addition of glycerol and/or hyaluronan did not affect the physico-chemical features of the vesicles. Indeed, no significant differences were detected in comparison with co-loaded liposomes and between the samples ($p > 0.05$). Glycerosomes, hyalurosomes and glycerol-hyalurosomes were able to incorporate finasteride and baicalin in the same amounts, similarly to co-loaded liposomes (reference), as the entrapment efficiency was ~80% for both molecules. The entrapment efficiency decreased when using finasteride alone or baicalin alone (~65%). The nanovesicles showed a good stability at room temperature, as no significant changes were detected after 30 days on storage at room temperature (~25 °C).

In vitro cytotoxicity assay

The biocompatibility of the formulations was evaluated by incubating hair follicle dermal papilla cells with samples at

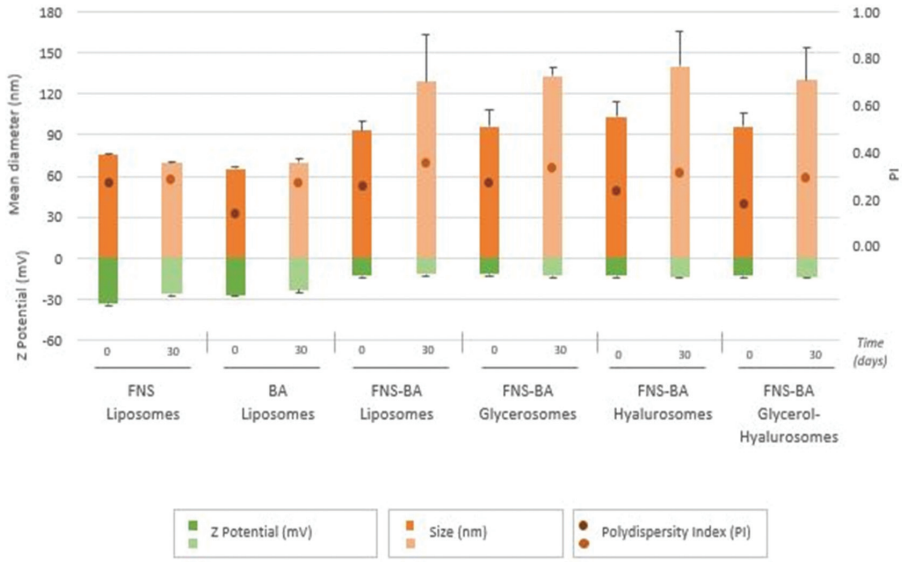

Fig. 2 Mean diameter, polydispersity index (PI) and zeta potential (ZP) values of finasteride (FNS) and baicalin (BA) loaded nanovesicles over 30 days of storage at room temperature (~25 °C). Values correspond to means ± standard deviations (n = 3).

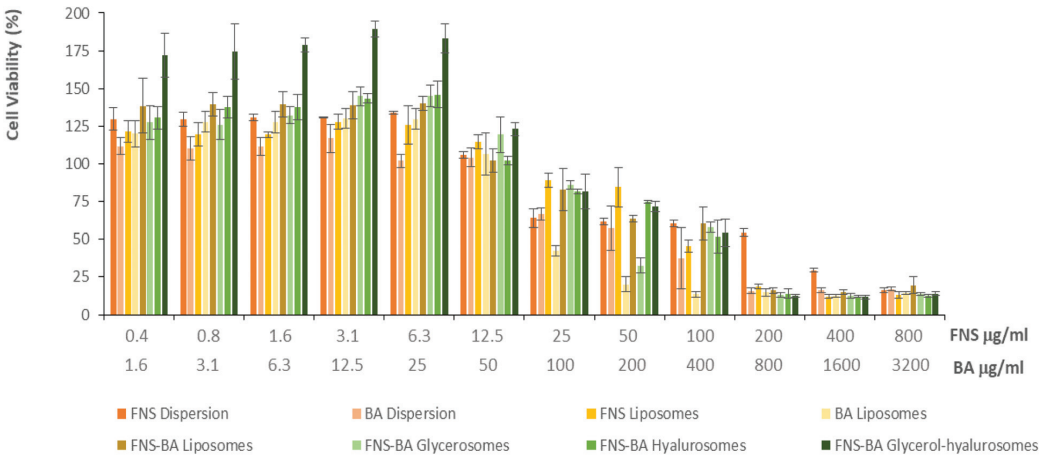

Fig. 3 Viability of hair follicle dermal papilla cells after 48 h of incubation with formulations at different dilutions. Finasteride (FNS) dispersion and baicalin (BA) dispersion were used as references along with finasteride loaded liposomes and baicalin loaded liposomes. Bars represent mean values ± standard deviations (n = 8).

different dilutions (corresponding to concentrations of finasteride ranging from 800 to 0.390 µg mL^{-1} and baicalin ranging from 3200 to 1.56 µg mL^{-1}) for 48 h (Fig. 3). The effect of finasteride or baicalin in dispersion or loaded individually in liposomes on the viability of papilla cells was concentration dependent: the viability was less than 50% when the lower dilutions (*i.e.*, higher concentrations) were used, while the viability was always ≥100% when using higher dilutions (*i.e.*, lower concentrations: ≤12.5 µg mL^{-1} of finasteride and ≤50 µg mL^{-1} of baicalin). The effect of finasteride and baicalin co-loaded glycerosomes and hyalurosomes was very similar to that of liposomes, while it was found that glycerol-hyalurosomes, at dilutions corresponding to finasteride concentrations ≥6.3 µg mL^{-1} and baicalin ≥25 µg mL^{-1}, stimulated cell proliferation leading to ~179% viability.

In vitro cell proliferation assay

Dermal papilla cells are considered the main responsible for controlling hair growth, and their proliferation can positively affect the process. Given that, the ability of the formulations to promote the proliferation of these cells, as a growth-related parameter, was investigated by using only non-cytotoxic

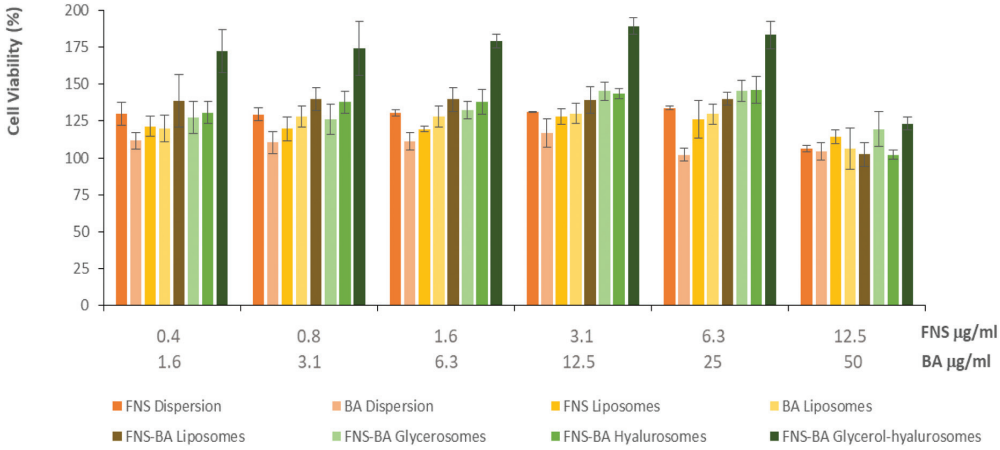

Fig. 4 Effect of finasteride and baicalin co-loaded nanovesicles on the proliferation of hair follicle dermal papilla cells after 48 h of treatment by using non-cytotoxic concentrations. Finasteride (FNS) dispersion and baicalin (BA) dispersion were used as references, along with finasteride loaded liposomes and baicalin loaded liposomes. Bars represent the means ± standard deviations (n = 8).

dilutions (Fig. 4). At these dilutions, finasteride and baicalin co-loaded into glycerol-hyalurosomes were able to stimulate cell growth to a greater extent (~179% viability) than the dispersions or the other vesicles, and irrespective of the concentration used ($p < 0.05$ *versus* untreated cells). The efficacy of both finasteride and baicalin co-loaded in phospholipid vesicles was compared with that of these molecules in dispersion or loaded individually in liposomes, in order to understand the positive contribution provided by both carrier and co-loading. The viability of the cells treated with the dispersions was ~122% using finasteride in dispersion or loaded in liposomes, and ~115% using baicalin in dispersion or loaded in liposomes. The co-loading in liposomes, glycerosomes and hyalurosomes led to a slight increase in cell proliferation (~132% viability without significant differences between these formulations), while the co-loading in glycerol-hyalurosomes significantly promoted the proliferation, as the cell viability reached ~179%. These results underline a synergistic effect of finasteride and baicalin on cell proliferation and an additional contribution of the glycerol-hyalurosomes on the achievement of the therapeutic efficacy. This can be mainly connected with their optimal carrier ability, which seems to be potentiated by the simultaneous presence of glycerol and sodium hyaluronate in phospholipid vesicles.

In vivo determination of hair length and anagen percentage

In vivo studies were performed by using C57BL/6 mice, which represent an ideal model to avoid fluctuations of results. The differences in hair growth and colour for each treated group was evaluated by visual inspection on days 12, 16 and 21 of treatment. The shaved area of all mice appeared pink on day 0, and the re-growth of dark hair was clearly visible on day 21 (Fig. 5). After 12 days, the finasteride or the baicalin in dispersion stimulated a moderate hair growth, which was more evident than that observed in untreated mice, but less than that provided by finasteride and baicalin loaded individually in liposomes. The co-loading of finasteride and baicalin in hyalurosomes and glycerol-hyalurosomes further improved the hair growth. On days 16 and 21, there were no significant differences between the treatments ($p > 0.05$), as the shaved area of all treated mice was completely covered by new hairs.

The length of the hair was also measured during the experiment to better evaluate the differences among the treatments (Table 1). On day 16, only finasteride and baicalin co-loaded glycerosomes, hyalurosomes and glycerol-hyalurosomes led to a significant improvement of the growth of hairs, with respect to untreated mice ($p < 0.01$). On day 21, all the treatments provided an increase in hair length (Enhancing effect, EE), especially using glycerol-hyalurosomes, which doubled the growth rate as compared to control untreated mice (EE = 2.1; Table 1). In addition, the anagen phase of hair follicles was immediately induced in the shaved area by using these formulations (Table 1).[36] After the completion of the anagen phase, the other phases (catagen and telogen phases) started spontaneously in a fairly homogeneous manner. The growth stages of hairs can be also detected by the colour of the skin, which became darker during the anagen phase because of the presence of melanocytes in hair follicles and the production of melanin, which in turn has an important role in controlling the cycle of hair growth. At the beginning of the experiment, immediately after the shaving procedure, the skin was pinkish, which is the characteristic colour of the telogen phase; during the treatment with the formulations, the colour of the skin surface turned to grey, which is the colour of the anagen phase.[12] The anagen phase started sooner when the mice were treated with the nanovesicles, as confirmed by visual inspection: the colour of the skin changed from pinkish to black due to an acceleration in hair growth rate.

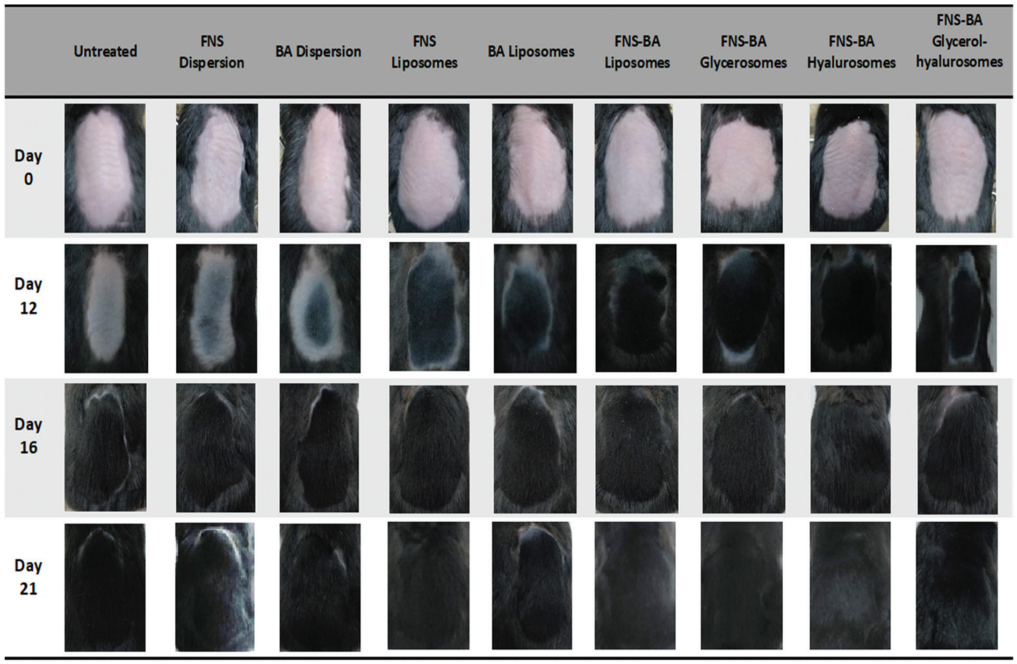

Fig. 5 Representative images of dorsal skin of C57BL/6 shaved mice on day 0 and after 12, 16 and 21 days of topical treatment with finasteride (FNS) and baicalin (BA) co-loaded in phospholipid nanovesicles or finasteride dispersion or baicalin dispersion or finasteride loaded liposomes and baicalin loaded liposomes used as references.

Table 1 Hair length on days 12, 16 and 21, enhancing effect (EE) and hair anagen percentage (% anagen) on day 21 (n = 10), recorded for each group of mice treated with finasteride (FNS) or baicalin (BA) co-loaded vesicles or finasteride dispersion and baicalin dispersion or finasteride loaded liposomes and baicalin loaded liposomes. The results are shown as means ± standard deviations (n = 5)

	Hair length (mm)			EE	% anagen
Treatment	Day 12	Day 16	Day 21	Day 21	Day 21
Control/no treatment	—	3.6 ± 0.4	5.7 ± 0.7	1	45
FNS dispersion	—	5.1 ± 0.4	6.5 ± 0.9	1.1	55
BA dispersion	—	4.2 ± 0.5	7.2 ± 1.1	1.3	70
FNS liposomes	2.4 ± 0.9	5.2 ± 0.8	8.1 ± 1.1	1.4	55
BA liposomes	2.6 ± 0.9	4.1 ± 0.4	7.1 ± 1.3	1.2	40
FNS-BA liposomes	3.4 ± 0.4	5.0 ± 0.7	10.1 ± 0.9	1.7	90
FNS-BA glycerosomes	3.7 ± 0.8	5.7 ± 0.7	9.8 ± 1.8	1.7	80
FNS-BA hyalurosomes	4.3 ± 0.4	8.6 ± 0.7	9.9 ± 1.4	1.7	75
FNS-BA glycerol-hyalurosomes	3.6 ± 0.5	7.4 ± 1.1	12.1 ± 1.6	2.1	80

Measurement of the number and diameter of follicles

Hair follicles are intimately connected with hair disorders: the higher the hair follicle number, the better the hair growth promotion. For this reason, the number and diameter of hair follicles were measured after 21 days of treatment. No significant differences were detected for the diameter of the follicles among the different groups *versus* control ($p > 0.05$). This parameter was not affected by the treatments with the formulations (data not shown). On the contrary, the number of follicles was significantly increased when the mice were treated with finasteride and baicalin co-loaded in the nanovesicles (Fig. 6). The treatment with finasteride or baicalin loaded individually in liposomes led to a slight increase in the number of follicles, which points to a crucial contribution provided by the co-loading.

Histological observation of hair follicles

In order to confirm the efficacy of the phospholipid vesicles in promoting hair growth, the dorsal skin of mice treated with the different formulations was excised, stained with haematoxylin and eosin, and observed under a light microscope. The morphological differences of the skin treated with finasteride and baicalin co-loaded vesicles were evaluated and compared with untreated skin and skin treated with finasteride in dis-

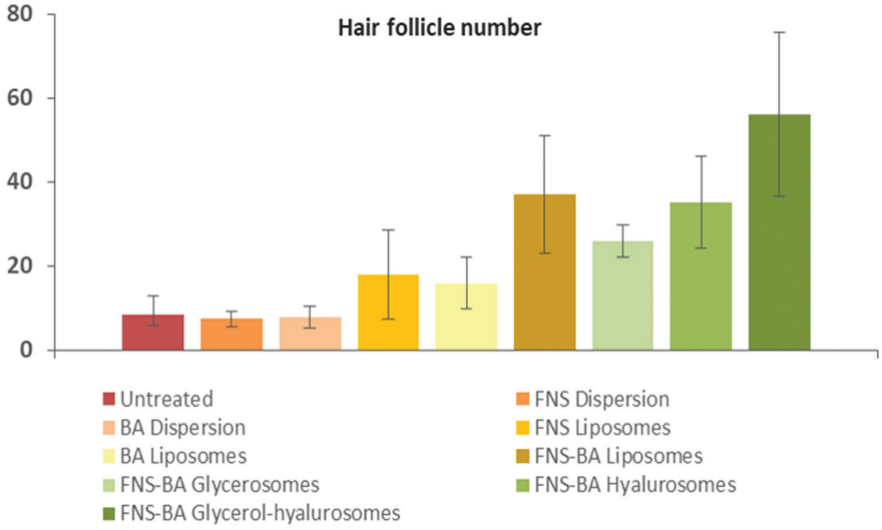

Fig. 6 Number of hair follicles in C57BL/6 mice after 21 days of treatment with finasteride (FNS) or baicalin (BA) co-loaded nanovesicles or finasteride dispersion or baicalin dispersion or finasteride loaded liposomes or baicalin loaded liposomes (references). Values are presented as means ± standard deviations (n = 5).

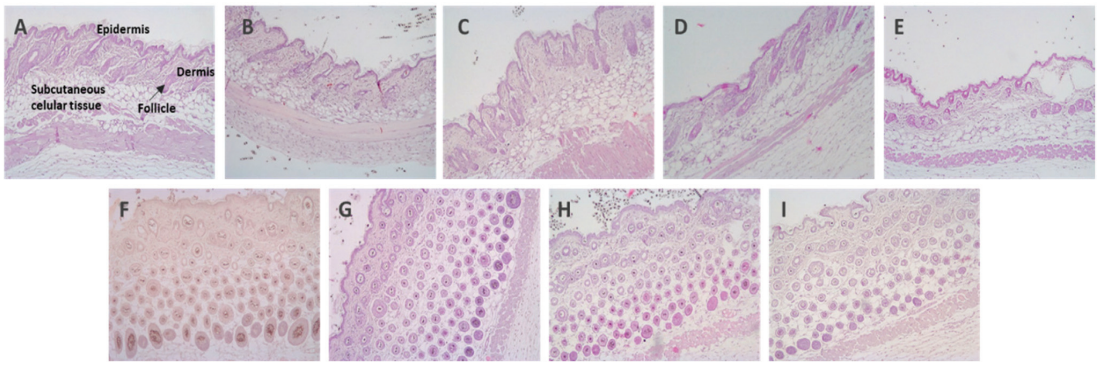

Fig. 7 Representative images of histological sections of mouse skin: untreated skin (A); skin treated with finasteride dispersion (B), baicalin dispersion (C), baicalin loaded liposomes (D), finasteride loaded liposomes (E), finasteride and baicalin co-loaded liposomes (F), glycerosomes (G), hyalurosomes (H) and glycerol-hyalurosomes (I). All images were taken at 10× magnification.

persion or loaded in liposomes and baicalin in dispersion or loaded in liposomes (Fig. 7). Histological results confirmed the promoting effect of the co-loading of finasteride and baicalin in all the vesicles in increasing the number of follicles in C57BL/6 mice.

Discussion

Considering the great number of patients affected by hair loss and alopecia and the lack of effective therapies, often associated with undesired side effects, in this work, glycerosomes, hyalurosomes and glycerol-hyalurosomes specifically tailored for the simultaneous delivery of finasteride and baicalin were developed and tested.[37,38] The use of phospholipid vesicles for the treatment of skin disorders seems to be a good strategy, as these nanocarriers can enhance skin bioavailability, penetration depth, and prolong the residence time of the payload.[21] Nanocarriers are also considered good candidates for the treatment of follicle diseases, such as hair loss or alopecia, as they may deliver the therapeutic agents specifically to the follicular area, improving their efficacy.[22] Finasteride and baicalin co-loaded liposomes, finasteride loaded liposomes and baicalin loaded liposomes were used as references to better evaluate the effect of additives (*i.e.*, glycerol and/or sodium hyaluronate) in phospholipid vesicles and the efficacy of the single therapeutic agents (*i.e.*, finasteride and baicalin).

Among the newest phospholipid vesicles developed in the last years, glycerosomes and hyalurosomes seemed to be the most appropriate for skin delivery.[30,39] Moreover, in this work, for the first time, sodium hyaluronate and glycerol were combined to obtain the so-called glycerol-hyalurosomes.

The combination of the co-solvent and the polymer strengthened the effectiveness of the single components, presumably because glycerol-hyalurosomes, by being highly viscous, were capable of staying in the application site for a prolonged time during which glycerol can modify the ordered structure of the stratum corneum allowing the diffusion of the vesicles, while sodium hyaluronate, by interacting with dermal papilla cells, can stimulate their proliferation and the hair growth cycle. Further, the ability of these vesicles to interact with cells ensures the entry of the payloads in the cytoplasm, where the therapeutic activity is exerted.

Finasteride is a drug widely used for the treatment of androgenetic alopecia but, because of the numerous side effects associated with the oral use, the long-term treatment is generally avoided, thus resulting in an ineffective therapeutic response.[40] In particular, the oral administration of finasteride (1 mg day^{-1}) resulted to be effective in men[41] and less in women.[42] The use of higher doses in women represents a possible alternative, which still is controversial and deserves further investigation.[43] The delivery of finasteride by phospholipid vesicles can represent a valuable alternative to ensure topical efficacy and avoid the side effects associated with oral administration.[44] In addition, the therapeutic efficacy of drugs can be potentiated by their association with natural adjuvants with complementary properties. Baicalin is a natural and safe active molecule capable of controlling and promoting hair growth,[12] thus it can be used to improve the local efficacy of finasteride. Our results confirmed that the co-loading of finasteride and baicalin accelerated the anagen phase and hair growth rate, as well as the number of follicles in treated mice, as compared to finasteride or baicalin loaded individually in liposomes. On the other hand, the co-loading was not as relevant to stimulating the proliferation of papilla cells *in vitro*.

The use of modified phospholipid vesicles (glycerosomes, hyalurosomes and glycerol-hyalurosomes) was expected to improve the skin and follicular delivery of the payloads.[44] Previous works reported the importance of the lamellarity and size of vesicles as key factors for the improvement of both bioavailability at skin and follicular levels and therapeutic efficacy of loaded drugs.[45] According to this, the mean diameter of the prepared vesicles was around 100 nm. Liposomes and hyalurosomes were mainly unilamellar and oligomellar and the number of lamellae increased in glycerosomes and glycerol-hyalurosomes, probably due to the presence of glycerol.[46] Previous studies disclosed optimal performances of ethosomes in favouring percutaneous absorption of finasteride, especially into the dermis layer,[47,48] thanks to the moisturizing properties of ethanol. In the present study, the phospholipid vesicles were modified with glycerol and/or sodium hyaluronate. The former is a trihydroxy alcohol widely used in dermatological preparations for its hydrating and moisturizing properties,[49] which can induce significant changes in the mechanical properties of human skin *in vivo*, even after a 10 min application.[50] Sodium hyaluronate is a naturally-occurring polyanionic polysaccharide present in the intercellular matrix of vertebrate connective tissues. It is present in the skin where it plays protective, stabilizing and shock-absorbing functions.[51] The combination of these components in phospholipid vesicles can improve skin hydration, facilitating the passage of intact vesicles to the dermis and follicles. In addition, they made the dispersions more viscous, facilitating the topical application, avoiding the loss of material and prolonging its residence time on the application site. Our results demonstrate that glycerol-hyalurosomes were able to promote the complete growth of hair in the shaved area of C57BL/6 mice at a faster rate than the other vesicles, besides providing a significant increase in hair length (12.1 ± 1.6 mm on day 21) and number of follicles. Therefore, the association of phospholipid, glycerol and sodium hyaluronate maximized the performances of the nanovesicles in the *in vivo* co-delivery of finasteride and baicalin. Moreover, glycerol-hyalurosomes were also the most effective formulation in promoting the growth of dermal papilla cells *in vitro*, which can positively affect hair growth process.

Conclusions

The results suggest that the co-loading of finasteride and baicalin in phospholipid vesicles can improve their efficacy against hair loss, but only if the vesicles are properly formulated. Indeed, when finasteride and baicalin were co-loaded in glycerol-hyalurosomes, hair follicle dermal papilla cells were stimulated to proliferate, hair growth was accelerated, and the number of follicles was increased in treated mice. These effects seem to be adequate to ensure the efficacy of the local treatment of hair loss and androgenetic alopecia.

Conflicts of interest

There are no conflicts to declare.

References

1 Y. Zhang, L. Han, S. S. Chen, J. Guan, F. Z. Qu and Y. Q. Zhao, *Biomed. Pharmacother.*, 2016, **83**, 641–647.
2 Z. Santos, P. Avci and M. R. Hamblin, *Expert Opin. Drug Discovery*, 2015, **10**, 269–292.
3 L. Dong, H. Hao, L. Xia, J. Liu, D. Ti, C. Tong, Q. Hou, Q. Han, Y. Zhao, H. Liu, X. Fu and W. Han, *Sci. Rep.*, 2014, **4**, 5432.
4 S. Müller-Röver, K. Foitzik and R. Paus, *B. H.-J. of I. and undefined*, Elsevier, 2001.
5 J. Ocampo-Garza, J. Griggs and A. Tosti, *Expert Opin. Invest. Drugs*, 2019, **28**, 275–284.

6 Y. Feng, L. Ma, X. Li and W. Ding, *X. C.-B. & Pharmacotherapy and undefined*, Elsevier, 2017.
7 M. Górecki, A. Dziedzic and R. Luboradzki, *A. O.-Steroids and undefined*, Elsevier, 2017.
8 N. Rattanachitthawat, T. Pinkhien, P. Opanasopit, T. Ngawhirunpat and P. Chanvorachote, *In Vivo*, 2019, **33**, 1209–1220.
9 M. Z. U. Khan, S. A. Khan, M. Ubaid, A. Shah, R. Kousar and G. Murtaza, *Curr. Drug Delivery*, 2018, **15**, 1100–1111.
10 A.-M. Hosking, M. Juhasz and N. A. Mesinkovska, *Skin Appendage Disord.*, 2018, **5**, 72–89.
11 G. Jakab, D. Bogdán, K. Mazák, R. Deme, Z. Mucsi, I. M. Mándity, B. Noszál, N. Kállai-Szabó and I. Antal, *AAPS PharmSciTech*, 2019, **20**, 314.
12 S. H. Shin, S. S. Bak, M. K. Kim, Y. K. Sung and J. C. Kim, *Naunyn-Schmiedeberg's Arch. Pharmacol.*, 2015, **388**, 583–586.
13 F. Xing, W. J. Yi, F. Miao, M. Y. Su and T. C. Lei, *Int. J. Mol. Med.*, 2018, **41**, 2079–2085.
14 A. R. Kim, S. N. Kim, I. K. Jung, H. H. Kim, Y. H. Park and W. S. Park, *Planta Med.*, 2014, **80**, 153–158.
15 Y. Qian, Y. Chen and L. Wang, *J. T.-A. cirurgica brasileira and undefined*, SciELO Bras, 2018.
16 C. Gao, Y. Zhou, H. Li, X. Cong, Z. Jiang, X. Wang, R. Cao and W. Tian, *Mol. Med. Rep.*, 2017, **16**, 8729–8734.
17 S. Mir-Palomo, A. Nácher, O. Díez-Sales, O. M. A. Vila Busó, C. Caddeo, M. L. Manca, M. Manconi, A. M. Fadda and A. R. Saurí, *Int. J. Pharm.*, 2016, **511**, 23–29.
18 J. Wang, H. Jiao, J. Meng, M. Qiao, H. Du, M. He, K. Ming, J. Liu, D. Wang and Y. Wu, *Front. Microbiol.*, 2019, **10**, 2800.
19 T. Ahmed, *M. K.-E. J. of P. Sciences and undefined*, Elsevier, 2016.
20 R. El-Gogary and S. Gaber, *M. N.-S. reports and undefined*, nature.com, 2019.
21 H. A. E. Benson, J. E. Grice, Y. Mohammed, S. Namjoshi and M. S. Roberts, *Curr. Drug Delivery*, 2019, **16**, 444–460.
22 C. L. Fang, I. A. Aljuffali, Y. C. Li and J. Y. Fang, *Ther. Delivery*, 2014, **5**, 991–1006.
23 A. Zeb, O. Qureshi and H. Kim, *J. C.-I. journal of and undefined*, ncbi.nlm.nih.gov, 2016.
24 M. L. Manca, I. Usach, J. E. Peris, A. Ibba, G. Orrù, D. Valenti, E. Escribano-Ferrer, J. C. Gomez-Fernandez, F. J. Aranda, A. M. Fadda and M. Manconi, *Pharmaceutics*, 2019, **11**, 263.
25 A. Ascenso, S. Raposo, C. Batista, P. Cardoso, T. Mendes, F. G. Praça, M. V. Bentley and S. Simões, *Int. J. Nanomed.*, 2015, **10**, 5837–5851.
26 I. Castangia, M. L. Manca, C. Caddeo, A. Maxia, S. Murgia, R. Pons, D. Demurtas, D. Pando, D. Falconieri, J. E. Peris, A. M. Fadda and M. Manconi, *Colloids Surf., B*, 2015, **132**, 185–193.
27 M. Manconi, F. Marongiu, M. L. Manca, C. Caddeo, G. Sarais, C. Cencetti, L. Pucci, V. Longo, G. Bacchetta and A. M. Fadda, *Int. J. Pharm.*, 2017, **523**, 159–166.
28 M. L. Manca, C. Cencetti, P. Matricardi, I. Castangia, M. Zaru, O. D. Sales, A. Nacher, D. Valenti, A. M. Maccioni, A. M. Fadda and M. Manconi, *Int. J. Pharm.*, 2016, **511**, 198–204.
29 N. Bavarsad, A. Akhgari, S. Seifmanesh, A. Salimi and A. Rezaie, *Daru, J. Pharm. Sci.*, 2016, **24**, 7.
30 M. L. Manca, I. Castangia, M. Zaru, A. Nácher, D. Valenti, X. Fernàndez-Busquets, A. M. Fadda and M. Manconi, *Biomaterials*, 2015, **71**, 100–109.
31 I. Castangia, C. Caddeo, M. L. Manca, L. Casu, A. C. Latorre, O. Díez-Sales, A. Ruiz-Saurí, G. Bacchetta, A. M. Fadda and M. Manconi, *Carbohydr. Polym.*, 2015, **134**, 657–663.
32 V. Truong, M. Bak, C. Lee and M. Jun, *W. J.- Molecules and undefined*, mdpi.com, 2017.
33 M. Manconi, J. Aparicio, A. O. Vila, J. Pendás, J. Figueruelo and F. Molina, *Colloids Surf., A*, 2003, **222**, 141–145.
34 A. Catalan-Latorre, M. Ravaghi, M. L. Manca, C. Caddeo, F. Marongiu, G. Ennas, E. Escribano-Ferrer, J. E. Peris, O. Diez-Sales, A. M. Fadda and M. Manconi, *Eur. J. Pharm. Biopharm.*, 2016, **107**, 49–55.
35 E. Abd, M. S. Roberts and J. E. Grice, *Skin Pharmacol. Physiol.*, 2016, **29**, 24–30.
36 R. Sennett and M. Rendl, *Semin. Cell Dev. Biol.*, 2012, **23**, 917–927.
37 L. L. Levy and J. J. Emer, *Int. J. Women's Health*, 2013, **5**, 541–556.
38 S. Arias-Santiago, A. Buendía-Eisman, M. T. Gutiérrez-Salmerón and S. Serrano-Ortega, in *Handbook of Hair in Health and Disease*, MDText.com, Inc., 2012, pp. 99–116.
39 M. L. Manca, M. Manconi, M. Zaru, D. Valenti, J. E. Peris, P. Matricardi, A. M. Maccioni and A. M. Fadda, *Int. J. Pharm.*, 2017, **532**, 401–407.
40 S. W. Lee, M. Juhasz, P. Mobasher, C. Ekelem and N. A. Mesinkovska, *J. Drugs Dermatol.*, 2018, **17**, 457–463.
41 J. Shapiro and K. D. Kaufman, *J. Invest. Dermatol. Symp. Proc.*, 2003, **8**, 20–23.
42 V. H. Price, J. L. Roberts, M. Hordinsky, E. A. Olsen, R. Savin, W. Bergfeld, V. Fiedler, A. Lucky, D. A. Whiting, F. Pappas, J. Culbertson, P. Kotey, A. Meehan and J. Waldstreicher, *J. Am. Acad. Dermatol.*, 2000, **43**, 768–776.
43 R. Oliveira-Soares, J. E. Silva, M. Correia and M. André, *Int. J. Trichol.*, 2013, **5**, 22–25.
44 M. Tabbakhian, N. Tavakoli, M. R. Jaafari and S. Daneshamouz, *Int. J. Pharm.*, 2006, **323**, 1–10.
45 D. D. Verma, S. Verma, G. Blume and A. Fahr, *Int. J. Pharm.*, 2003, **258**, 141–151.
46 M. Manconi, S. Mura, C. Sinico, A. M. Fadda, A. O. Vila and F. Molina, *Colloids Surf., A*, 2009, **342**, 53–58.
47 Y. Rao, F. Zheng, X. Zhang, J. Gao and W. Liang, *AAPS PharmSciTech*, 2008, **9**, 860–865.
48 Y. Rao, F. Zheng, X. Liang, H. Wang, J. Zhang and X. Lu, *Drug Delivery*, 2015, **22**, 1003–1009.
49 J. W. Fluhr, R. Darlenski and C. Surber, *Br. J. Dermatol.*, 2008, **159**, 23–34.
50 L. Overgaard Olsen and G. B. E. Jemec, *Acta Derm.-Venereol.*, 1993, **73**, 404–406.
51 M. B. Brown and S. A. Jones, *J. Eur. Acad. Dermatol. Venereol.*, 2005, **19**, 308–318.

GENERALITAT VALENCIANA
CONSELLERIA DE AGRICULTURA, MEDIO AMBIENTE, CAMBIO CLIMÁTICO Y DESARROLLO RURAL
DIRECCIÓN GENERAL DE AGRICULTURA, GANADERÍA Y PESCA

Unión Europea

AUTORIZACION PROCEDIMIENTO 2016/VSC/PEA/00112

Vista la solicitud realizada en fecha **01/06/16** con nº reg. entrada **21725** por D/Dª. **Pilar Campins Falcó**, Vicerrectora de Investigación y Política Científica, centro usuario **ES460780001001**, para realizar el procedimiento:

"Evaluación de la eficacia antiinflamatoria de flavonoides vehiculizados en nanotransportadores para el tratamiento de enfermedades inflamatorias cutáneas"

Teniendo en cuenta la documentación aportada, según se indica en el artículo 33, punto 5 y 6, y puesto que dicho procedimiento se halla sujeto a autorización en virtud de lo dispuesto en el artículo 31 del Real Decreto 53/2013, de 1 de febrero,

Vista la propuesta del jefe del servicio de Ganadería y Sanidad y Bienestar Animal.

AUTORIZO:

la realización de dicho procedimiento al que se le asigna el código: **2016/VSC/PEA/00112** tipo **2,** de acuerdo con las características descritas en la propia documentación para el número de animales, especie y periodo de tiempo solicitado. Todo ello sin menoscabo de las autorizaciones pertinentes, por otras Administraciones y entidades, y llevándose a cabo en las siguientes condiciones:

Usuario: **Universitat de Valencia**

Responsable del proyecto: **Amparo Nácher Alonso**

Establecimiento: **Sección de Producción Animal SCIE-Campus Burjassot**

Necesidad de evaluación restrospectiva:

Condiciones específicas:

Observaciones:

Valencia a, 27 de junio de 2016

El director general de Agricultura, Ganadería y Pesca

Rogelio Llanes Ribas

GENERALITAT VALENCIANA
CONSELLERIA D'AGRICULTURA, MEDI AMBIENT, CANVI CLIMÀTIC I DESENVOLUPAMENT RURAL

GENERALITAT VALENCIANA
Conselleria d'Agricultura, Medi Ambient, Canvi Climàtic i Desenvolupament Rural

Dirección General de Agricultura, Ganadería y Pesca
Ciutat Administrativa 9 d'Octubre
Calle de La Democracia, 77 · Edif. B3 P2
46018 València

AUTORIZACION PROCEDIMIENTO 2019/VSC/PEA/0113

Vista la solicitud realizada en fecha **16/04/19** con nº reg. entrada **263378** por D/Dª. **Carlos Hermenegildo Caudevilla**, **Vicerrector de Investigación y Política Científica**, centro usuario **ES460780001001**, para realizar el procedimiento:

"Determinación de la eficacia de polifenoles encapsulados en nanoliposomas en el tratamiento de diversas formas de alopecia."

Teniendo en cuenta la documentación aportada, según se indica en el artículo 33, punto 5 y 6, y puesto que dicho procedimiento se halla sujeto a autorización en virtud de lo dispuesto en el artículo 31 del Real Decreto 53/2013, de 1 de febrero,

Vista la propuesta del jefe del servicio de Producción y Sanidad Animal.

AUTORIZO:

la realización de dicho procedimiento al que se le asigna el código: **2019/VSC/PEA/0113** tipo **2,** de acuerdo con las características descritas en la propia documentación para el número de animales, especie y periodo de tiempo solicitado. Todo ello sin menoscabo de las autorizaciones pertinentes, por otras Administraciones y entidades, y llevándose a cabo en las siguientes condiciones:

Usuario: **Universitat de Valencia**

Responsable del proyecto: **Amparo Nacher Alonso**

Establecimiento: **Sección de Producción Animal SCIE-Campus Burjassot**

Necesidad de evaluación restrospectiva:

Condiciones específicas:

Observaciones:

Valencia a, fecha de la firma electrónica
El director general de Agricultura, Ganadería y Pesca

Firmat per Rogelio Llanes Ribas el 25/04/2019 14:19:12
Càrrec: Dirección General